NASA TECHNICAL MEMORANDUM

NASA TM X-3461

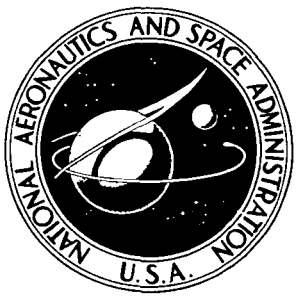

NASA TM X-3461

SUPERSONIC AERODYNAMIC CHARACTERISTICS OF A SERIES OF WRAP-AROUND-FIN MISSILE CONFIGURATIONS

Roger H. Fournier

Langley Research Center
Hampton, Va. 23665

NATIONAL AERONAUTICS AND SPACE ADMINISTRATION · WASHINGTON, D. C. · MARCH 1977

1. Report No.	2. Government Accession No.	3. Recipient's Catalog No.
NASA TM X-3461		

4. Title and Subtitle	5. Report Date
SUPERSONIC AERODYNAMIC CHARACTERISTICS OF A SERIES OF WRAP-AROUND-FIN MISSILE CONFIGURATIONS	March 1977
	6. Performing Organization Code

7. Author(s)	8. Performing Organization Report No.
Roger H. Fournier	L-11153
	10. Work Unit No. 505-11-22-01
9. Performing Organization Name and Address NASA Langley Research Center Hampton, VA 23665	11. Contract or Grant No.
	13. Type of Report and Period Covered Technical Memorandum
12. Sponsoring Agency Name and Address National Aeronautics and Space Administration Washington, DC 20546	14. Sponsoring Agency Code

15. Supplementary Notes

16. Abstract

A parametric study of wrap-around-fin missile configurations has been conducted at Mach numbers from 1.60 to 2.86 in the Langley Unitary Plan wind tunnel. The fin configurations investigated included variations in chord length, leading-edge sweep, thickness ratio, and leading-edge shape. The investigation also included a smooth and a stepped-down afterbody required for flush retraction of the wrap-around-fin configuration.

The investigation indicated no unusual longitudinal characteristics; however, all the wrap-around-fin configurations tested indicated erratic lateral behavior, particularly in the form of induced roll at zero angle of attack and irregular variations of roll with angle of attack and Mach number. The magnitude of rolling moment at an angle of attack of 0° is estimated to represent approximately 0.25° or less roll control deflection. The stepped-down afterbody had a marked effect on reducing the induced roll.

17. Key Words (Suggested by Author(s))	18. Distribution Statement
Missile Wrap-around-fin Tube-launch missile Compact-storage missile	Unclassified - Unlimited Subject Category 02

19. Security Classif. (of this report)	20. Security Classif. (of this page)	21. No. of Pages	22. Price*
Unclassified	Unclassified	172	$6.25

* For sale by the National Technical Information Service, Springfield, Virginia 22161

SUPERSONIC AERODYNAMIC CHARACTERISTICS OF A SERIES OF WRAP-AROUND-FIN MISSILE CONFIGURATIONS

Roger H. Fournier
Langley Research Center

SUMMARY

A parametric study of wrap-around-fin missile configurations has been conducted at Mach numbers from 1.60 to 2.86 in the Langley Unitary Plan wind tunnel. The fin configurations investigated included variations in chord length, leading-edge sweep, thickness ratio, and leading-edge shape. The investigation also included a smooth and a stepped-down afterbody required for flush retraction of the wrap-around-fin configurations.

The investigation indicated no unusual longitudinal characteristics; although for the smaller fins, a more forward moment center would be required to provide adequate longitudinal stability at the higher Mach numbers. All the wrap-around-fin configurations tested indicated erratic lateral behavior, particularly in the form of induced roll at zero angle of attack, and irregular variations of roll with angle of attack and Mach number. The magnitude of rolling moment at an angle of attack of 0° is estimated to represent approximately 0.25° or less control deflection. The stepped-down afterbody had a marked effect on reducing the induced roll.

INTRODUCTION

The requirements for compact storage of tube-launch missile configurations often result in serious compromise of aerodynamic performance. One method of satisfying these requirements involves the use of wrap-around folding fins. These fins are contoured to fit around the body when stored and are deployed for increased stability when launched. Several missile configurations with wrap-around fins have been proposed. References 1 to 3 include some results of previous tests of wrap-around-fin (WAF) configurations. These results indicate that erratic aerodynamic rolling-moment characteristics are inherent in these configurations.

In order to provide additional information for missile designers, a parametric study on wrap-around-fin missile configurations has been conducted in the Langley Unitary Plan wind tunnel to determine their static aerodynamic characteristics at supersonic speeds.

The study included fins with variations in thickness ratio, leading-edge sweep, leading-edge bevel, fin curvature, and chord length. Tests were performed at Mach numbers from 1.60 to 2.86 through an angle-of-attack range of about -8° to 6° at a Reynolds number per meter of 9.84×10^{6} and at model roll attitudes of 0° and 45°.

SYMBOLS

The aerodynamic data are referred to the body axis system. The moment reference was located 61.976 cm (61 percent of the body length) aft of the model nose.

A reference area (based on body diameter, 10.16 cm), 0.008107 m^2

A_b base area, Basic = 0.008107 m^2, Stepped = 0.006567 m^2

C_A axial-force coefficient, $\frac{\text{Axial force}}{qA}$

$C_{A,b}$ base axial-force coefficient, $\frac{\text{Base axial force}}{qA_b}$

C_l rolling-moment coefficient, $\frac{\text{Rolling moment}}{qAd}$

C_m pitching-moment coefficient, $\frac{\text{Pitching moment}}{qAd}$

C_N normal-force coefficient, $\frac{\text{Normal force}}{qA}$

$C_{N,F}$ fin normal-force coefficient (number after F denotes fin position), $\frac{\text{Fin normal force}}{qS_F}$

C_n yawing-moment coefficient, $\frac{\text{Yawing moment}}{qAd}$

C_Y side-force coefficient, $\frac{\text{Side force}}{qA}$

c fin root chord, cm

d reference diameter, 10.16 cm

M Mach number

q dynamic pressure, kN/m^2

S_F fin area of each fin (fin designated by number after F), m^2

t fin thickness, cm

α angle of attack, deg

Λ_f fin leading-edge sweep, deg

ϕ model roll orientation, deg ($\phi = 0^\circ$ when roots of fins are in horizontal and vertical planes)

Model component designations:

B_1 basic body

B_2 body with stepped afterbody

F_1 long-chord curved fin (17.78 cm long, $t/c = 0.0285$, $S_{F1} = 0.01192\ m^2$)

F_2 short-chord curved fin (10.16 cm long, $t/c = 0.0153$, $S_{F2} = 0.00671\ m^2$)

F_6 same as F_1 except with beveled leading edge

F_7 same as F_1 except $t/c = 0.0153$

F_9 long-chord straight fin (17.78 cm long, $t/c = 0.0285$, $S_{F9} = 0.01187\ m^2$)

F_{13} same as F_1 except with a leading-edge sweep of 34° $\left(\frac{\text{Tip chord}}{\text{Root chord}} = 0.75\right)$, $S_{F13} = 0.01040\ m^2$

F_{16} same as F_2 except with a leading-edge sweep of 21° $\left(\frac{\text{Tip chord}}{\text{Root chord}} = 0.75\right)$, $S_{F16} = 0.00694\ m^2$

Fin position 1 is in top vertical plane (concave side to right) for $\phi = 0^\circ$ and fin positions are numbered consecutively in clockwise direction looking upstream.

APPARATUS AND METHODS

Tunnel

The investigation was conducted in the low Mach number test section of the Langley Unitary Plan wind tunnel, which is a variable-pressure continuous-flow facility. The test section is approximately 2.13 m long and 1.22 m square. The nozzle leading to the test section is of the asymmetric sliding-block type, which permits a continuous variation in Mach number from about 1.50 to 2.90.

Model

Dimensional details of the model are shown in figure 1 and tunnel installation photographs are shown in figure 2. The body of the basic model consisted of a two-caliber, secant-ogive nose and an eight-caliber cylindrical afterbody which was 10.16 cm in diameter. Four sets (cruciform) of wrap-around fins (WAF) with root chords 17.78 cm in length were furnished. Three sets of these fins had a 0° leading-edge sweep and a thickness ratio of 0.0285. One set of fins

had a thickness ratio of 0.0153, a second set of fins had a leading-edge sweep of 34°, and a third set of fins had beveled leading edges used for producing rolling moment. A set of straight fins was also provided. In addition, two other sets of fins with root chords 10.16 cm in length were furnished. These two sets of fins differed only in leading-edge sweep. Both the long- and short-chord fins were attached to the body with the fin trailing edges at the body base. An alternate afterbody was provided that had a 10-percent reduction in diameter for a length sufficient to allow installation of any of the fins.

Test Conditions

The tests were performed at the following conditions:

Mach number	Stagnation temperature, K	Stagnation pressure, kN/m^2	Reynolds number per meter
1.60	339	81.9	9.84×10^6
1.90	339	91.3	9.84
2.36	339	113.4	9.84
2.86	339	147.7	9.84

The dewpoint was maintained sufficiently low to insure negligible condensation effects in the test section. The angles of attack were varied from about -8° to 6° at an angle of sideslip of 0° and at model roll angles of 0° and 45°. Boundary-layer transition strips 0.16 cm wide, composed of No. 60 sand grains were placed 3.05 cm aft of the model nose and 1.02 cm aft of the leading edges in a streamwise direction on the fins.

Measurements

Aerodynamic forces and moments were measured on the model by means of a six-component electrical strain-gage balance housed within the model. The balance, in turn, was rigidly fastened to a sting. Each fin was instrumented with a three-component strain-gage balance for measuring the fin normal force. Model cavity and base pressures were measured by means of static-pressure orifices located in the vicinity of the balance and at the model base.

Corrections

The angles of attack have been corrected for deflections of the balance and sting due to aerodynamic loads and for tunnel flow angularity. The results have been adjusted to a condition of free-stream static pressure acting over the entire base of the model. Typical base corrections are shown in figure 3.

PRESENTATION OF RESULTS

Longitudinal Aerodynamic Characteristics

Lateral Aerodynamic Characteristics

DISCUSSION

Longitudinal Characteristics

In the investigation of the aerodynamics of the wrap-around fin, a curved fin was compared with a straight fin with equal projected planform area. The

results indicated that there are no significant effects of fin curvature on the longitudinal characteristics through the test angle-of-attack and Mach number ranges (figs. 4 and 5).

Reducing the chord length (and area) of the wrap-around fins (figs. 6 to 9) causes a reduction in normal force and pitching moment with increasing α and a slight reduction in axial force. For the moment reference center used, the reduced area results in the difference between static stability or instability at the higher Mach numbers.

Results of figures 10 to 13 indicate that the wrap-around fins with the swept leading edges show a slight reduction in C_A, C_N, and C_m with increasing α and Mach number, resulting most likely from the reduction in fin area. Reduction of fin thickness ratio has little effect on the longitudinal characteristics of the vehicle other than a slight reduction in C_A (figs. 14 and 15). The results of figures 16 and 17 indicate that beveling the leading edges of the fins to produce rolling moment had little effect on the longitudinal characteristics. Indentation of the afterbody with either the unswept long-chord fins (figs. 18 and 19) or the long-chord fins with swept leading edges (figs. 20 and 21) leads to a reduction in C_N and C_m with increasing α whereas C_A is relatively unaffected.

Body-alone data are presented in figure 22 in order that fin contributions can be determined.

Lateral Characteristics

The data on effects of fin curvature for the long-chord fins (figs. 23 and 24) indicate that the curved fins produce a negative rolling moment at $\alpha = 0^\circ$ in the test Mach number range and that these rolling moments increase with increasing positive or negative angles of attack. The curved fins also result in a small induced yawing moment that varies in direction and magnitude with both Mach number and angle of attack. The nature of the induced roll produced by the curved fins is graphically illustrated by pressure distribution measurements that have been reported in reference 2. The integrated pressure measurements from these investigations indicate that at supersonic speeds, a net lateral force is directed toward the concave side of the WAF, particularly over the leading-edge region, even at $\alpha = 0^\circ$. This force results in a rolling moment in the direction of the convex side of the WAF when viewed from the rear. The magnitude of the rolling moment at $\alpha = 0^\circ$ is estimated to represent approximately 0.25° or less, if all four fins were deflected for roll control. (This estimate is based on data from similar models.)

The effect of fin length for the unswept curved fins (figs. 25 and 26) indicates somewhat erratic behavior since the short fins produce slightly higher values of induced roll near $\alpha = 0^\circ$ for the lower Mach numbers and slightly lower values at $M = 2.86$. In general, however, the variation of C_l with α is less for the short fins. In addition, with the exception of $M = 2.86$, the short fins, when compared with the long fins, produced higher values of induced yaw with a greater variation with α and, in some cases, a reversal in direction. These results must be further tempered, however, by the fact that the

short-chord fin is thinner than the long-chord fin, and the thickness effects cannot be isolated from the chord effects in this comparison.

The effects of fin leading-edge sweep on the lateral characteristics of the vehicle with long-chord curved fins are presented in figures 29 and 30, respectively. Sweeping the leading edge of the long-chord fins was again the cause for erratic behavior. For example, at $M = 1.60$ the swept fin had essentially no effect on the magnitude of C_l at $\alpha = 0^\circ$ in comparison with the unswept fin, but the swept fin reduced the variation of C_l with α. However, at $M = 1.90$, the magnitude of C_l was substantially increased, but the variation with α remained small. At $M = 2.36$, there was essentially no effect on either the magnitude or the variation of C_l and at $M = 2.86$, the magnitude of C_l was measurably reduced whereas the variation with α was unchanged. Sweeping the leading edge of the short-chord curved fins (figs. 31 and 32) resulted in a large decrease in C_l at $\alpha = 0^\circ$ while maintaining only a small variation over the angle-of-attack range at all test Mach numbers. This particular fin (F_{16}) thus appears to be one of the more promising fins used in this investigation insofar as maintaining reasonably low and well-behaved induced lateral effects over the angle-of-attack and Mach number ranges considered. This observation is further illustrated by figures 27 and 28, wherein both the long-chord and the short-chord curved swept fins are compared. This comparison clearly shows the lower values of C_l at $\alpha = 0^\circ$ and the more orderly variation of induced effects with α and M for the short-chord swept fin (F_{16}).

Decreasing the thickness of the long-chord fins (figs. 33 and 34) generally leads to a decrease in C_l at all positive angles of attack in the test Mach number range. The magnitude of C_l at $\alpha = 0^\circ$ is not significantly affected by fin thickness except at $M = 2.86$ where the thinner fin (F_7) results in a reduced value of C_l. A 22.5° bevel on the leading edge of the long-chord fins (figs. 35 and 36) provides an increase in rolling moment at the two higher Mach numbers while showing relatively small and inconsistent effects at the two lower Mach numbers.

Indenting the afterbody in the vicinity of either the unswept or swept long-chord curved fins (figs. 37 and 38) generally leads to a reduction in the rolling moment and in the case of the swept fin (F_{13}) (figs. 39 and 40) results in essentially no induced roll particularly near $\alpha = 0^\circ$ at all test Mach numbers. This phenomenon is not fully understood but suggests that a disruption to the flow field immediately ahead of a WAF results in a more symmetrical fin pressure distribution.

Body-alone (B_1) data are presented in figure 41 in order that fin contributions can be determined.

Component Data

The normal-force values for each of the four fins, mounted on body B_1, are shown in figures 42 to 48 for all the configurations tested. It should be pointed out that any comparison of these data must recognize that the coefficients presented are based on the reference dimensions of the individual fins.

CONCLUDING REMARKS

A parametric study of wrap-around-fin missile configurations has been conducted at Mach numbers from 1.60 to 2.86 in the Langley Unitary Plan wind tunnel. The investigation indicated no unusual longitudinal characteristics. The small fins would, however, require a more forward moment center in order to provide adequate longitudinal stability at the higher Mach numbers.

All the wrap-around-fin configurations indicated somewhat erratic behavior, particularly in the form of induced roll at zero angle of attack and irregular variations of roll with angle of attack and Mach number. The magnitude of rolling moment at an angle of attack of 0° is estimated to represent approximately 0.25° or less if all four fins are deflected for roll control. (This estimate is based on data from similar models.) Other investigations have shown that a pressure difference exists between the convex and concave sides of the wrap-around fin, especially near the leading edge. This pressure difference results in the induced lateral characteristics. The results of the present investigation tend to verify this finding.

Geometric modifications that change the fin pressure distribution - leading-edge sweep, leading-edge shape, and thickness ratio - produced somewhat inconsistent effects with variations in angle of attack and Mach number. However, the effect of the stepped-down or reduced diameter afterbody has a marked effect on reducing the induced roll.

Langley Research Center
National Aeronautics and Space Administration
Hampton, VA 23665
December 8, 1976

REFERENCES

1. Wells, R. Franklin: Investigation of the Aerodynamic Characteristics of a Model of a Rocket Missile With Several Arrangements of Folding Fins at Mach Numbers of 1.75, 2.15, 2.48, and 2.87. NASA TM X-234, 1960.

2. Holmes, John E.: Wrap-Around Fin (WAF) Aerodynamics. Proceedings of 9th Navy Symposium on Aeroballistics, Volume 1, Appl. Physics Lab., The John Hopkins Univ., May 1972, pp. 13-22.

3. Dahlke, Calvin W.: Aerodynamics of Wrap-Around-Fins, a Survey of the Literature. Report No. RD-TR-71-7, U.S. Army Missile Command, Mar. 1971.

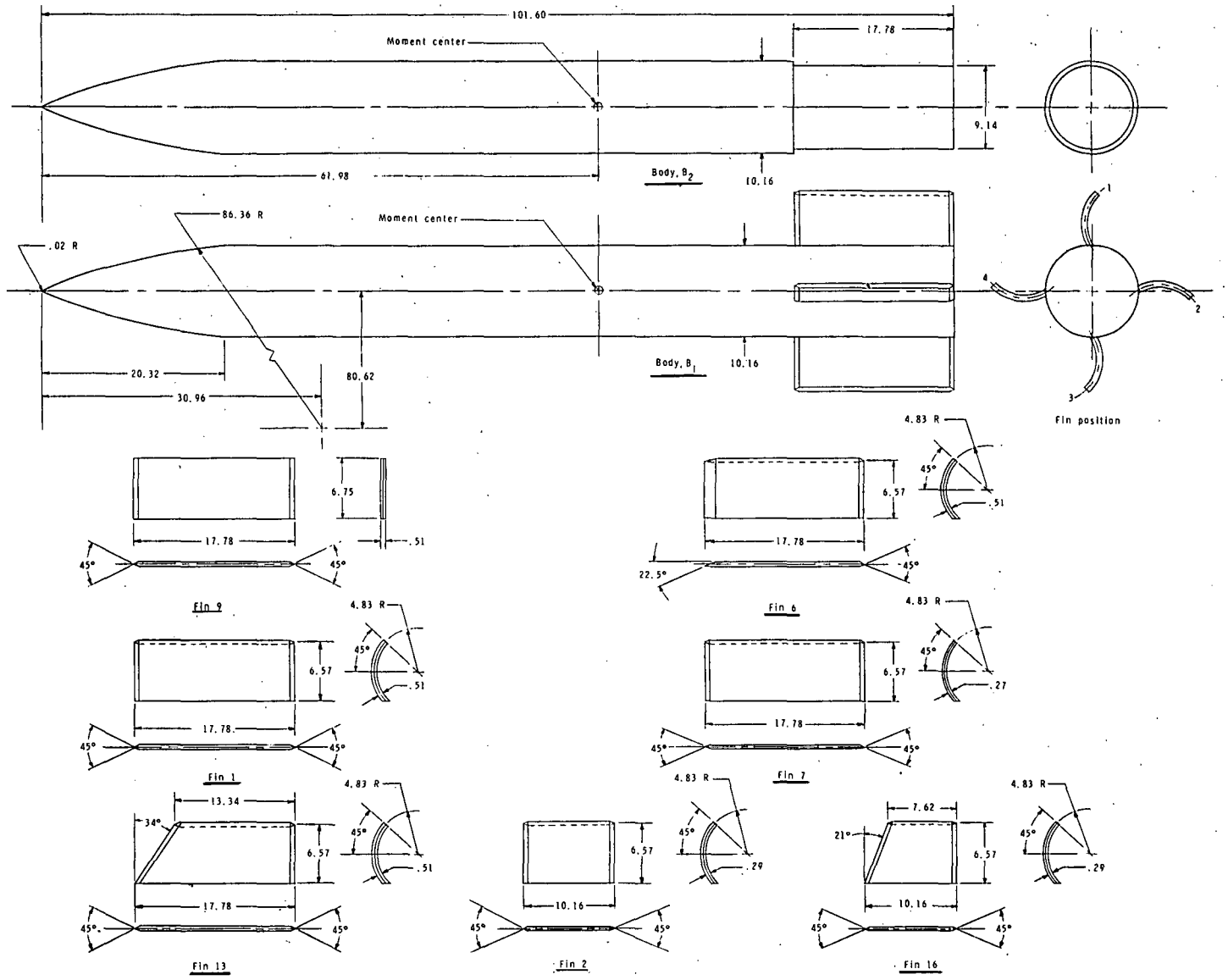

Figure 1.- Details of model. All dimensions are in centimeters unless otherwise noted.

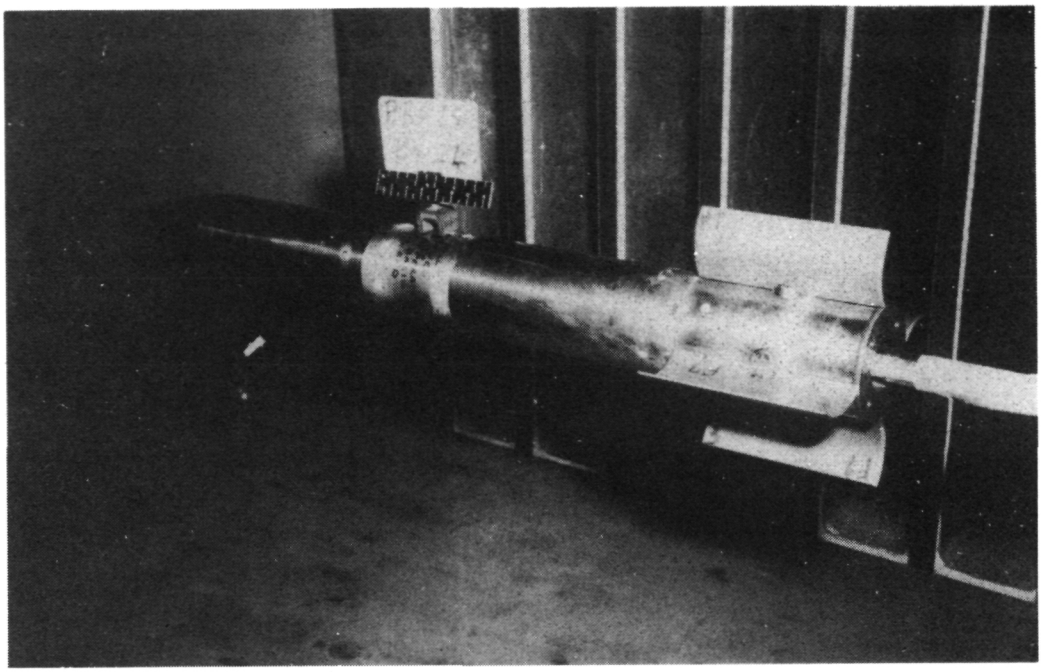

(a) Basic body and long-chord unswept curved fins (B_1F_7).

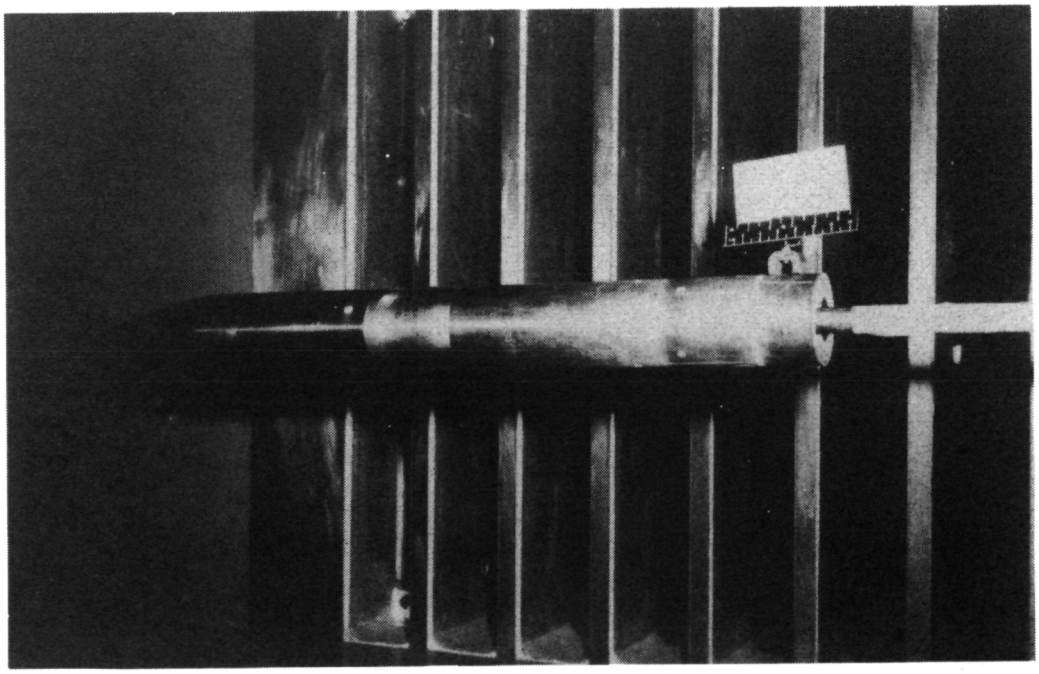

(b) Basic body (B_1).

L-76-7514

Figure 2.- Typical model photographs. $\phi = 0^{\circ}$.

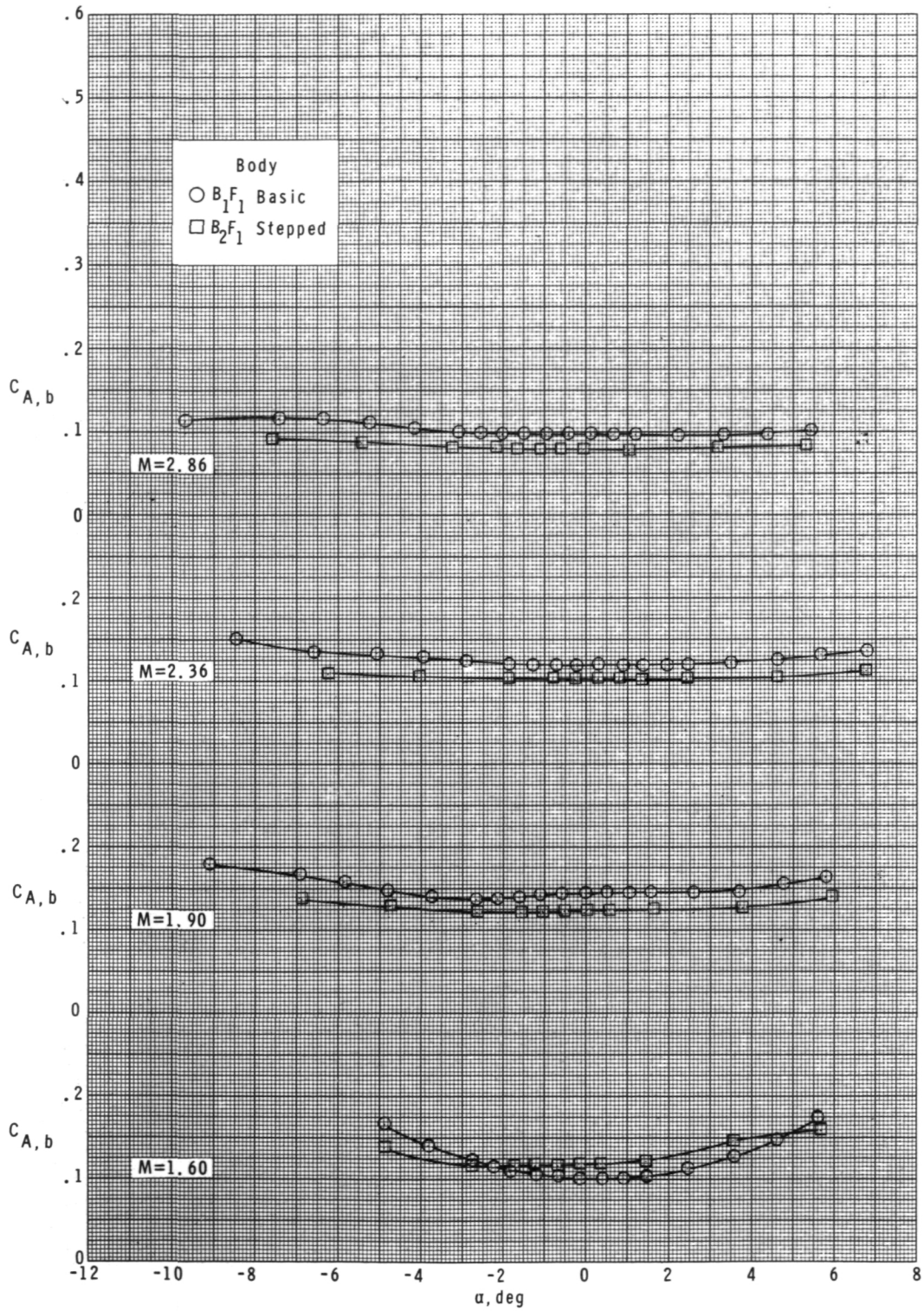

Figure 3.- Typical values of base axial-force coefficient for the basic (B_1) and stepped (B_2) afterbody with long-chord curved unswept fin (F_1).

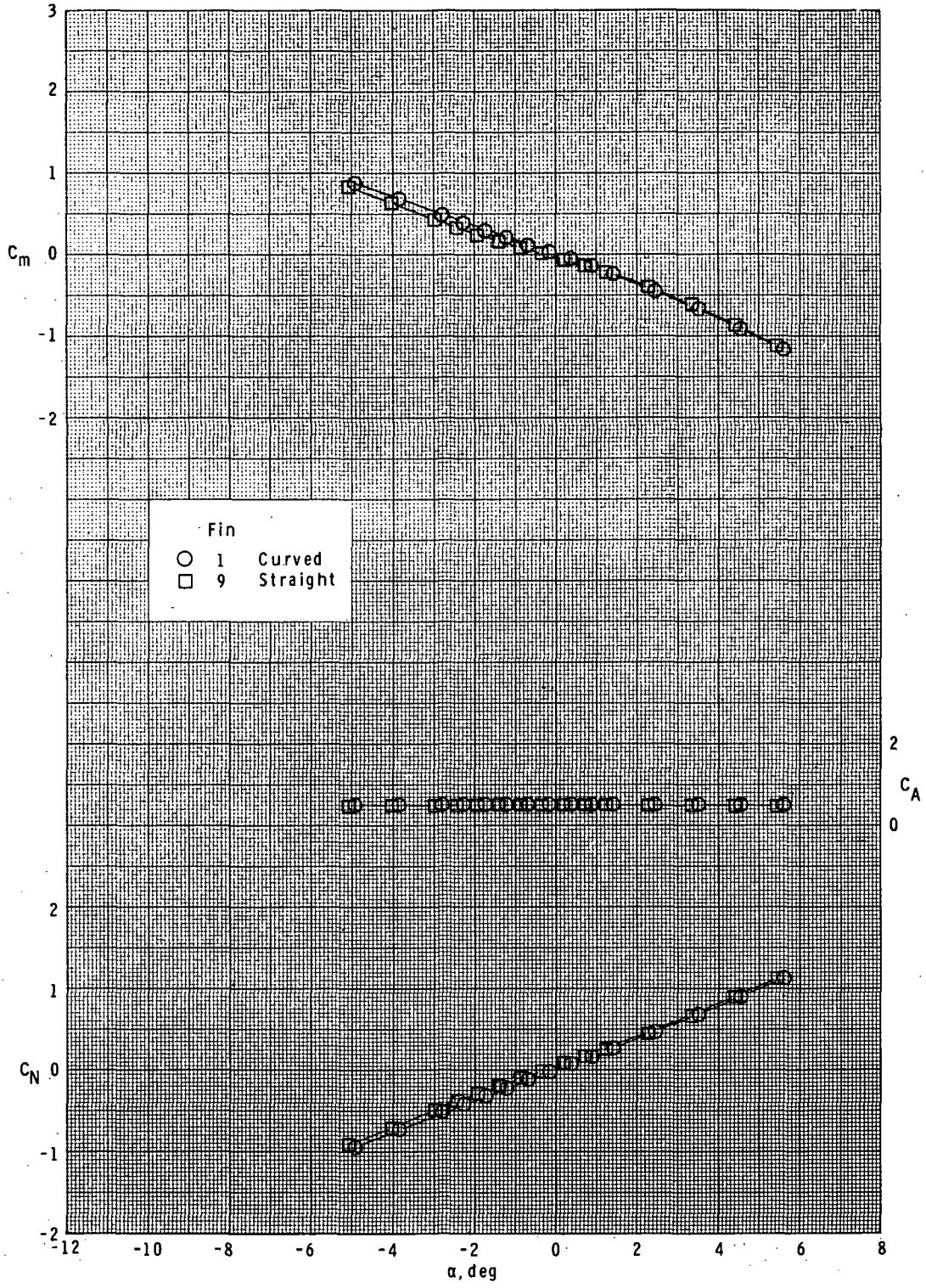

(a) M = 1.60.

Figure 4.- Effect of fin curvature on longitudinal characteristics. Basic body (B_1); long-chord fins (F_1 and F_9); $\phi = 0^\circ$.

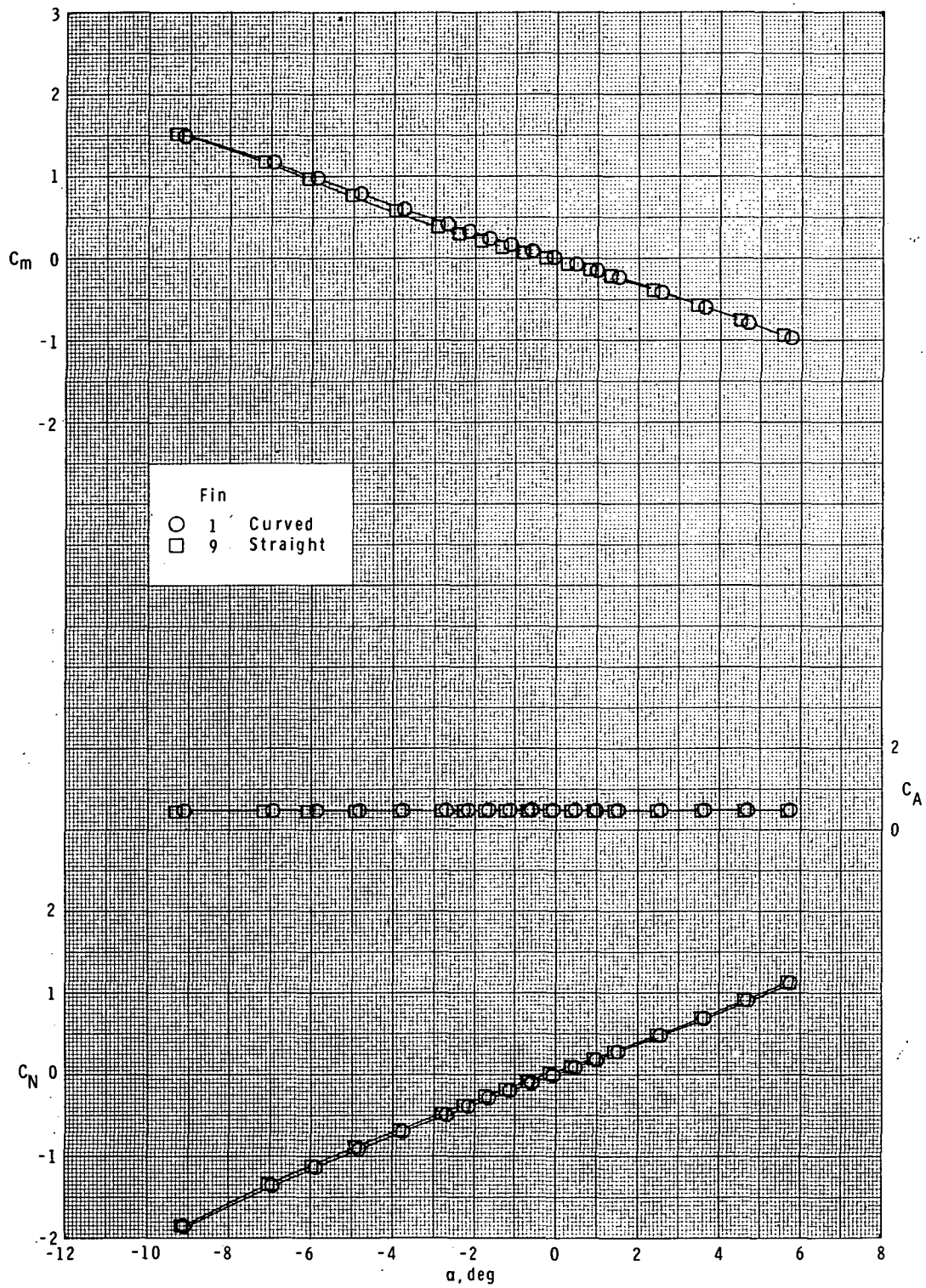

(b) M = 1.90.

Figure 4.- Continued.

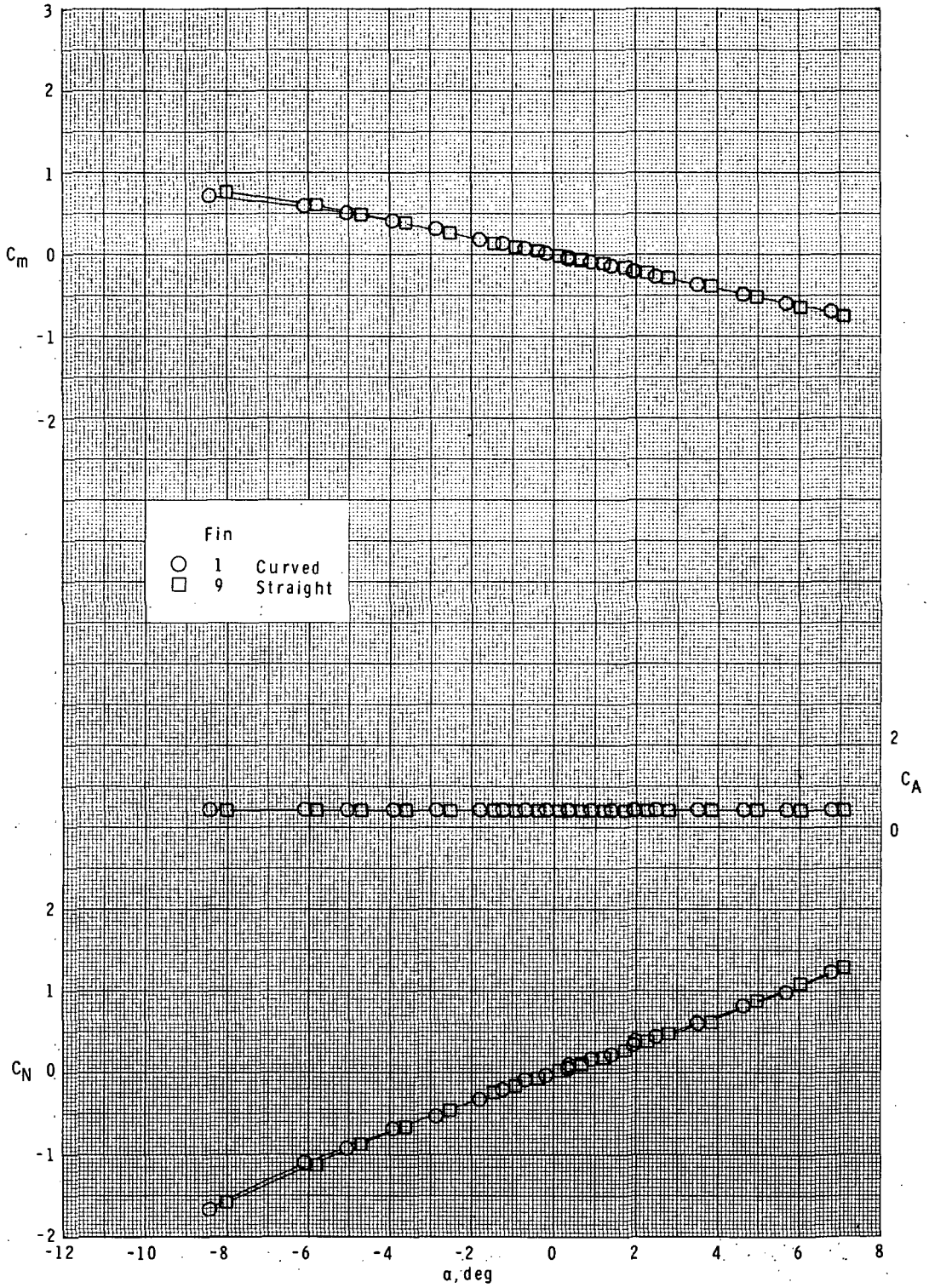

(c) M = 2.36.

Figure 4.- Continued.

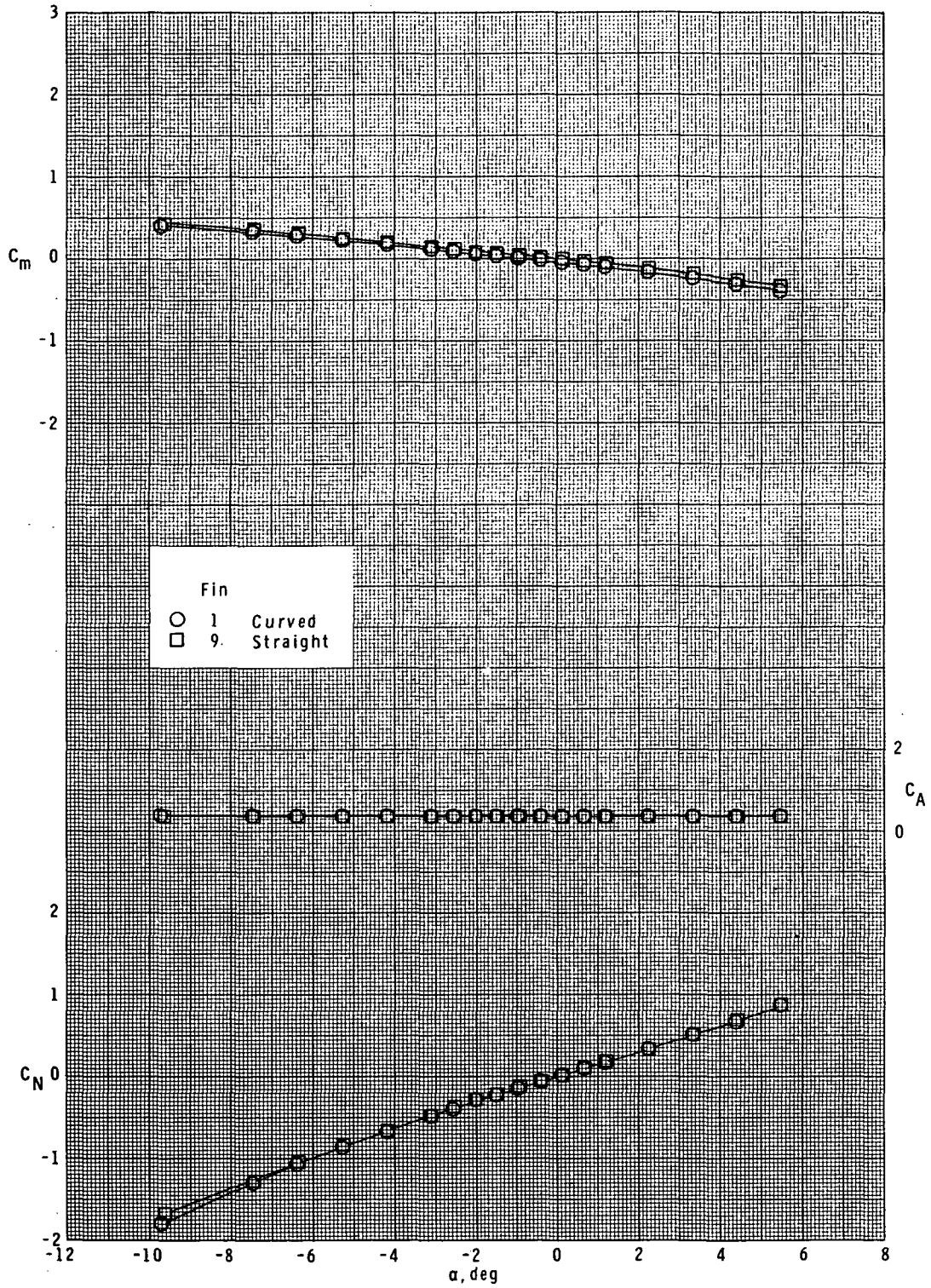

(d) M = 2.86.

Figure 4.- Concluded.

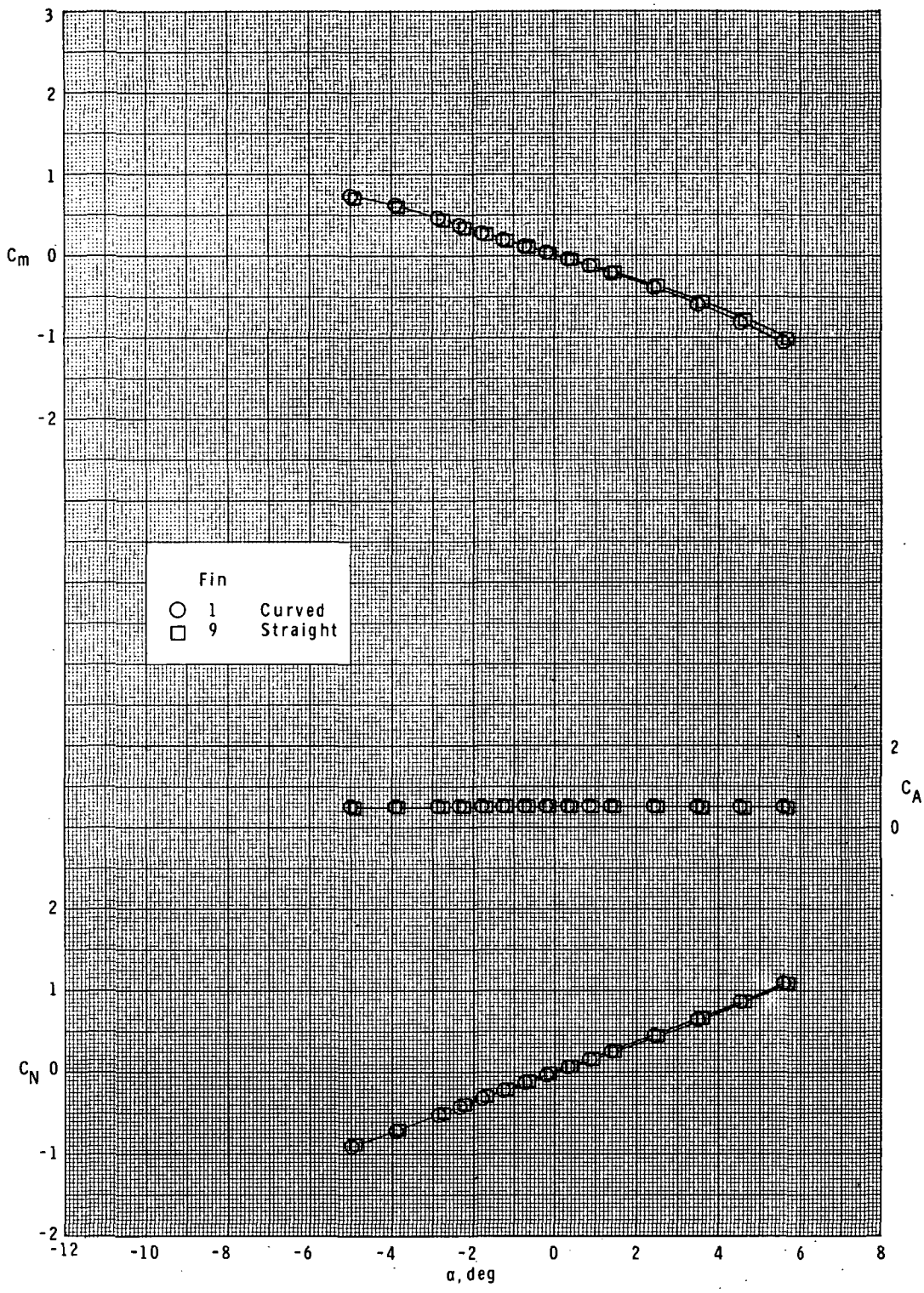

(a) M = 1.60.

Figure 5.- Effect of fin curvature on longitudinal characteristics. Basic body (B_1); long-chord fins (F_1 and F_9); $\phi = 45^\circ$.

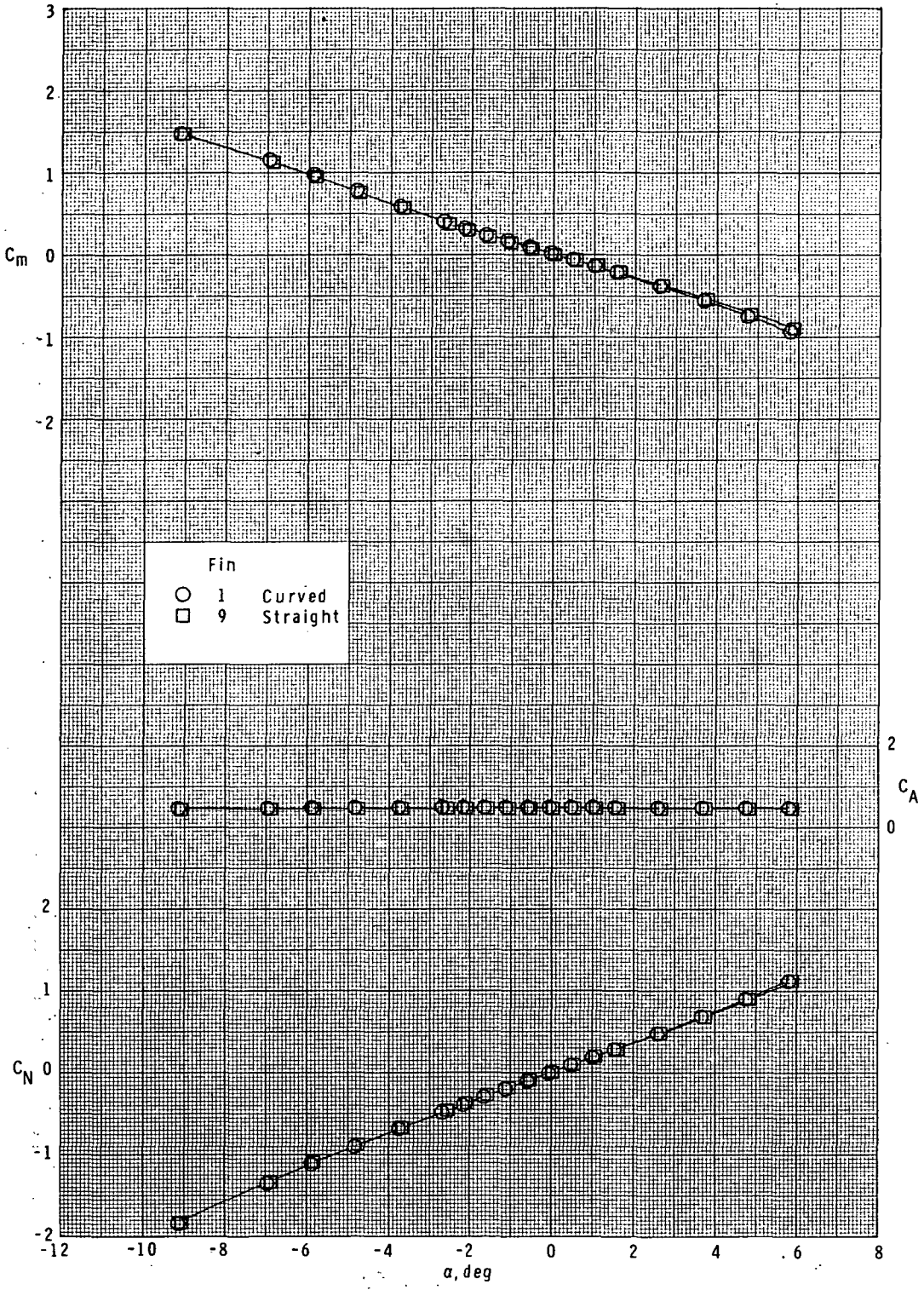

(b) M = 1.90.

Figure 5.- Continued.

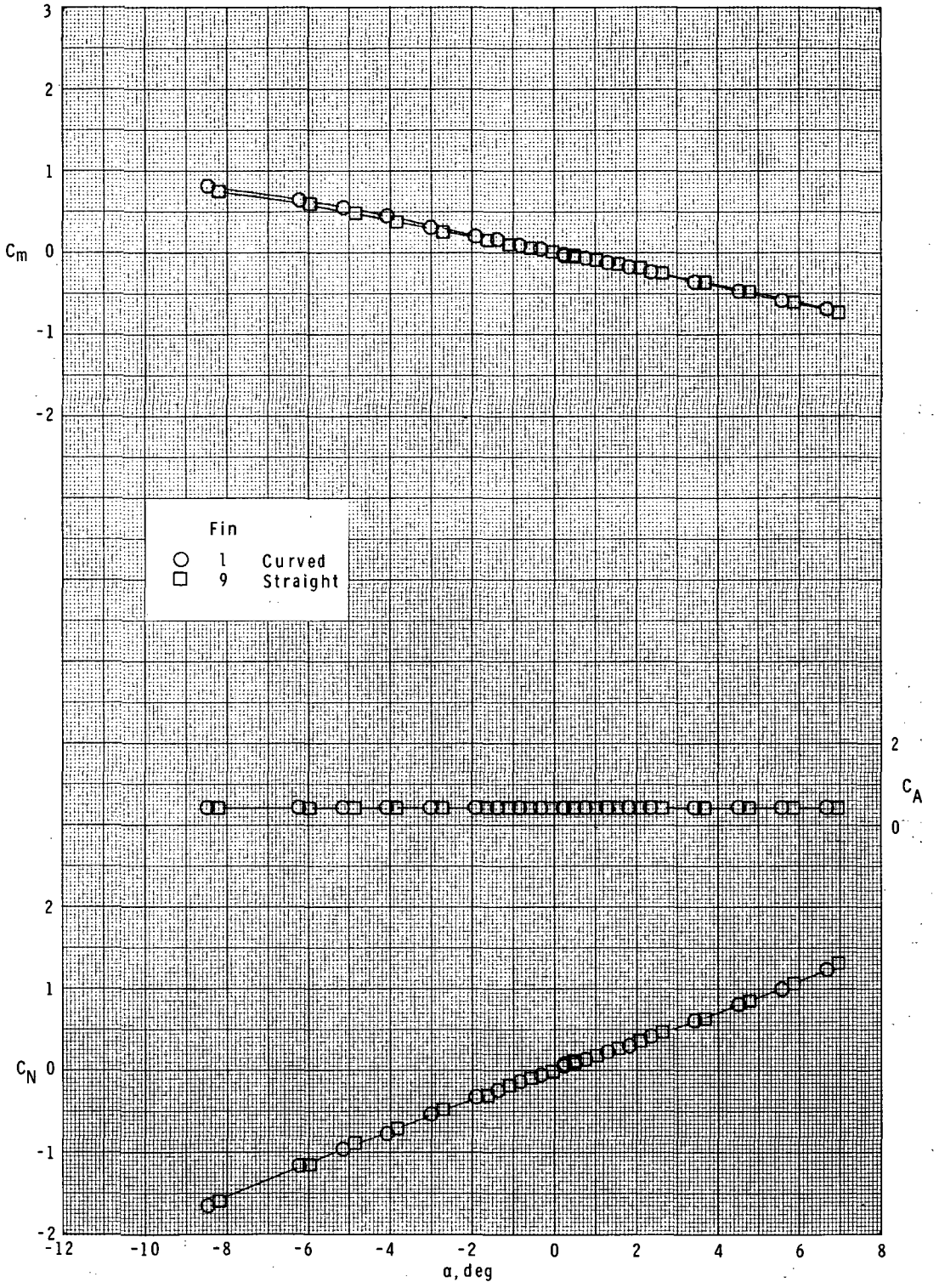

(c) M = 2.36.

Figure 5.- Continued.

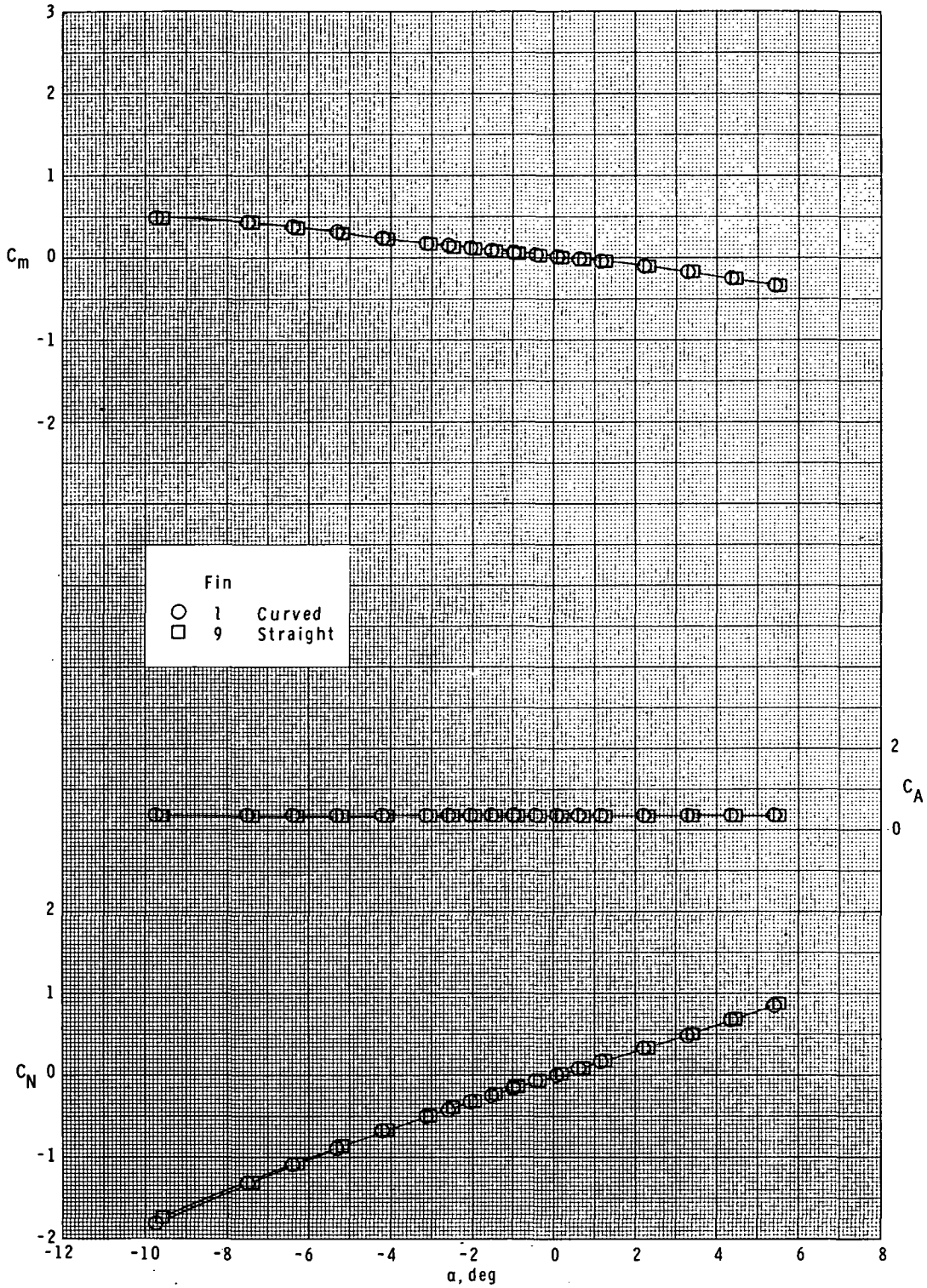

(d) M = 2.86.

Figure 5.- Concluded.

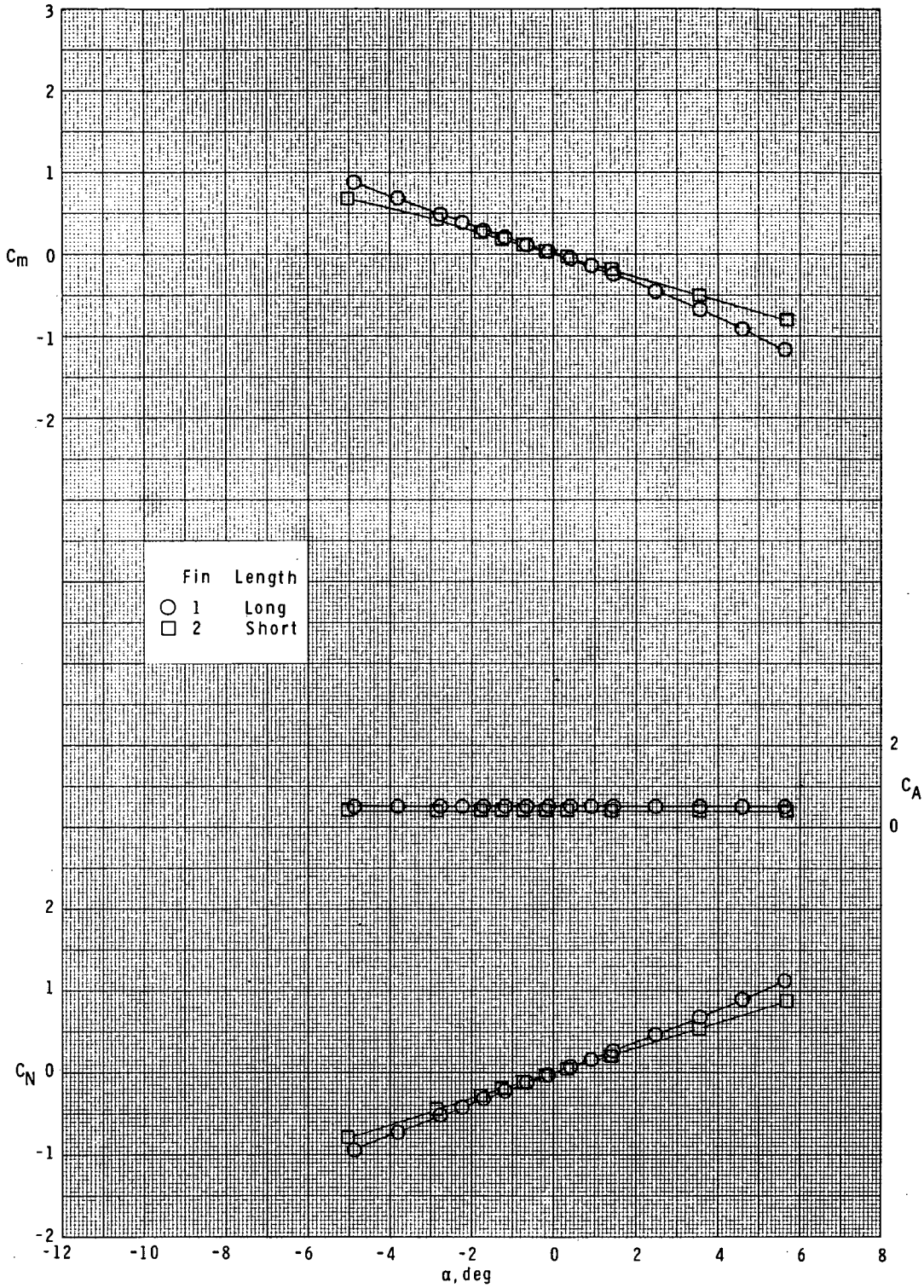

(a) M = 1.60.

Figure 6.- Effect of fin length on longitudinal characteristics. Basic body (B_1); unswept curved fins (F_1 and F_2); $\phi = 0^\circ$.

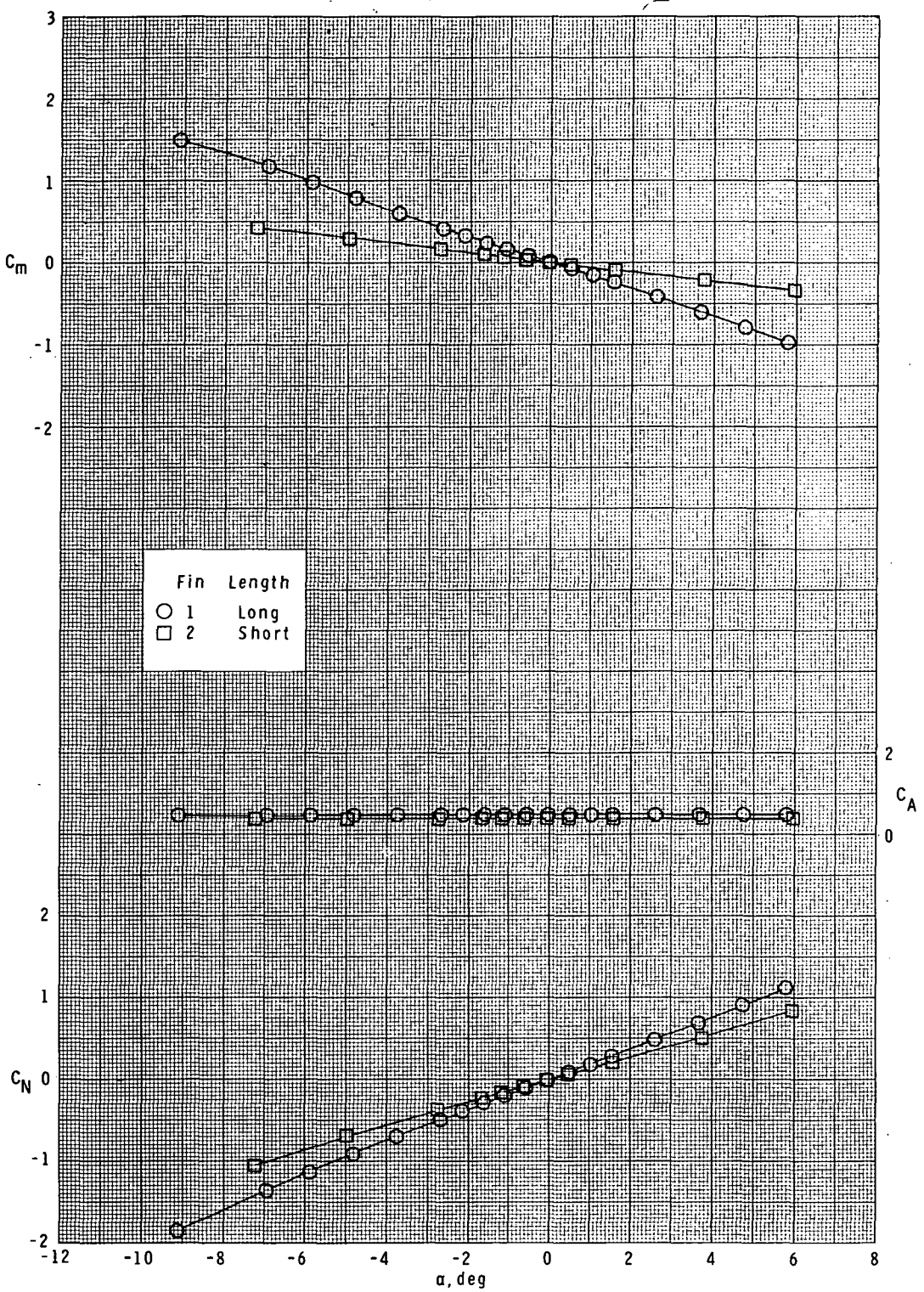

(b) M = 1.90.

Figure 6.- Continued.

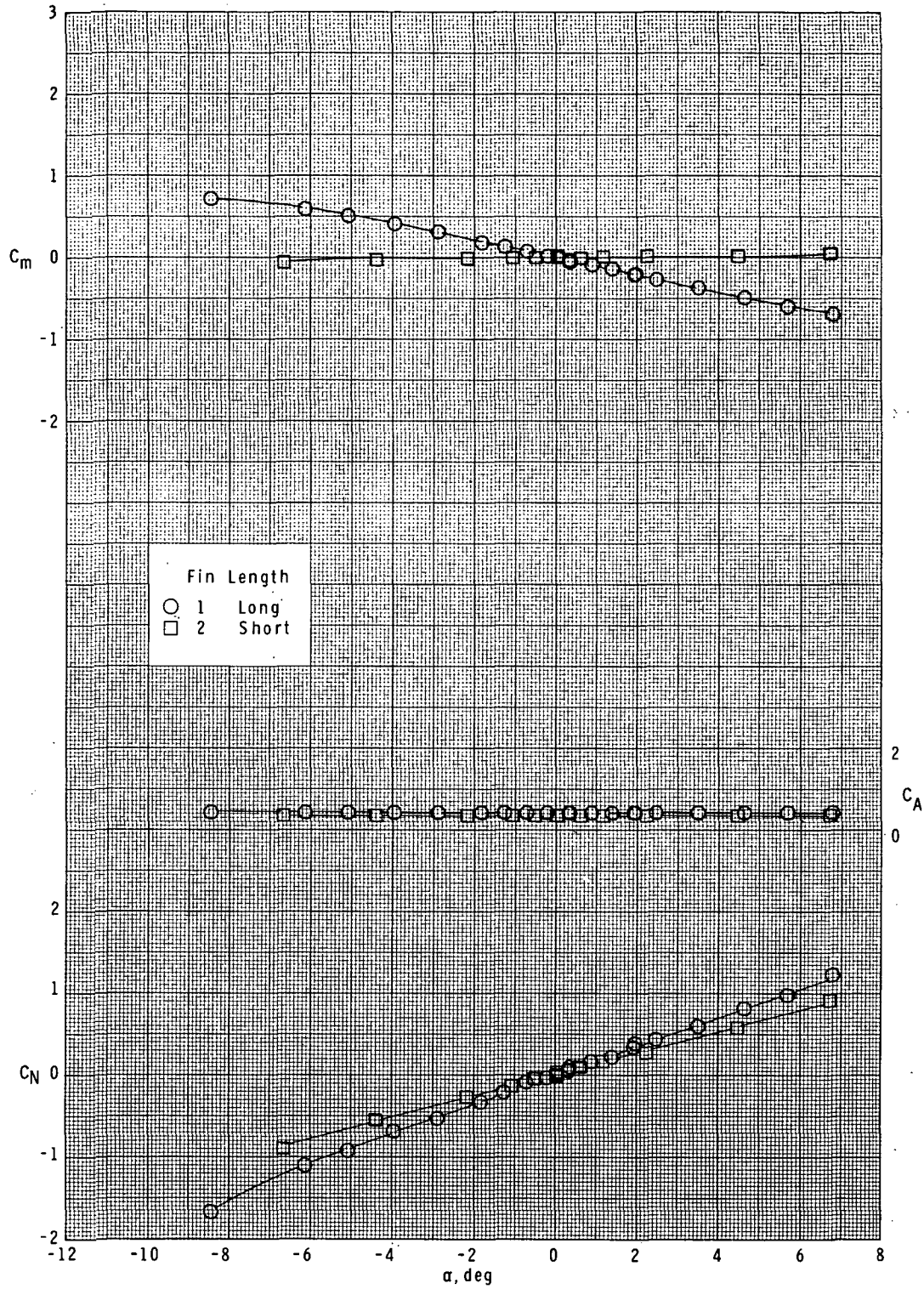

(c) M = 2.36.

Figure 6.- Continued.

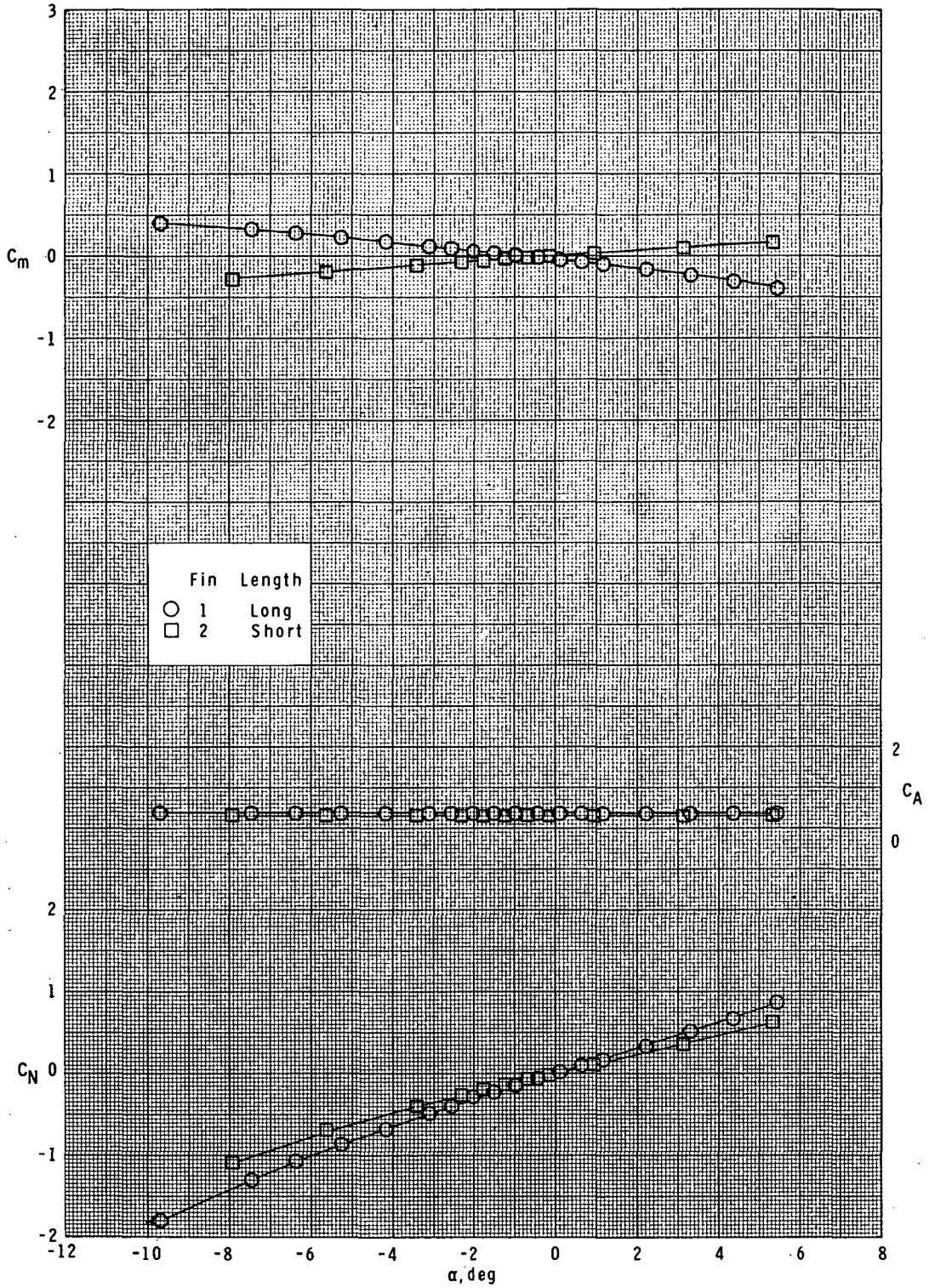

(d) M = 2.86.

Figure 6.- Concluded.

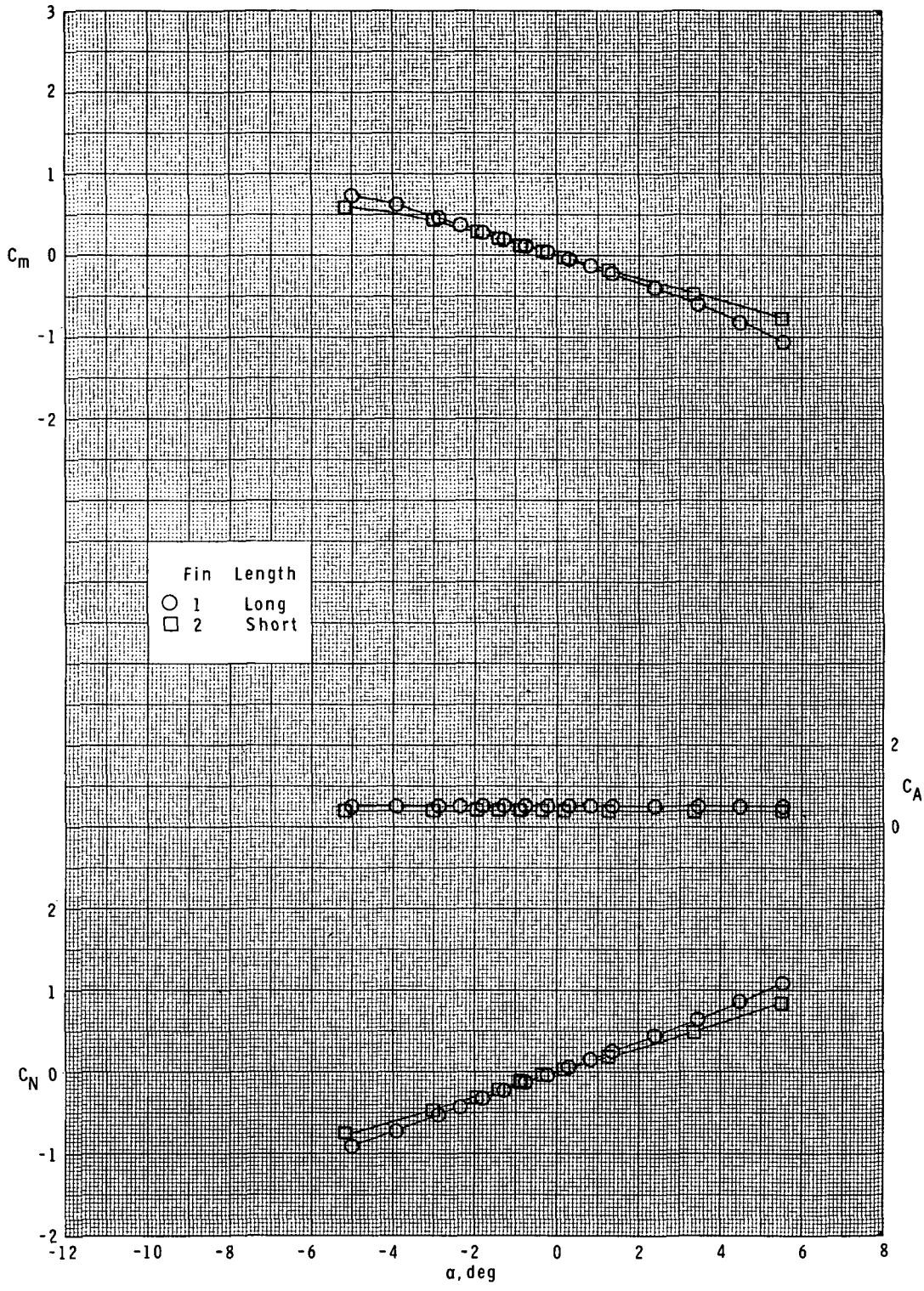

(a) M = 1.60.

Figure 7.- Effect of fin length on longitudinal characteristics. Basic body (B_1); unswept curved fins (F_1 and F_2); $\phi = 45^\circ$.

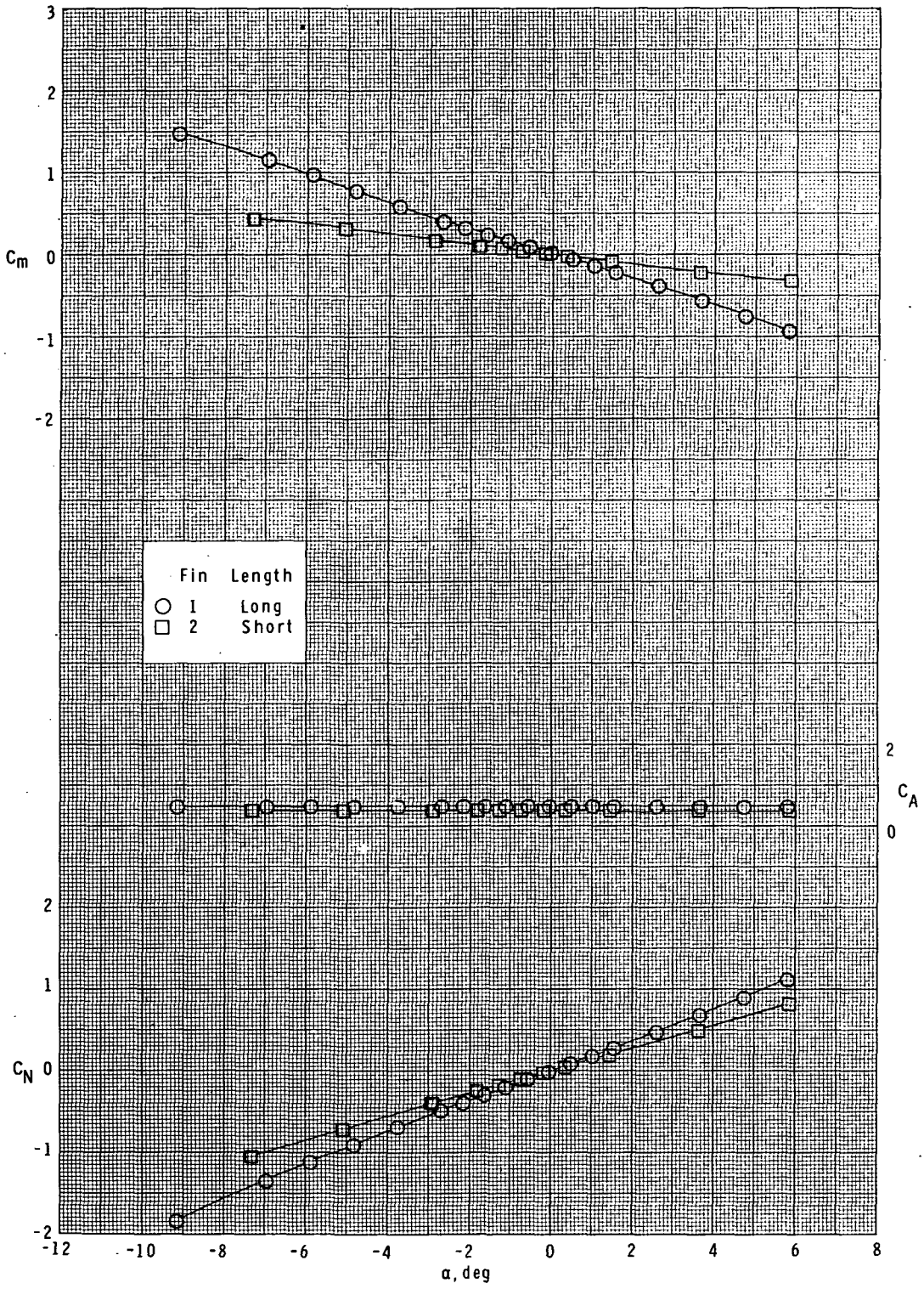

(b) M = 1.90.

Figure 7.- Continued.

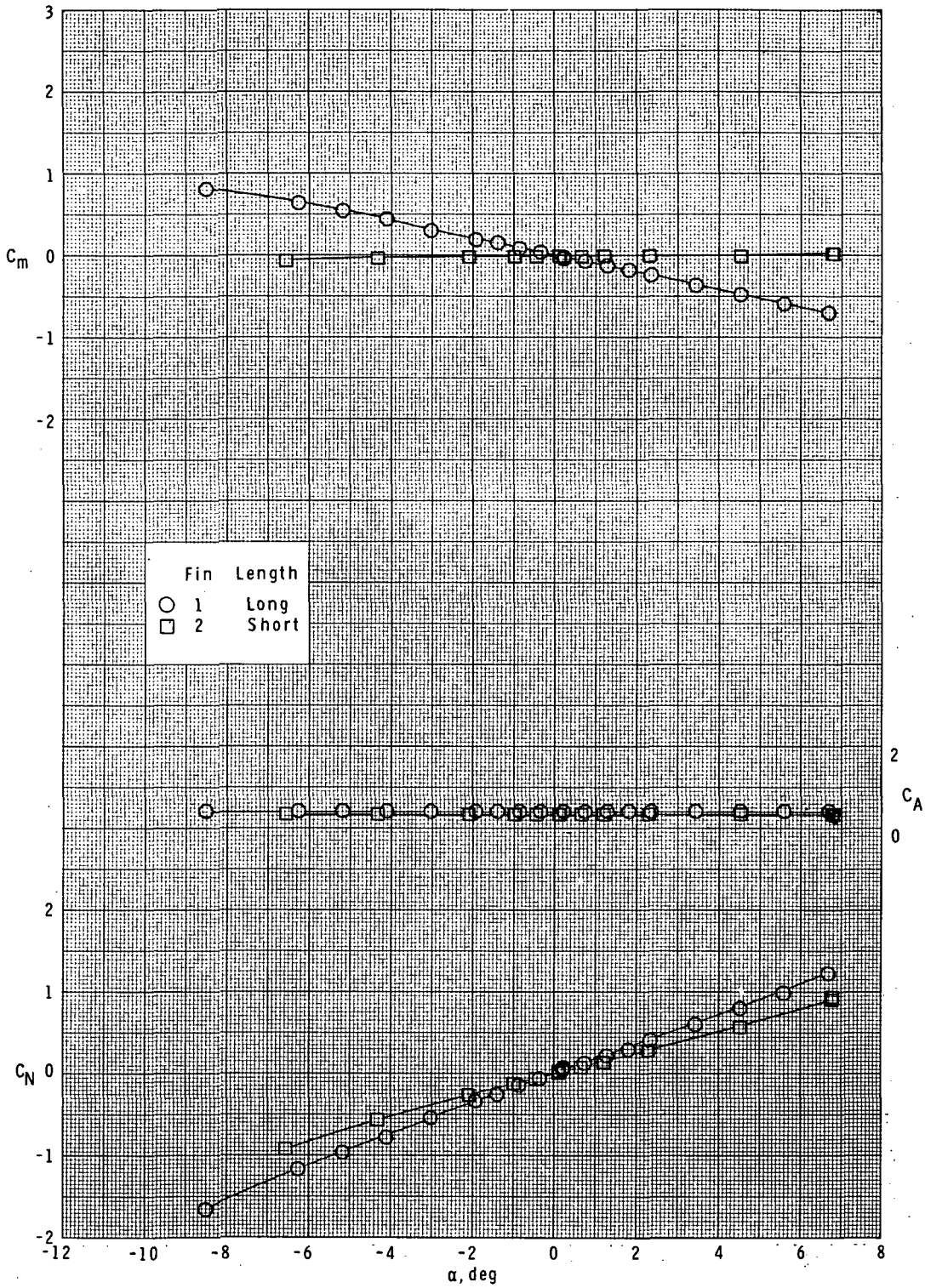

(c) M = 2.36.

Figure 7.- Continued.

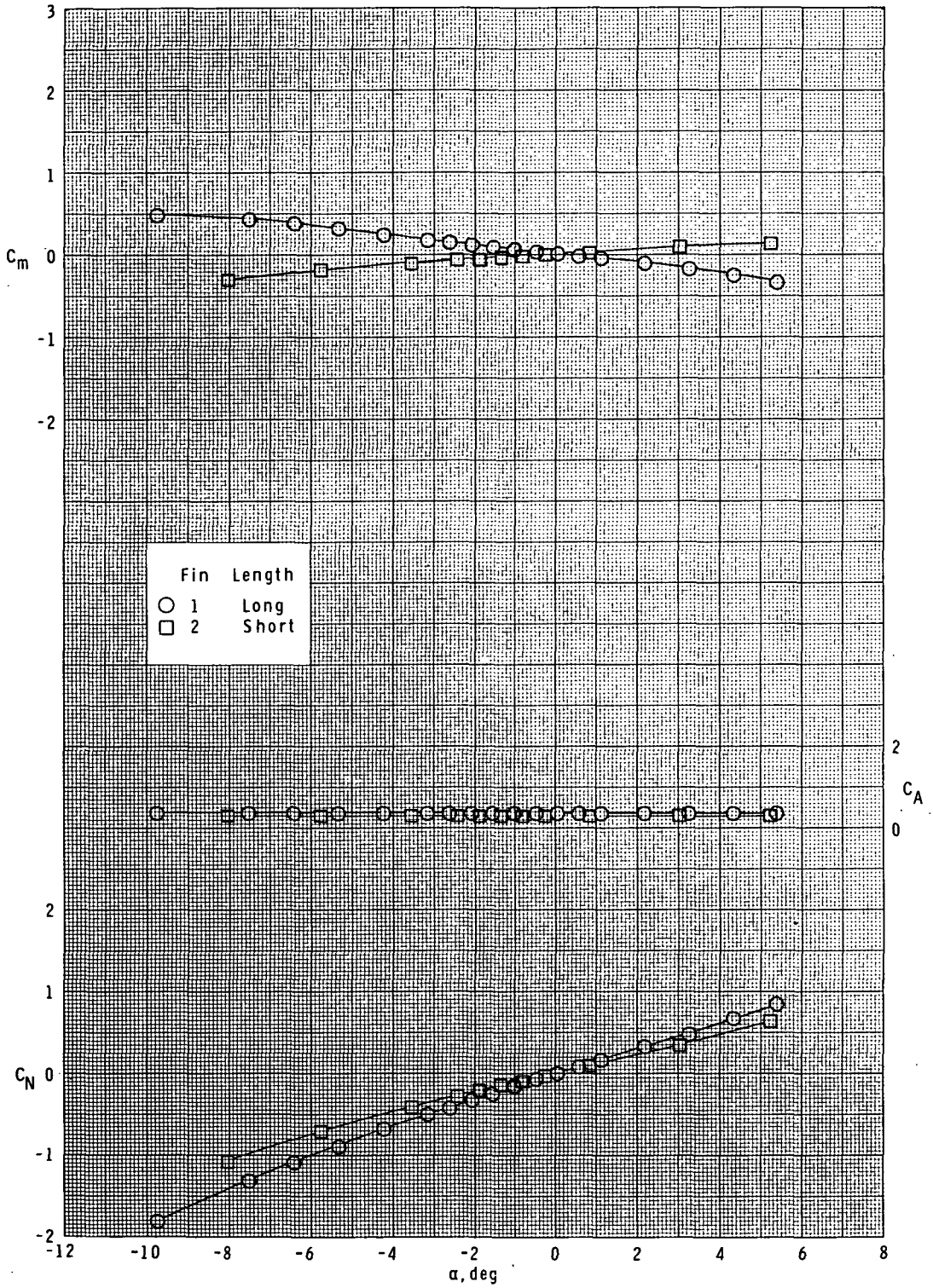

(d) M = 2.86.

Figure 7.- Concluded.

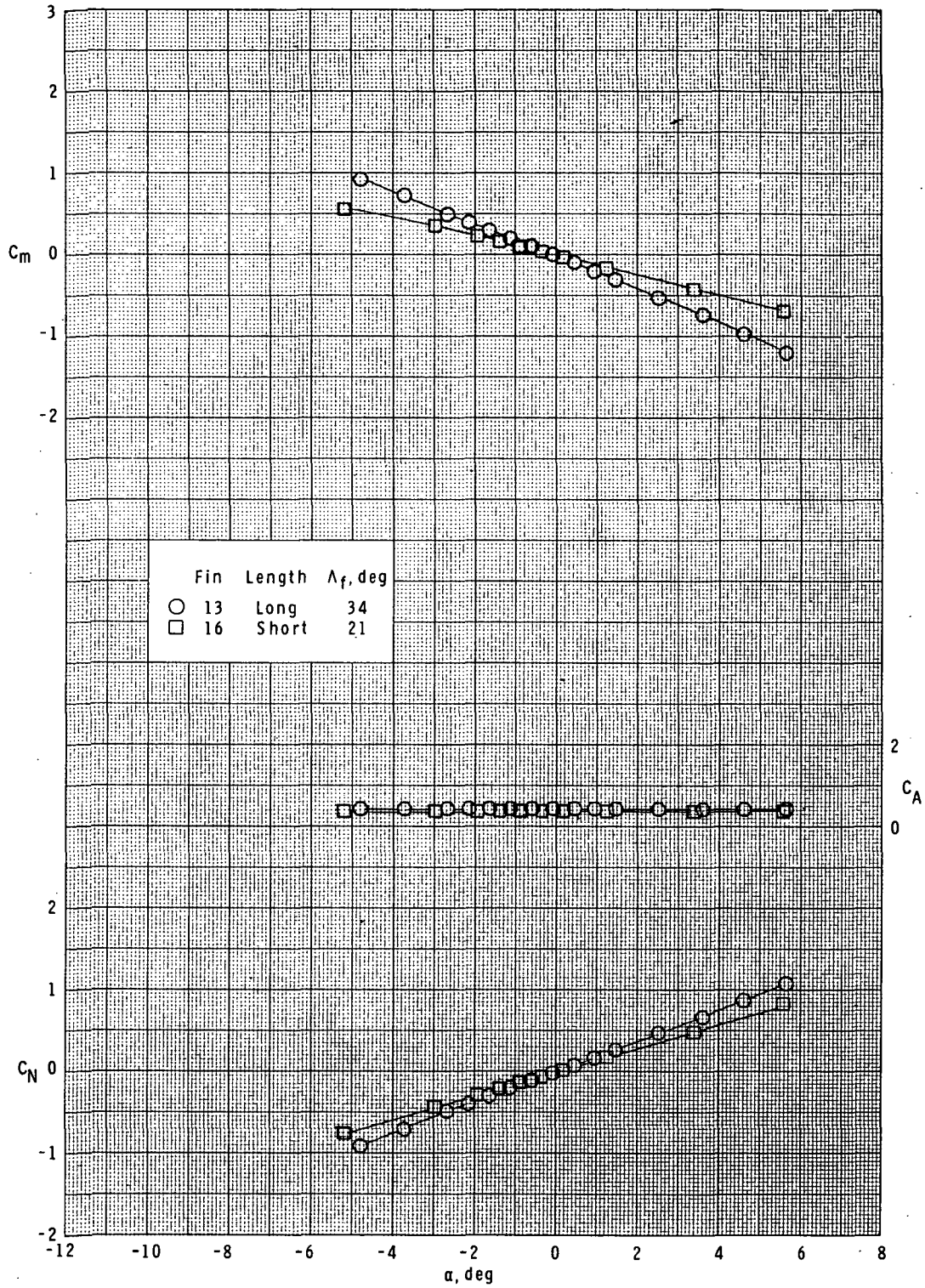

(a) M = 1.60.

Figure 8.- Effect of fin length on longitudinal characteristics. Basic body (B_1); swept curved fins (F_{13} and F_{16}); $\phi = 0^o$.

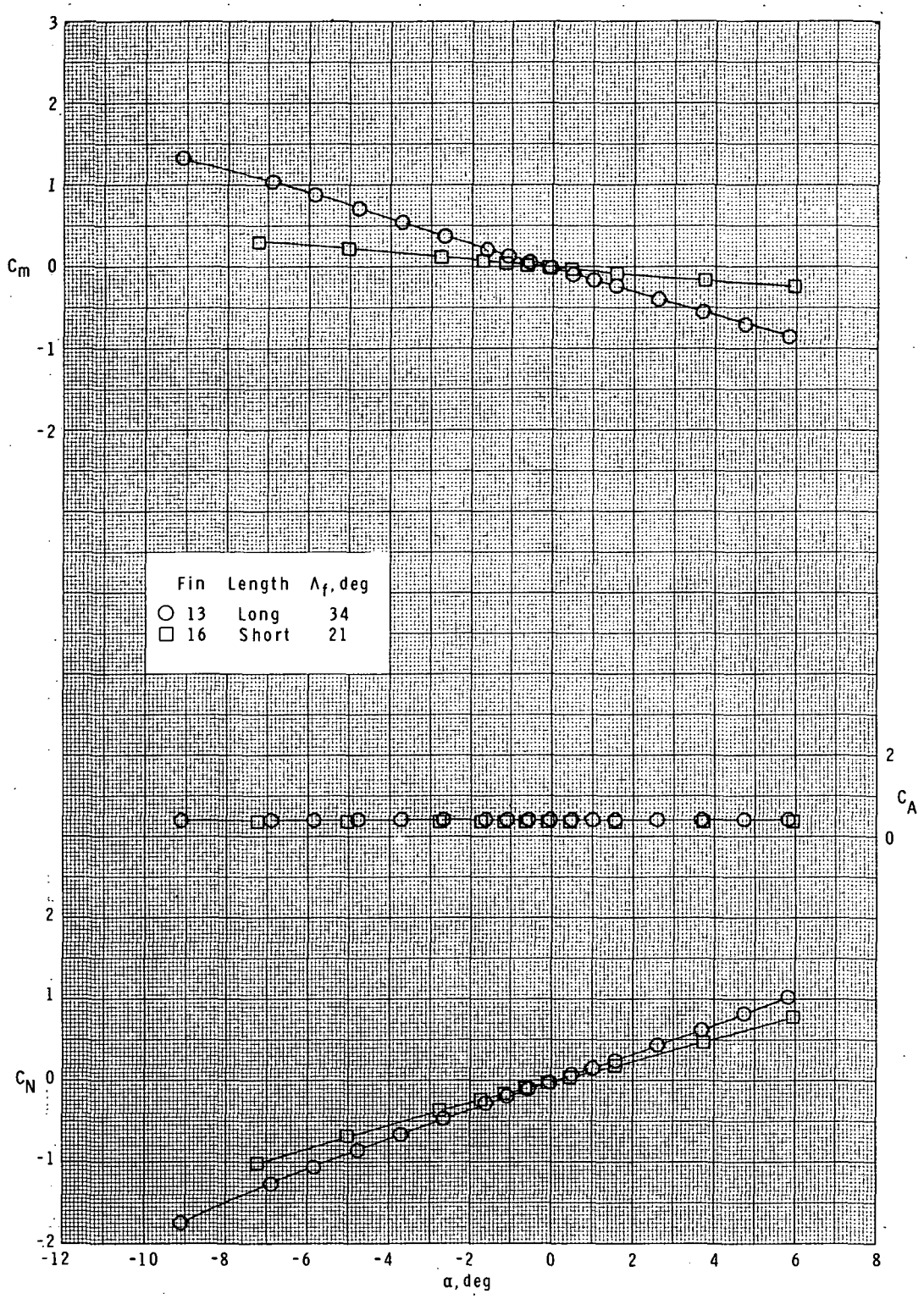

(b) M = 1.90.

Figure 8.- Continued.

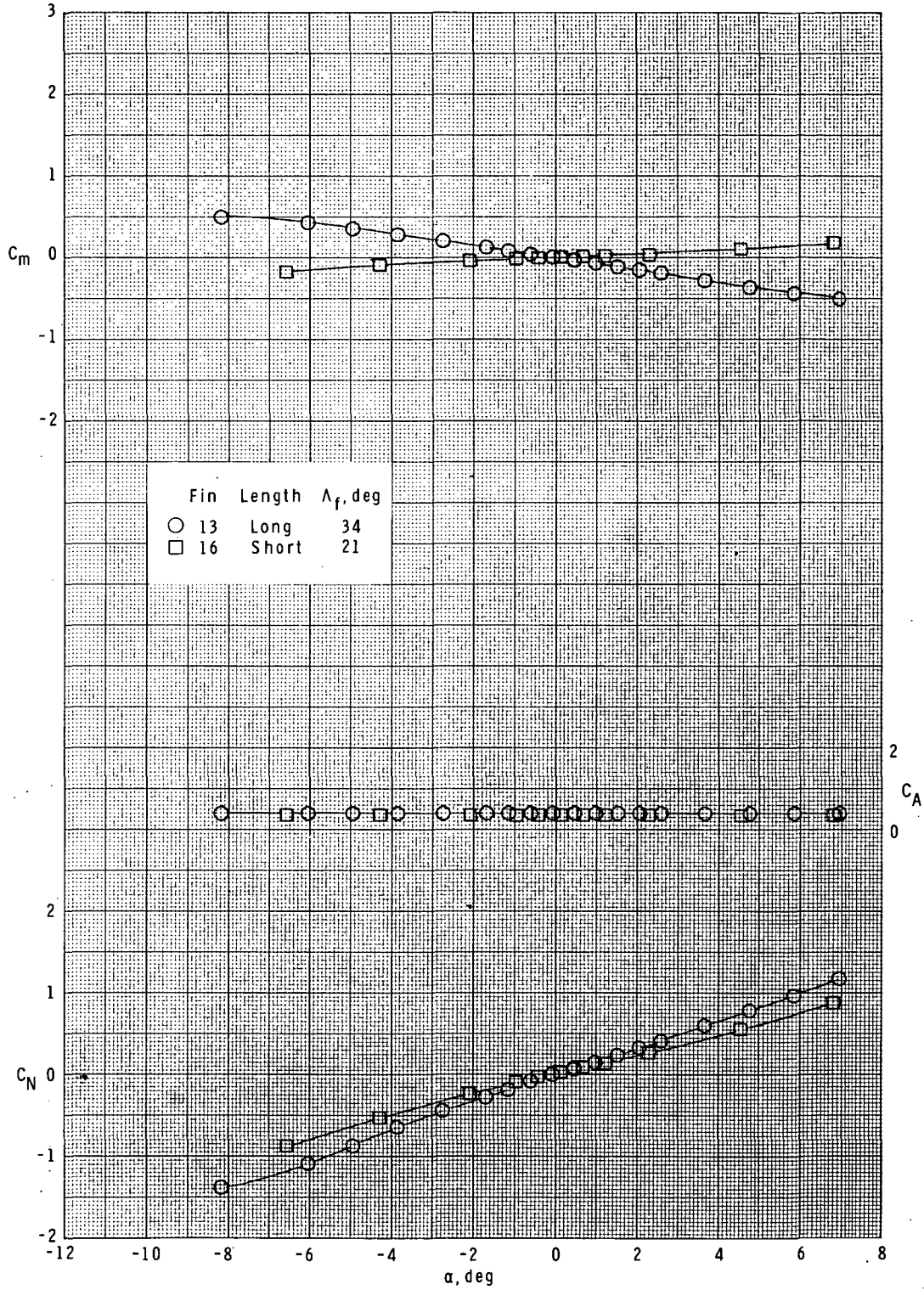

(c) M = 2.36.

Figure 8.- Continued.

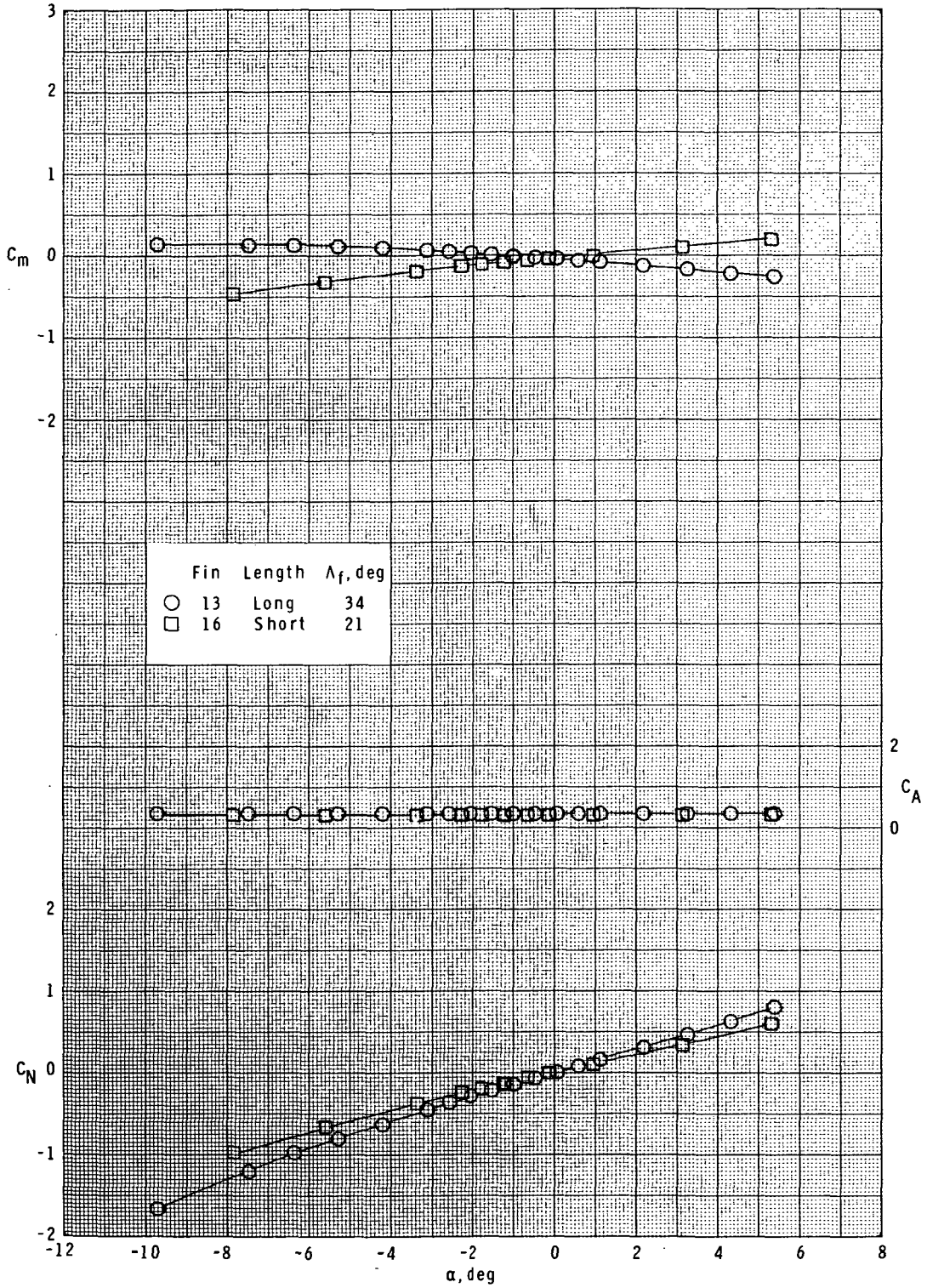

(d) M = 2.86.

Figure 8.- Concluded.

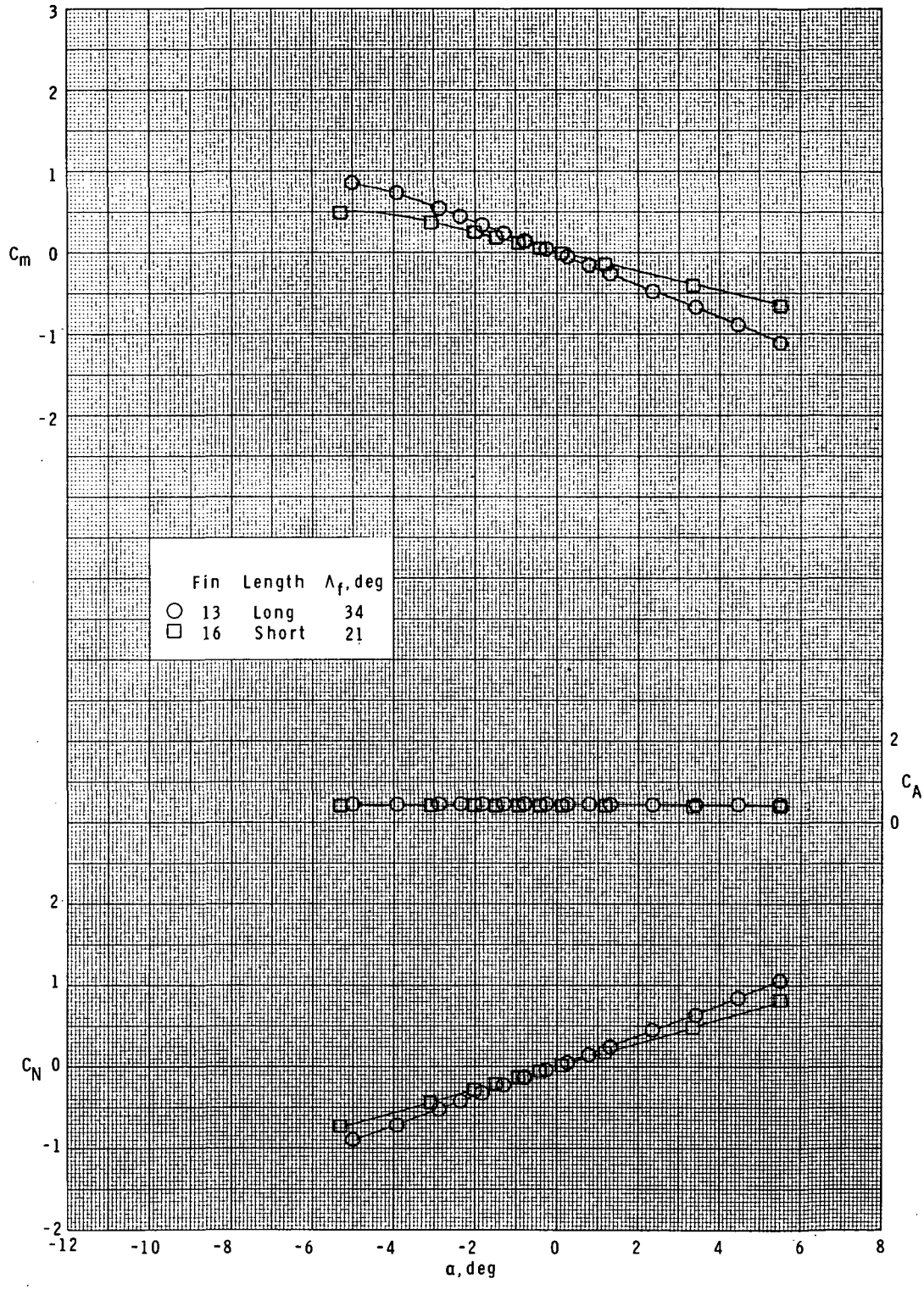

(a) M = 1.60.

Figure 9.- Effect of fin length on longitudinal characteristics. Basic body (B_1); swept curved fins (F_{13} and F_{16}); $\phi = 45^\circ$.

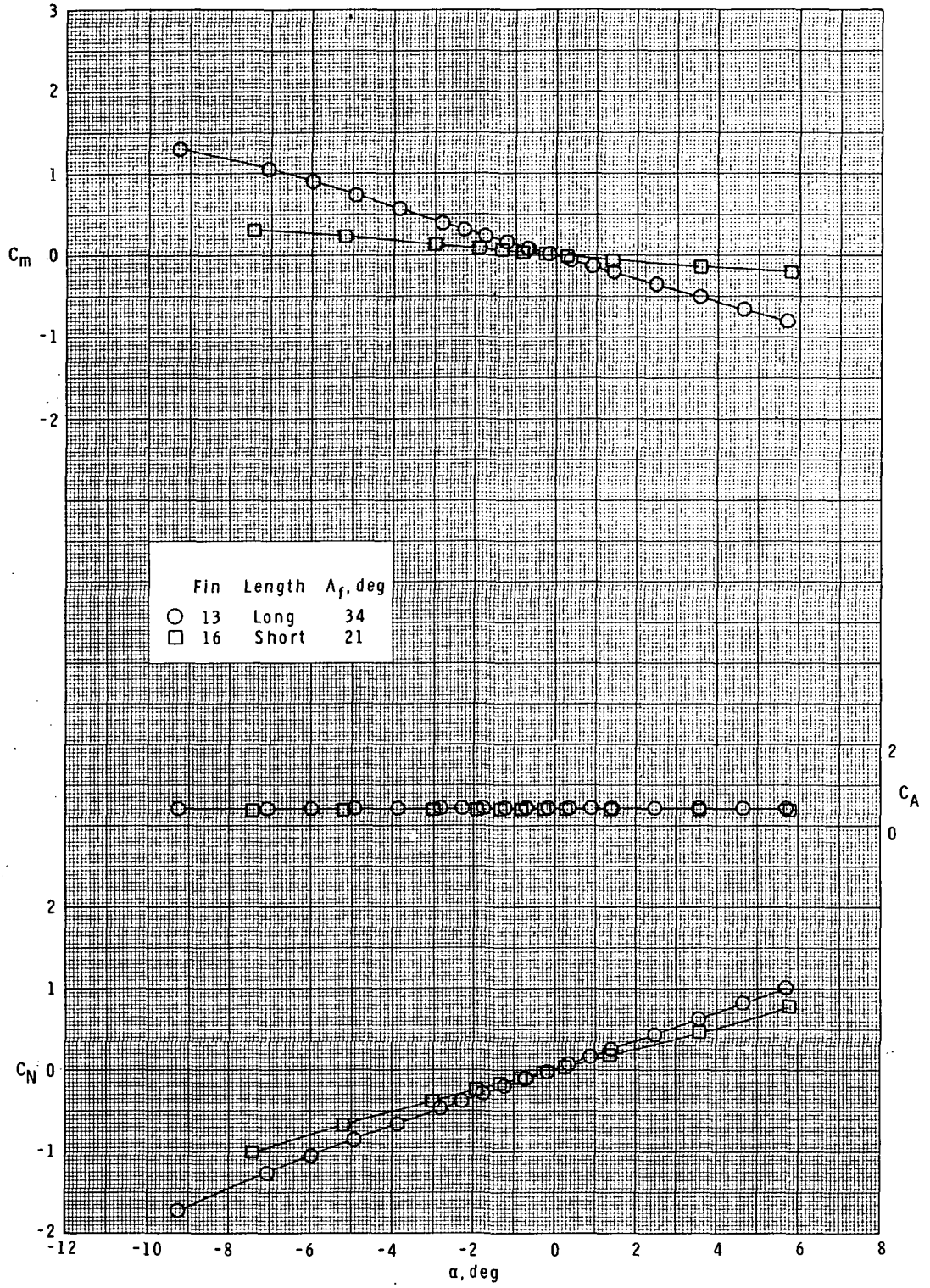

(b) M = 1.90.

Figure 9.- Continued.

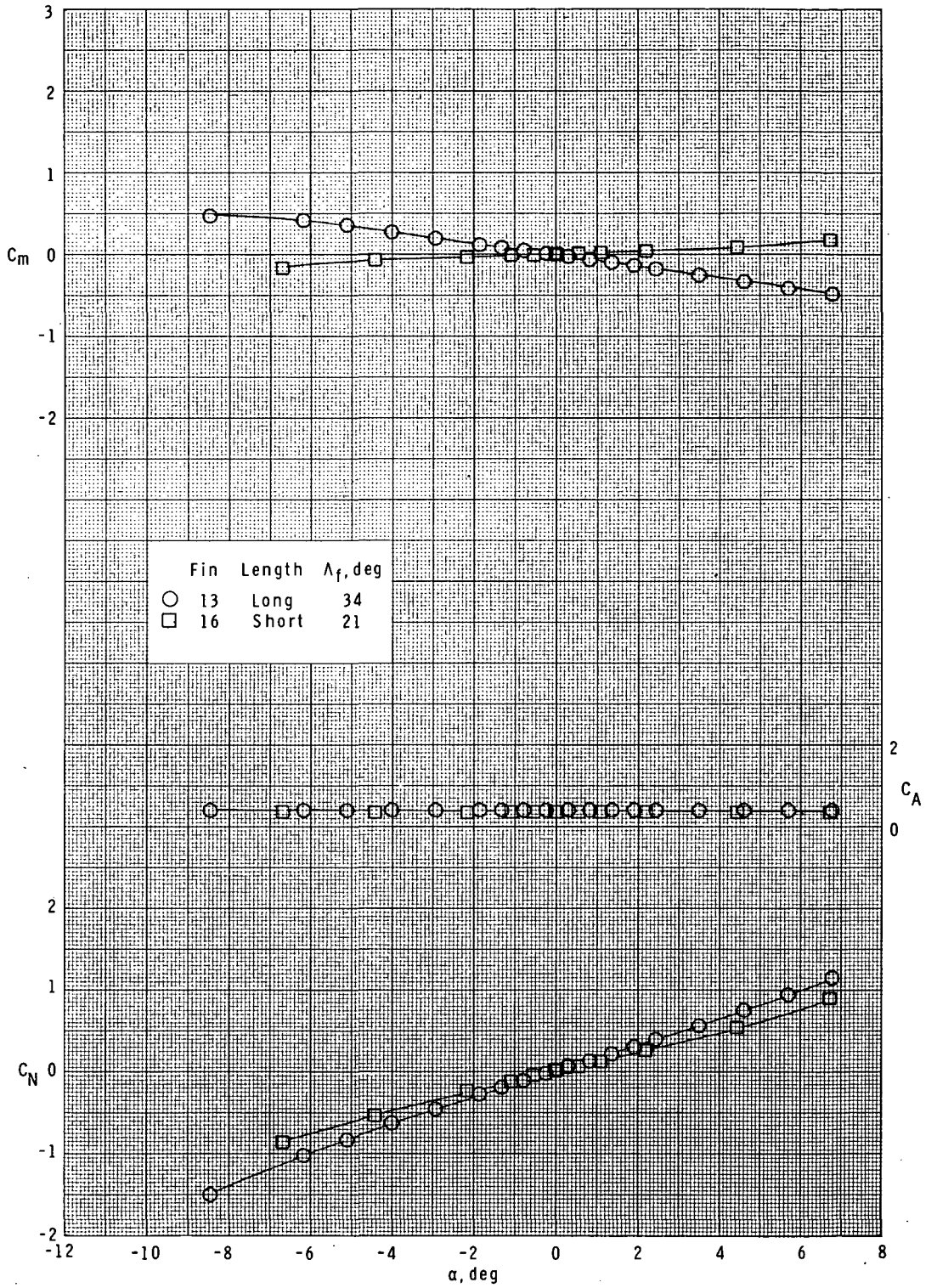

(c) M = 2.36.

Figure 9.- Continued.

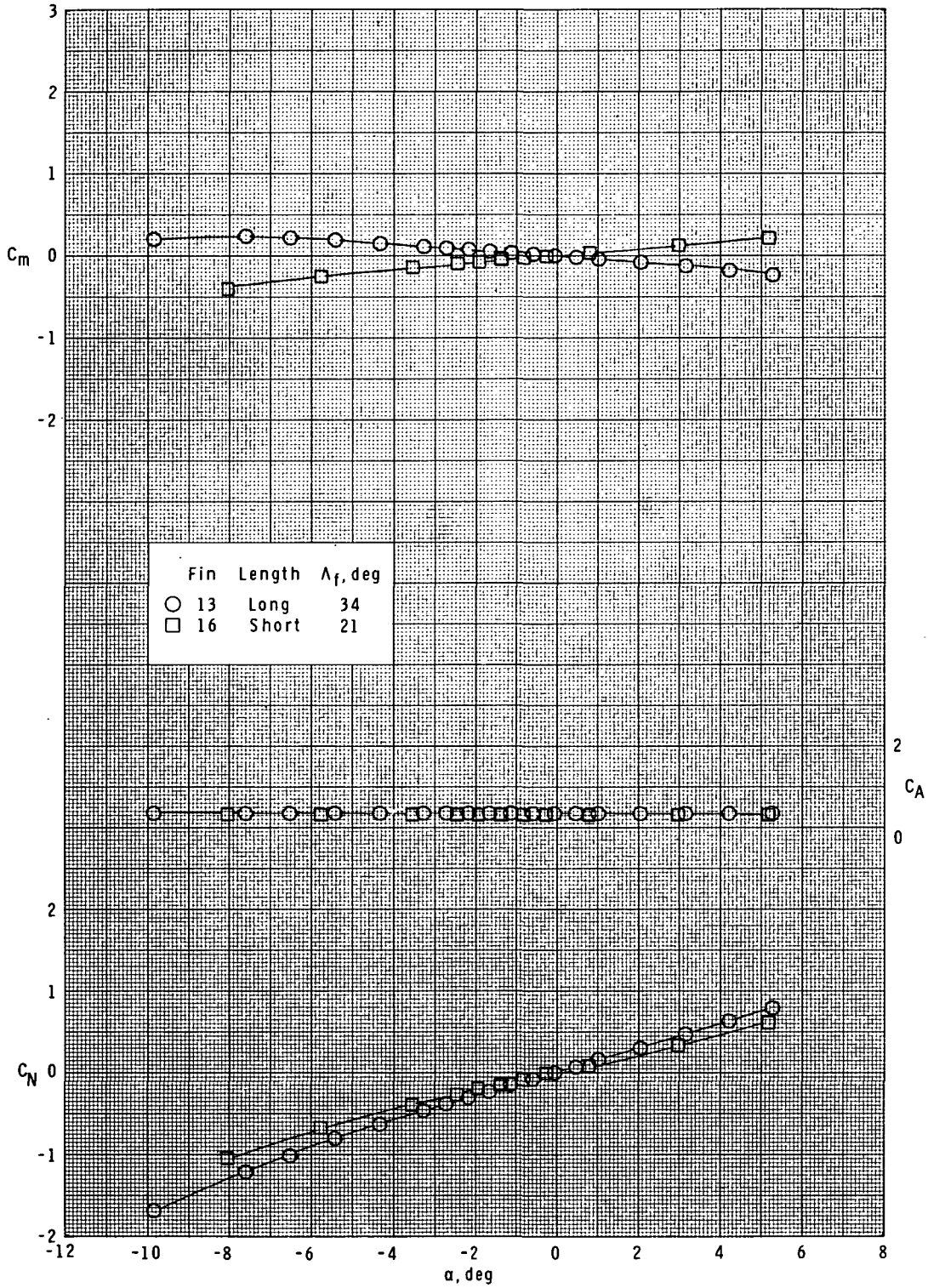

(d) M = 2.86.

Figure 9.- Concluded.

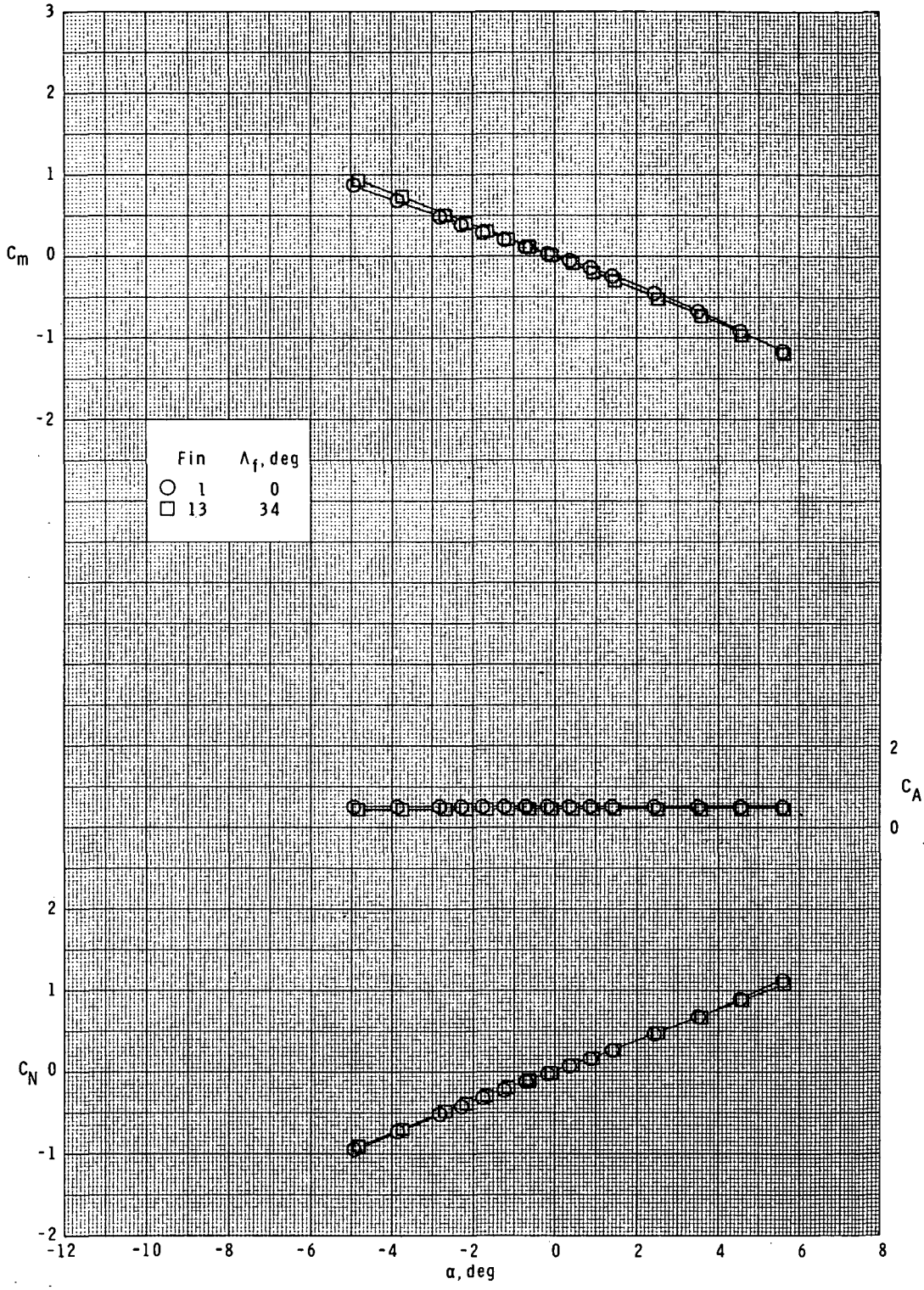

(a) M = 1.60.

Figure 10.- Effect of fin leading-edge sweep on longitudinal characteristics. Basic body (B_1); long-chord curved fins (F_1 and F_{13}); $\phi = 0^\circ$.

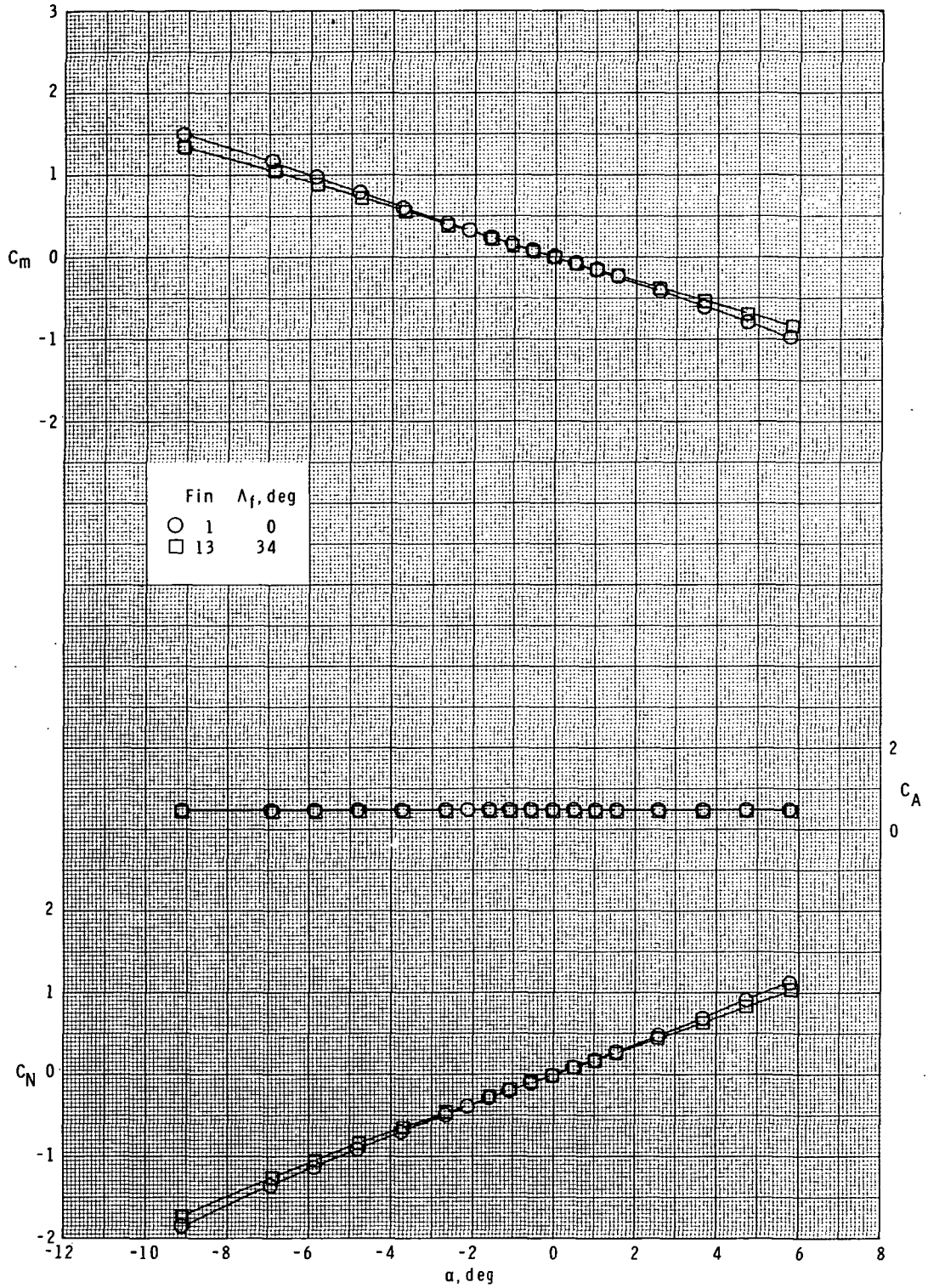

(b) M = 1.90.

Figure 10.- Continued.

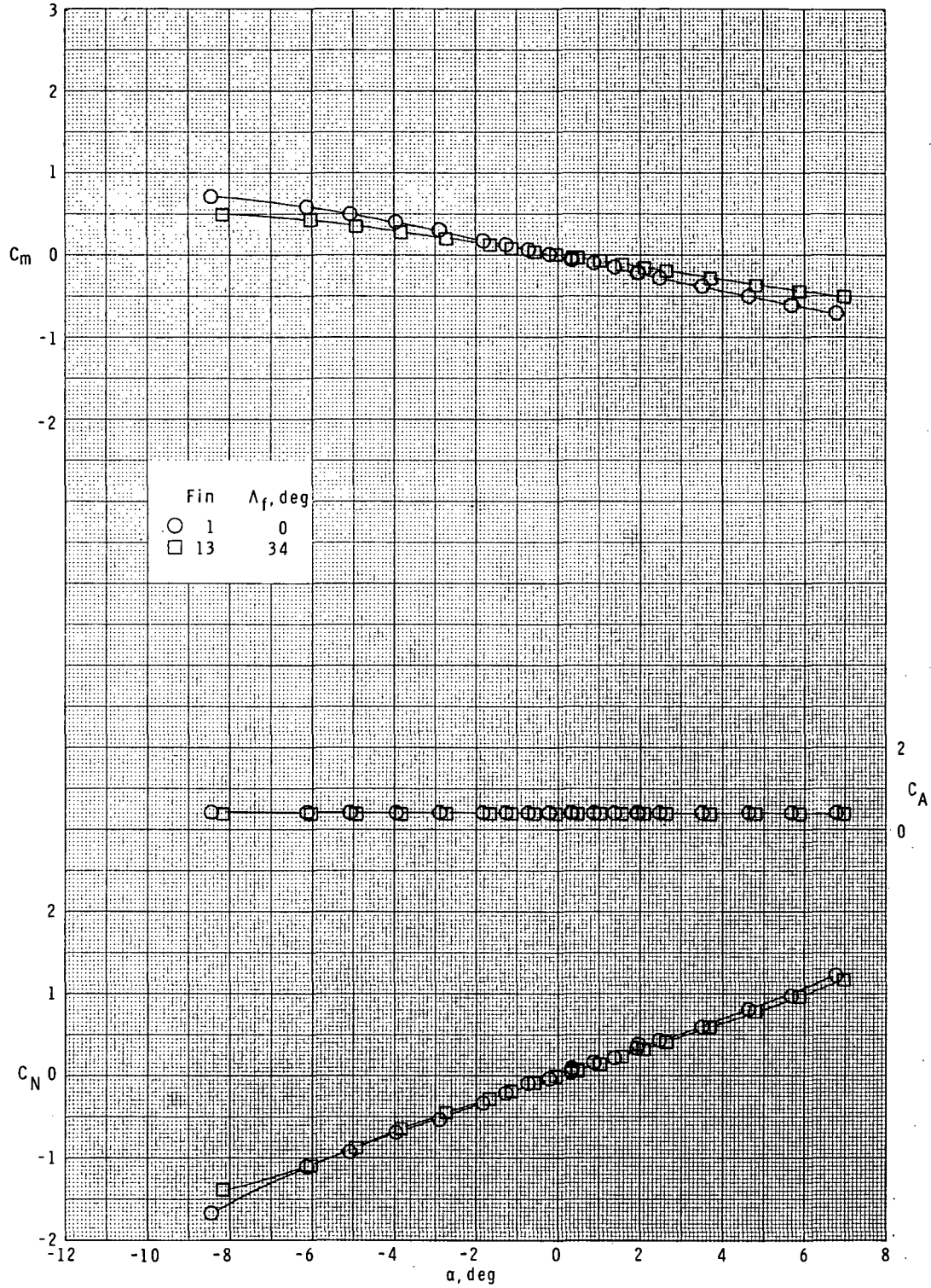

(c) M = 2.36.

Figure 10.- Continued.

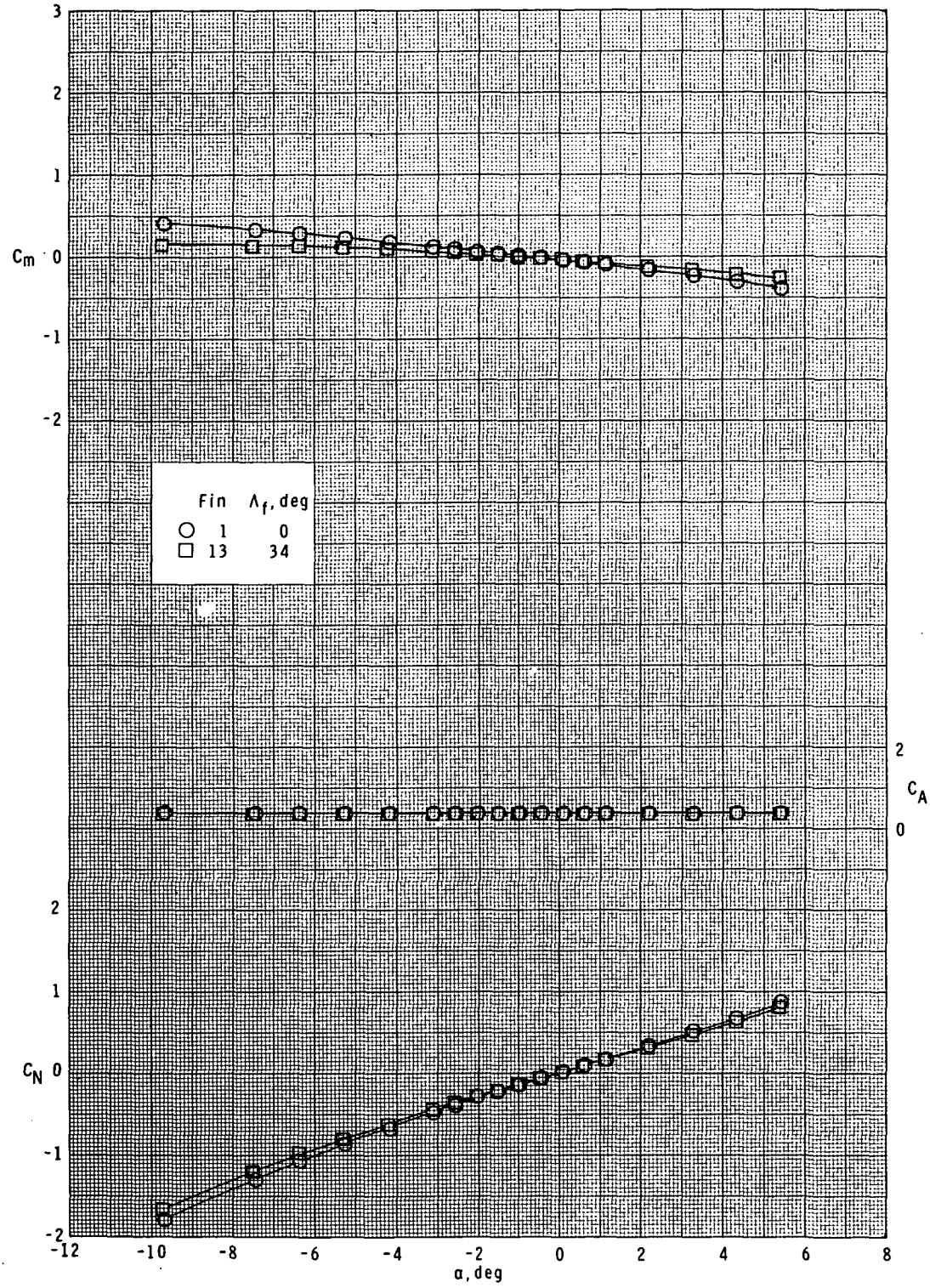

(d) M = 2.86.

Figure 10.- Concluded.

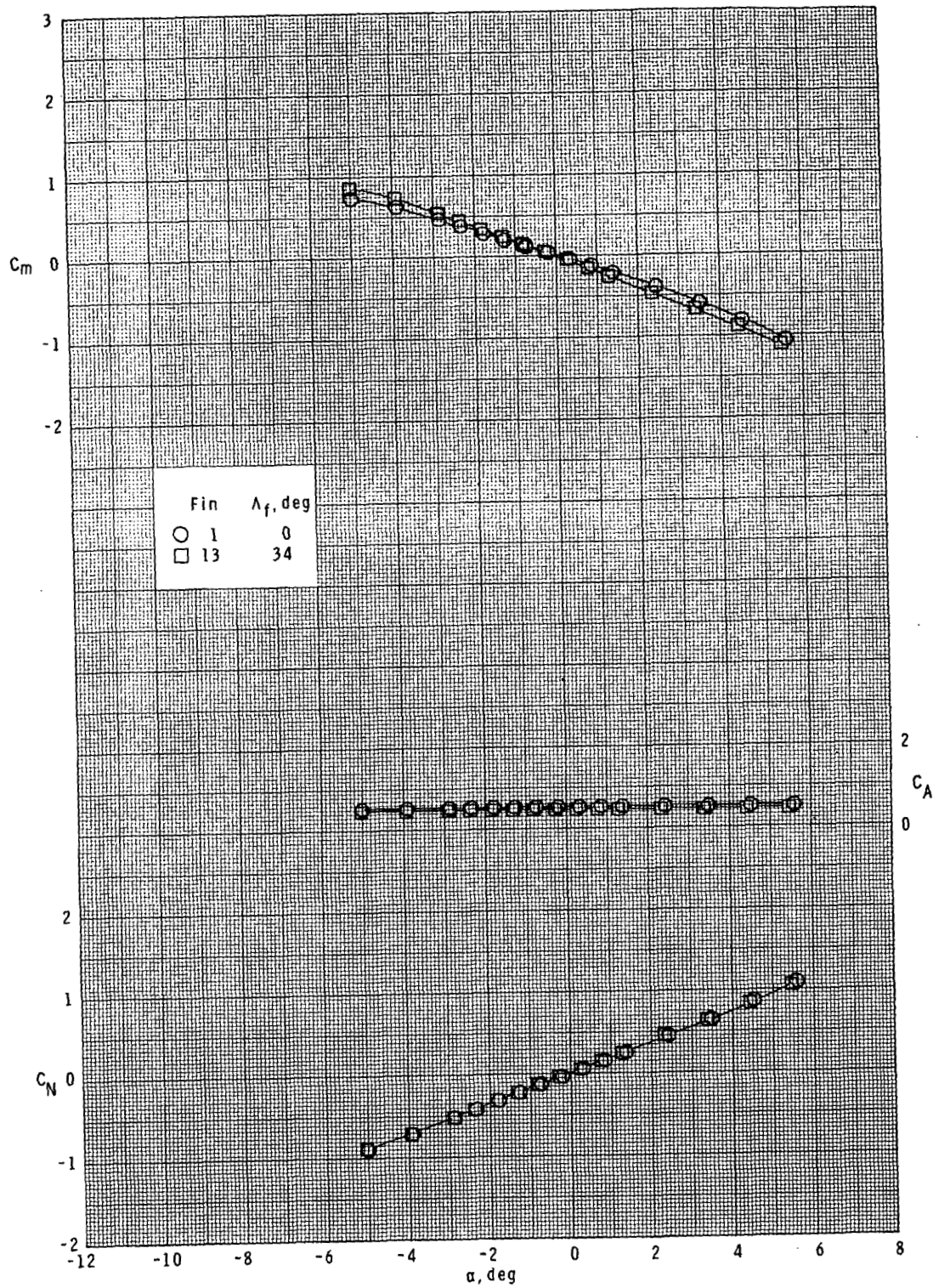

(a) M = 1.60.

Figure 11.- Effect of fin leading-edge sweep on longitudinal characteristics. Basic body (B_1); long-chord curved fins (F_1 and F_{13}); $\phi = 45^o$.

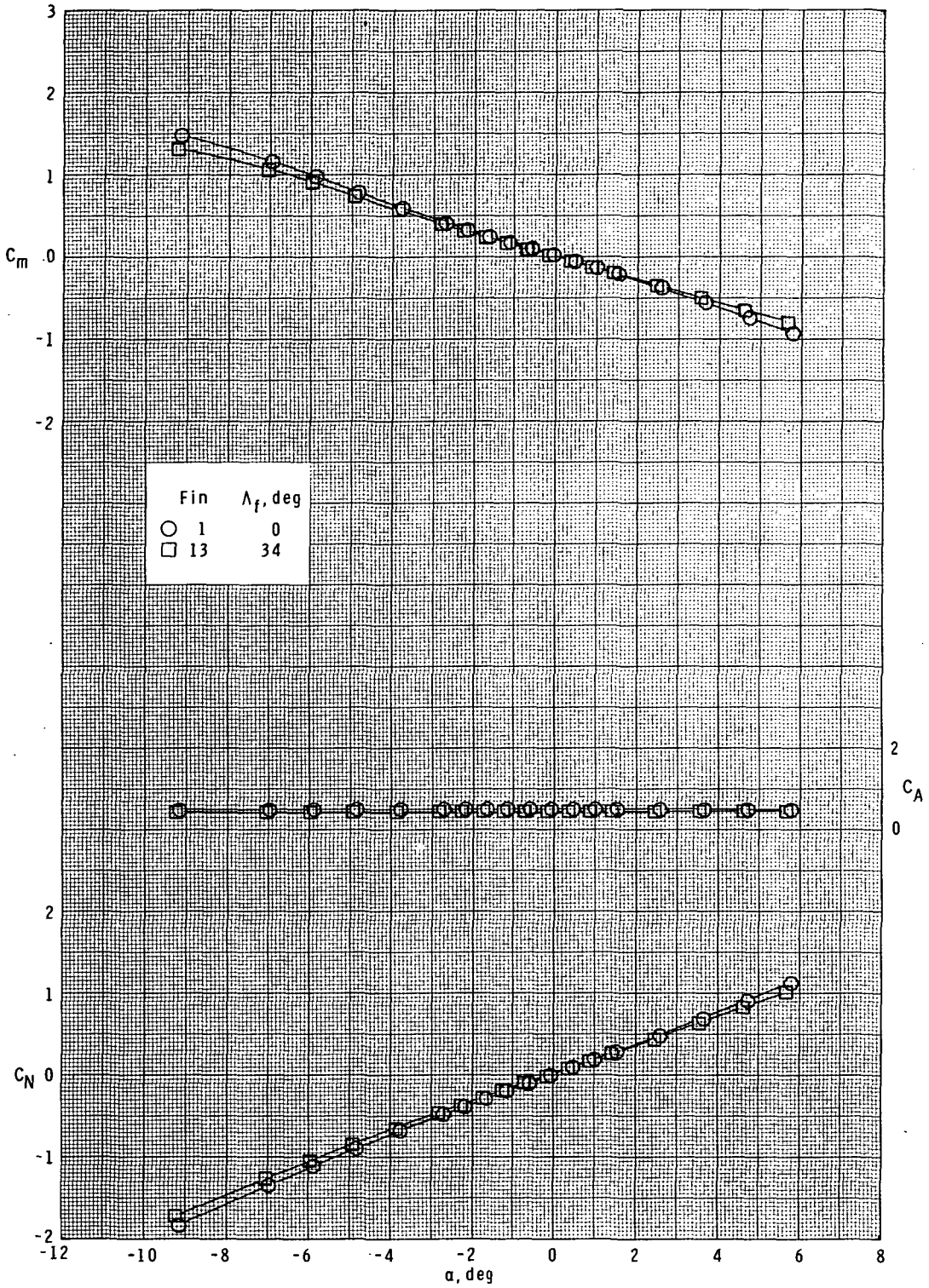

(b) M = 1.90.

Figure 11.- Continued.

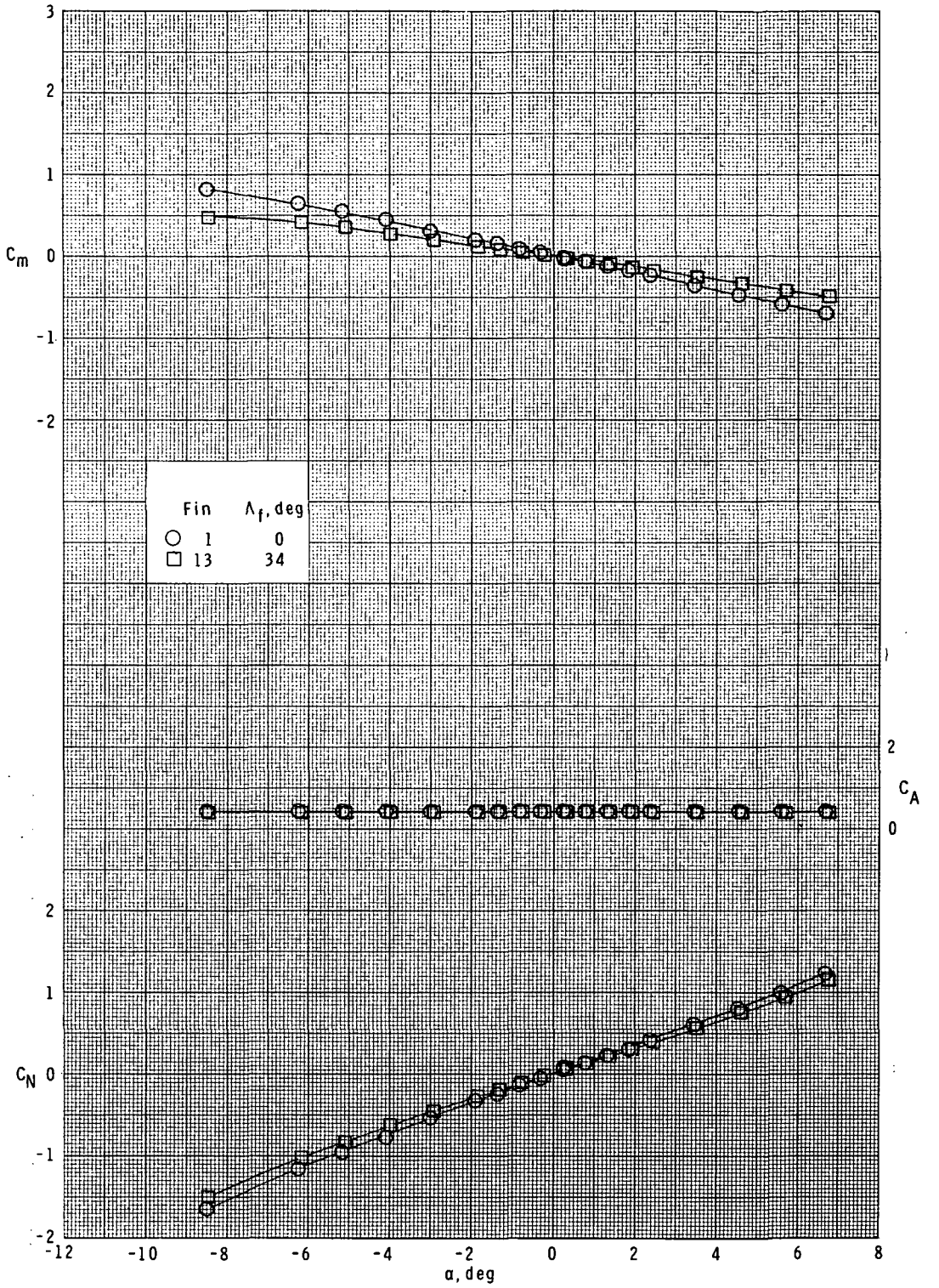

(c) M = 2.36.

Figure 11.- Continued.

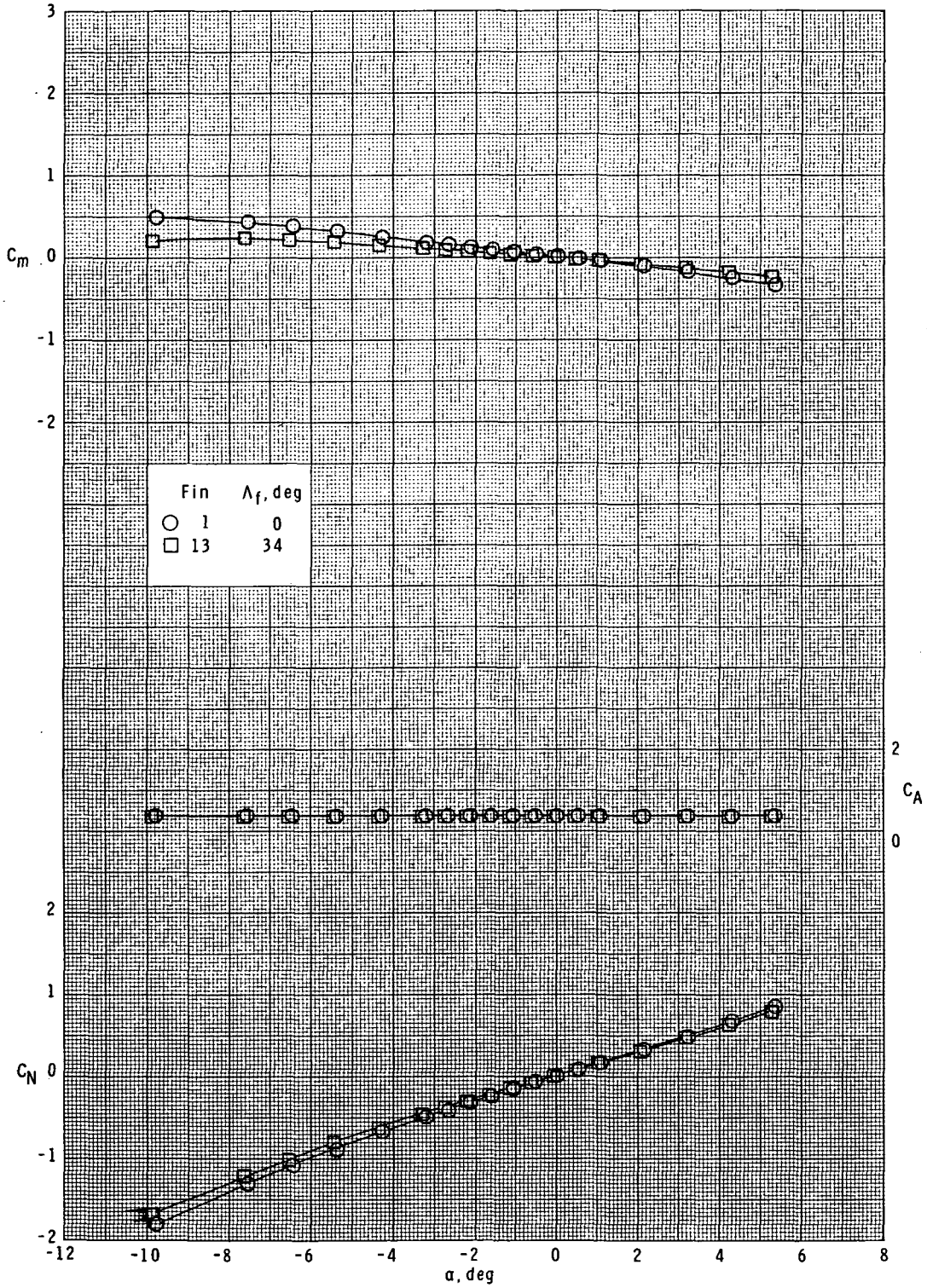

(d) M = 2.86.

Figure 11.- Concluded.

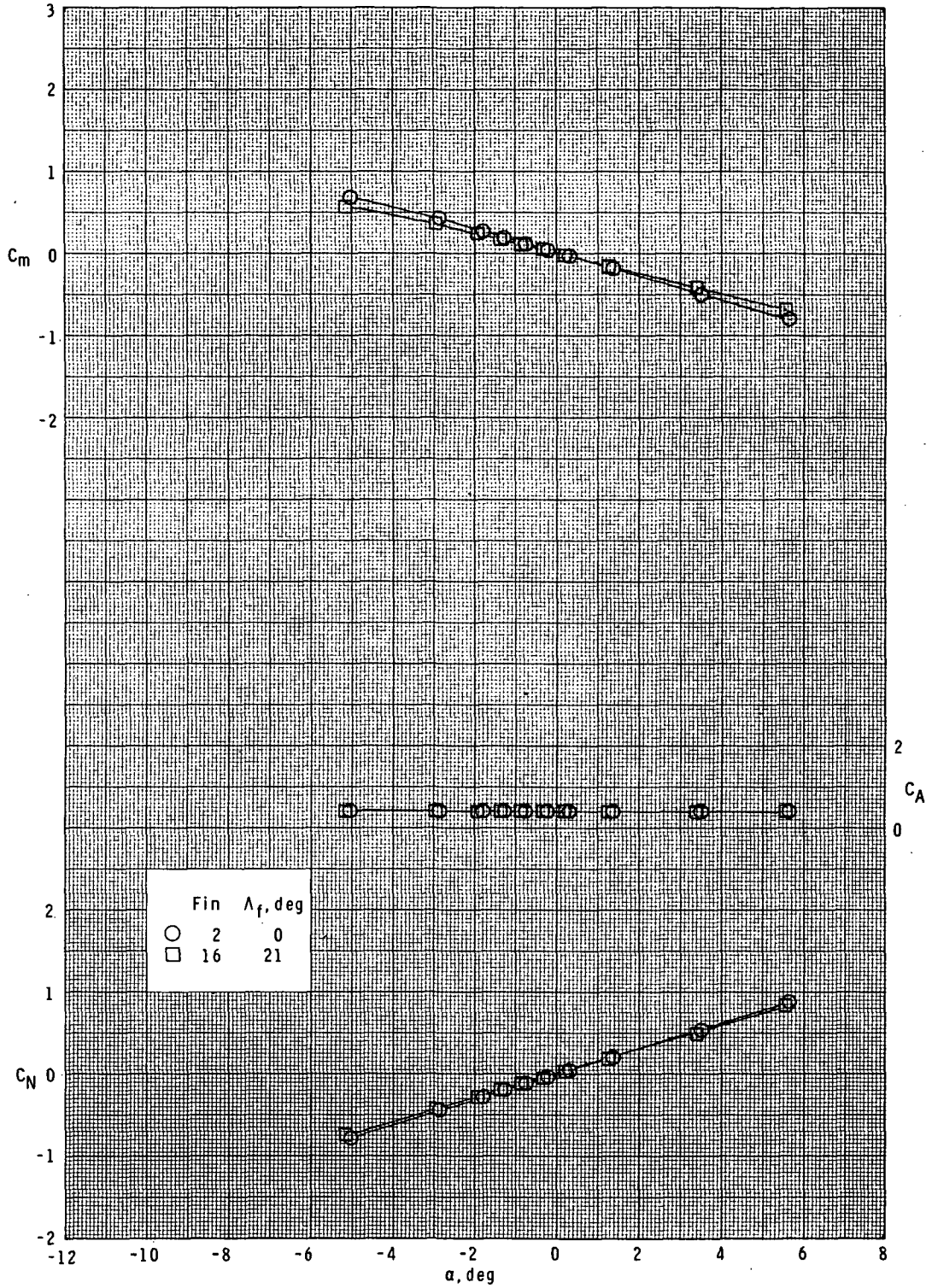

(a) M = 1.60.

Figure 12.- Effect of fin leading-edge sweep on longitudinal characteristics. Basic body (B_1); short-chord curved fins (F_2 and F_{16}); $\phi = 0^\circ$.

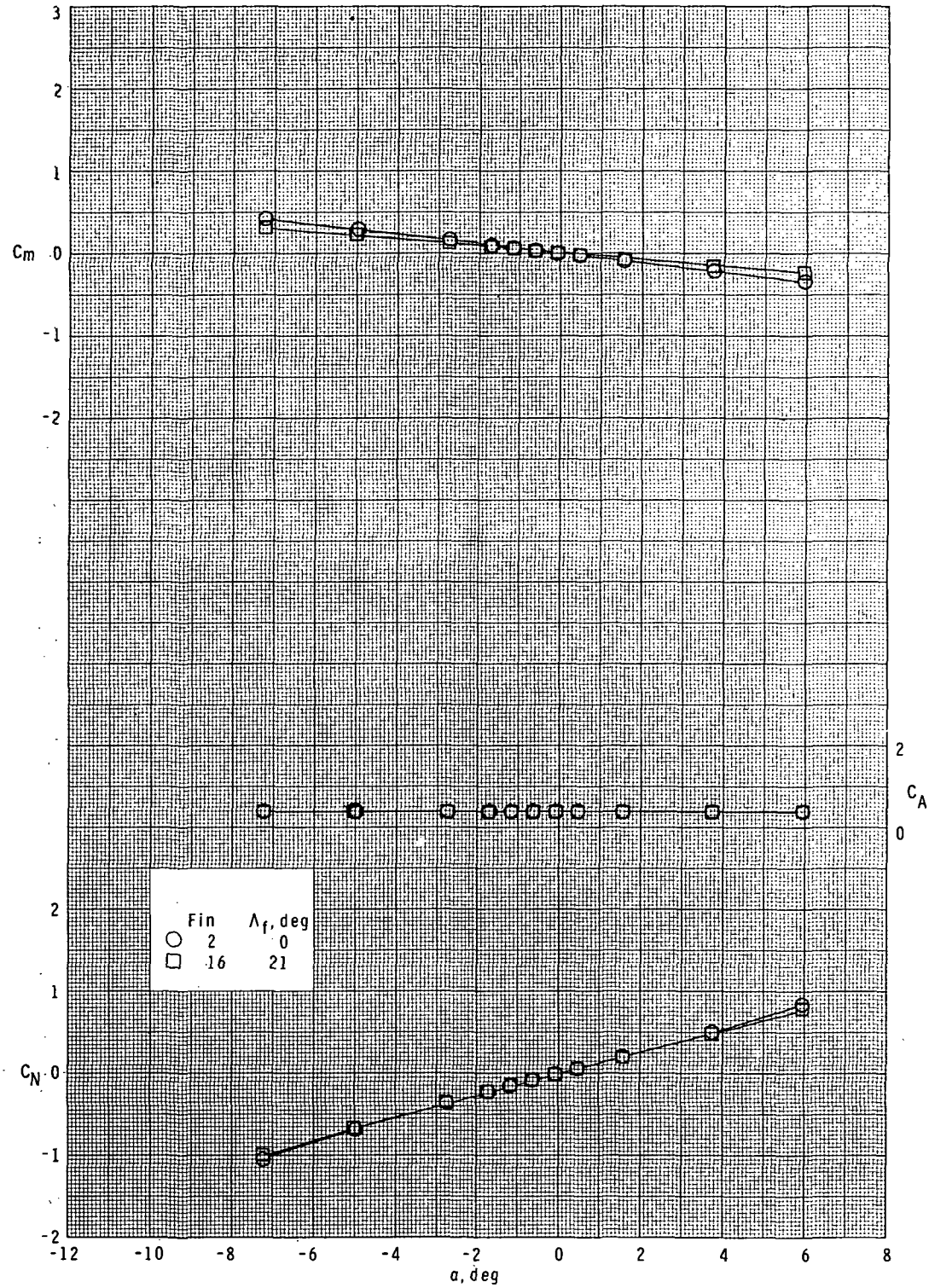

(b) M = 1.90.

Figure 12.- Continued.

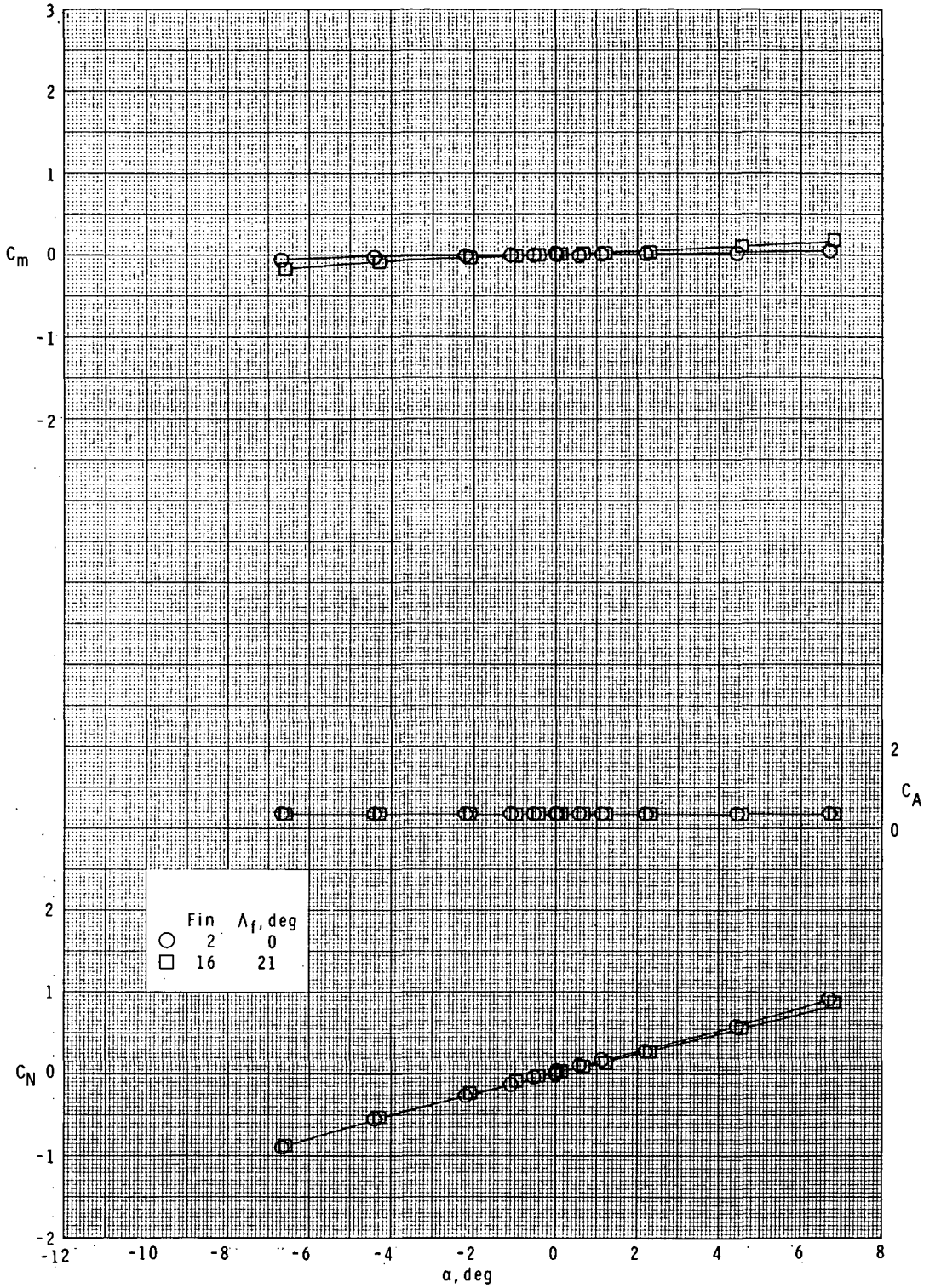

(c) M = 2.36.

Figure 12.- Continued.

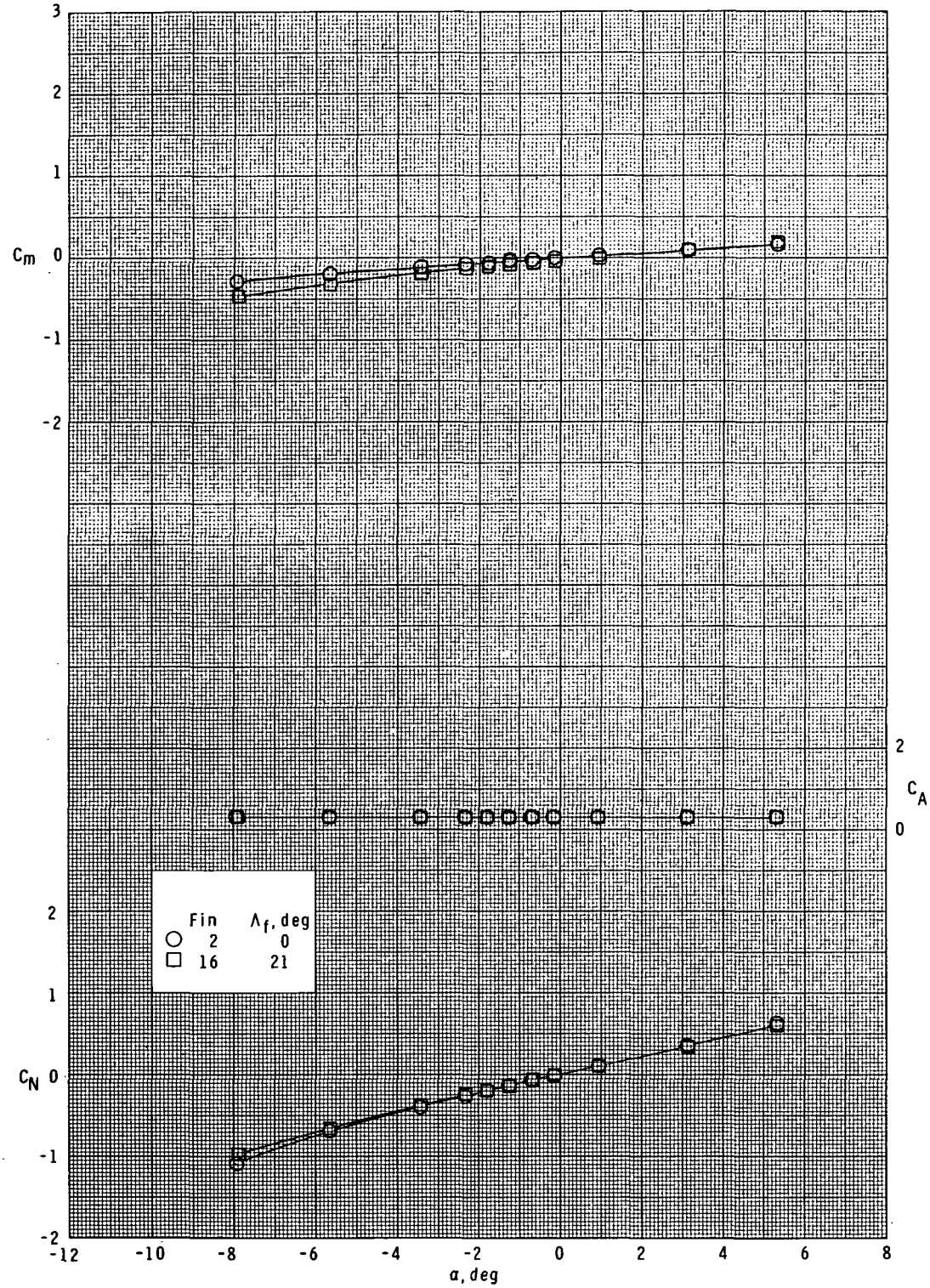

(d) M = 2.86.

Figure 12.- Concluded.

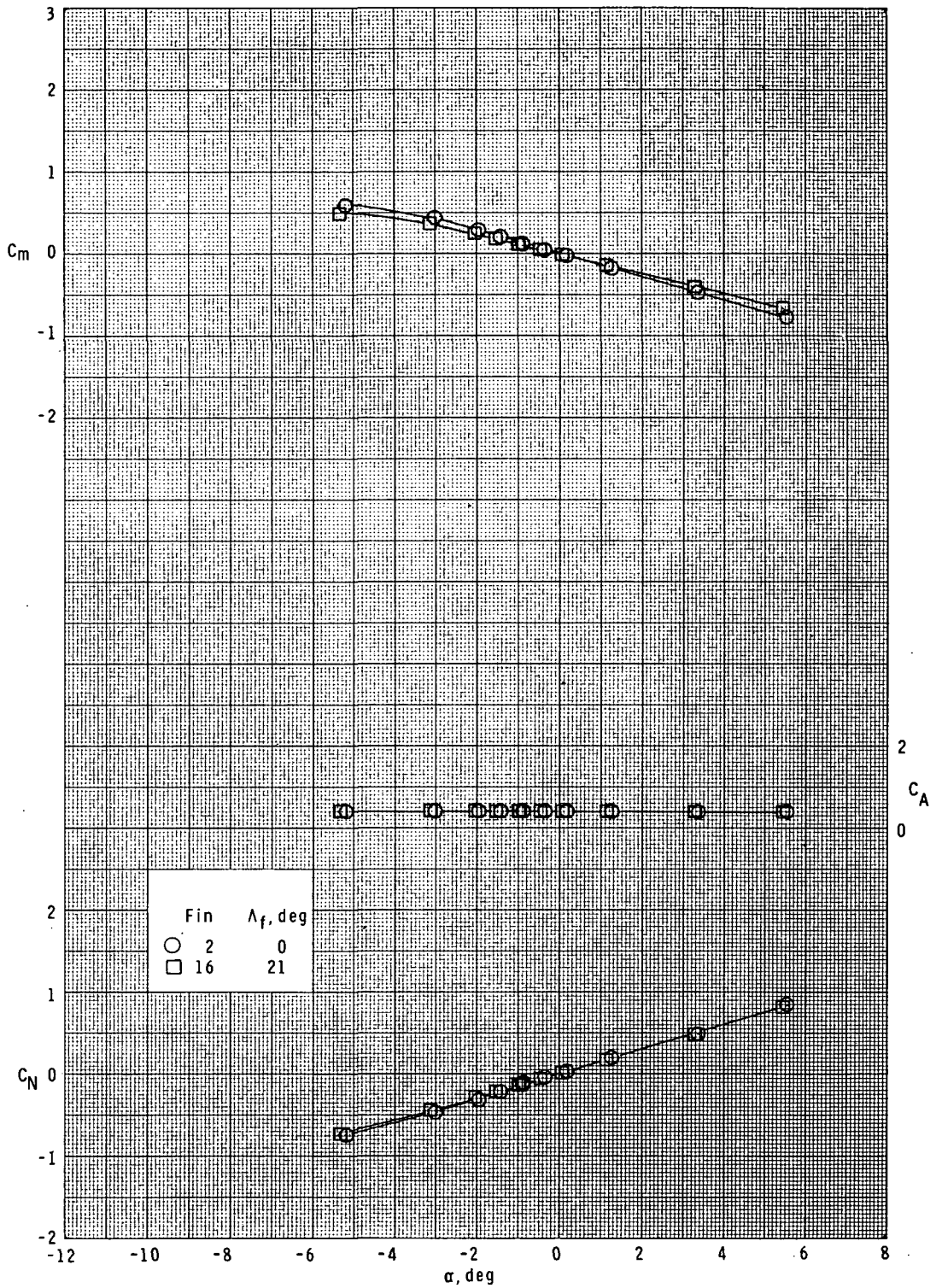

(a) M = 1.60.

Figure 13.- Effect of fin leading-edge sweep on longitudinal characteristics. Basic body (B_1); short-chord curved fins (F_2 and F_{16}); $\phi = 45^\circ$.

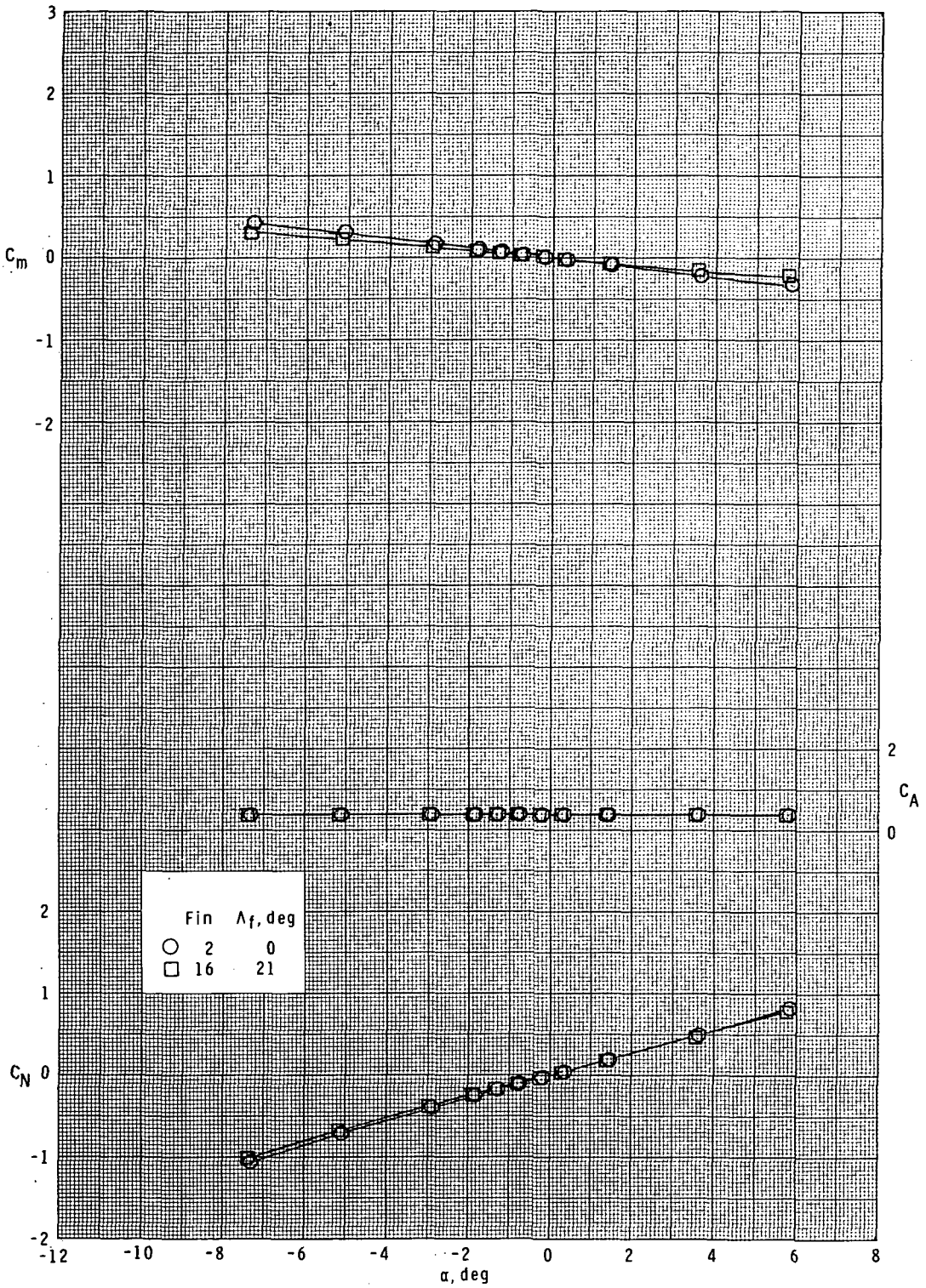

(b) M = 1.90.

Figure 13.- Continued.

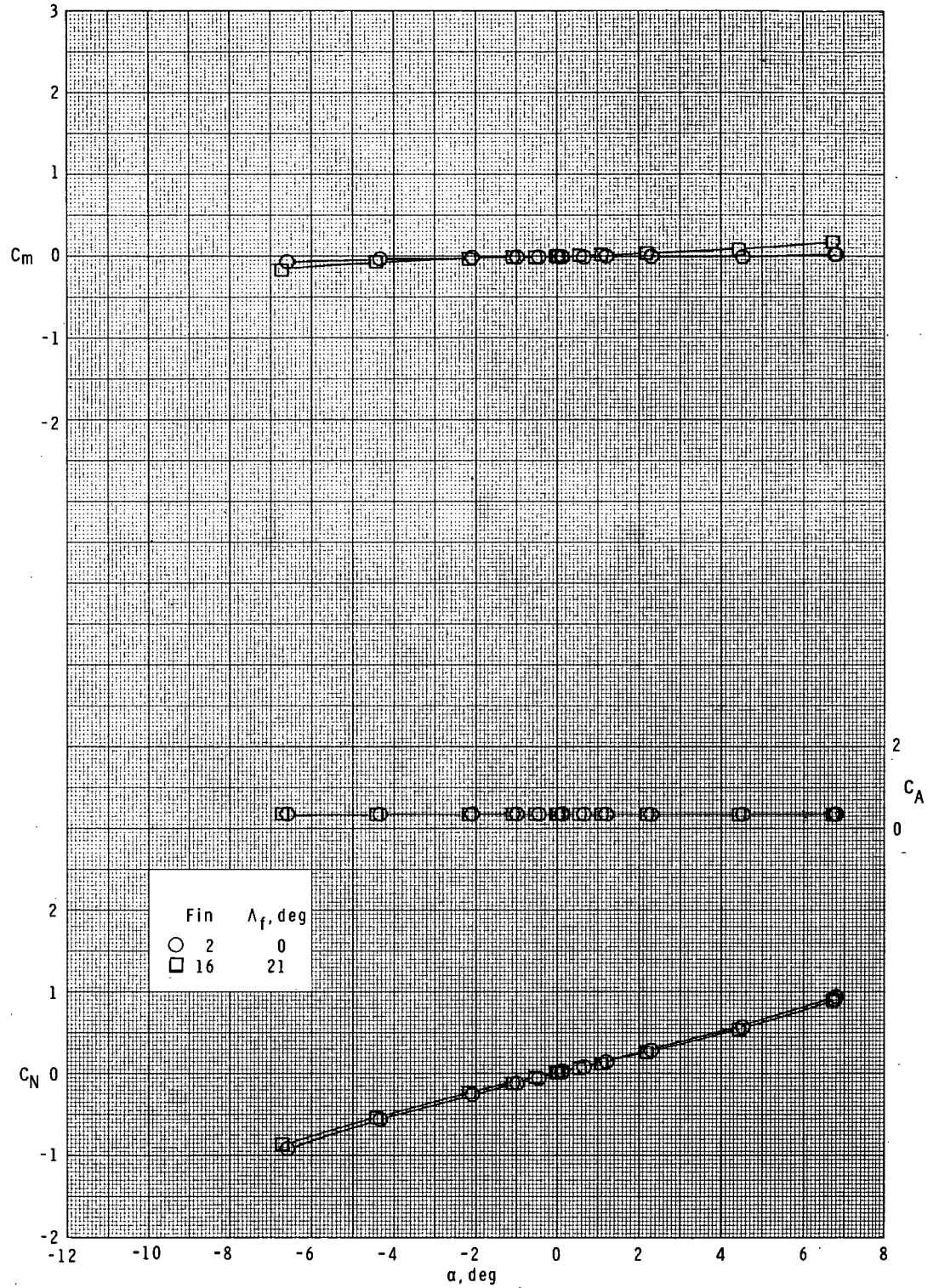

(c) M = 2.36.

Figure 13.- Continued.

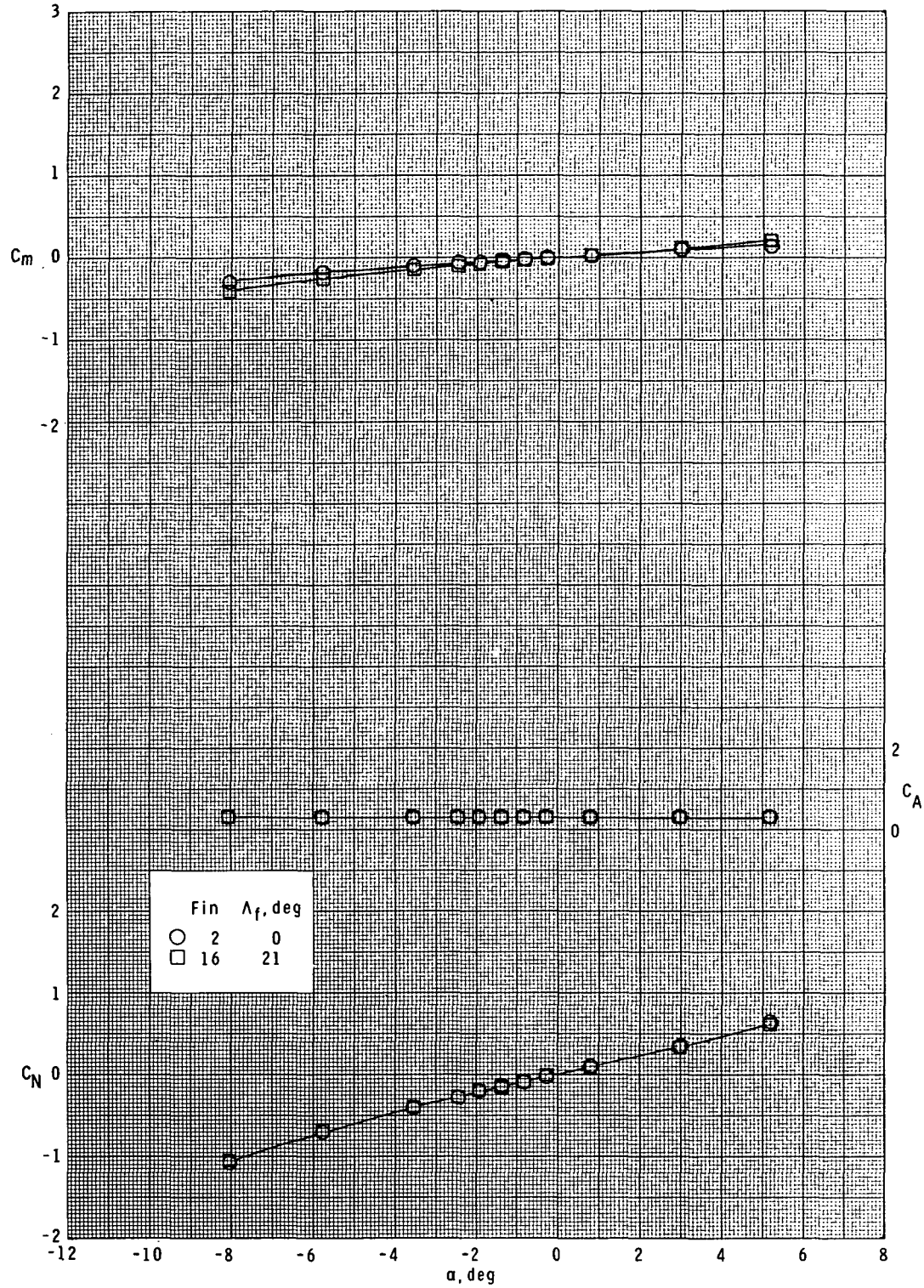

(d) M = 2.86.

Figure 13.- Concluded.

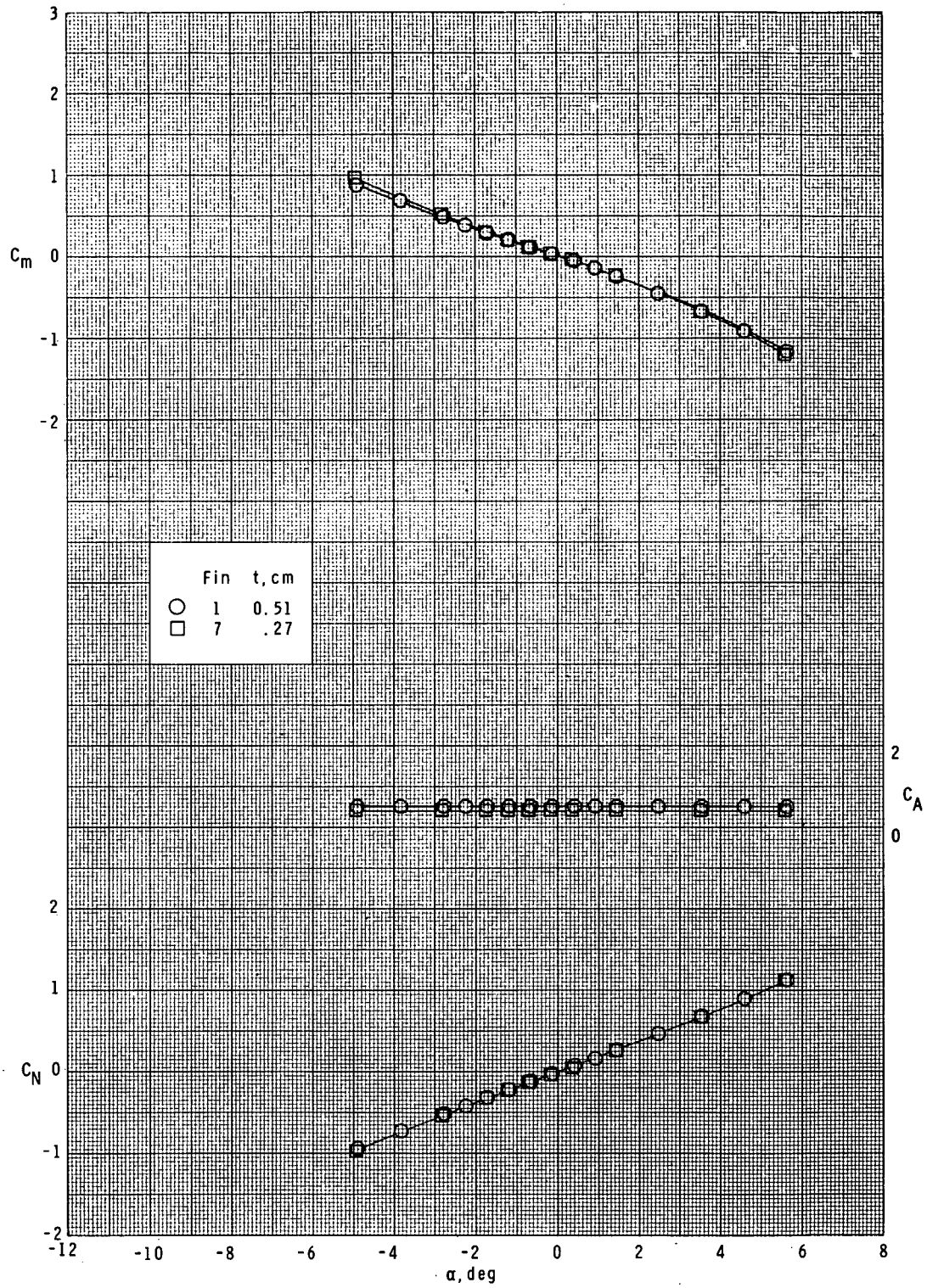

(a) M = 1.60.

Figure 14.- Effect of fin thickness on longitudinal characteristics. Basic body (B_1); long-chord curved fins (F_1 and F_7); $\phi = 0^o$.

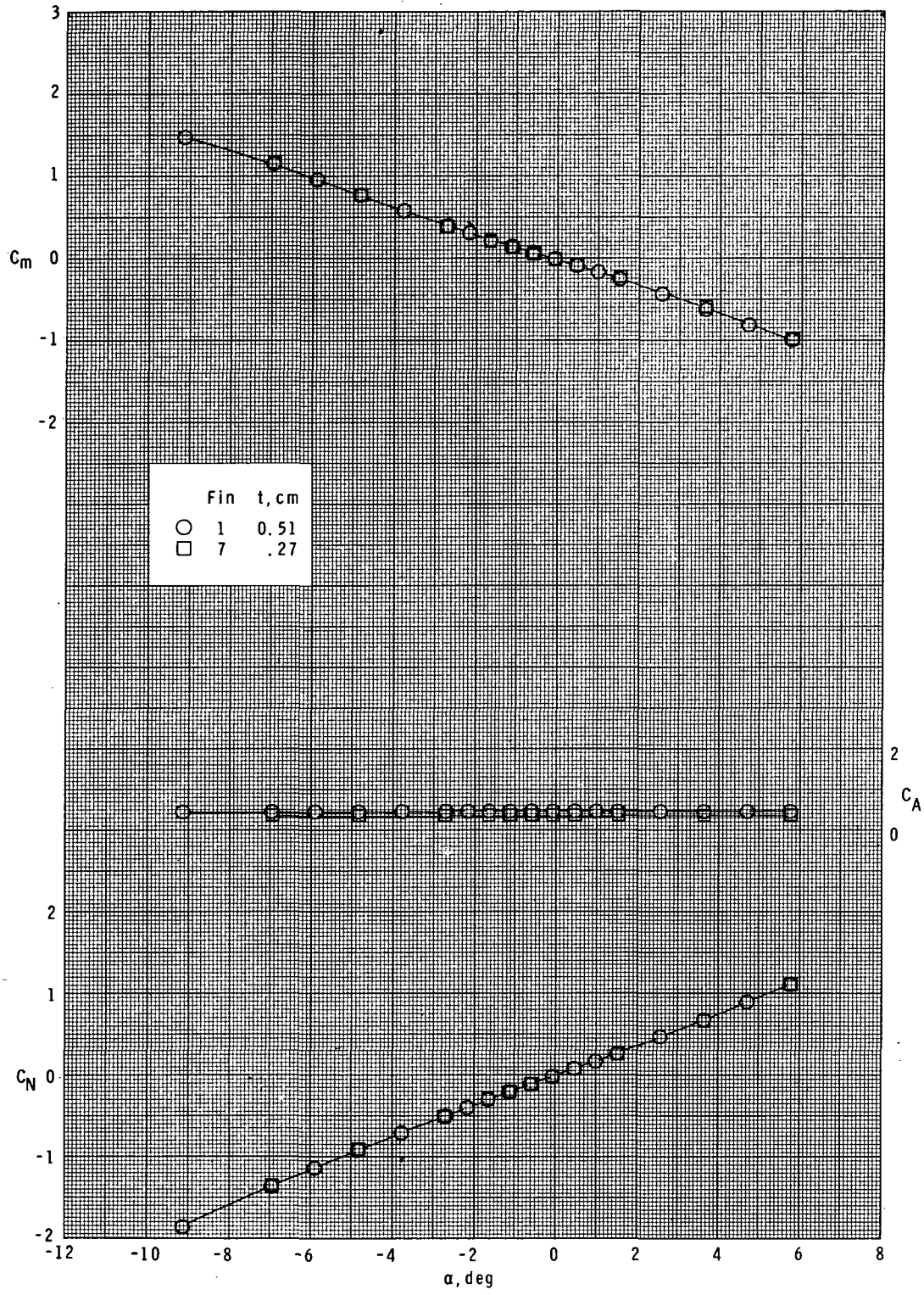

(b) M = 1.90.

Figure 14.- Continued.

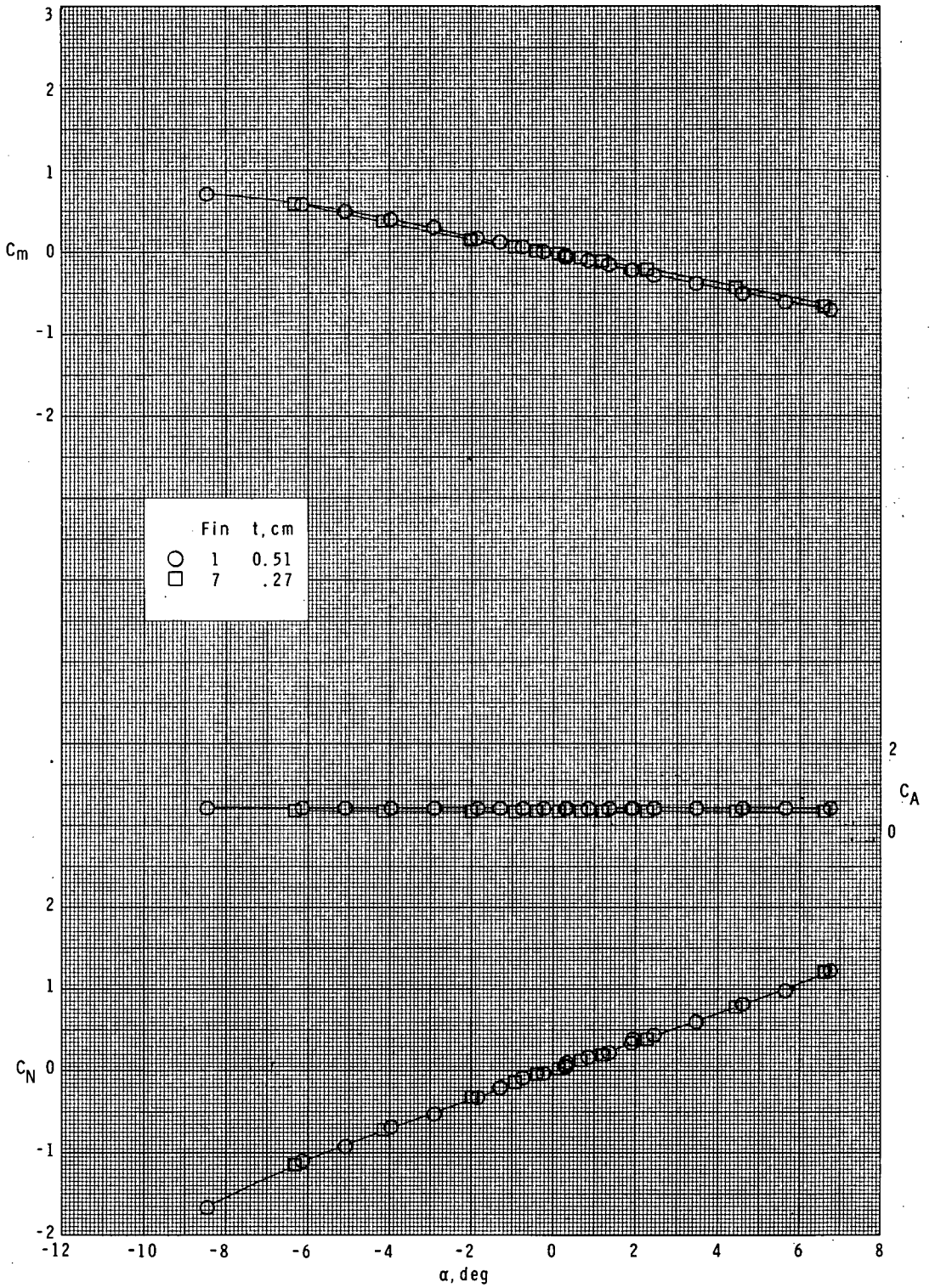

(c) M = 2.36.

Figure 14.- Continued.

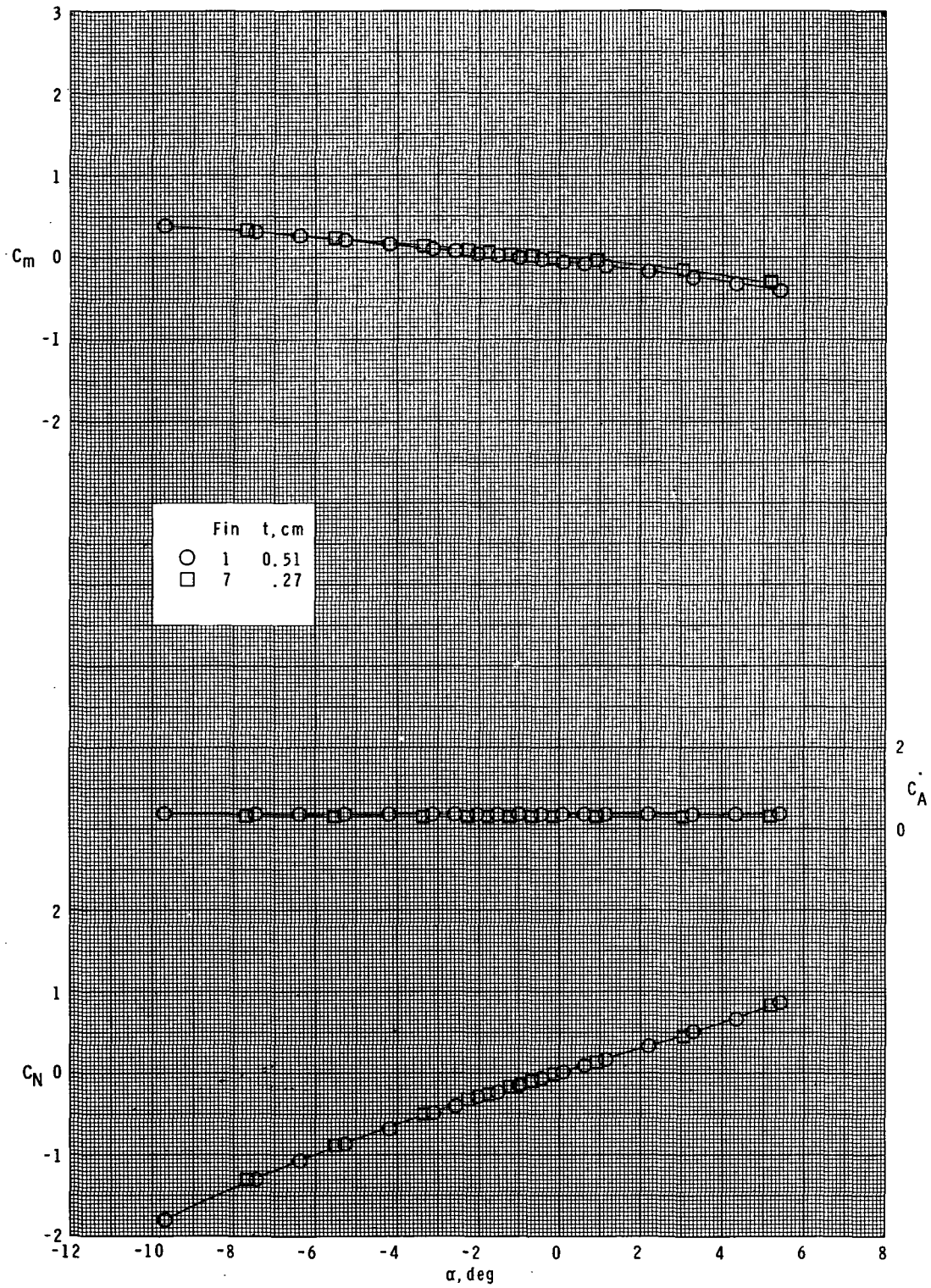

(d) M = 2.86.

Figure 14.- Concluded.

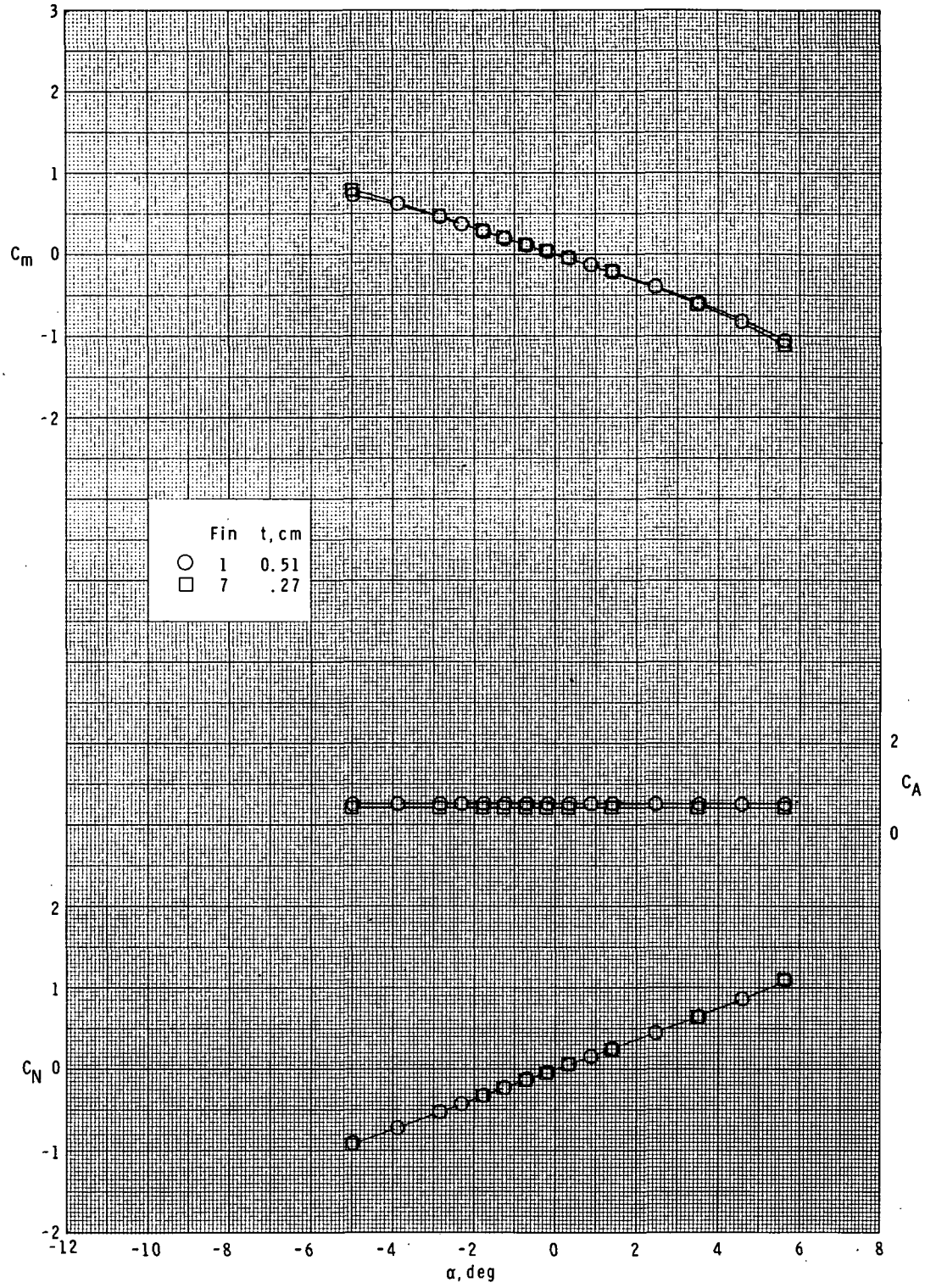

(a) M = 1.60.

Figure 15.- Effect of fin thickness on longitudinal characteristics. Basic body (B_1); long-chord curved fins (F_1 and F_7); $\phi = 45^\circ$.

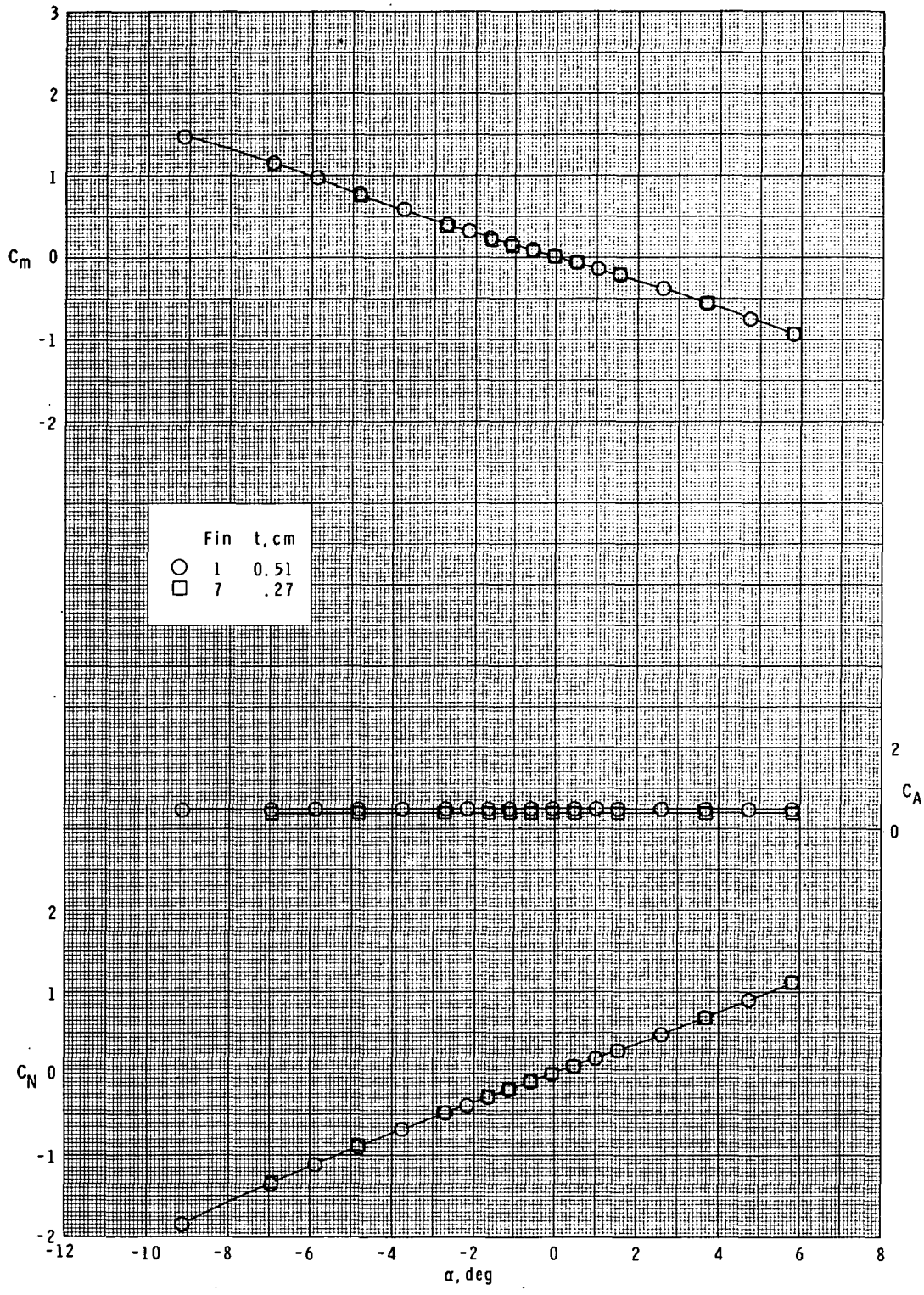

(b) M = 1.90.

Figure 15.- Continued.

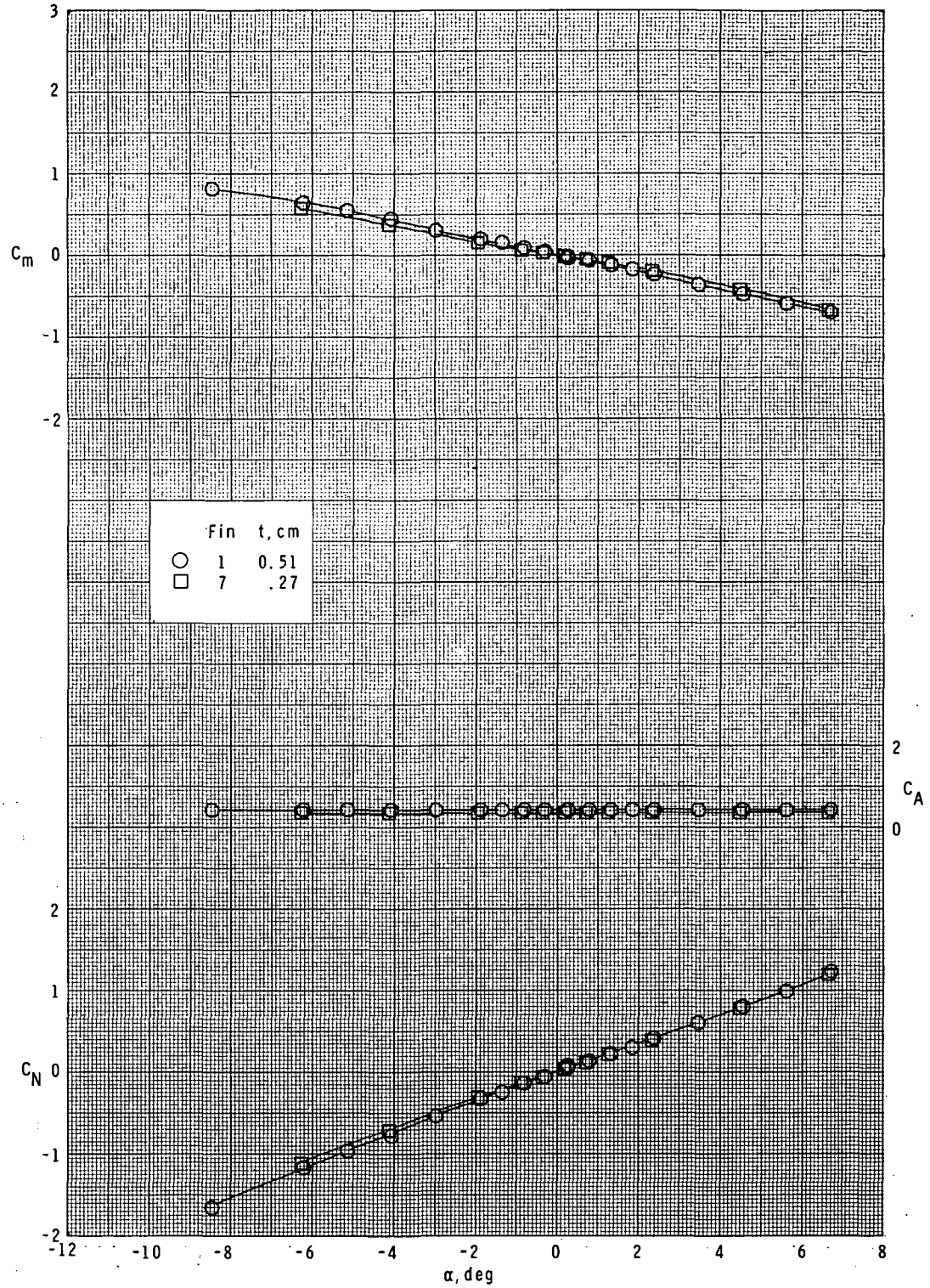

(c) M = 2.36.

Figure 15.- Continued.

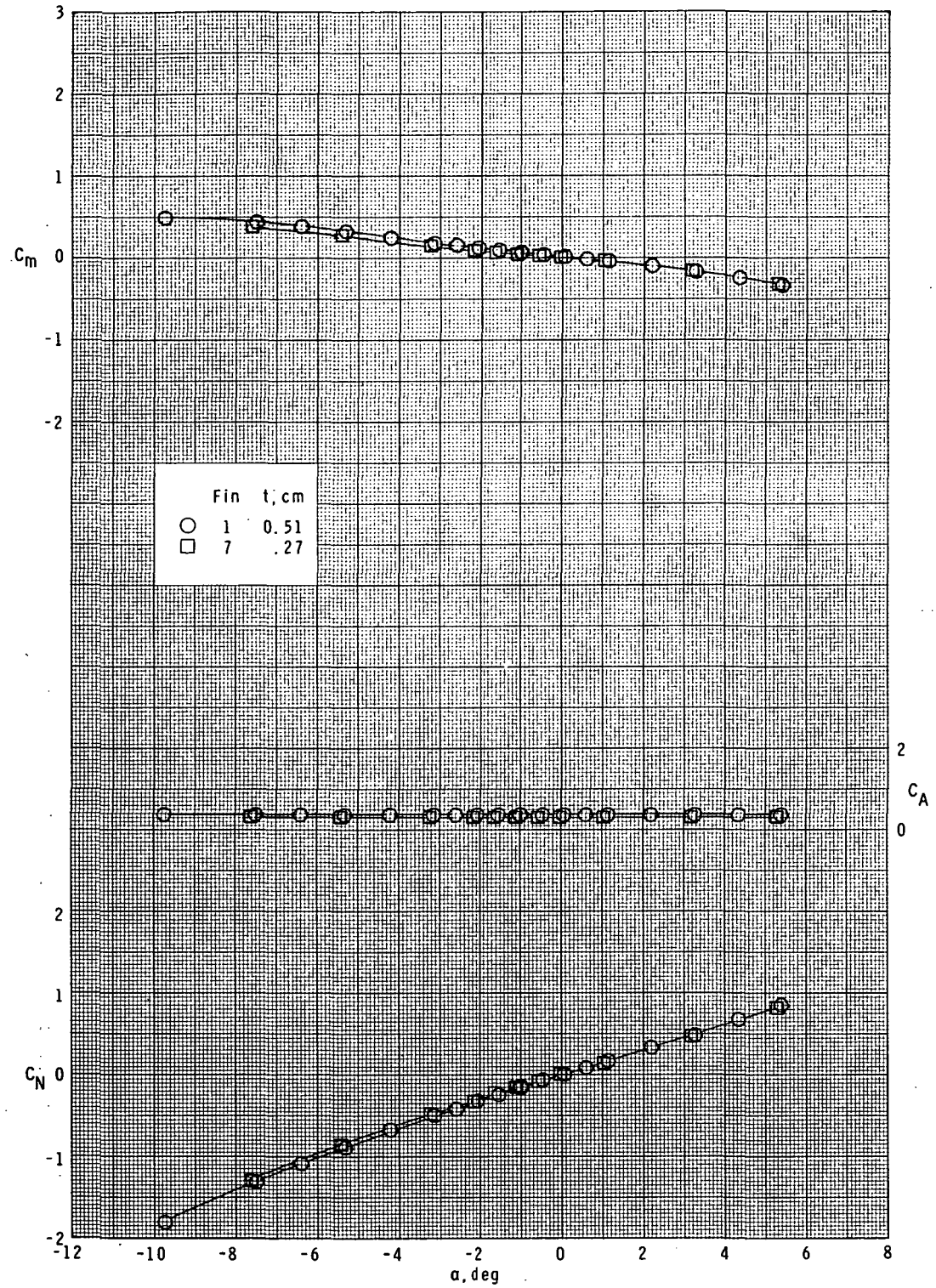

(d) M = 2.86.

Figure 15.- Concluded.

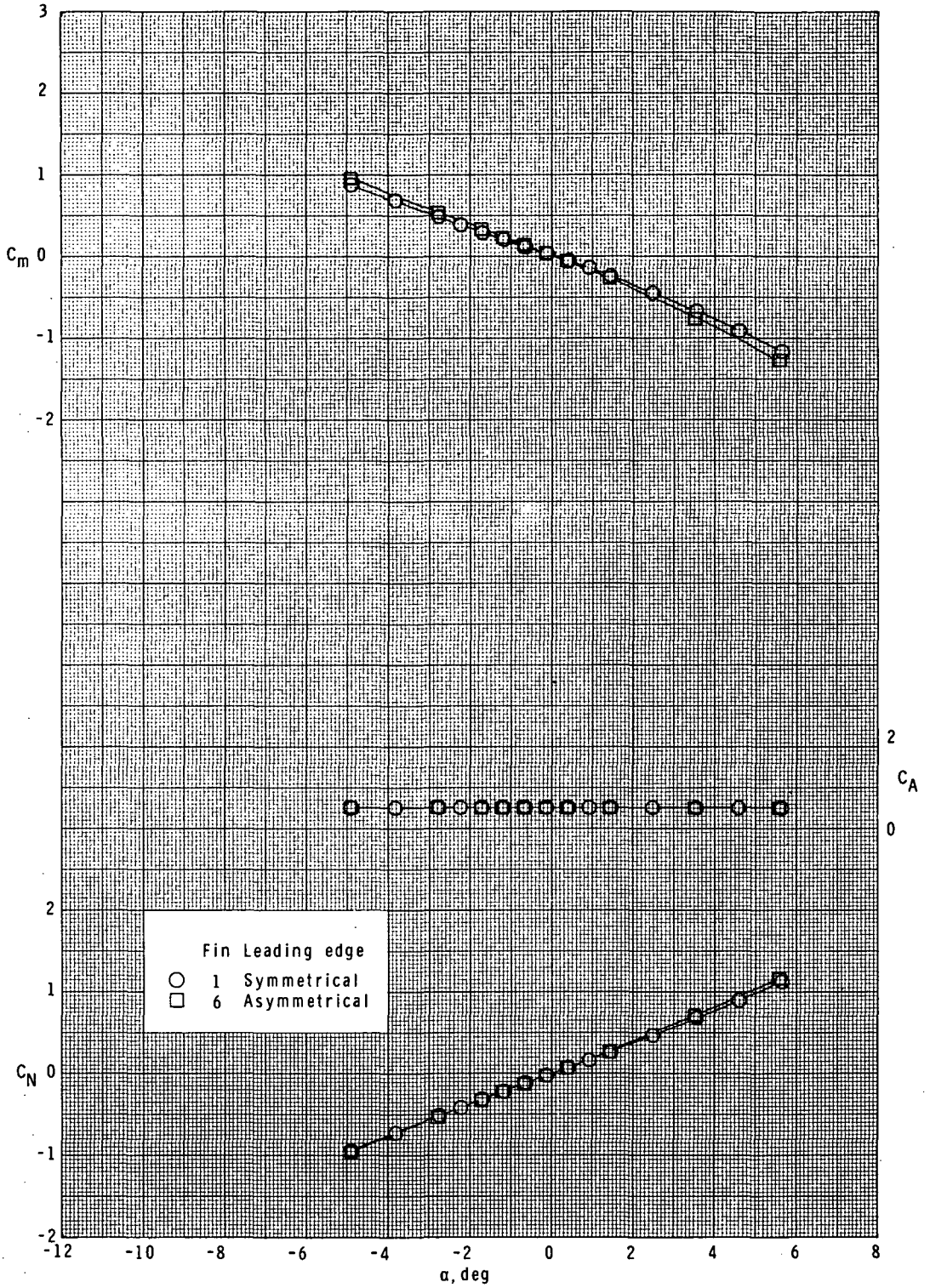

(a) M = 1.60.

Figure 16.- Effect of fin leading-edge shape on longitudinal characteristics. Basic body (B_1); long-chord curved fins (F_1 and F_6); $\phi = 0^o$.

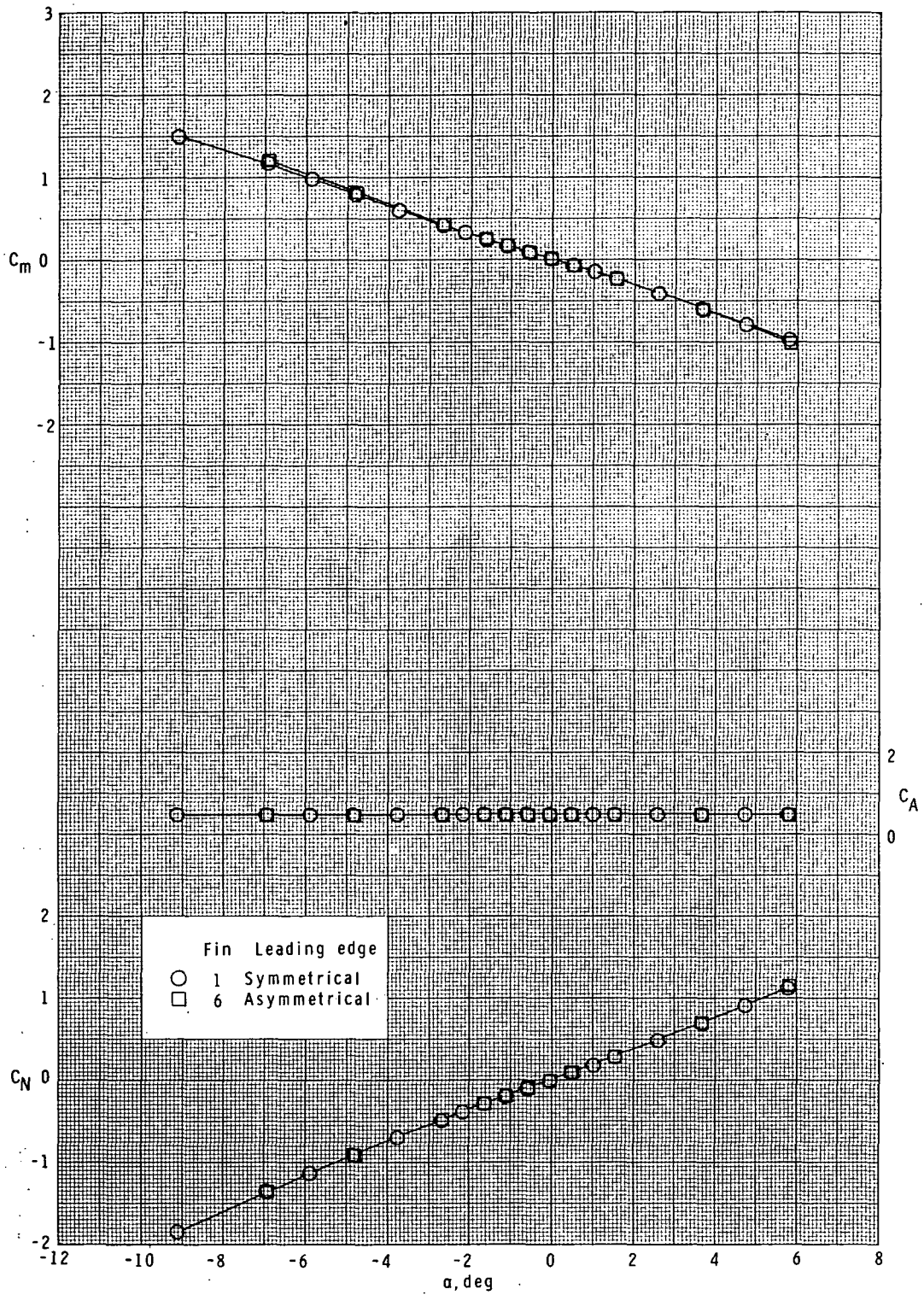

(b) M = 1.90.

Figure 16.- Continued.

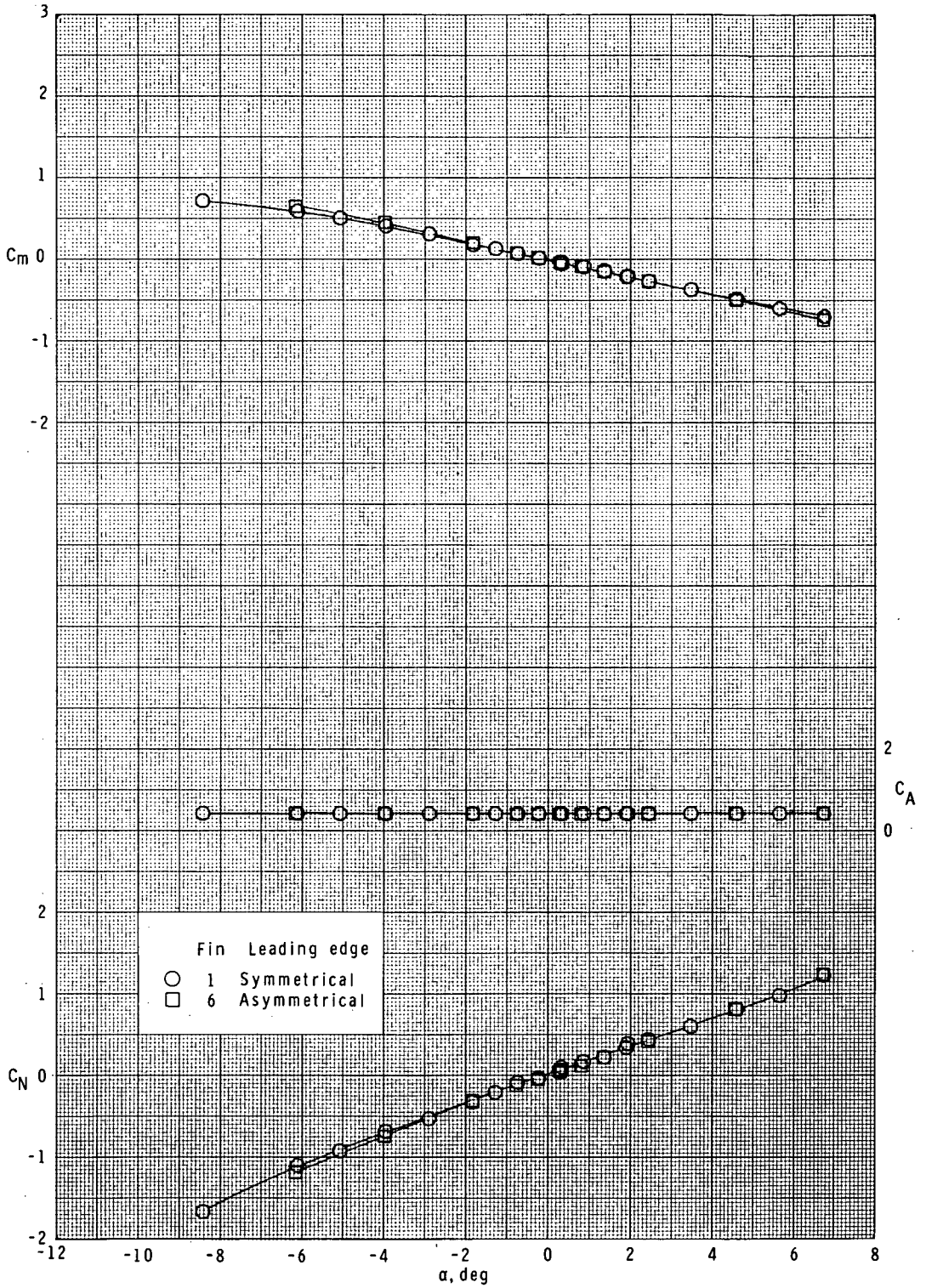

(c) M = 2.36.

Figure 16.- Continued.

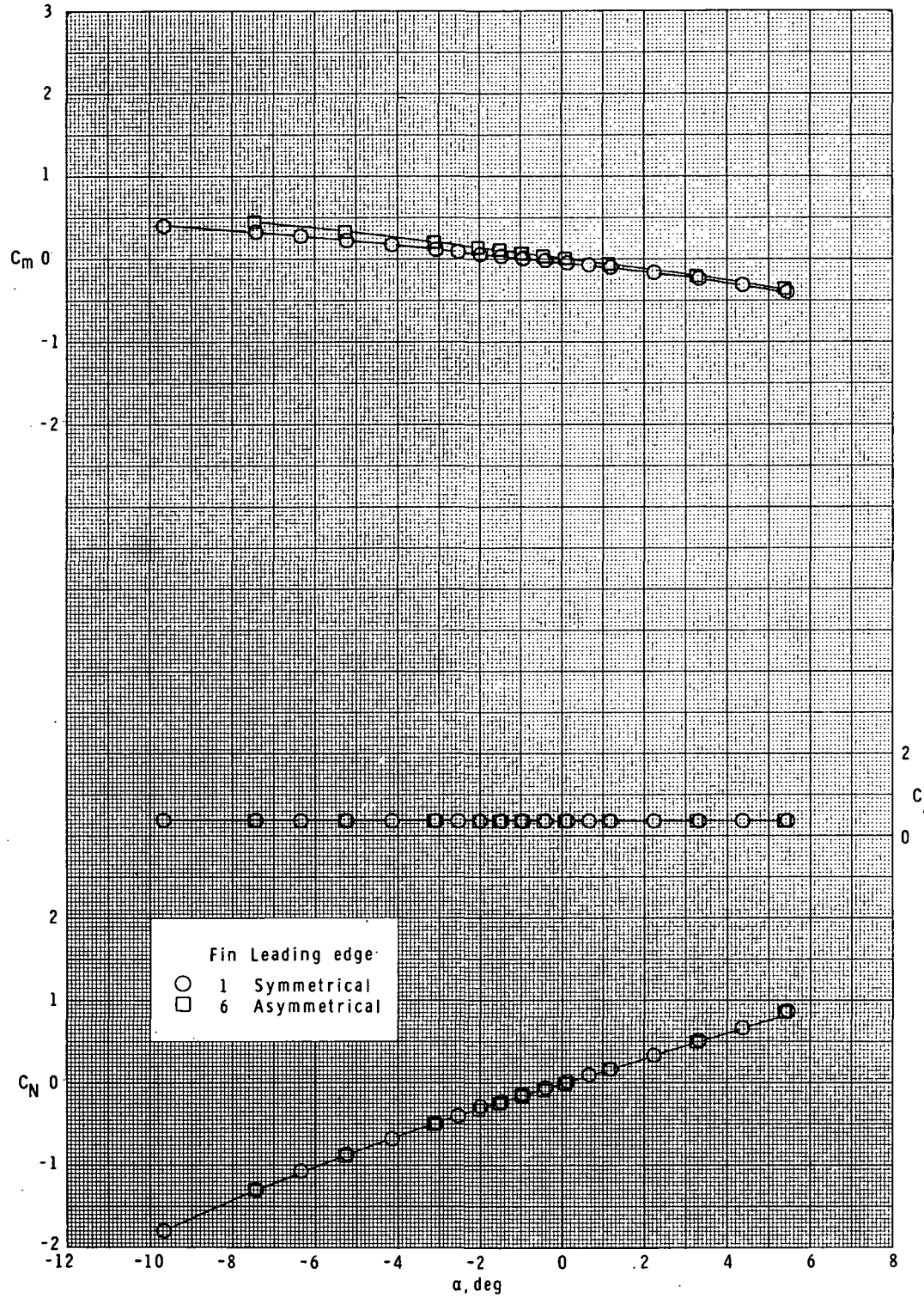

(d) M = 2.86.

Figure 16.- Concluded.

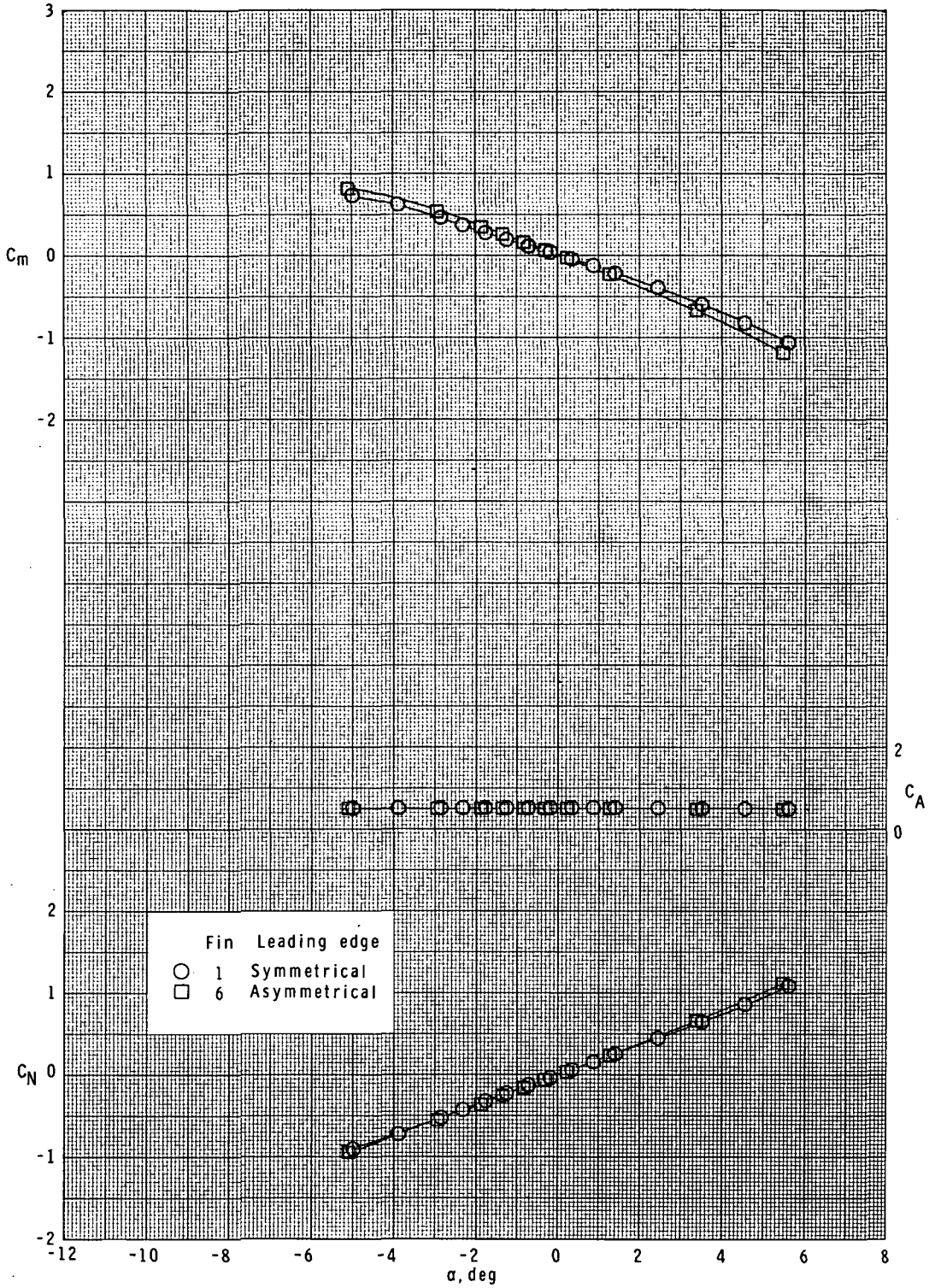

(a) M = 1.60.

Figure 17.- Effect of fin leading-edge shape on longitudinal characteristics. Basic body (B_1); long-chord curved fins (F_1 and F_6); $\phi = 45^\circ$.

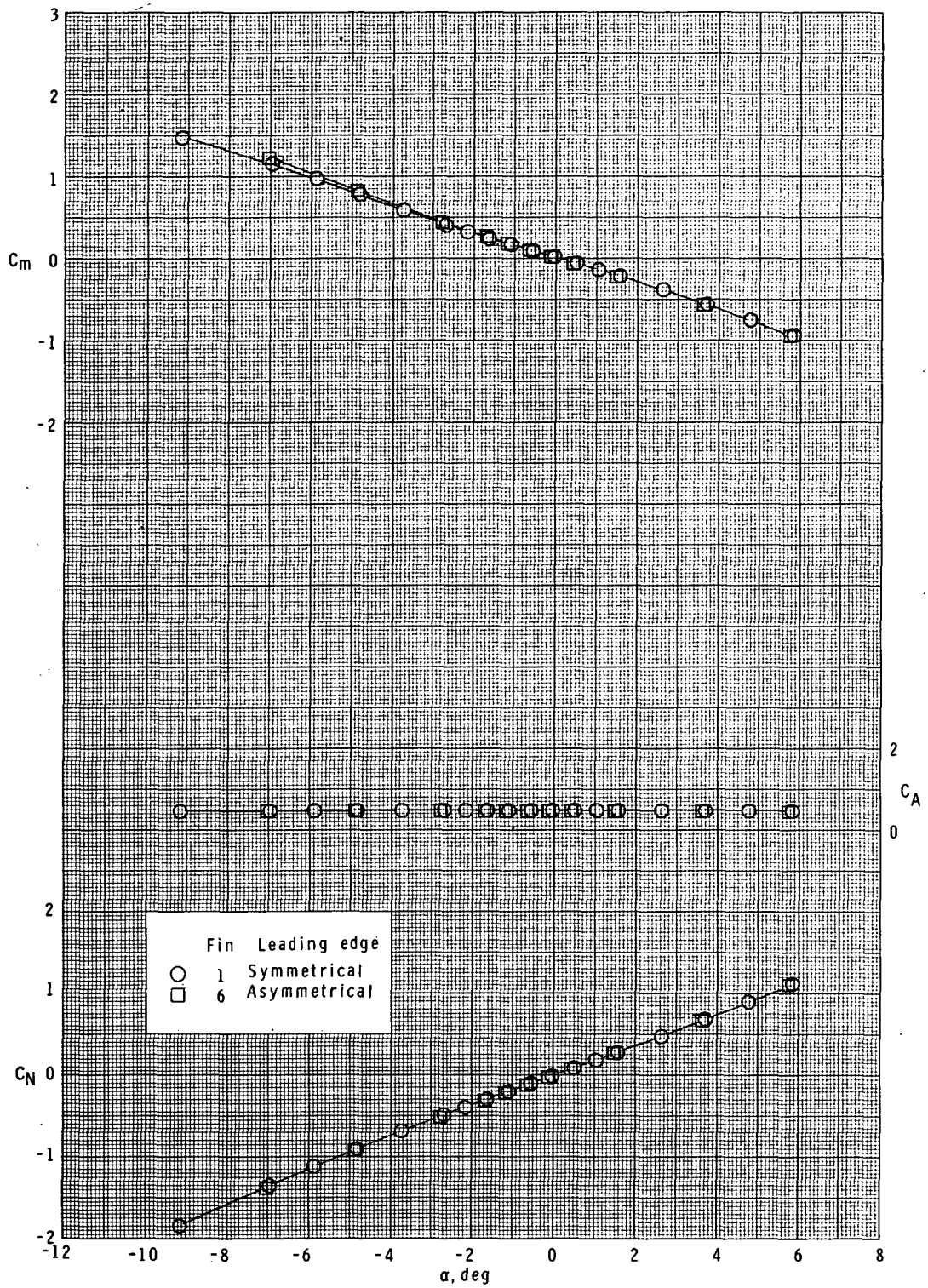

(b) M = 1.90.

Figure 17.- Continued.

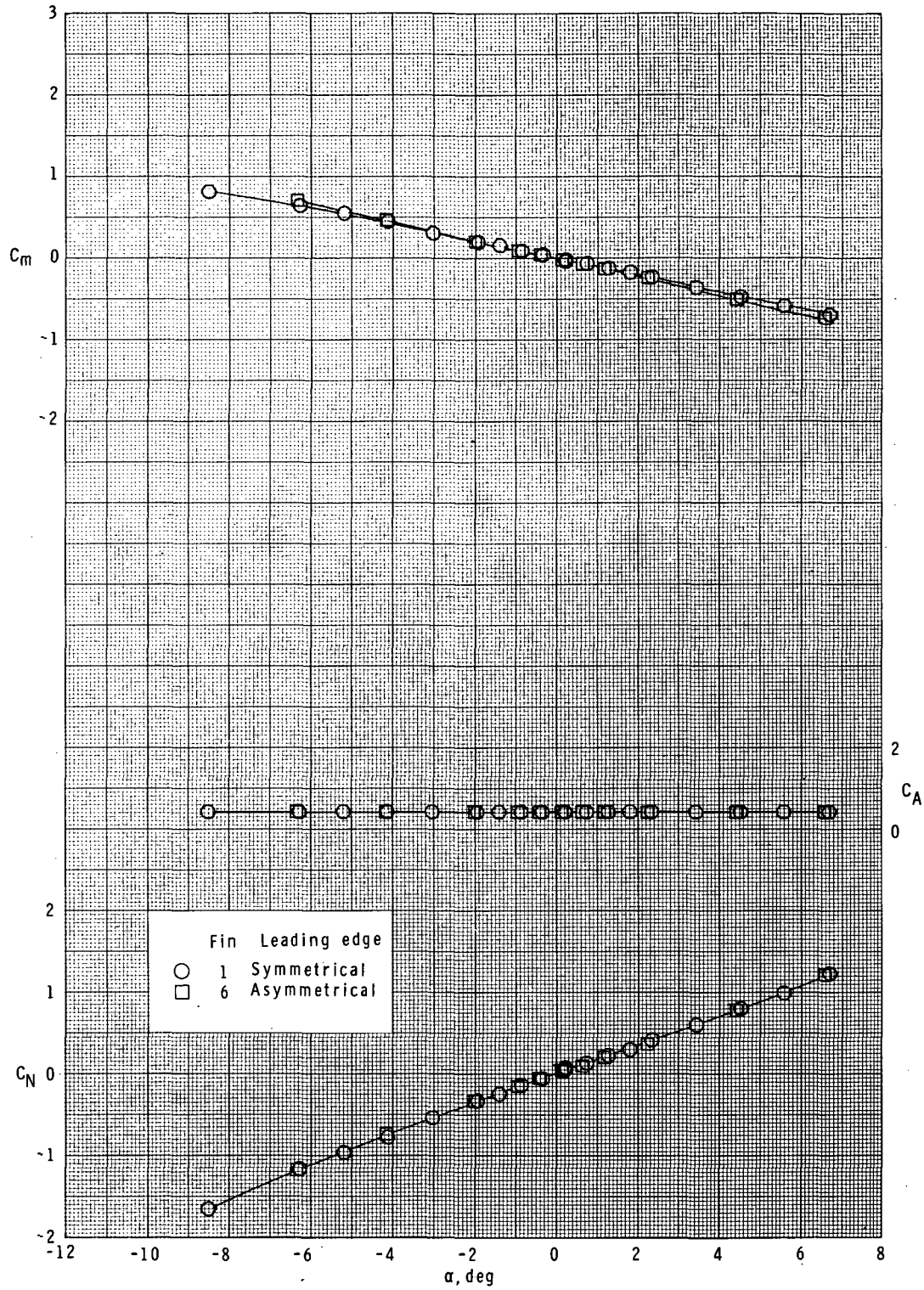

(c) M = 2.36.

Figure 17.- Continued.

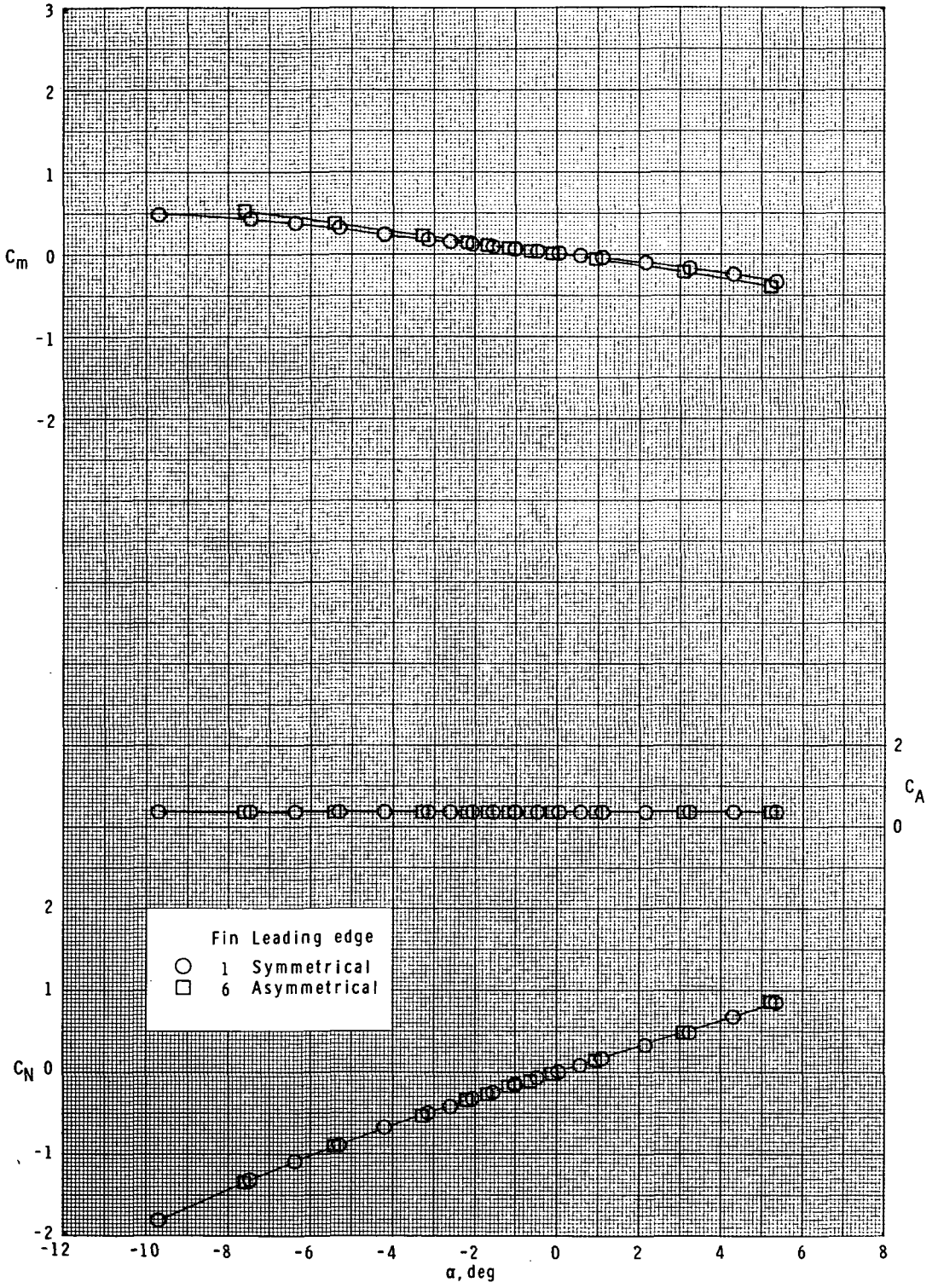

(d) M = 2.86.

Figure 17.- Concluded.

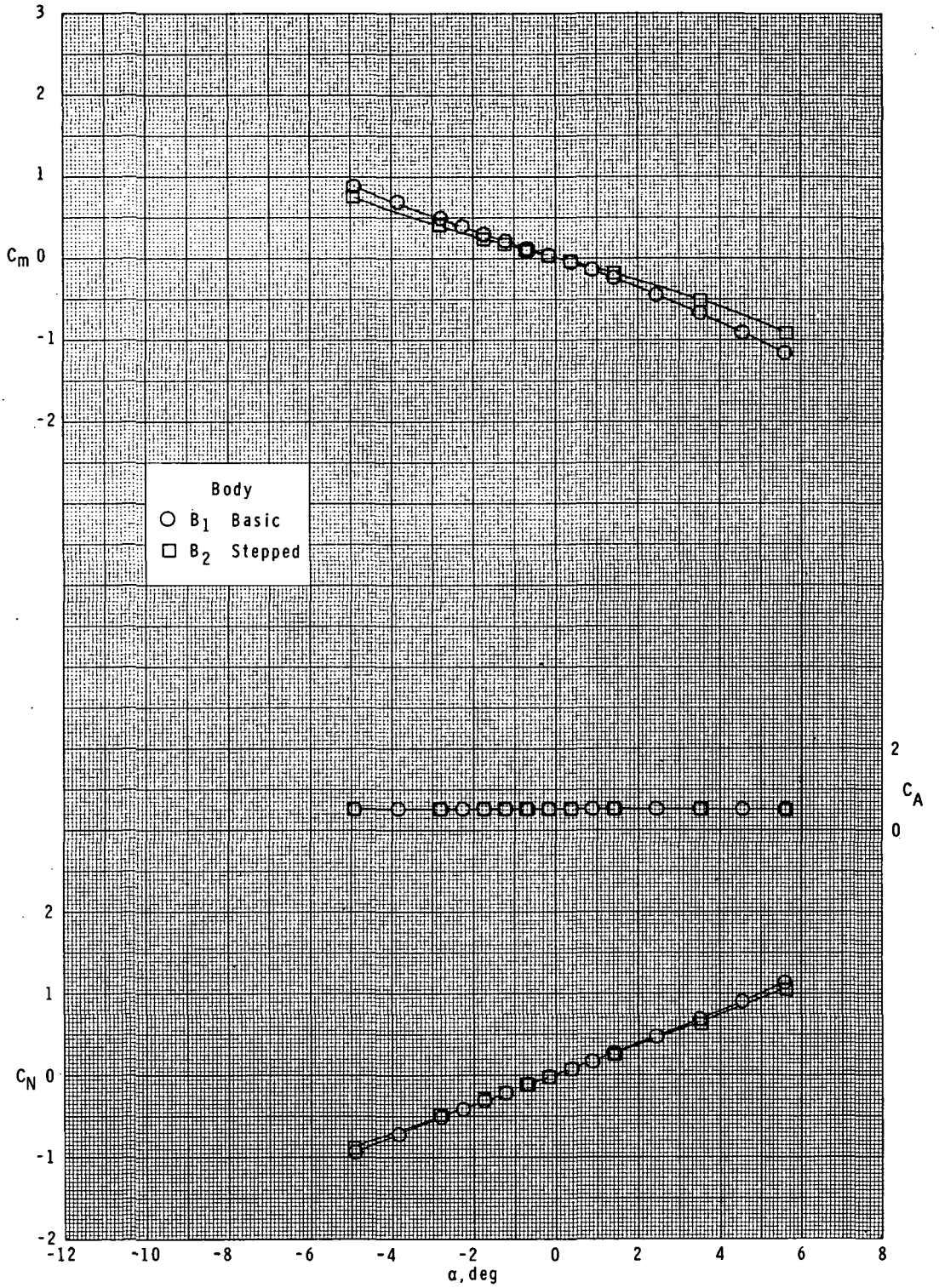

(a) M = 1.60.

Figure 18.- Effect of afterbody diameter on longitudinal characteristics. Long-chord unswept curved fin (F_1); bodies (B_1 and B_2); $\phi = 0^o$.

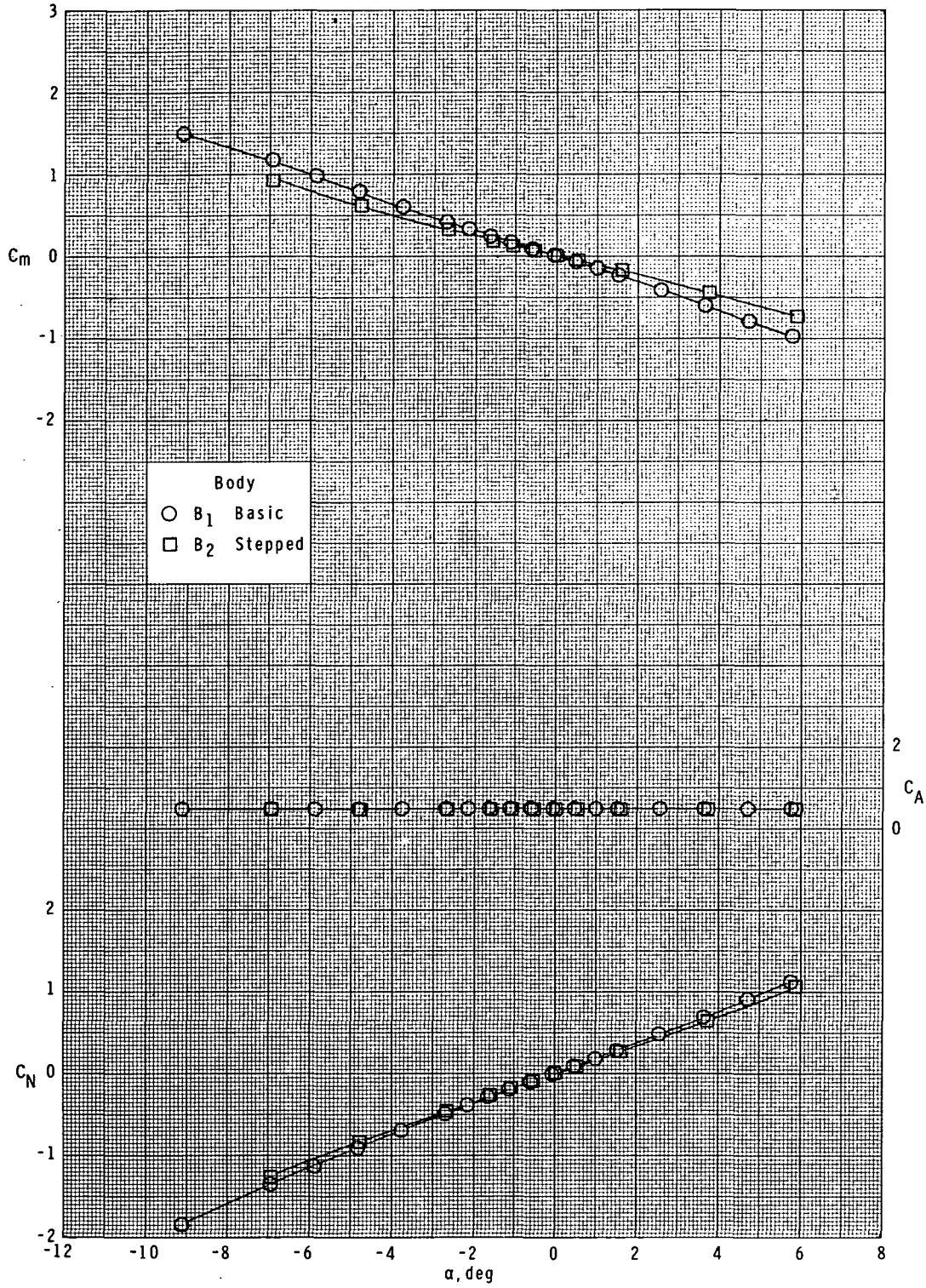

(b) M = 1.90.

Figure 18.- Continued.

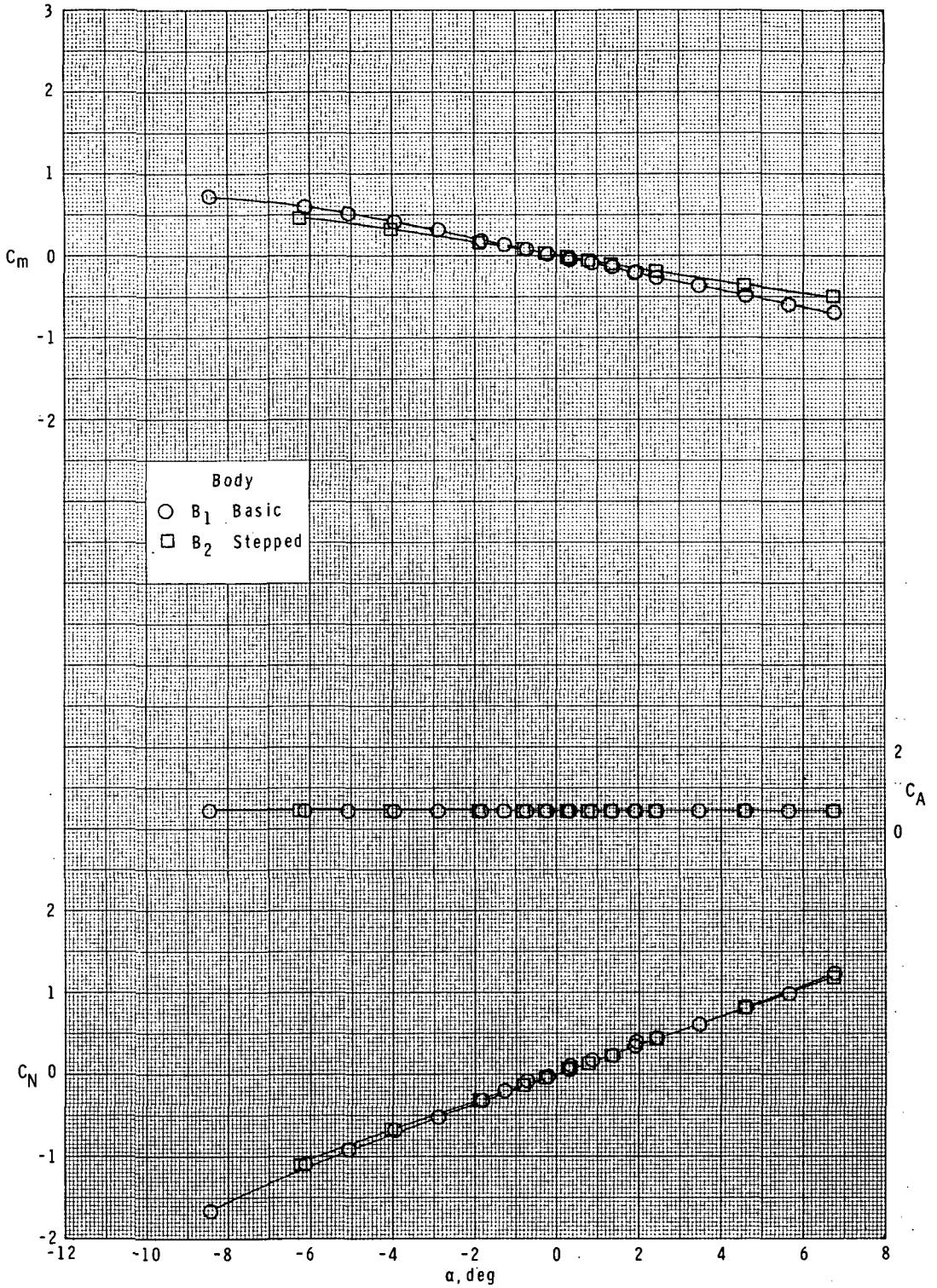

(c) M = 2.36.

Figure 18.- Continued.

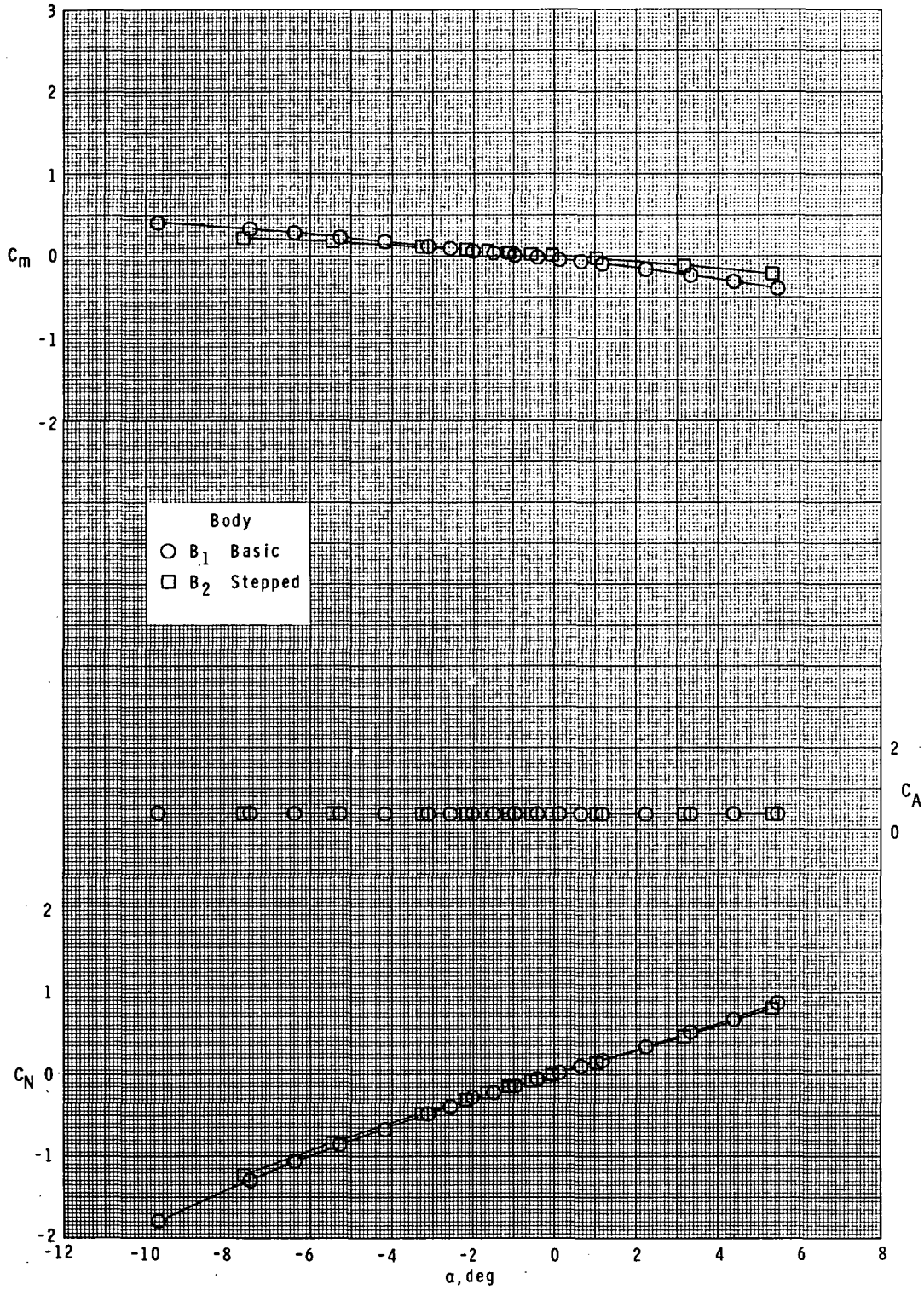

(d) M = 2.86.

Figure 18.- Concluded.

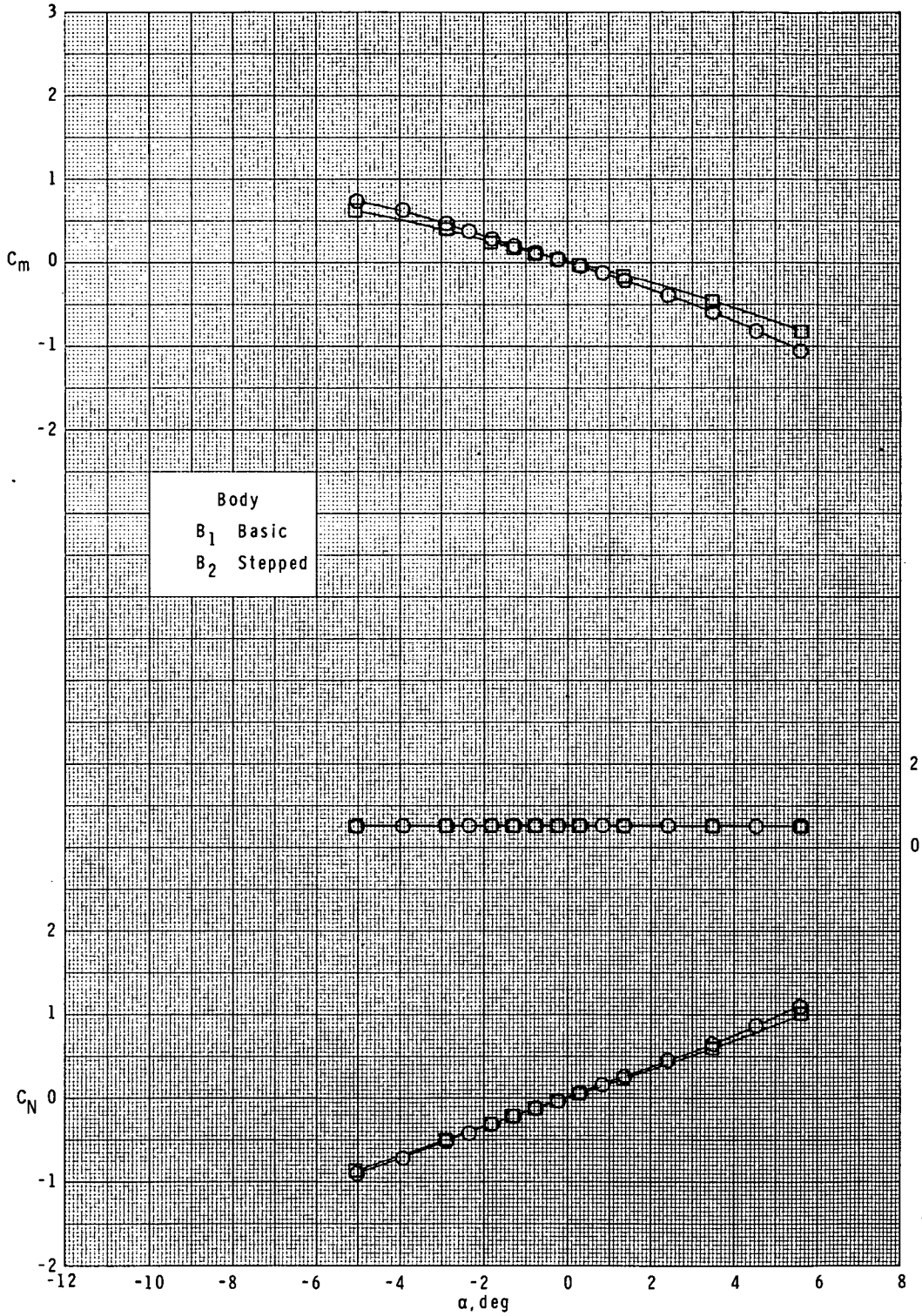

(a) M = 1.60.

Figure 19.- Effect of afterbody diameter on longitudinal characteristics. Long-chord unswept curved fin (F_1); bodies (B_1 and B_2); $\phi = 45^o$.

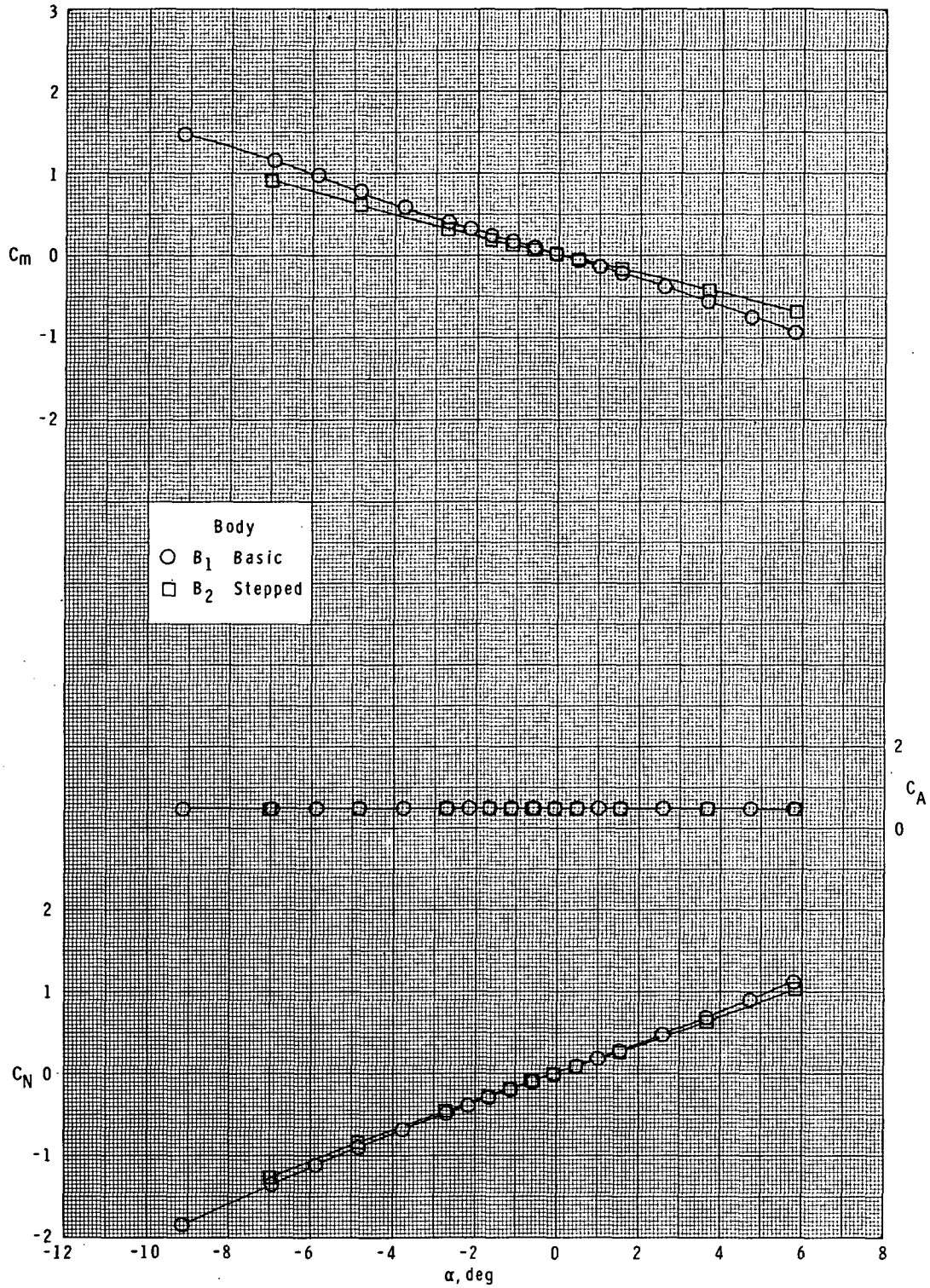

(b) M = 1.90.

Figure 19.- Continued.

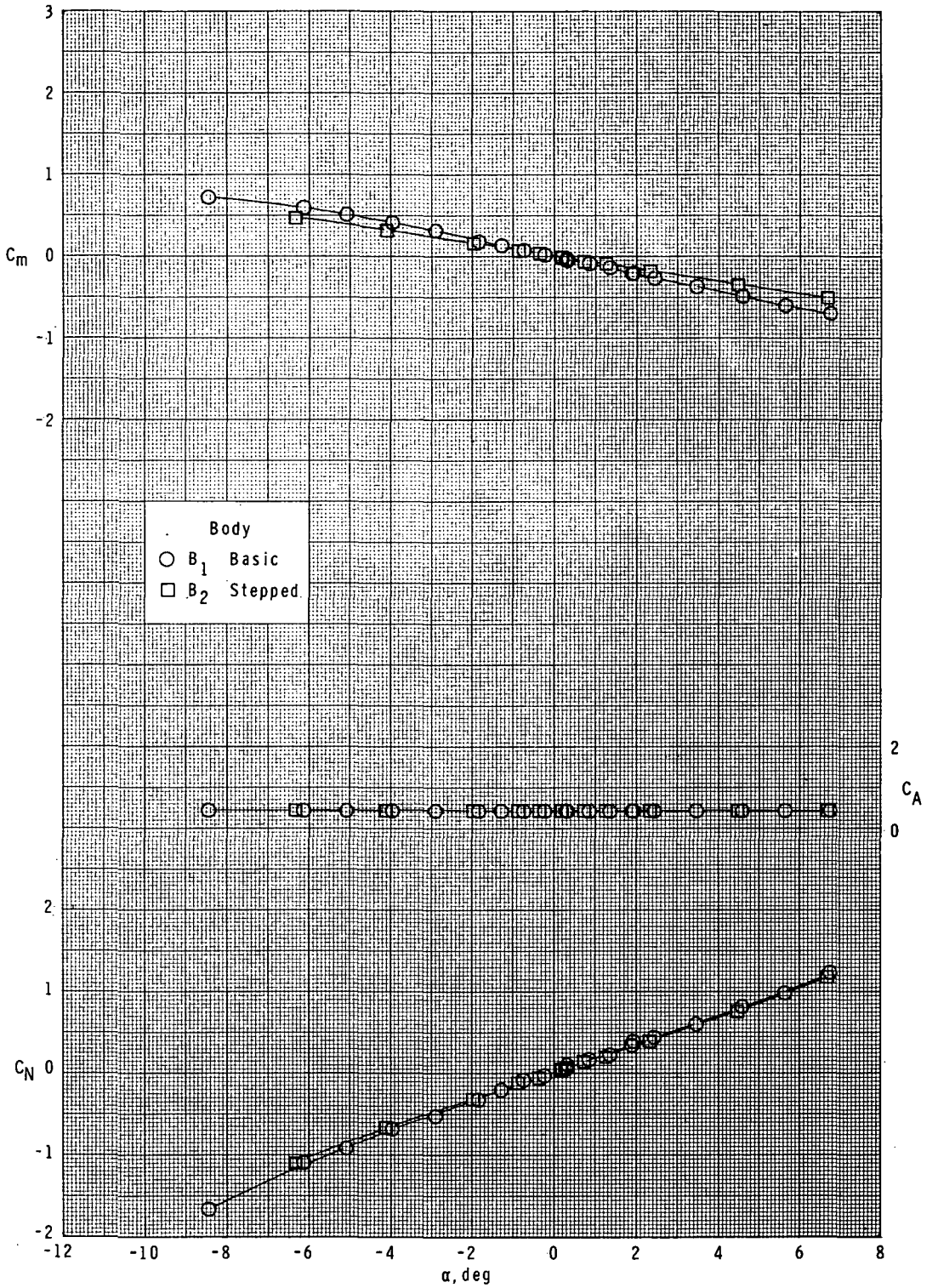

(c) M = 2.36.

Figure 19.- Continued.

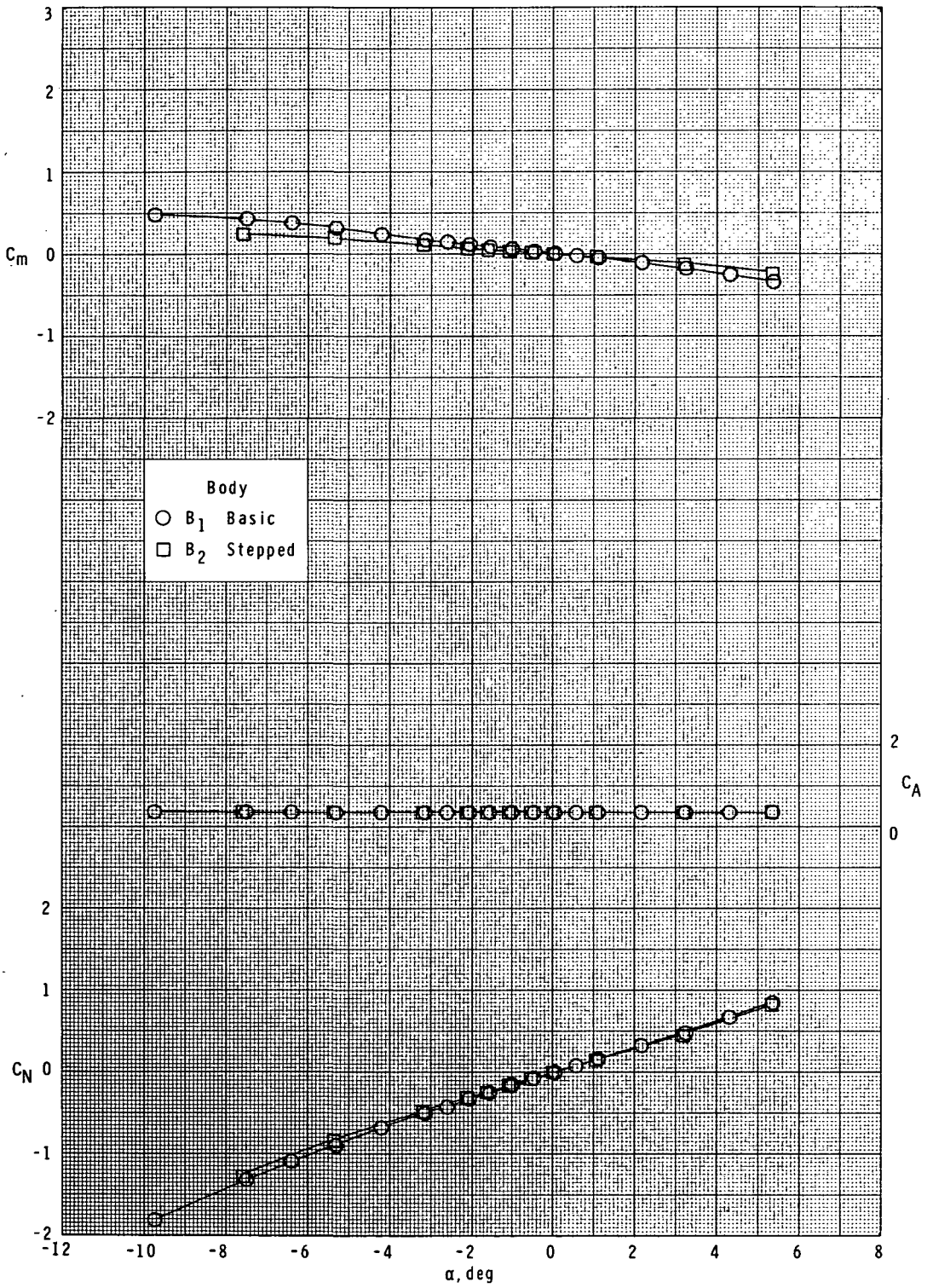

(d) M = 2.86.

Figure 19.- Concluded.

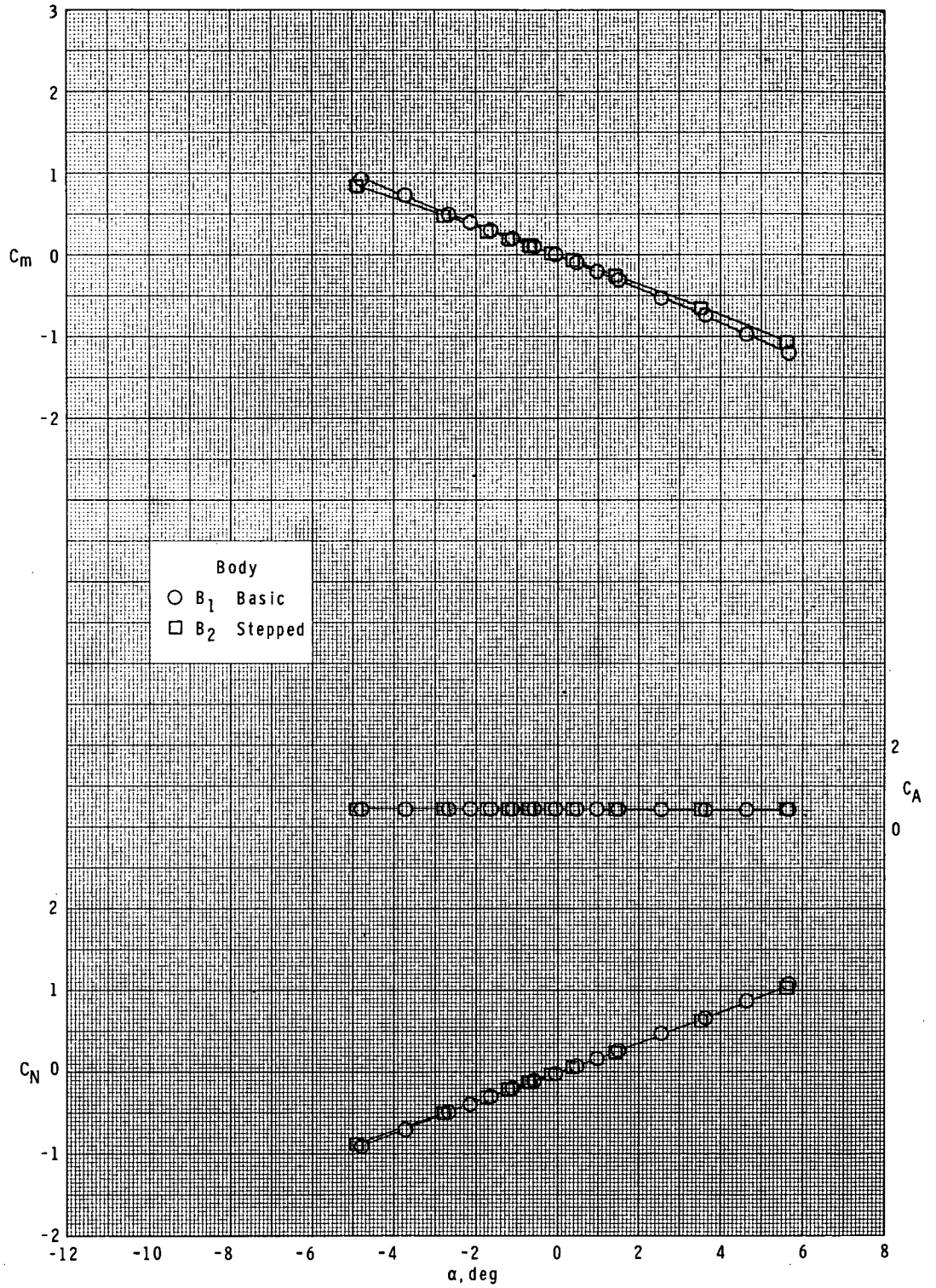

(a) M = 1.60.

Figure 20.- Effect of afterbody diameter on longitudinal characteristics. Long-chord swept curved fin (F_{13}); bodies (B_1 and B_2); $\phi = 0^{o}$.

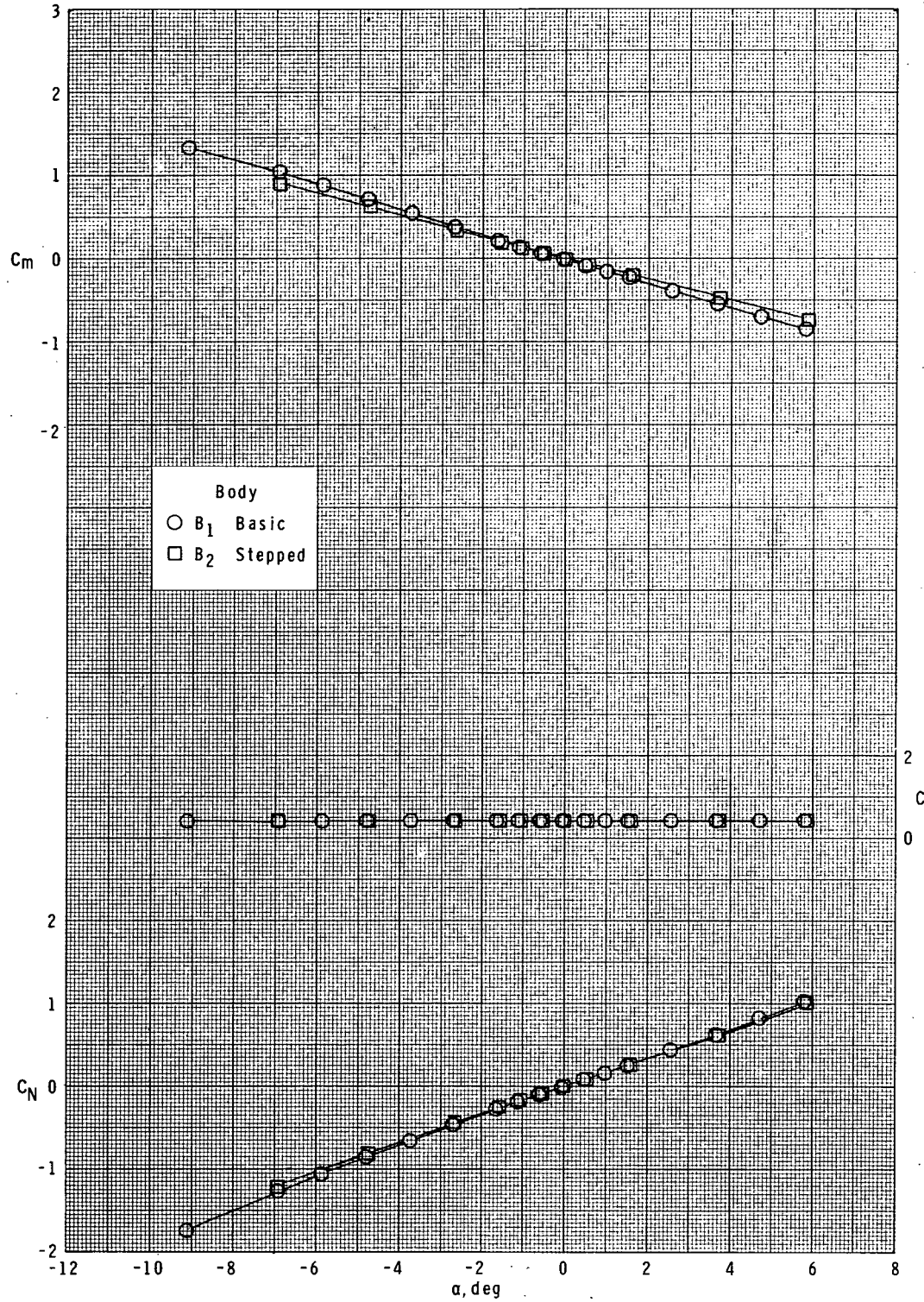

(b) M = 1.90.

Figure 20.- Continued.

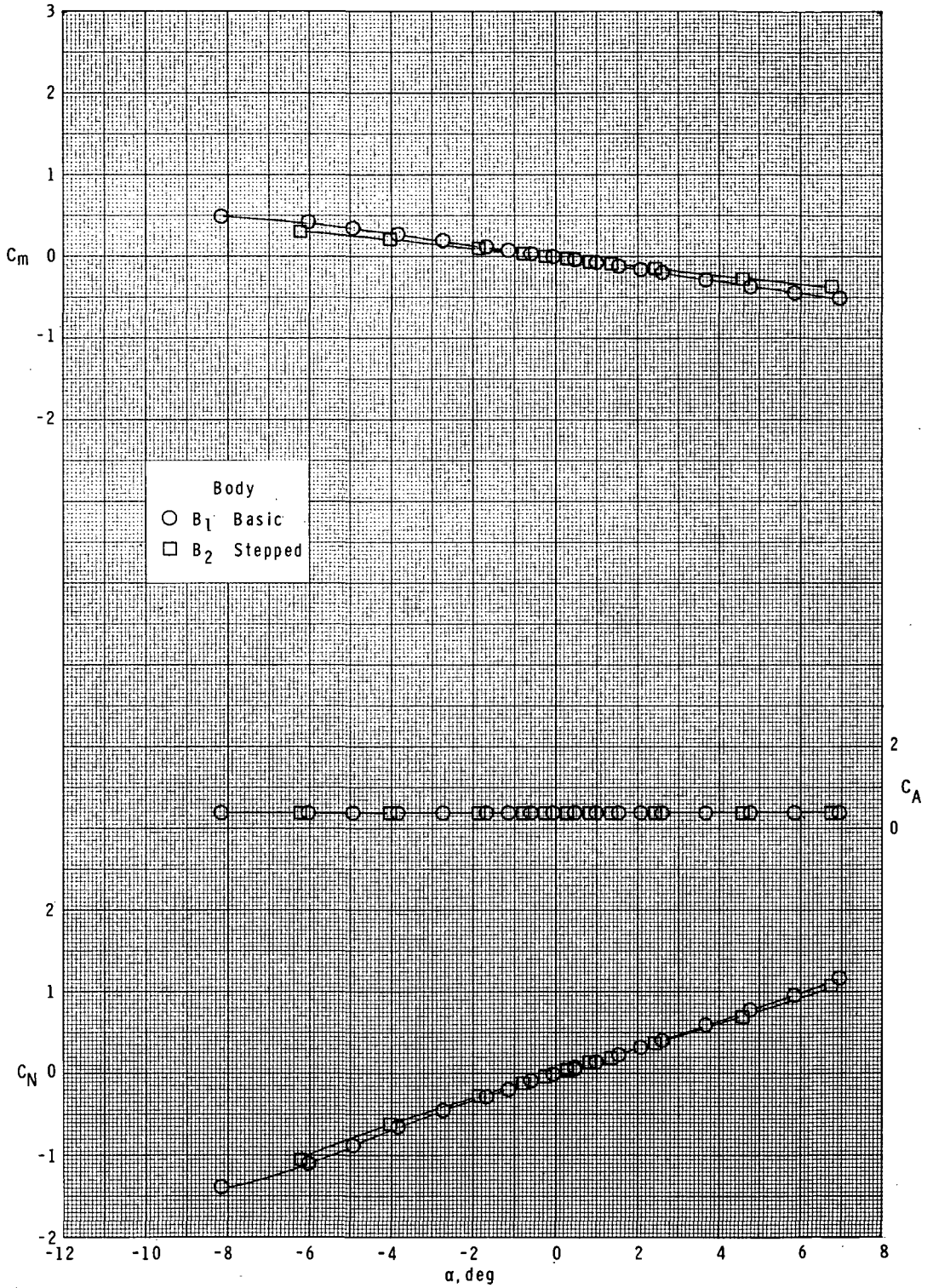

(c) M = 2.36.

Figure 20.- Continued.

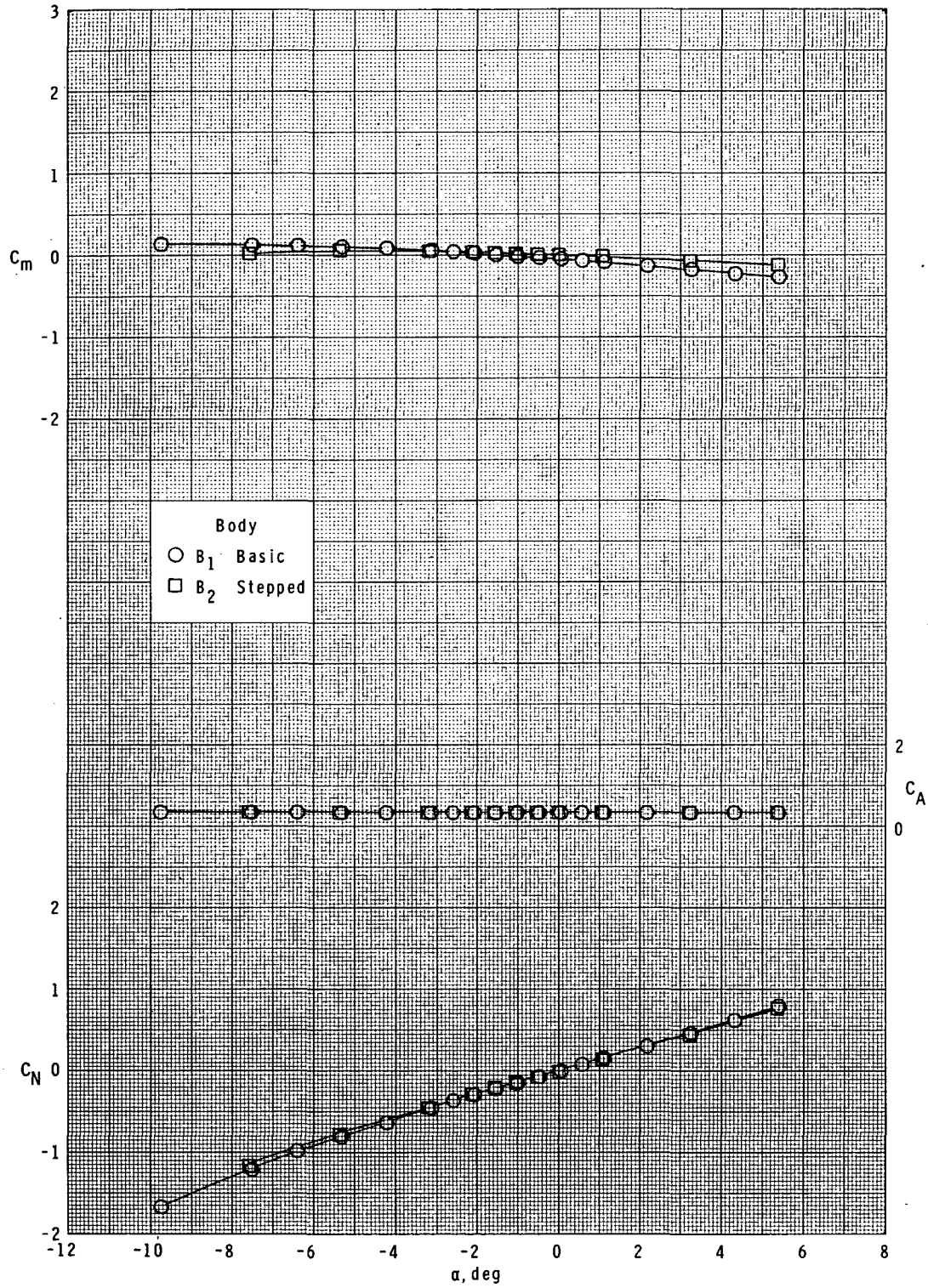

(d) M = 2.86.

Figure 20.- Concluded.

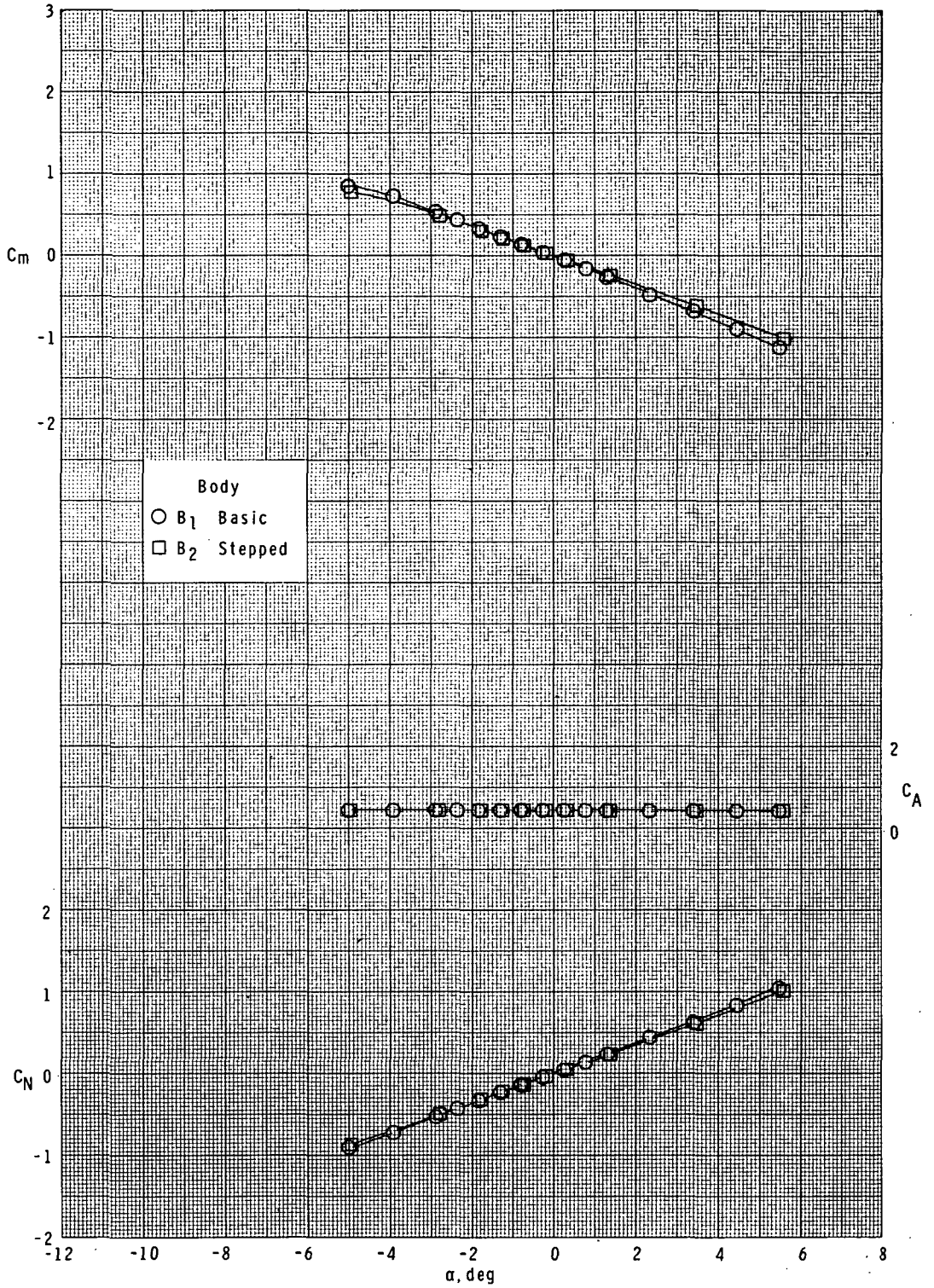

(a) M = 1.60.

Figure 21.- Effect of afterbody diameter on longitudinal characteristics. Long-chord swept curved fin (F_{13}); bodies (B_1 and B_2); $\phi = 45^{\circ}$.

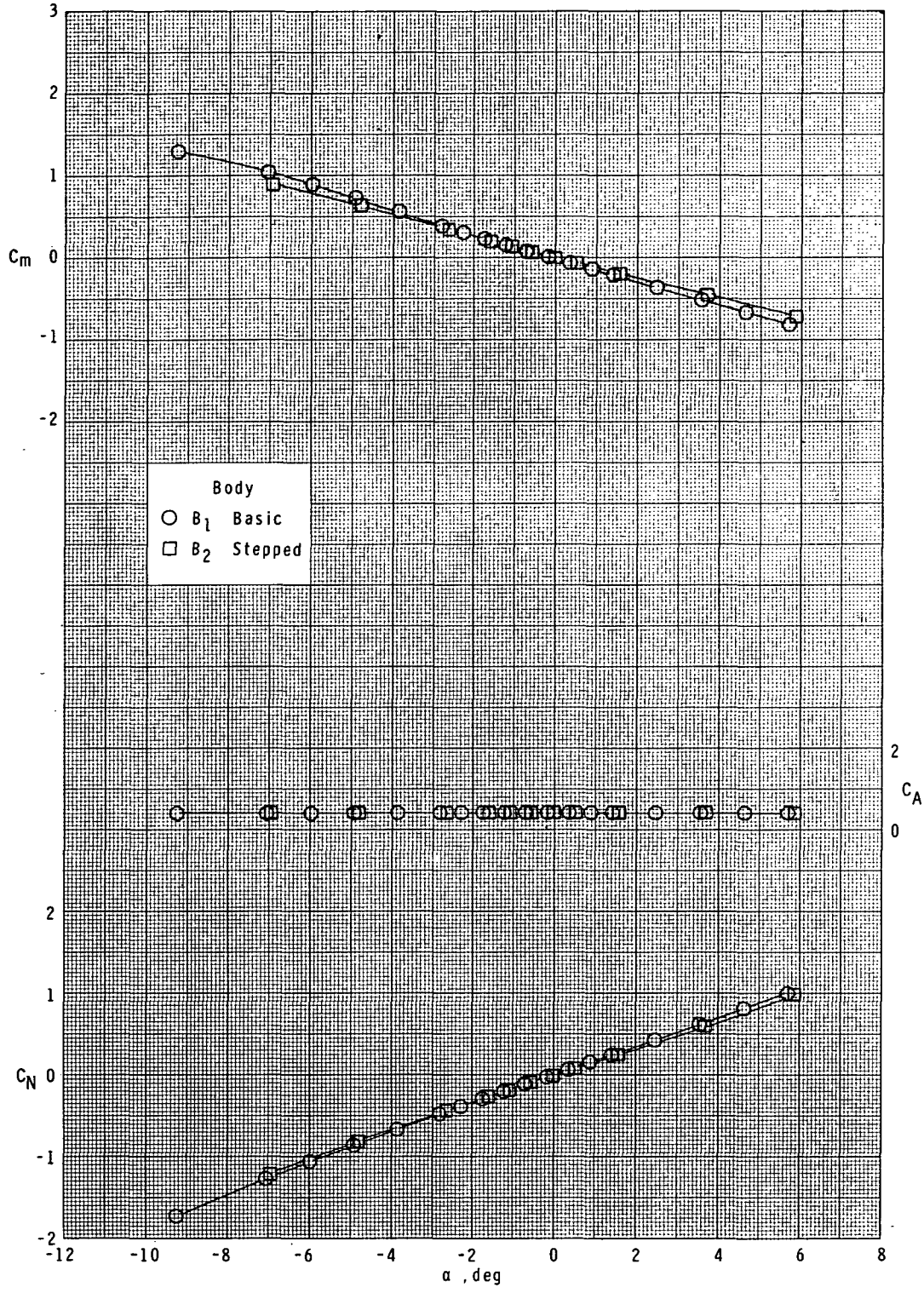

(b) M = 1.90.

Figure 21.- Continued.

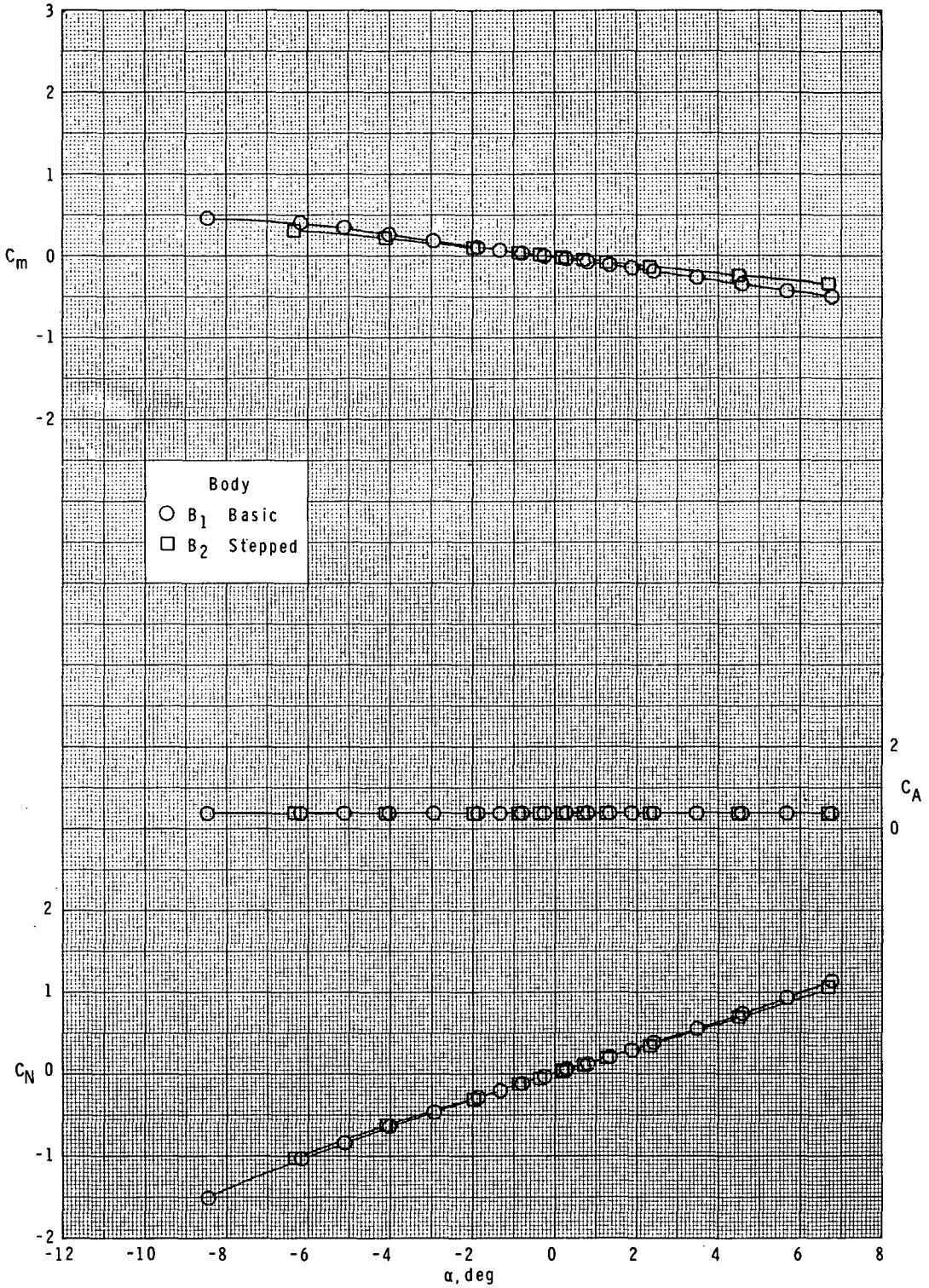

(c) M = 2.36.

Figure 21.- Continued.

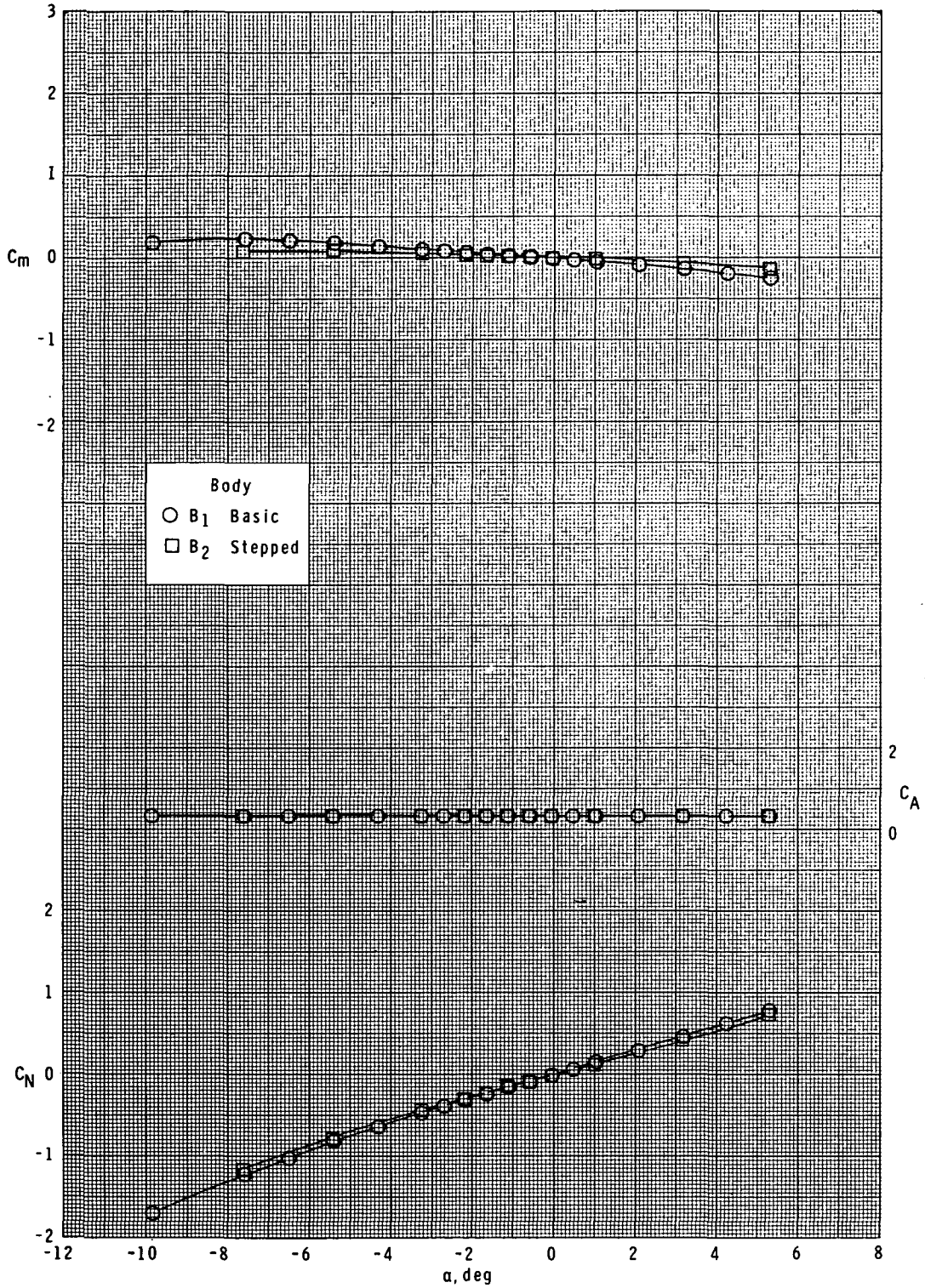

(d) M = 2.86.

Figure 21.- Concluded.

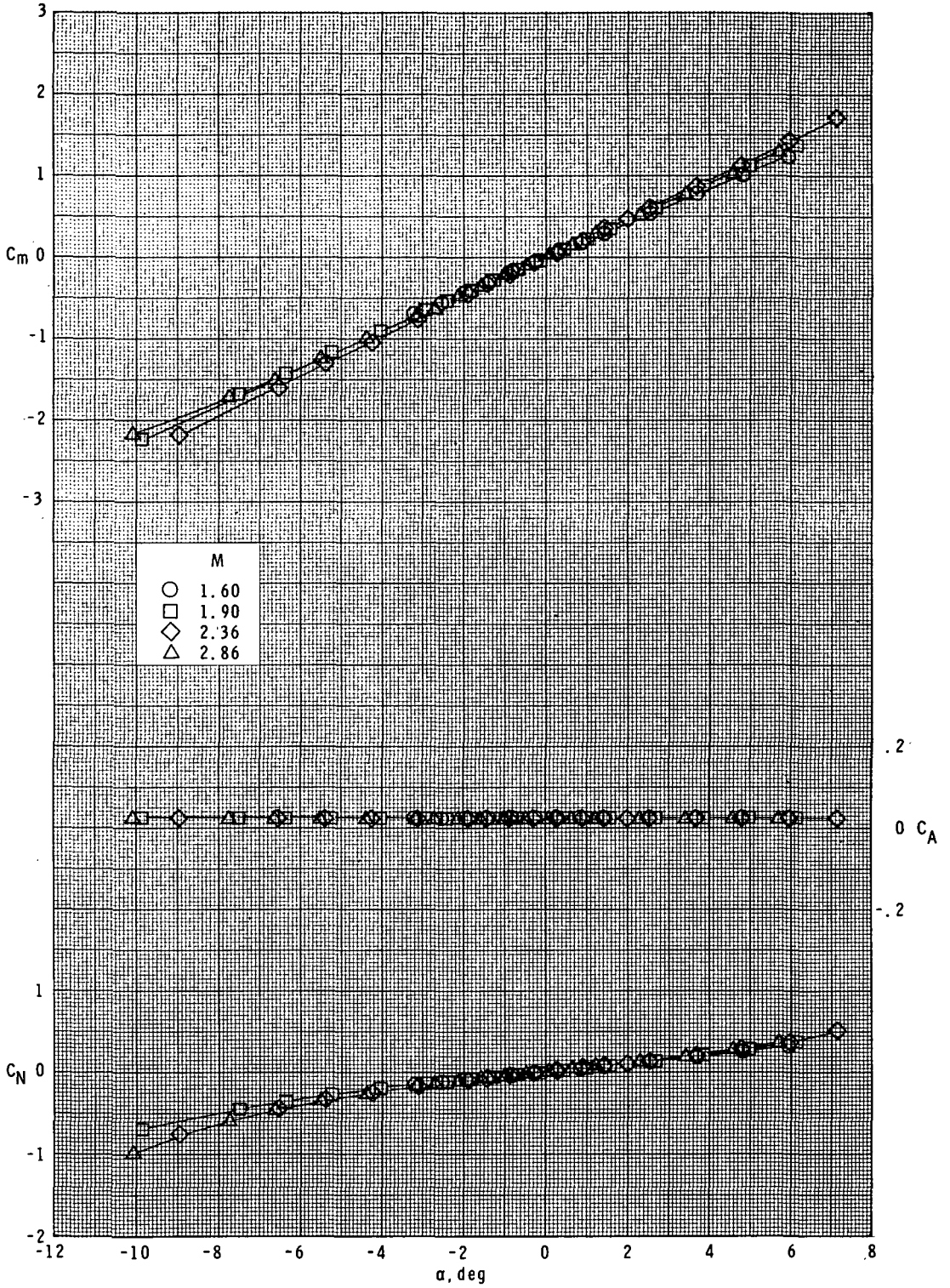

Figure 22.- Longitudinal characteristics of basic body (B_1).

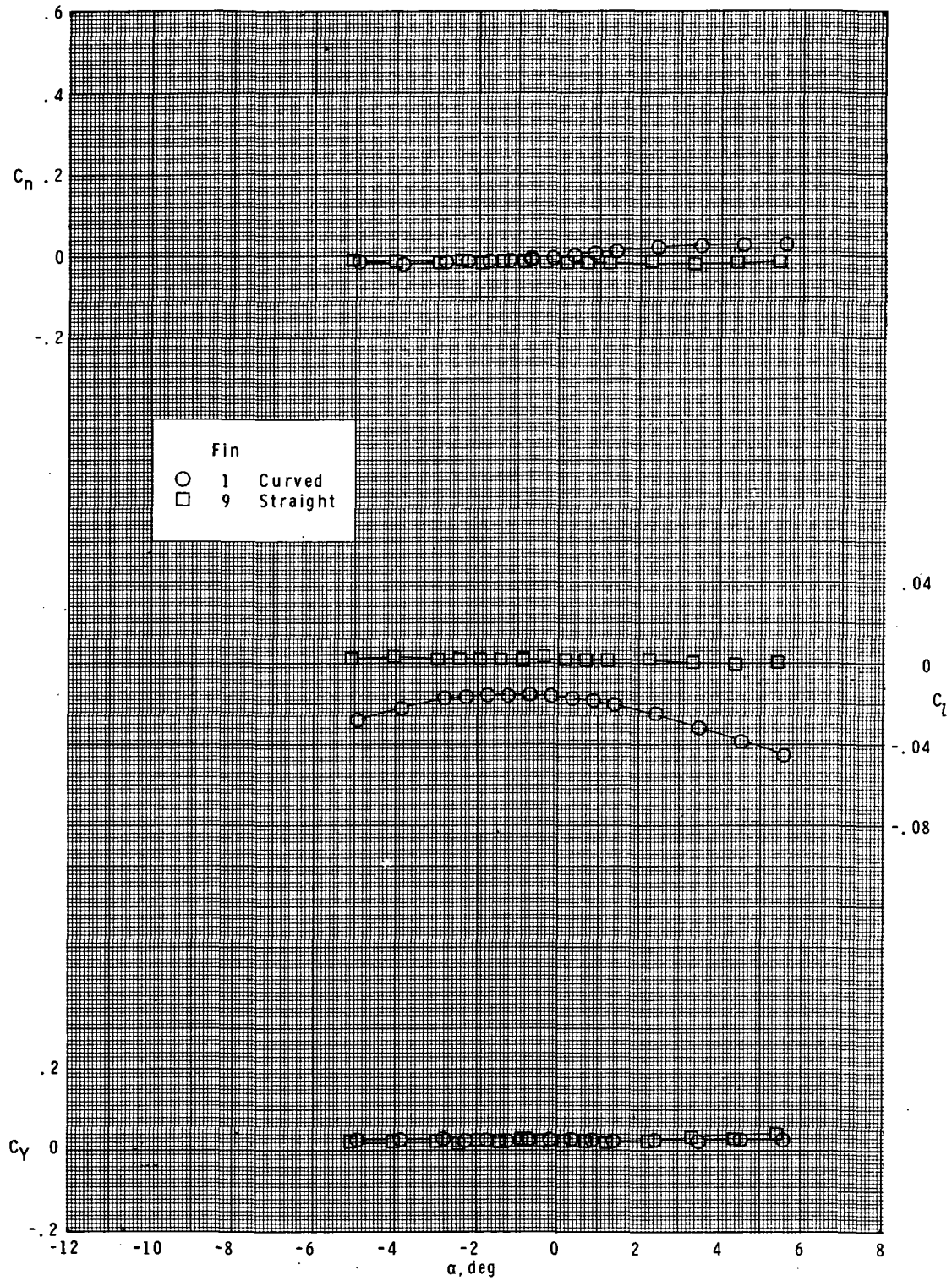

(a) M = 1.60.

Figure 23.- Effect of fin curvature on lateral characteristics. Basic body (B_1); long-chord fins (F_1 and F_9); $\phi = 0^o$.

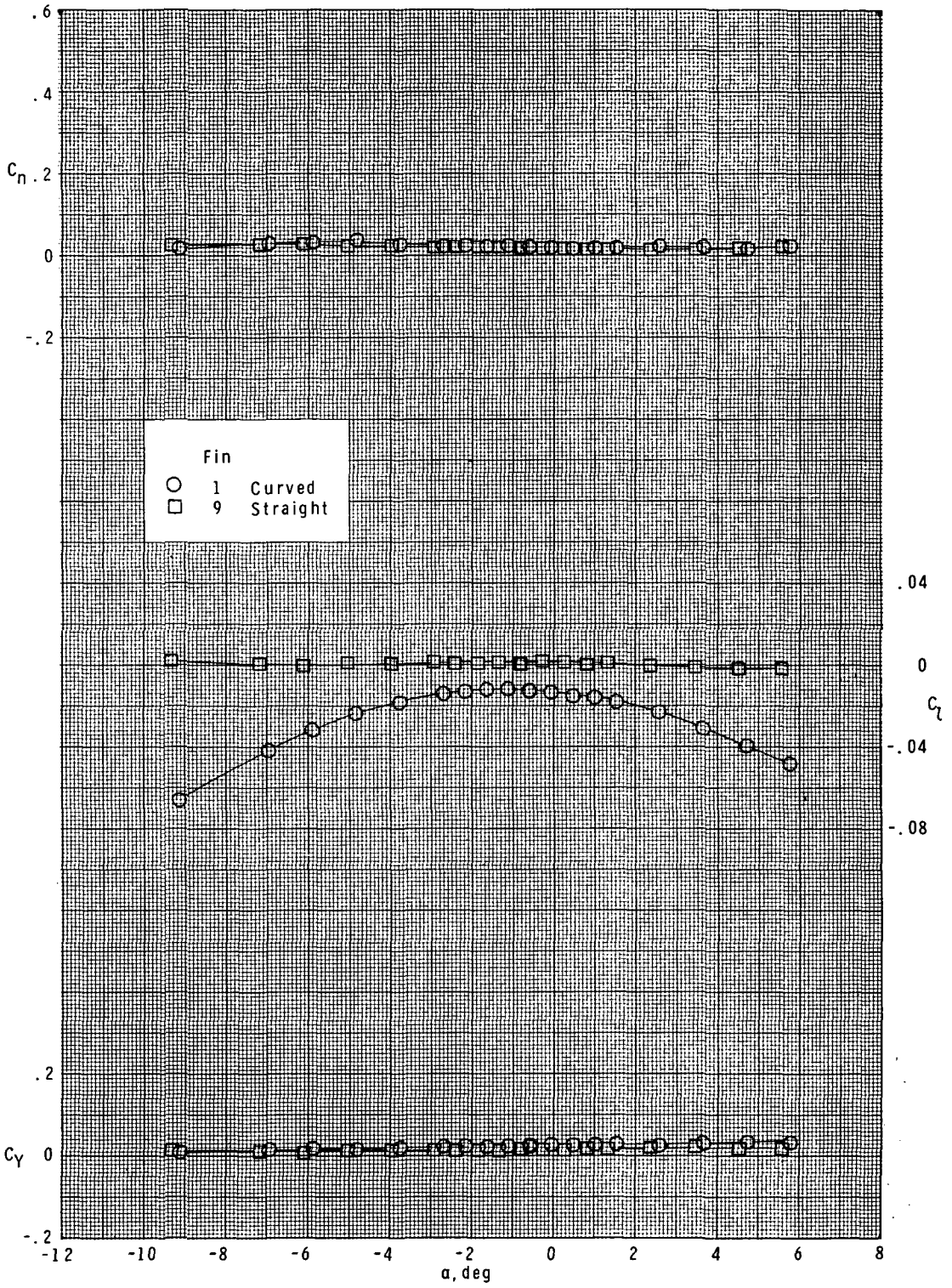

(b) M = 1.90.

Figure 23.- Continued.

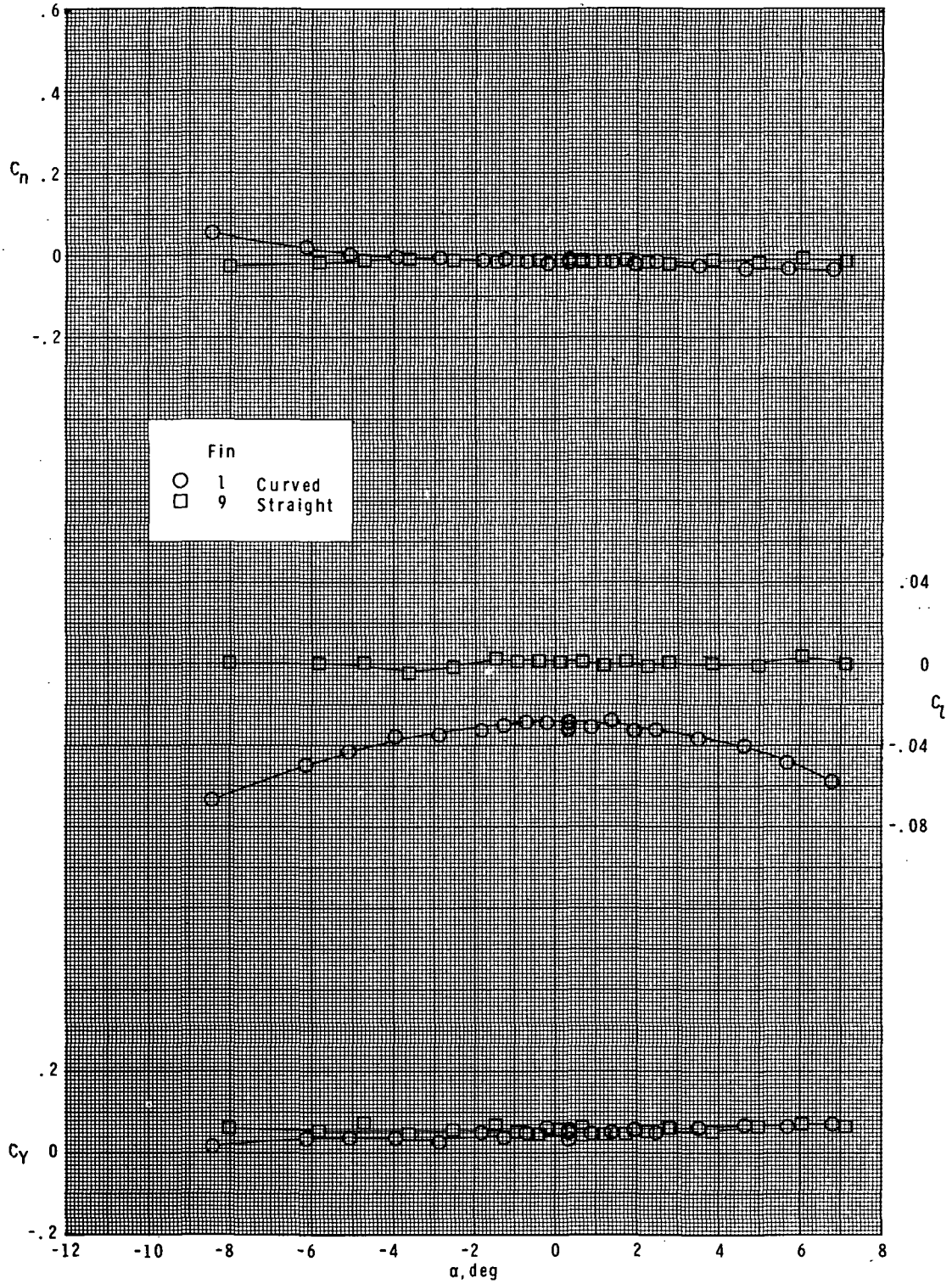

(c) M = 2.36.

Figure 23.- Continued.

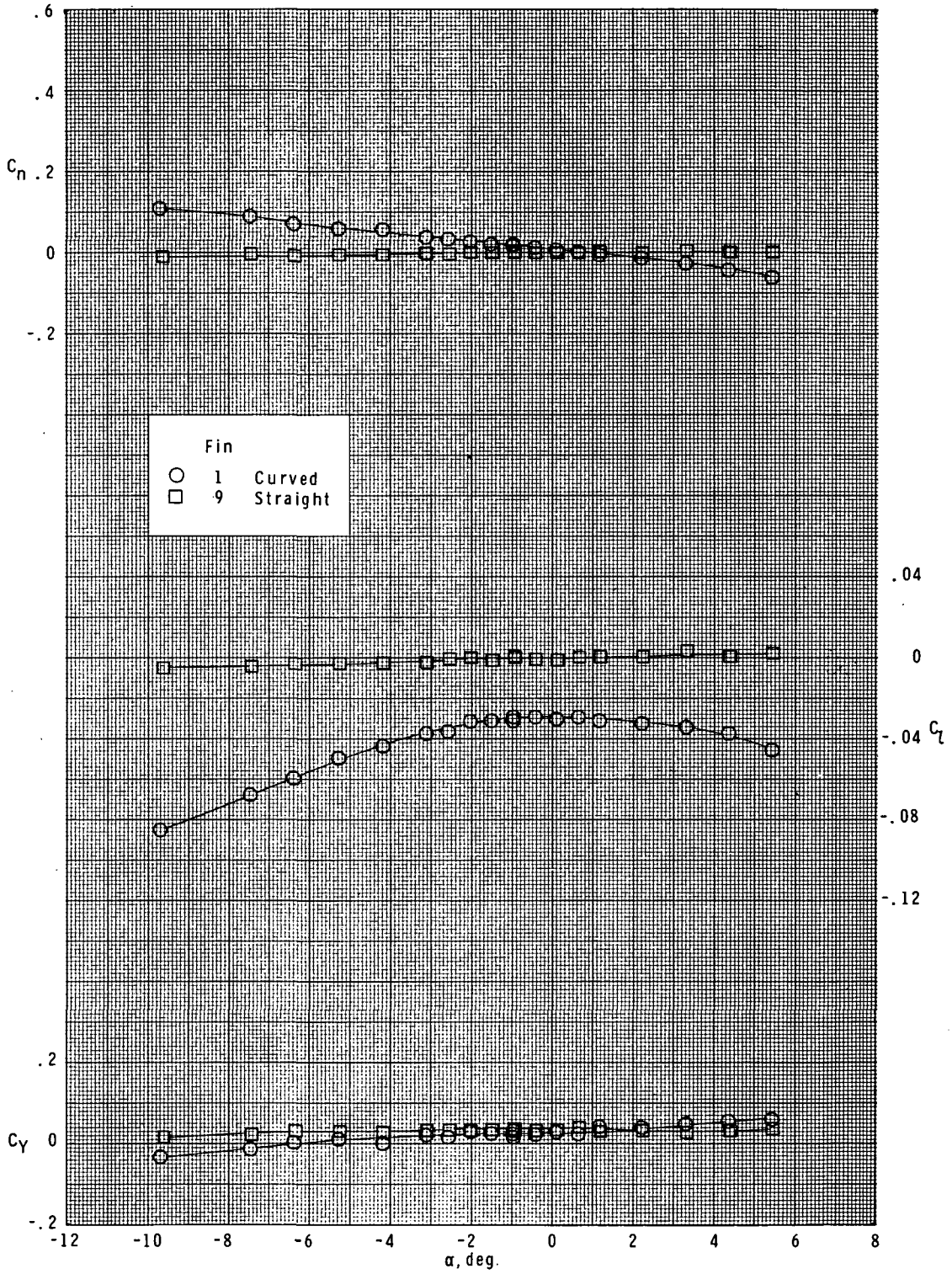

(d) M = 2.86.

Figure 23.- Concluded.

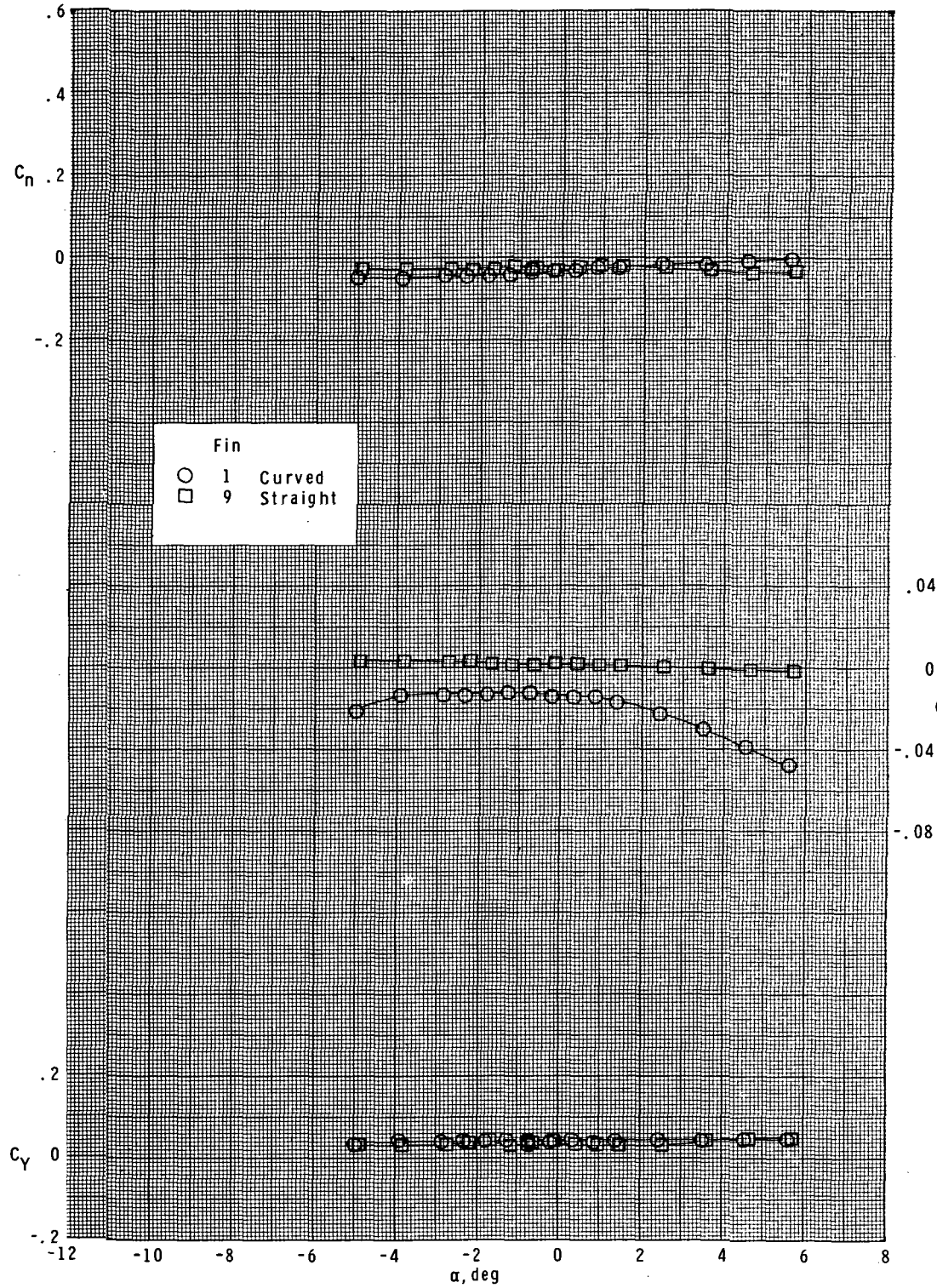

(a) M = 1.60.

Figure 24.- Effect of fin curvature on lateral characteristics. Basic body (B_1); long-chord fins (F_1 and F_9); $\phi = 45^o$.

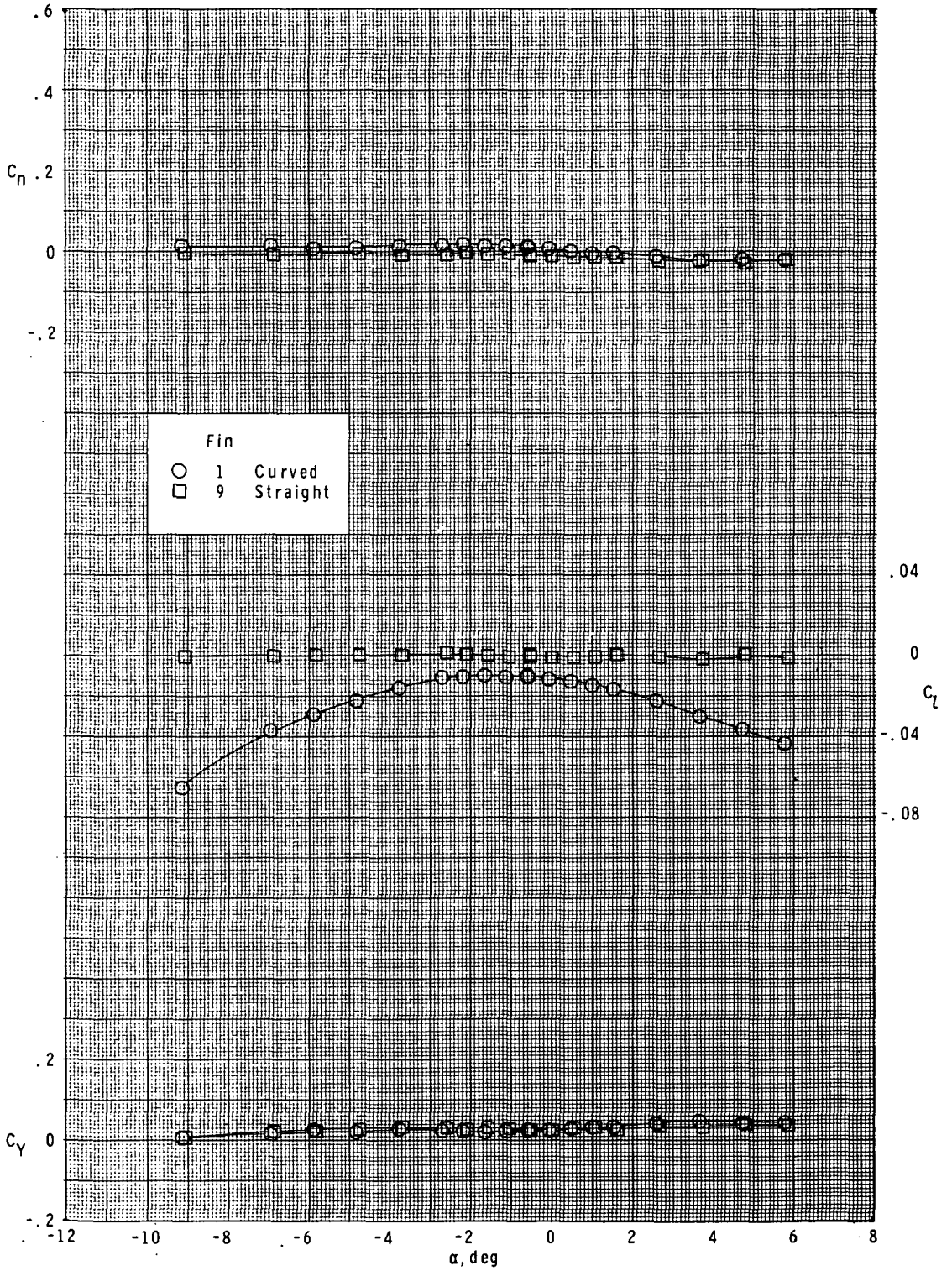

(b) M = 1.90.

Figure 24.- Continued.

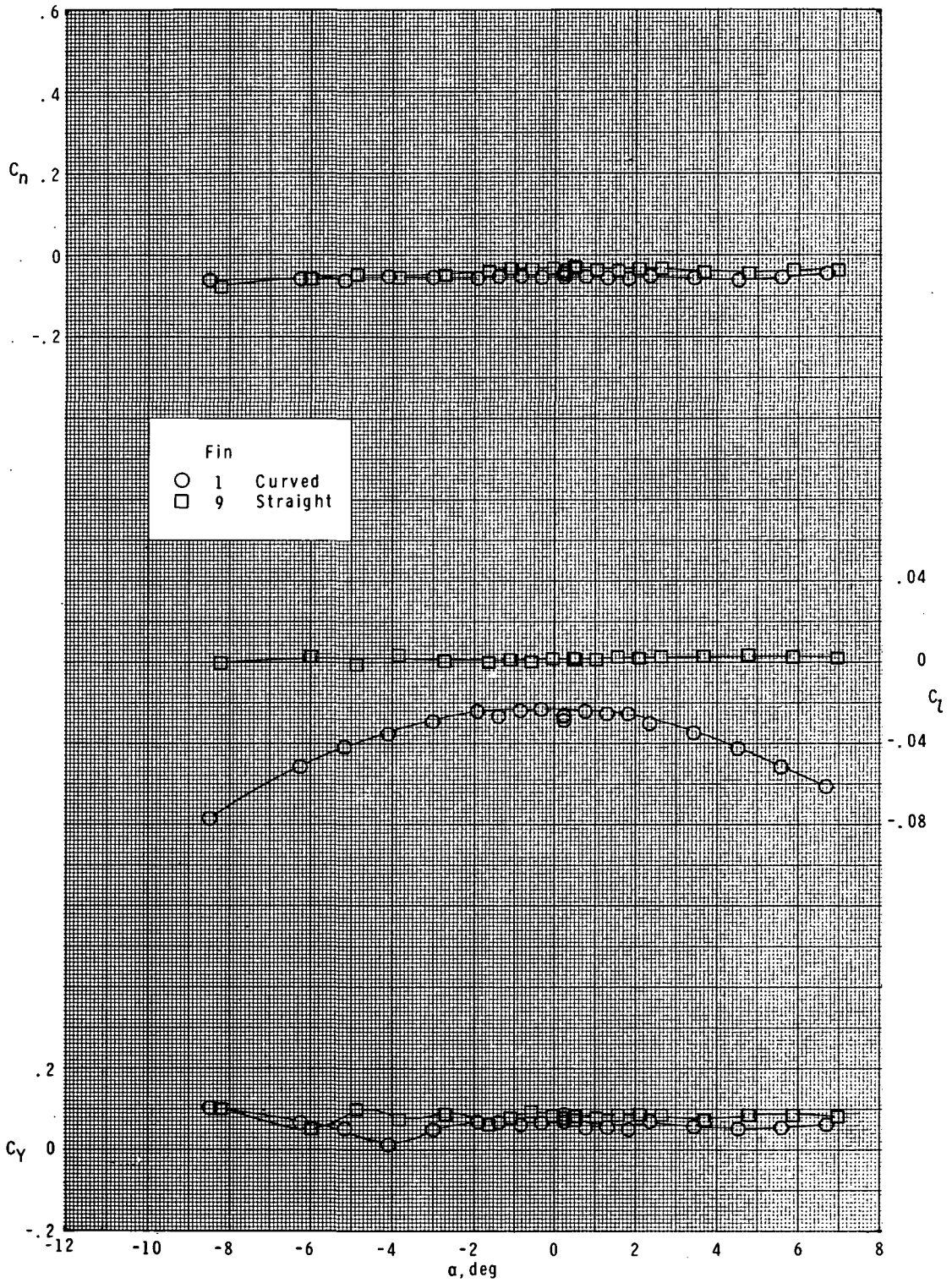

(c) M = 2.36.

Figure 24.- Continued.

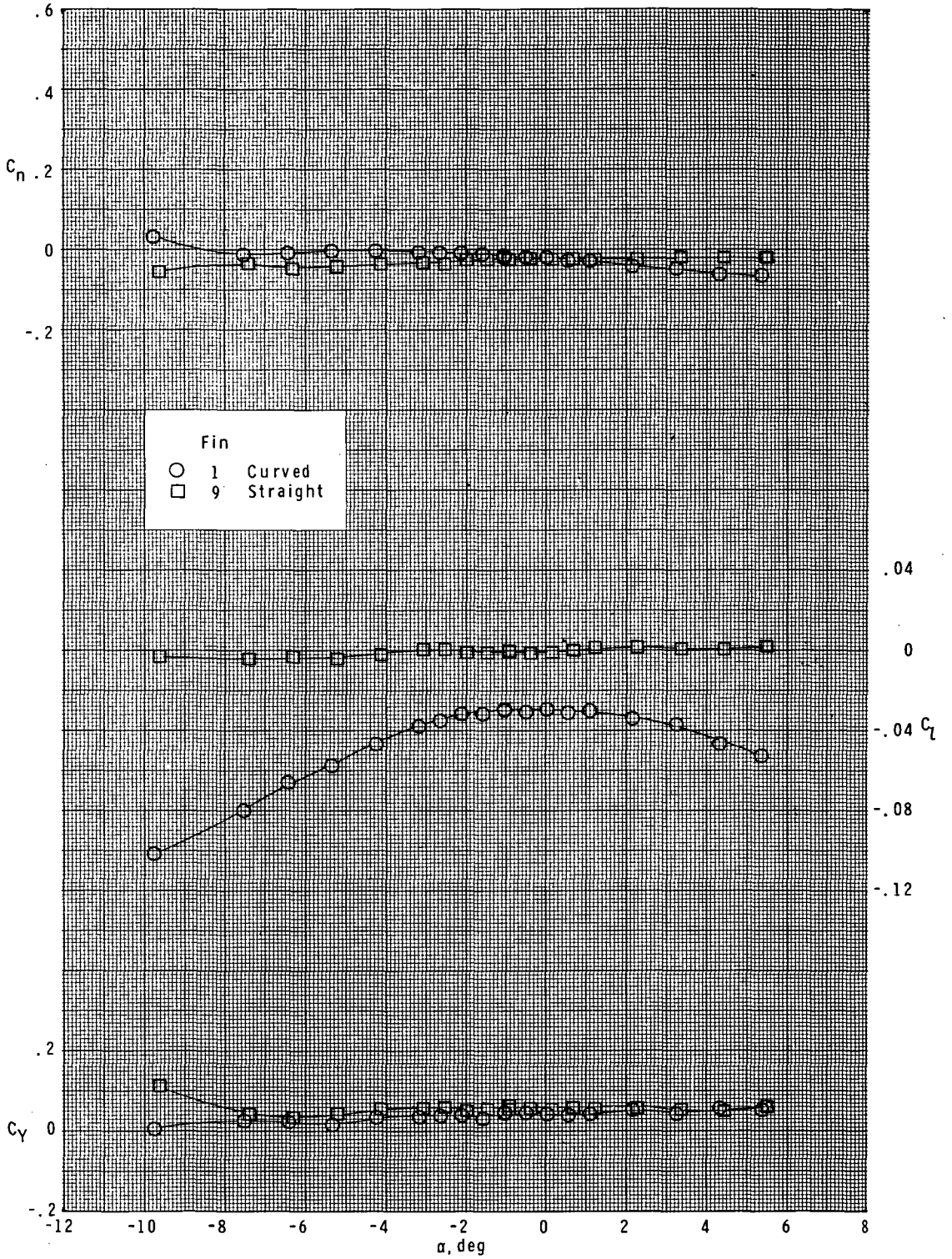

(d) M = 2.86.

Figure 24.- Concluded.

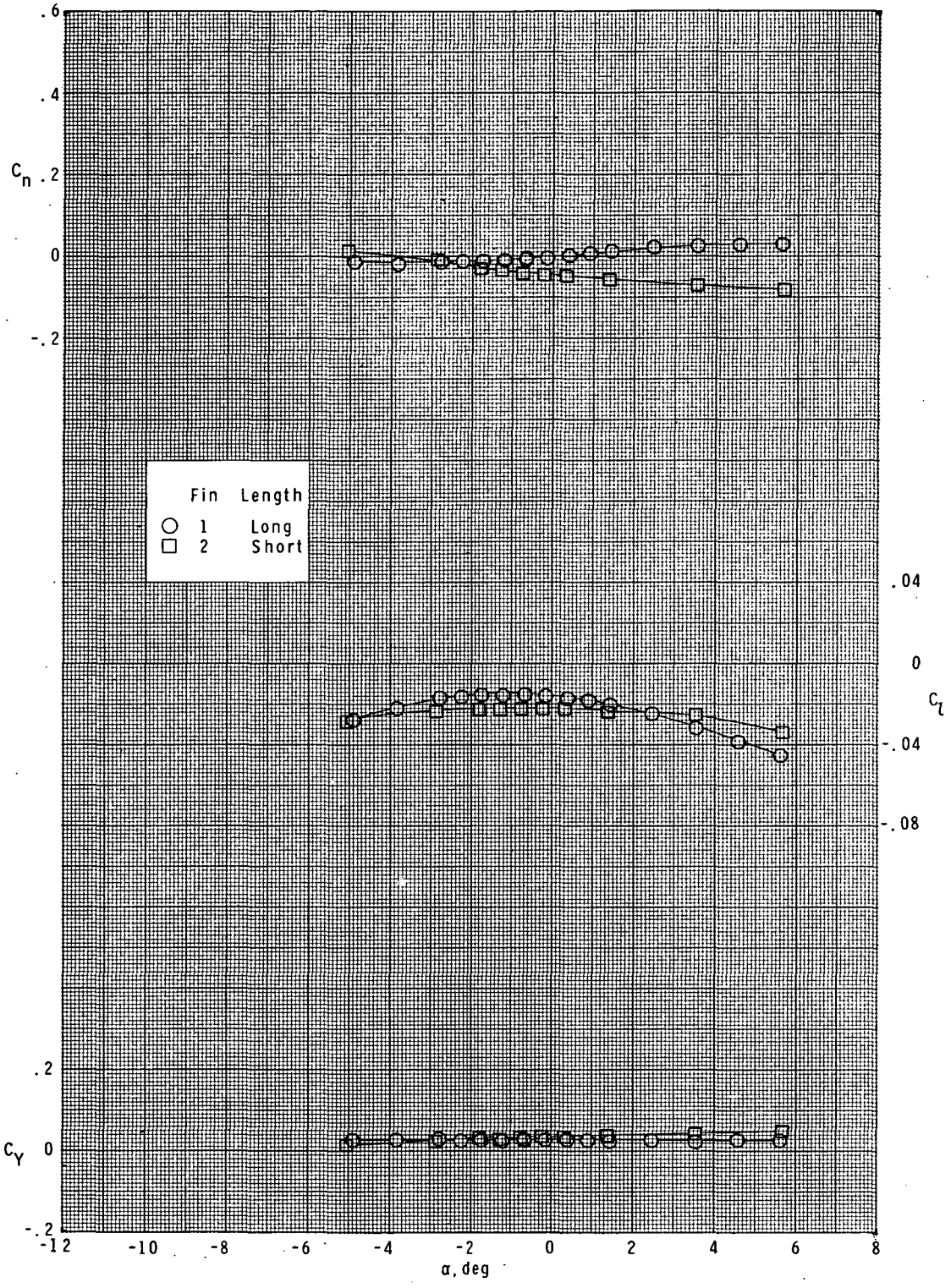

(a) M = 1.60.

Figure 25.- Effect of fin length on lateral characteristics. Basic body (B_1); unswept curved fins (F_1 and F_2); $\phi = 0^o$.

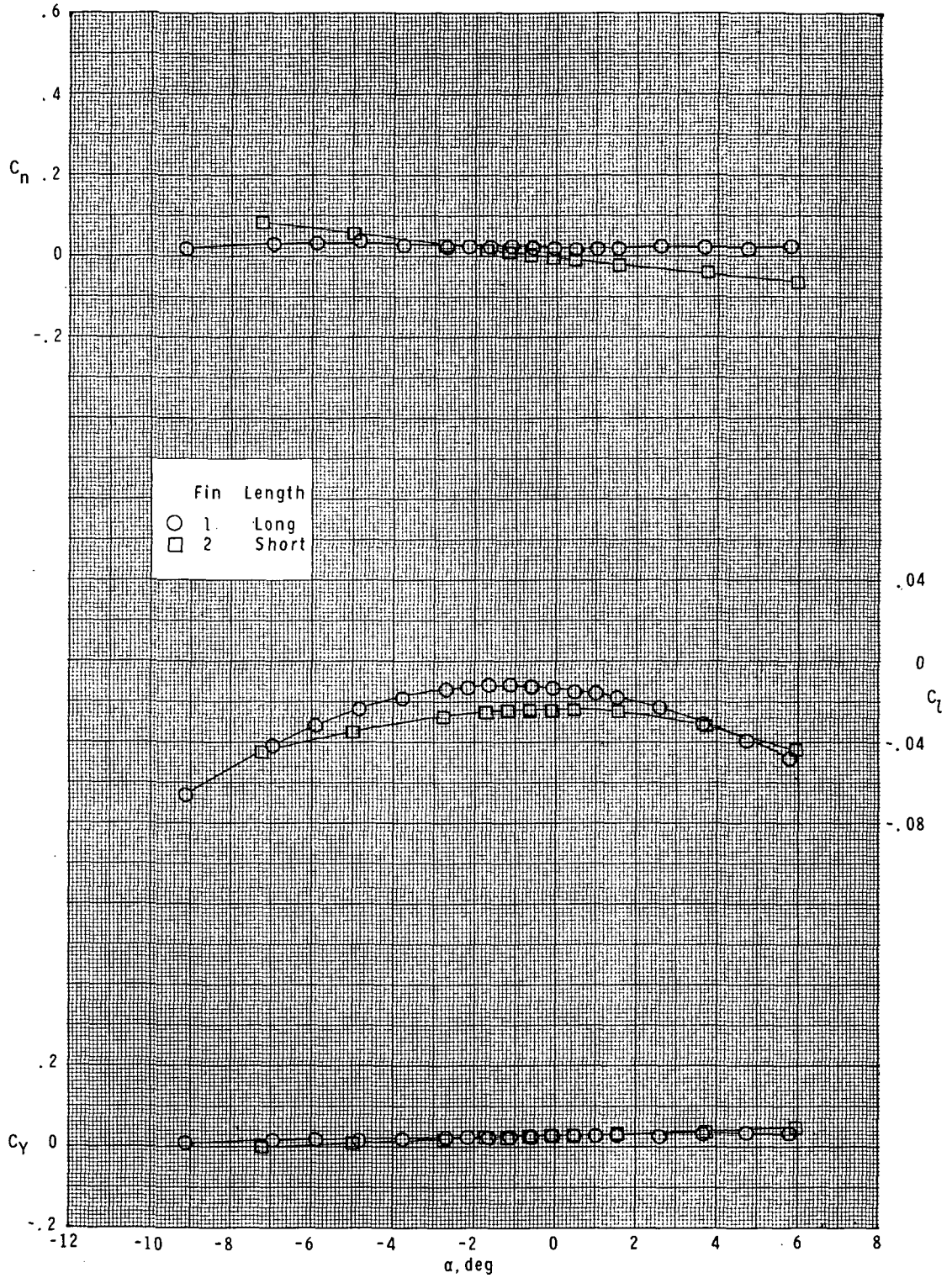

(b) M = 1.90.

Figure 25.- Continued.

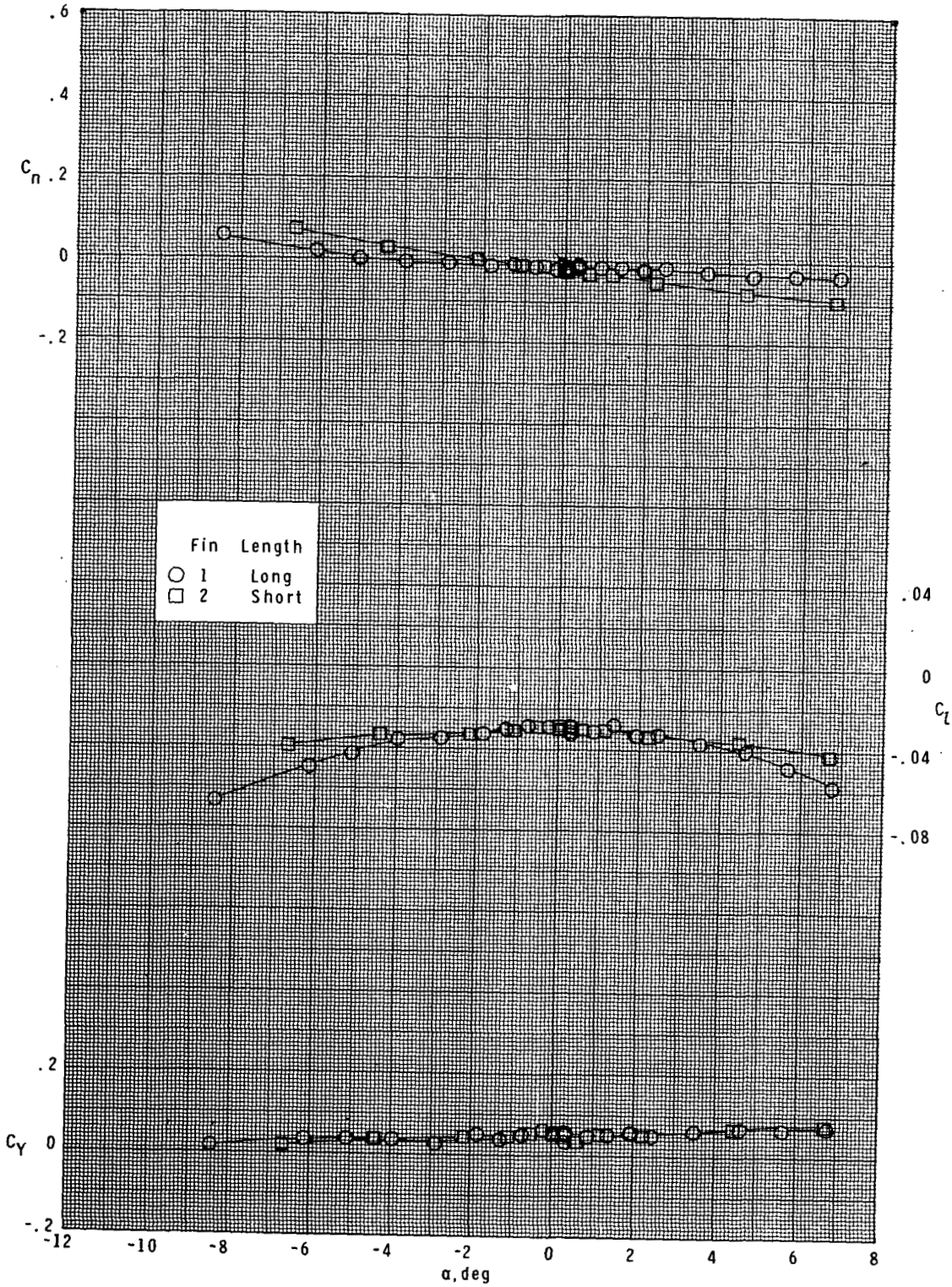

(c) M = 2.36.

Figure 25.- Continued.

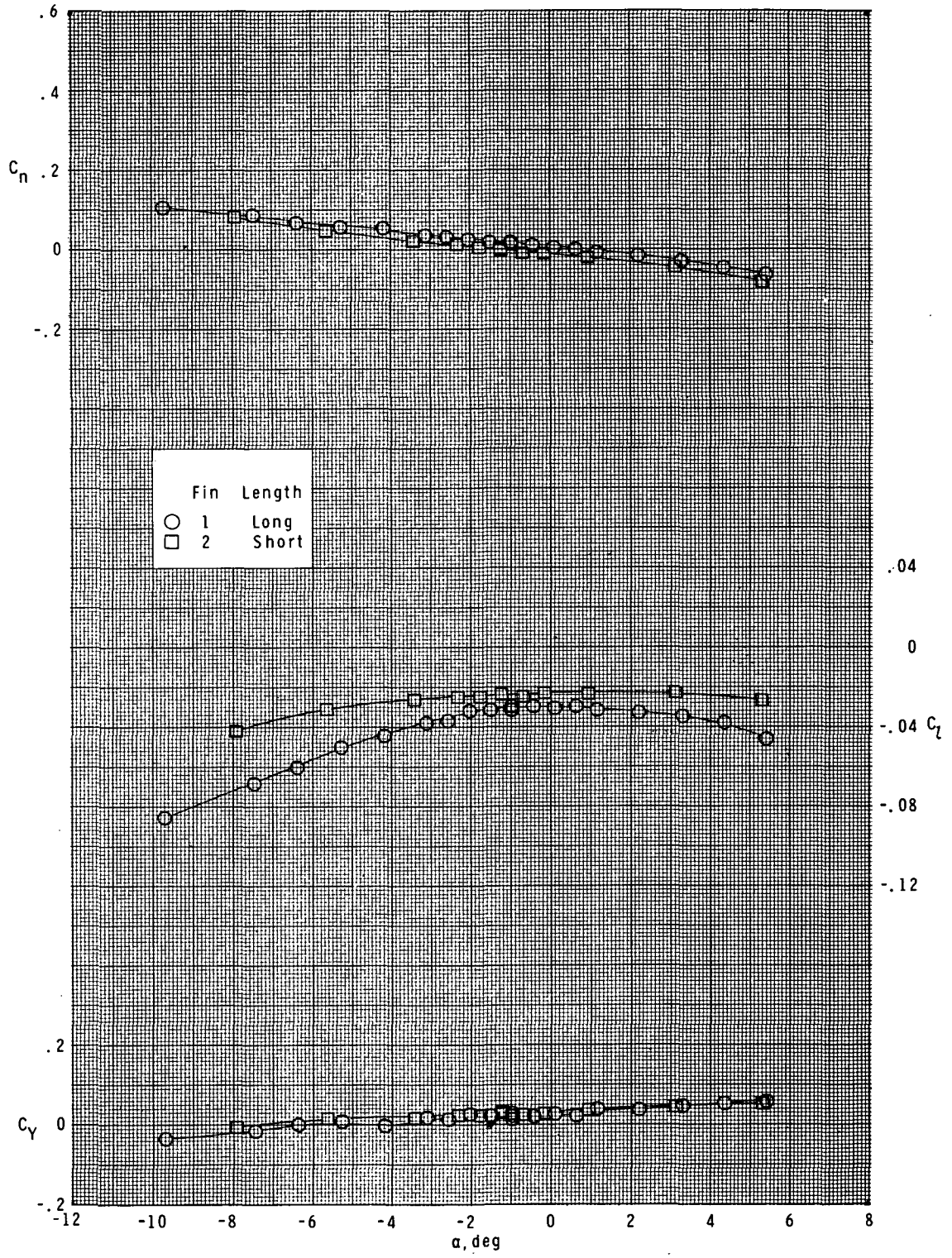

(d) M = 2.86.

Figure 25.- Concluded.

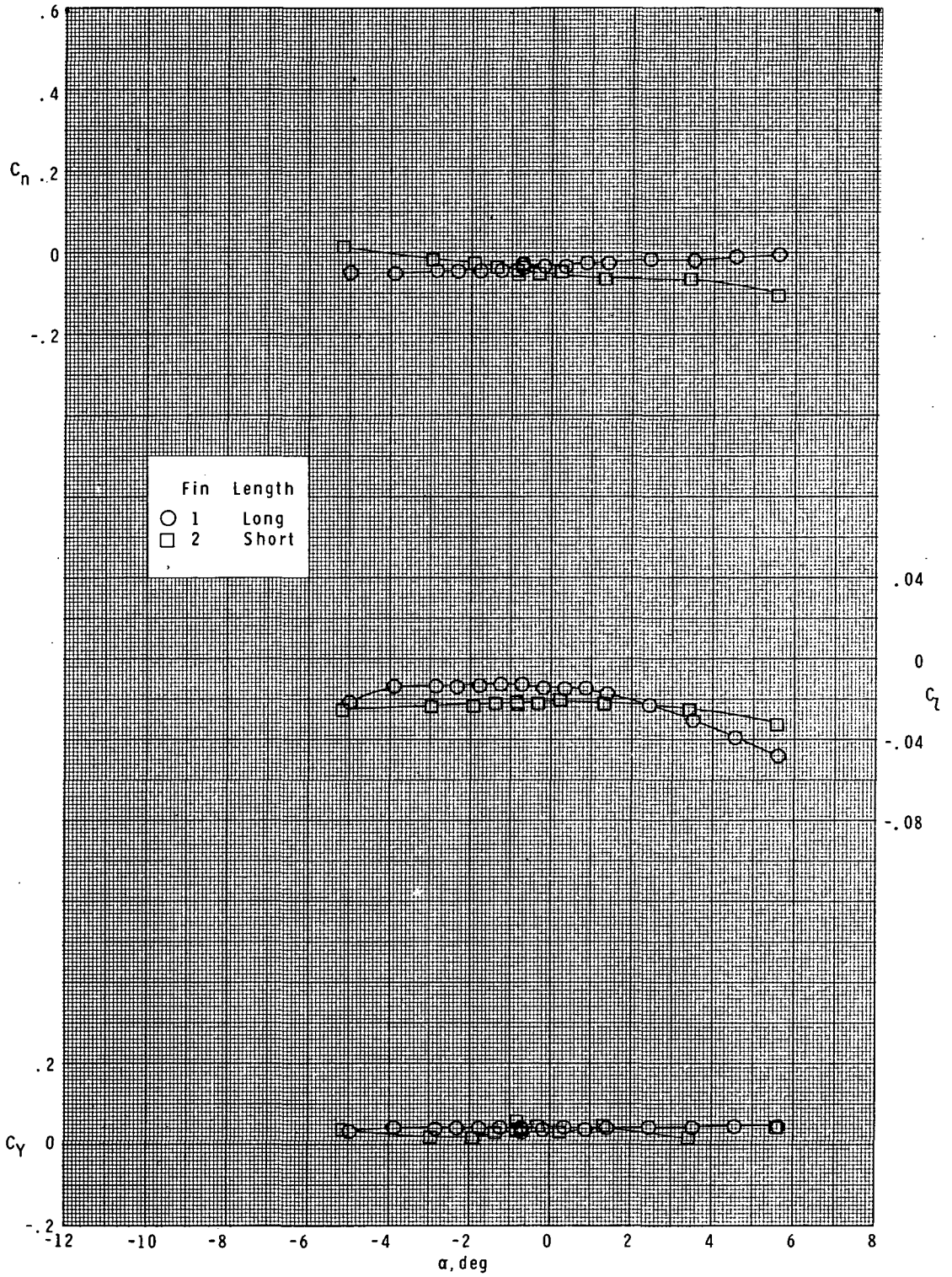

(a) M = 1.60.

Figure 26.- Effect of fin length on lateral characteristics. Basic body (B_1); unswept curved fins (F_1 and F_2); $\phi = 45^\circ$.

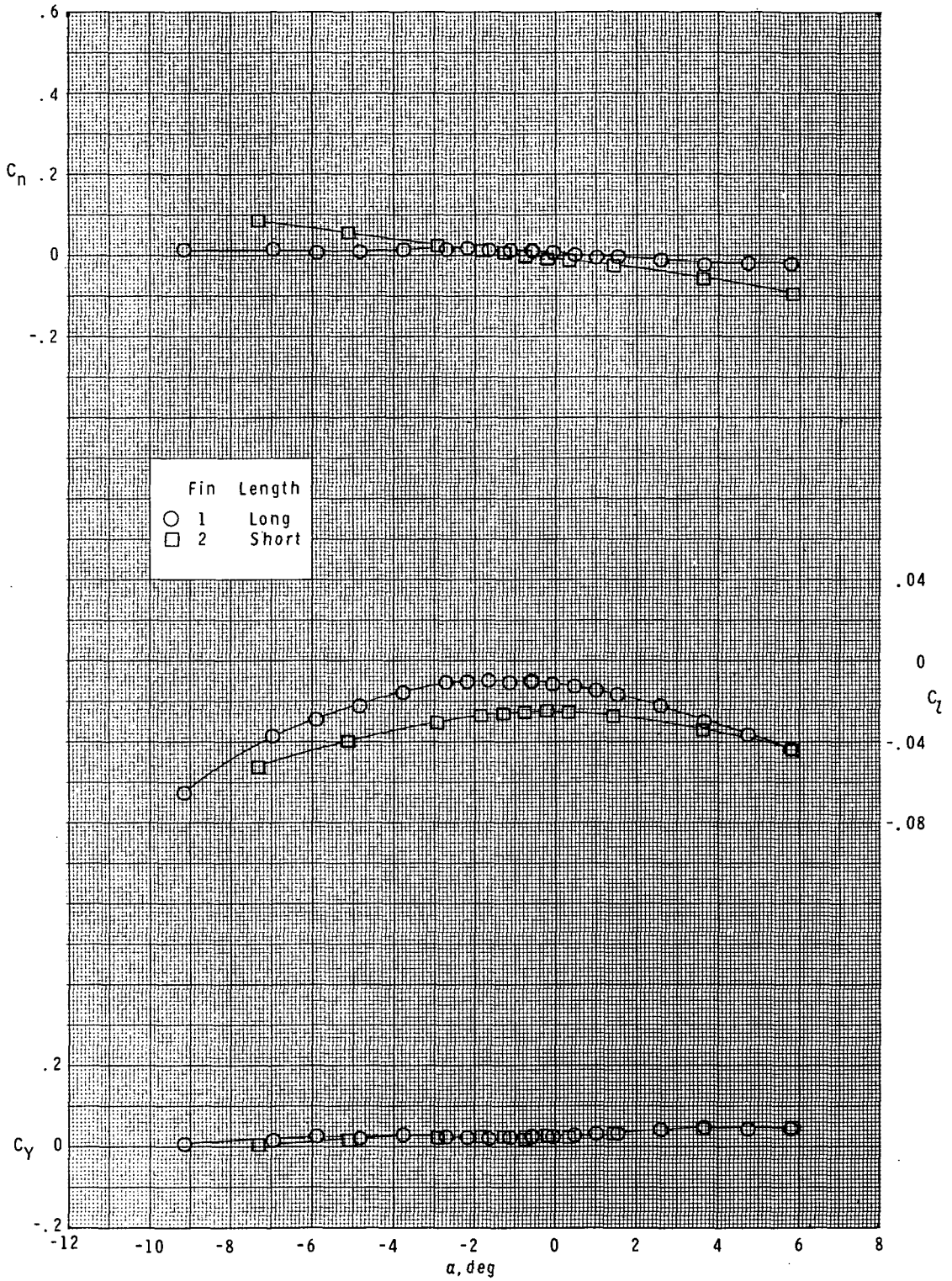

(b) M = 1.90.

Figure 26.- Continued.

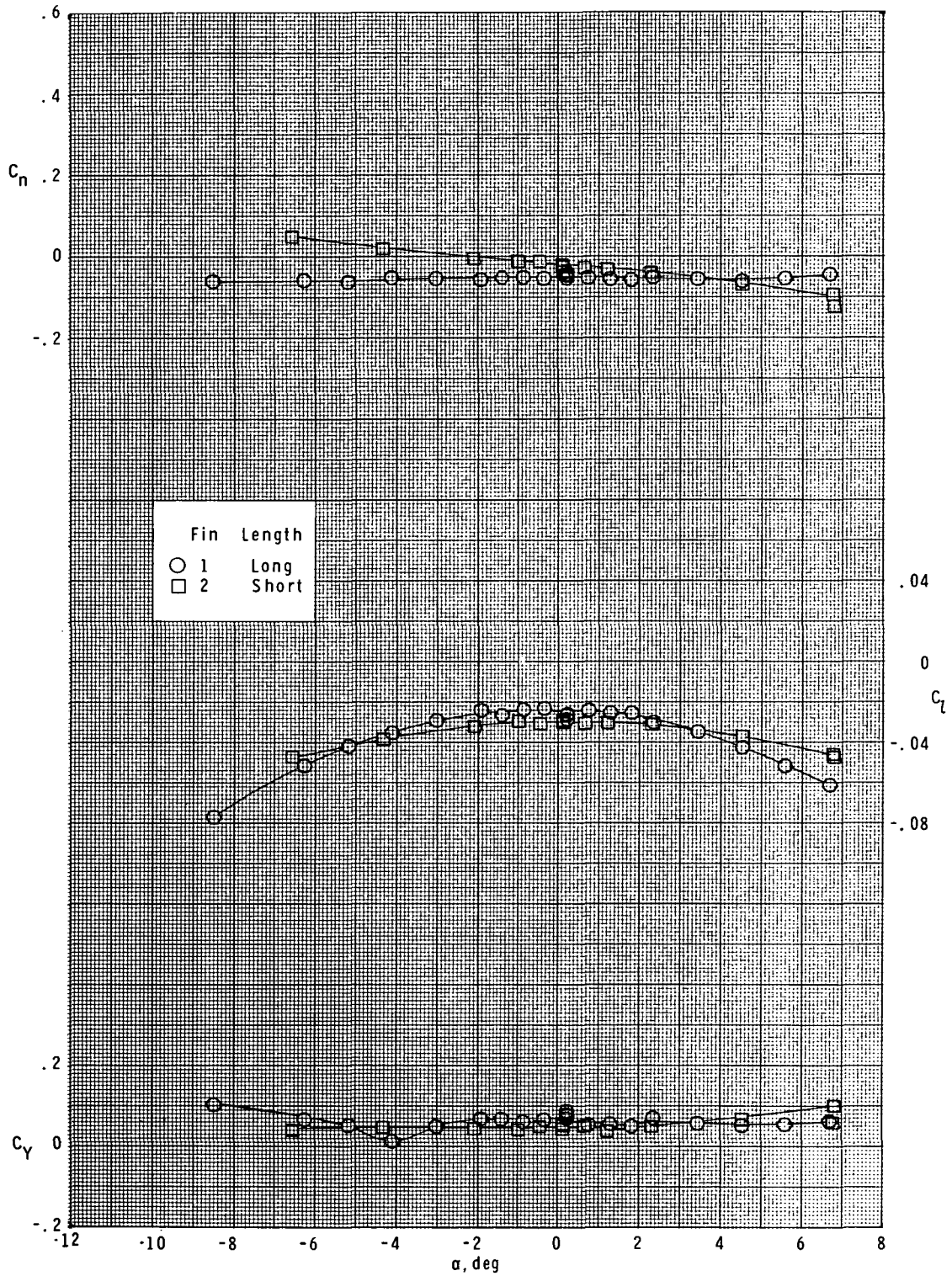

(c) M = 2.36.

Figure 26.- Continued.

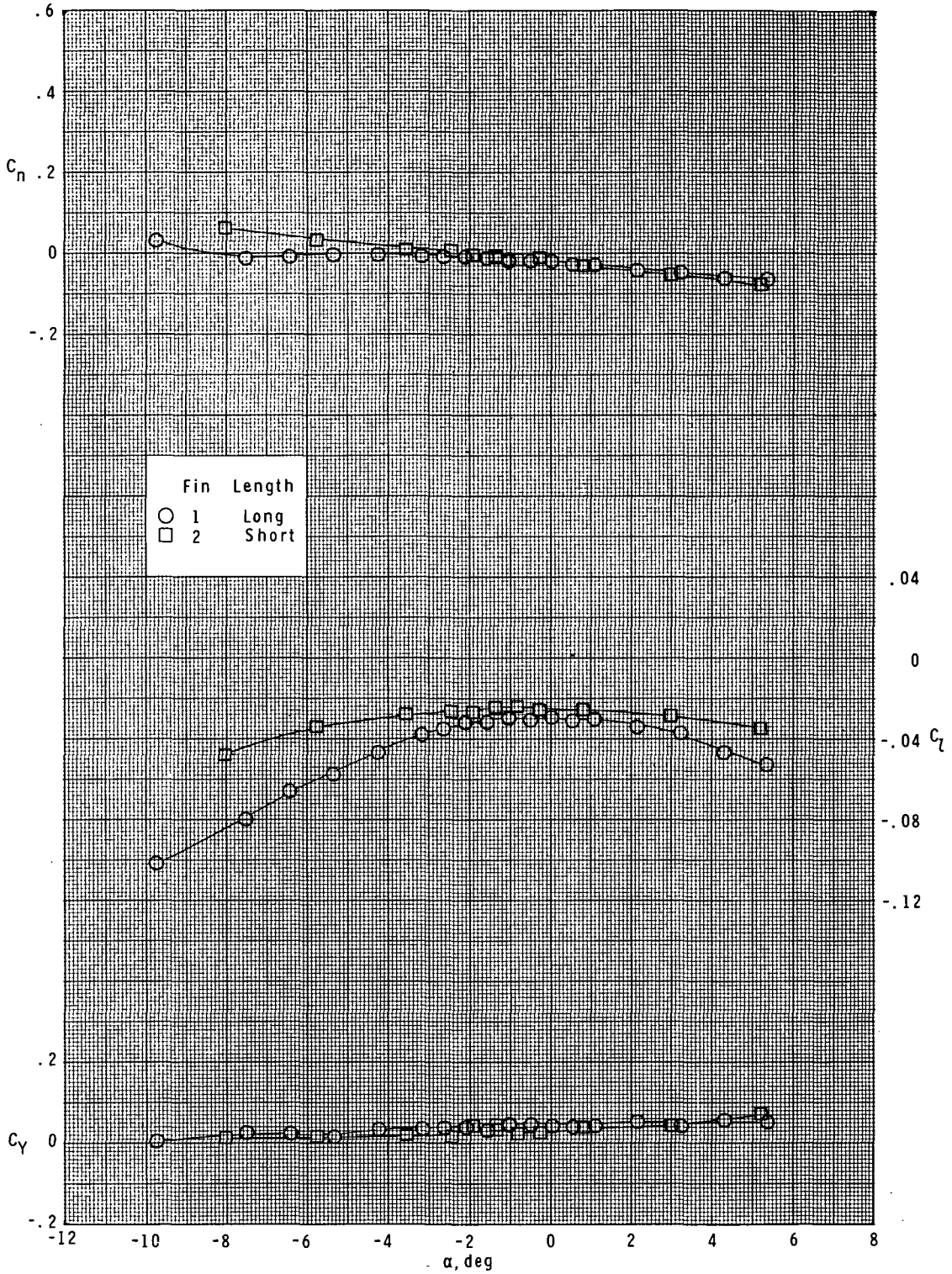

(d) M = 2.86.

Figure 26.- Concluded.

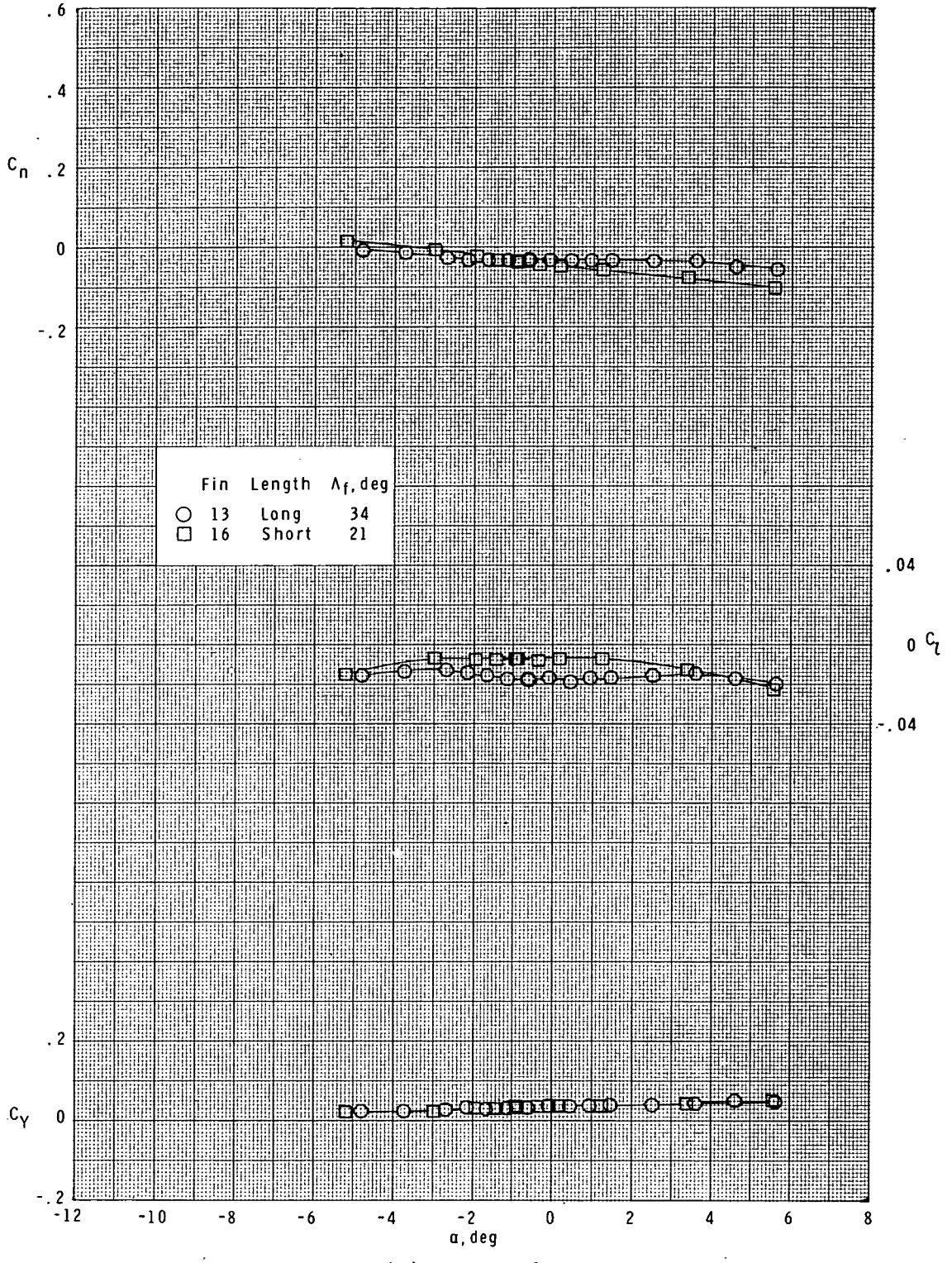

(a) M = 1.60.

Figure 27.- Effect of fin length on lateral characteristics. Basic body (B_1); swept curved fins (F_{13} and F_{16}); $\phi = 0^o$.

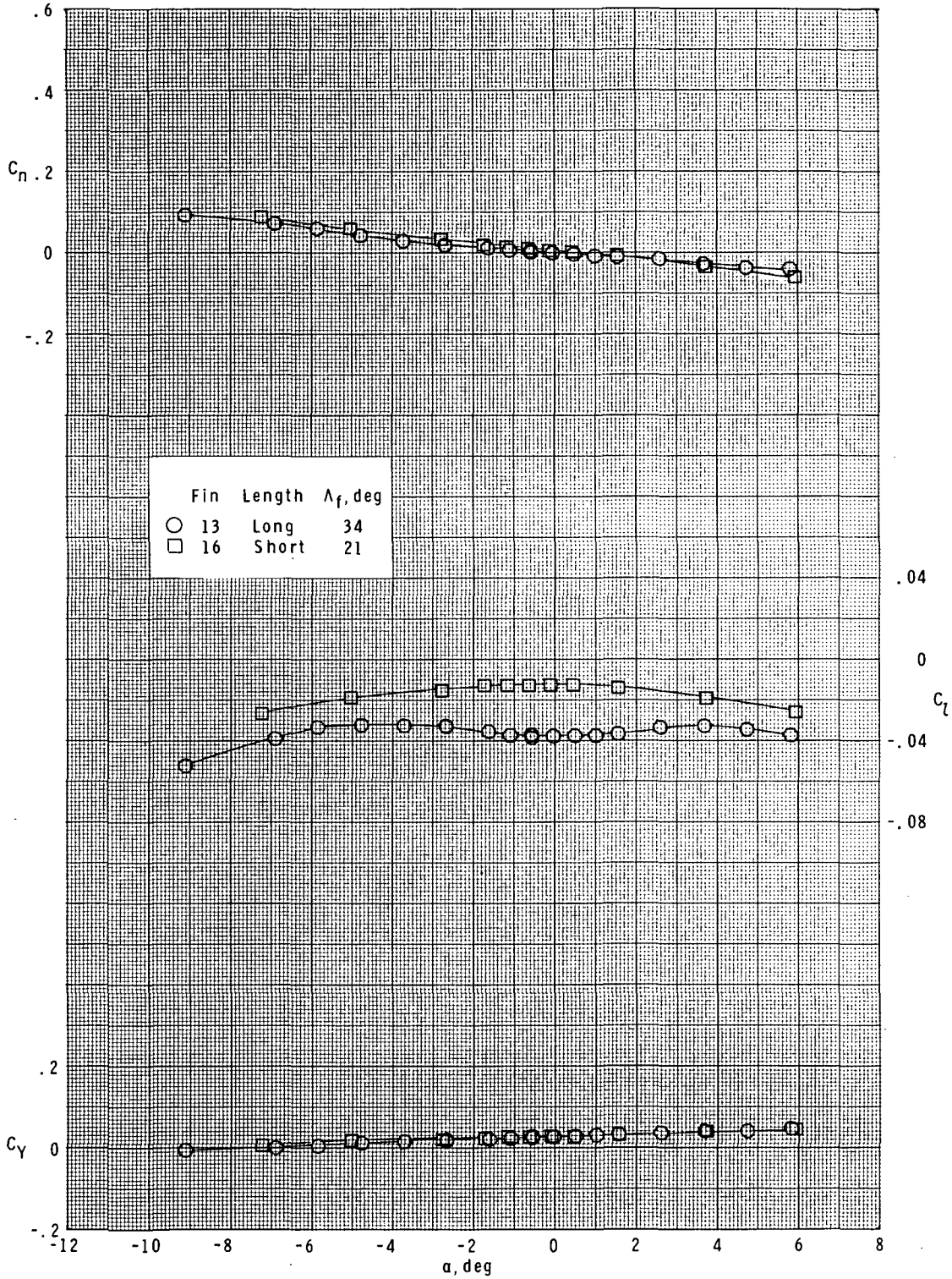

(b) M = 1.90.

Figure 27.- Continued.

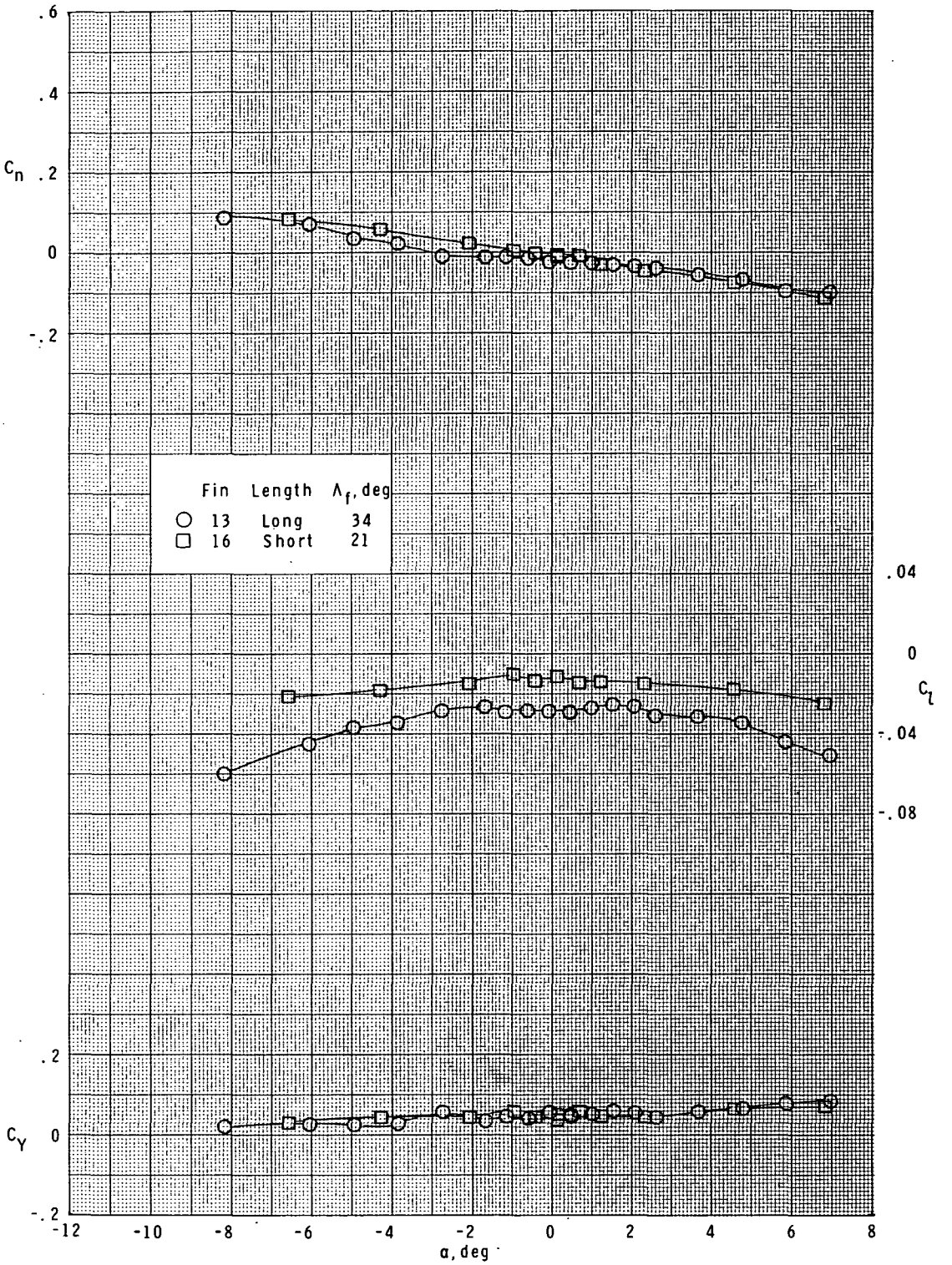

(c) M = 2.36.

Figure 27.- Continued.

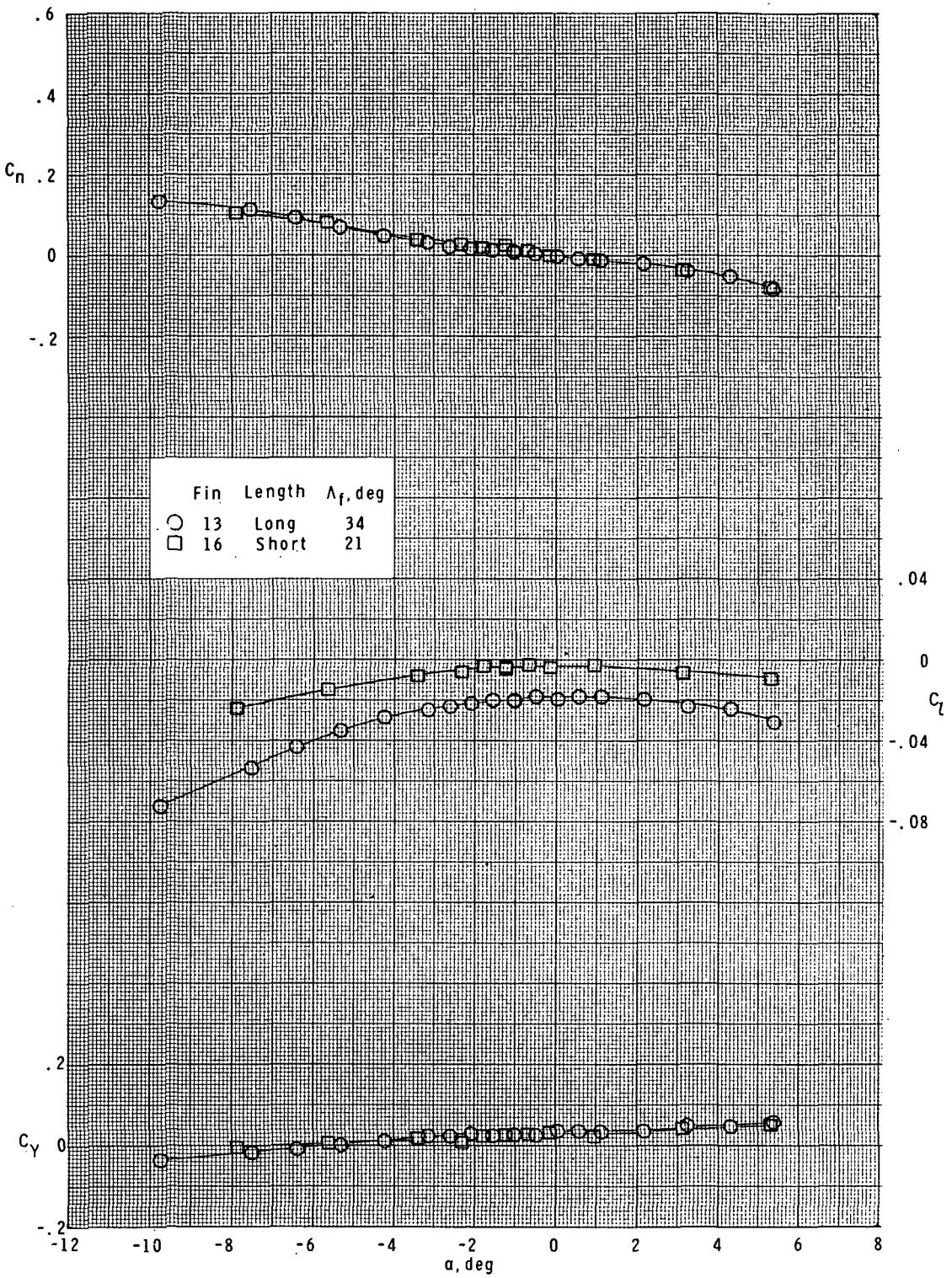

(d) M = 2.86.

Figure 27.- Concluded.

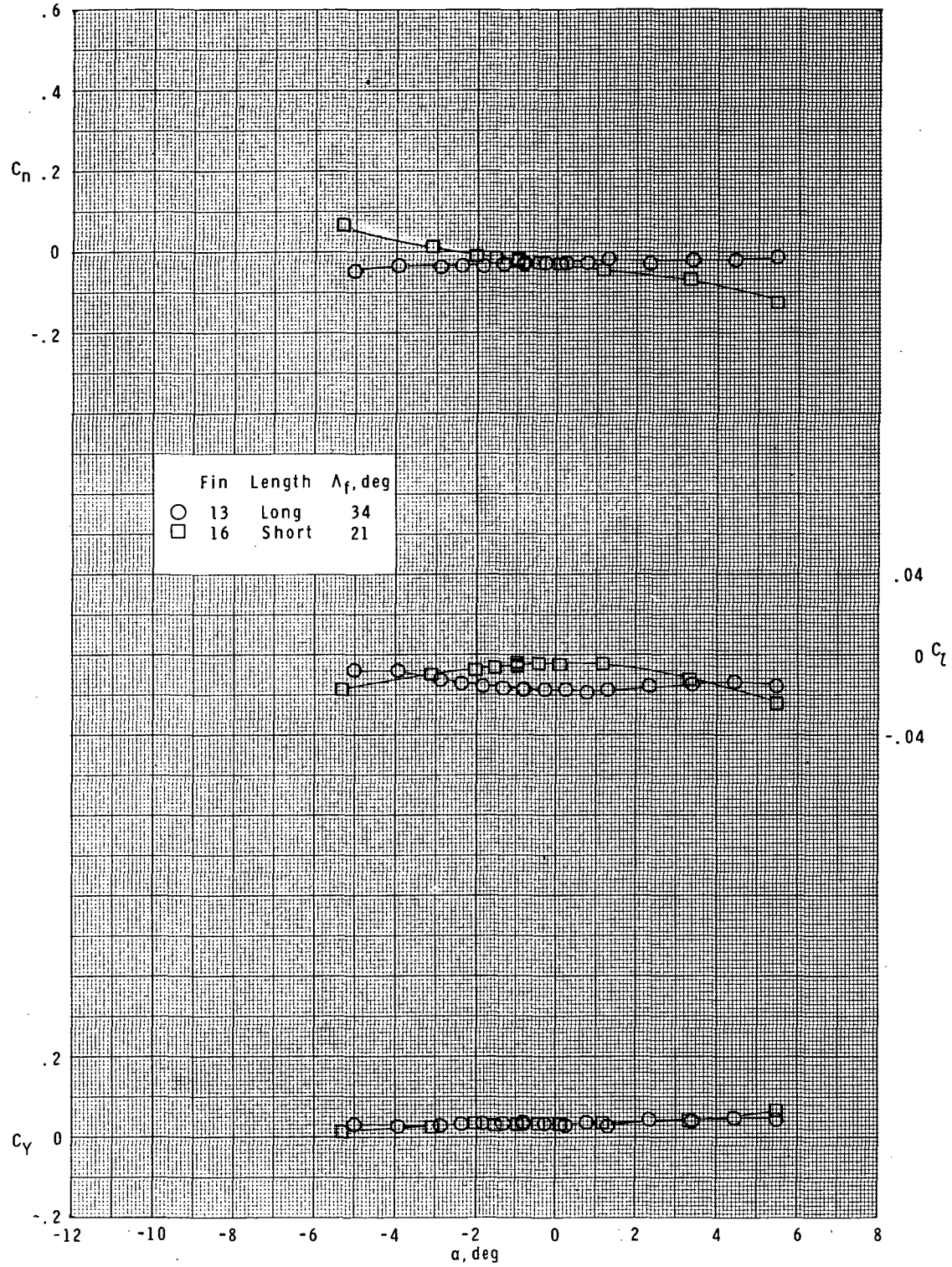

(a) M = 1.60.

Figure 28.- Effect of fin length on lateral characteristics. Basic body (B_1); swept curved fins (F_{13} and F_{16}); $\phi = 45^\circ$.

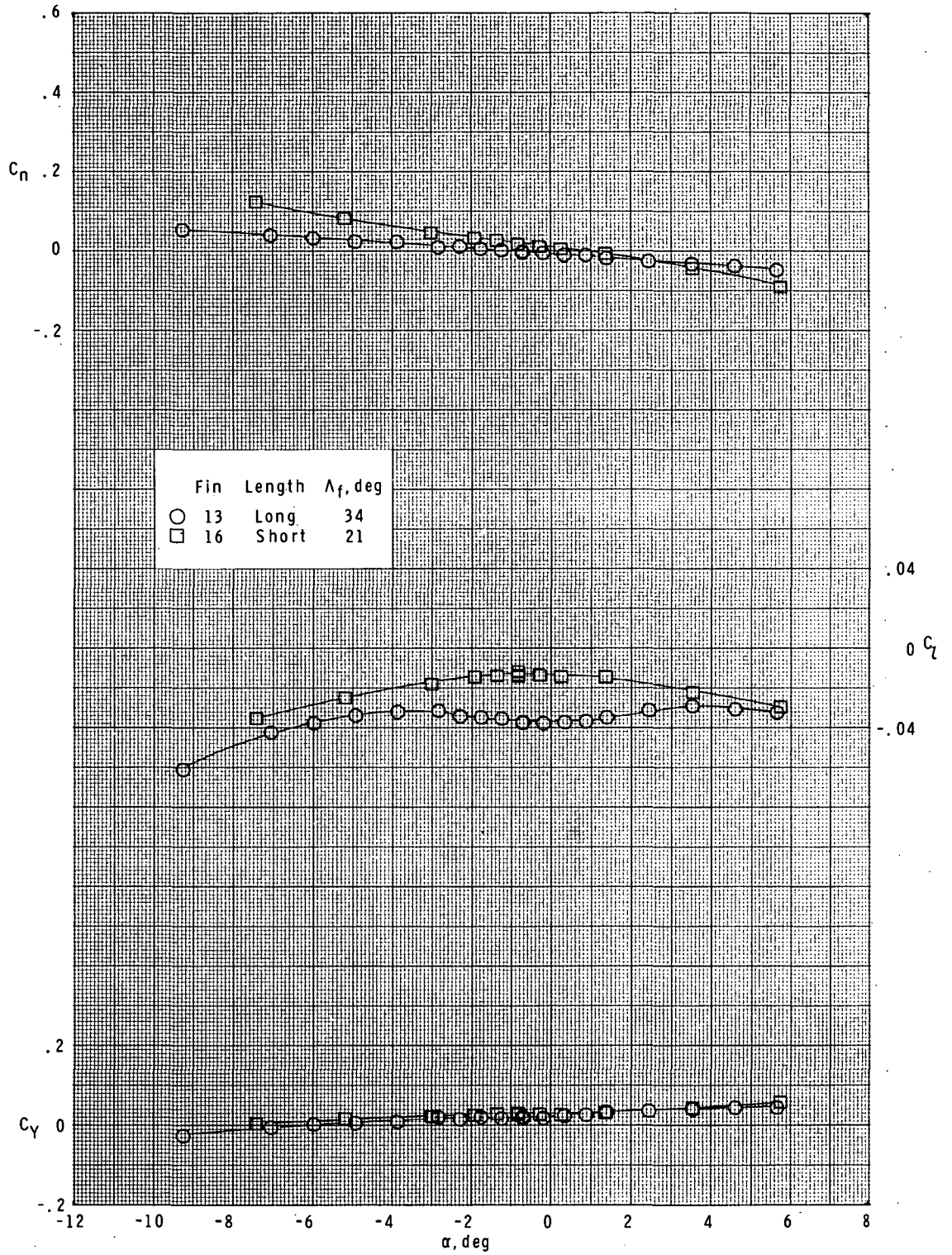

(b) M = 1.90.

Figure 28.- Continued.

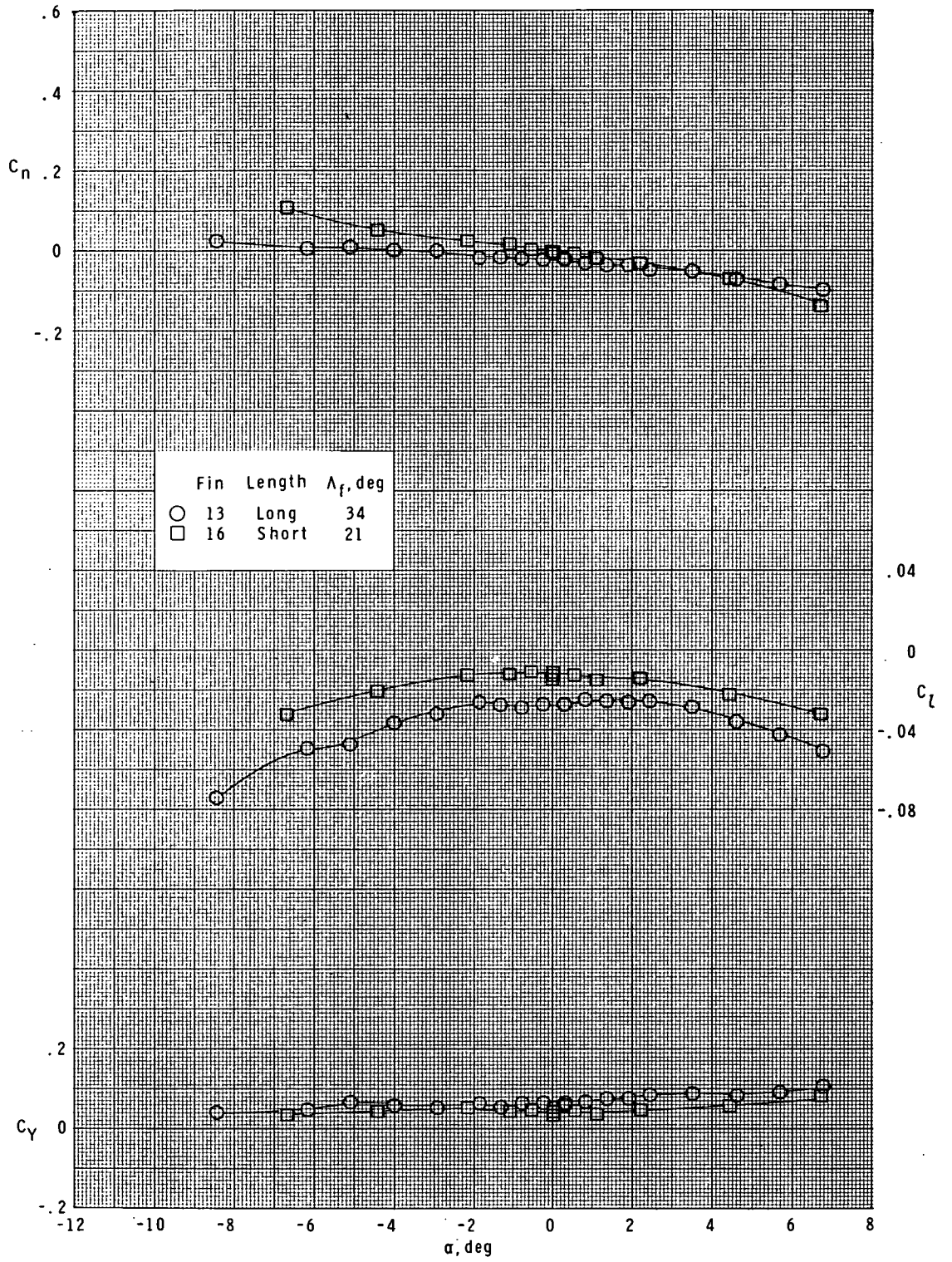

(c) M = 2.36.

Figure 28.- Continued.

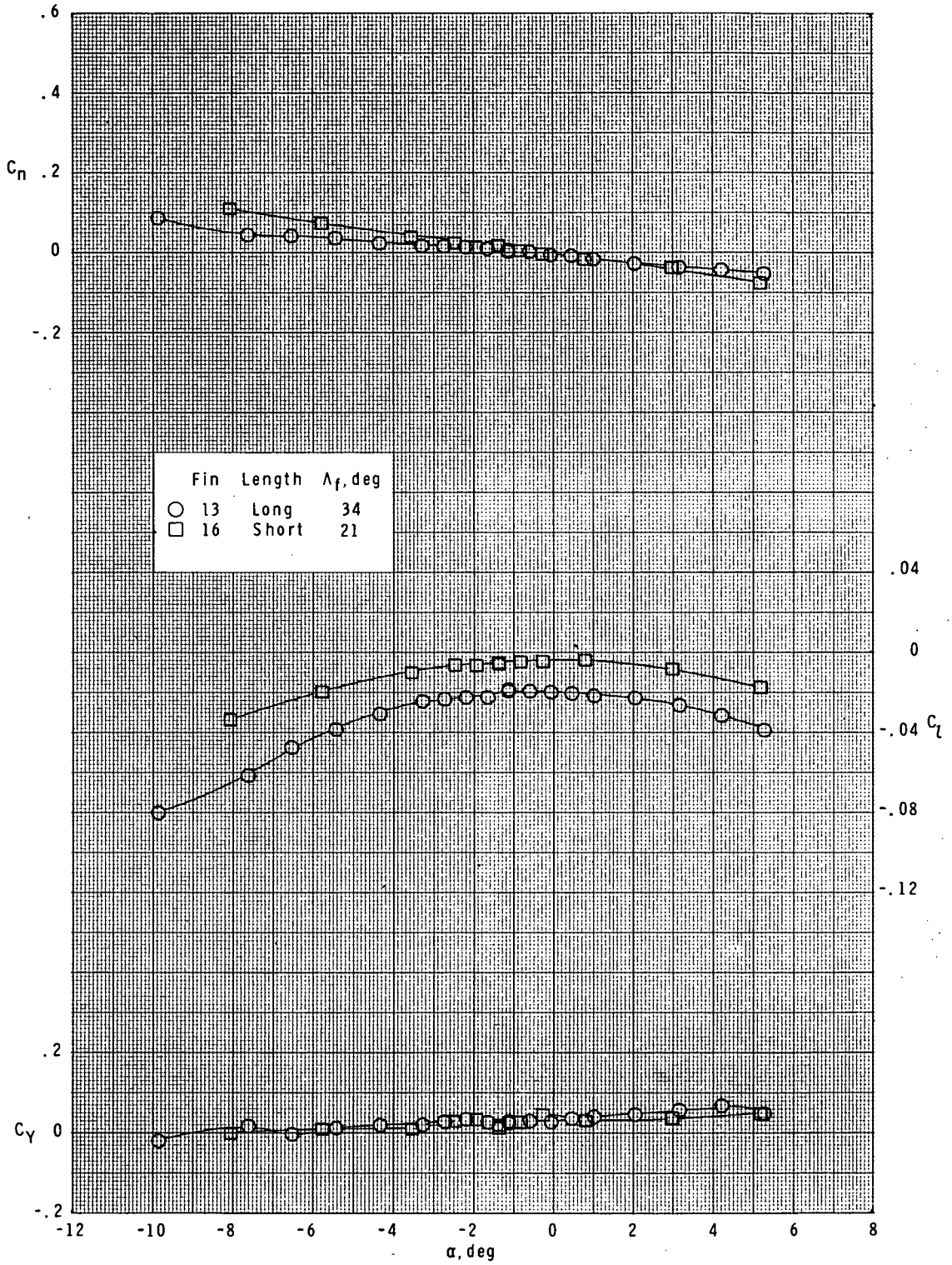

(d) M = 2.86.

Figure 28.- Concluded.

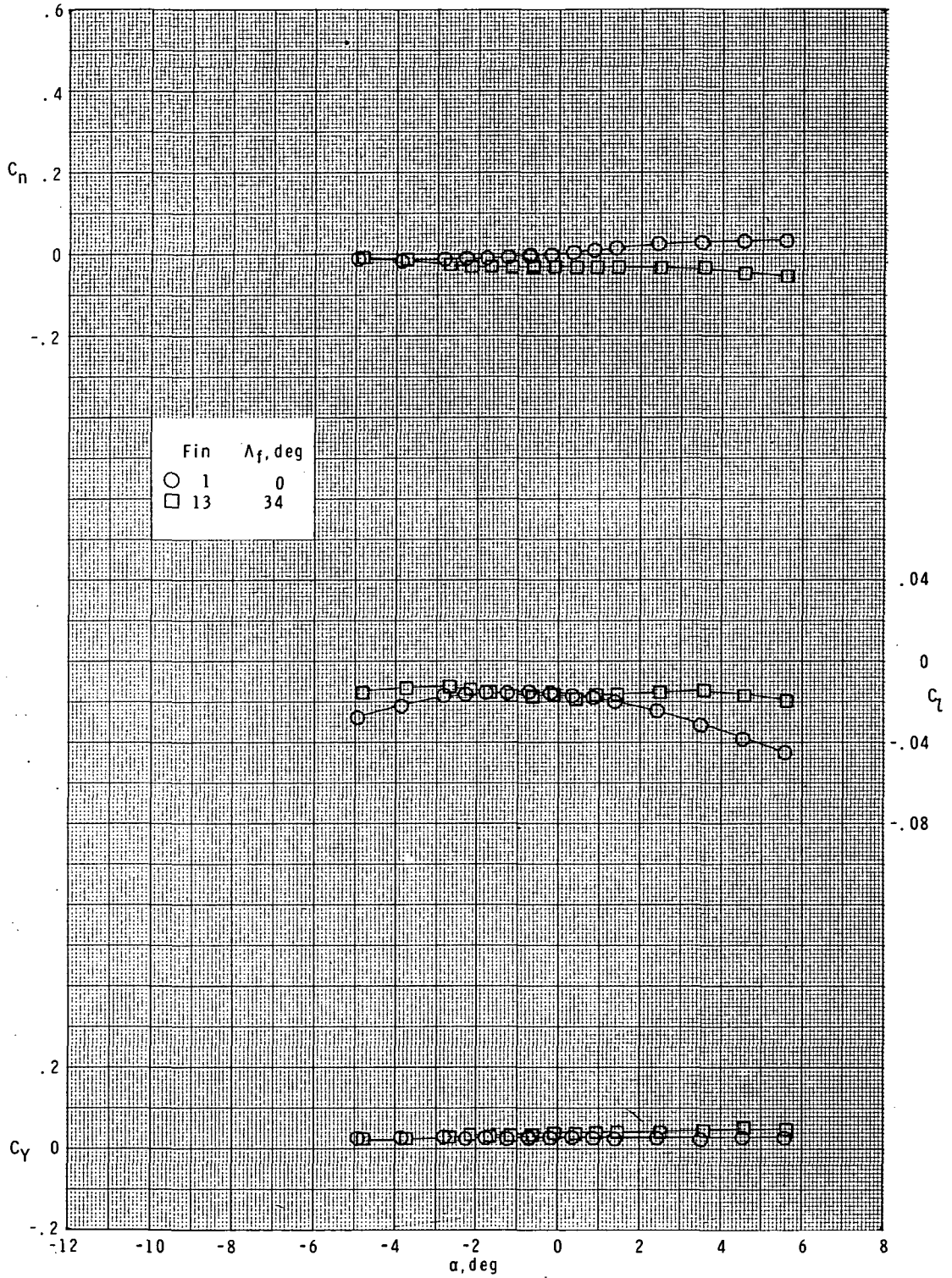

(a) M = 1.60.

Figure 29.- Effect of fin leading-edge sweep on lateral characteristics. Basic body (B_1); long-chord curved fins (F_1 and F_{13}); $\phi = 0^o$.

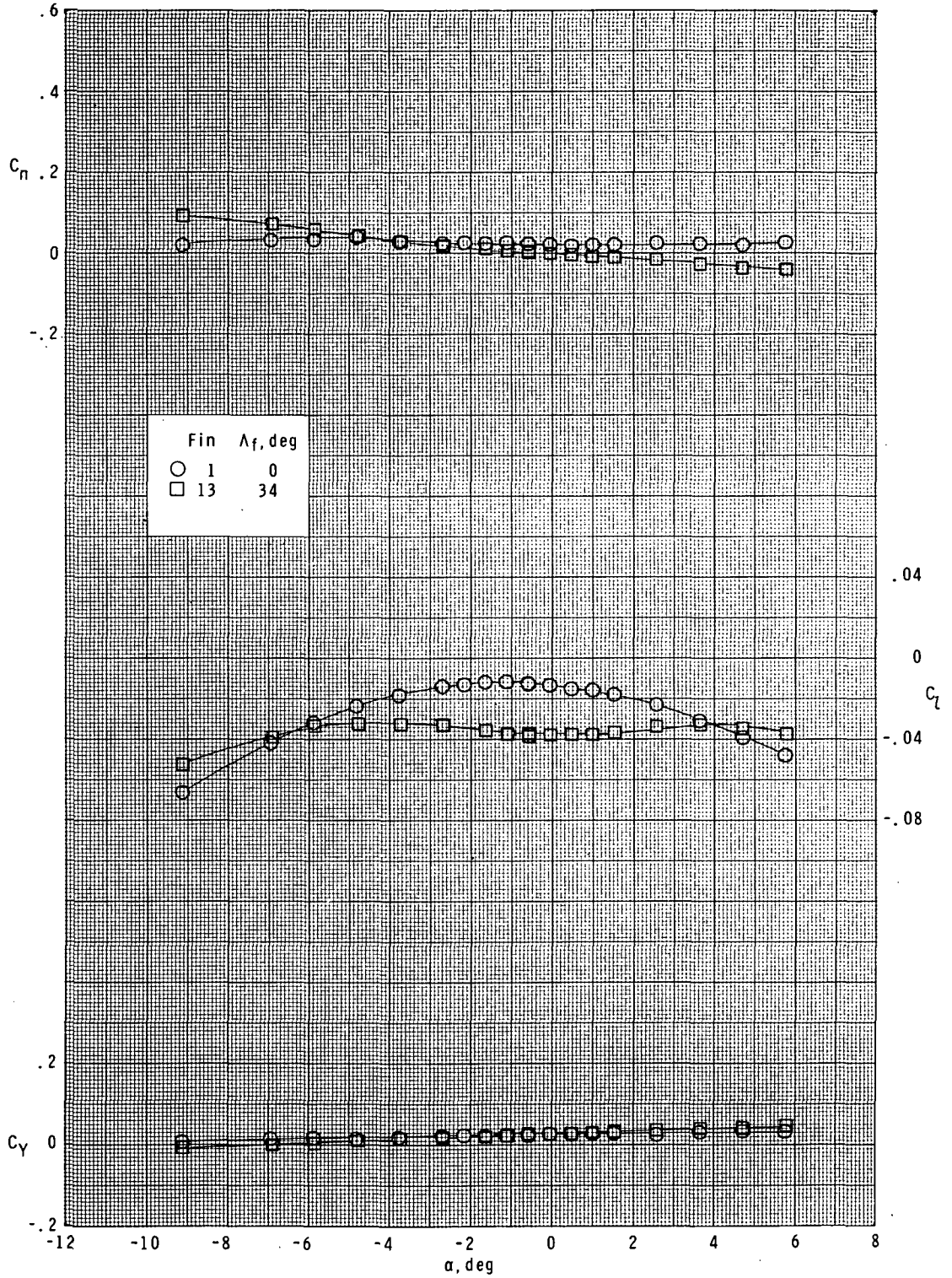

(b) M = 1.90.

Figure 29.- Continued.

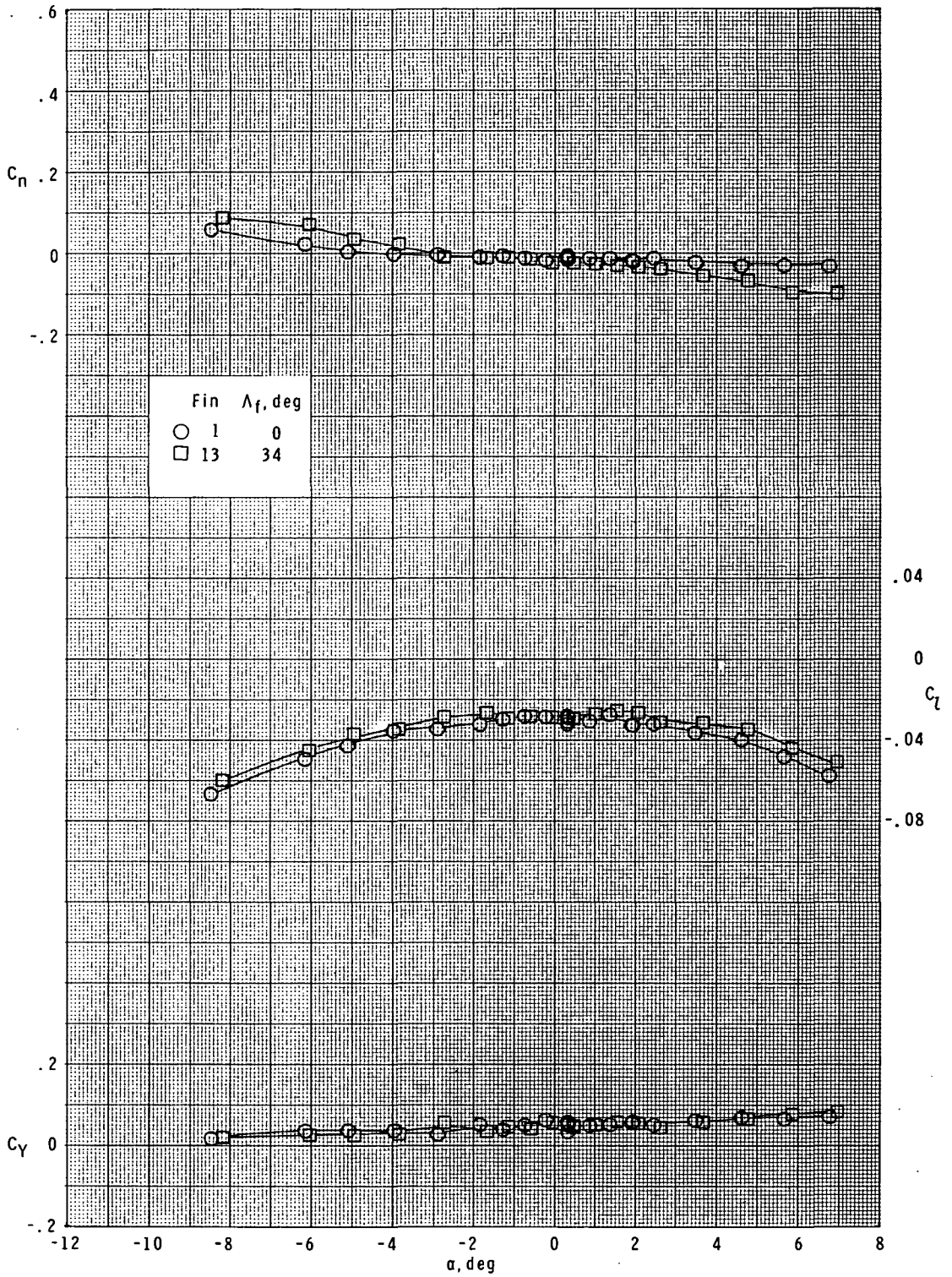

(c) M = 2.36.

Figure 29.- Continued.

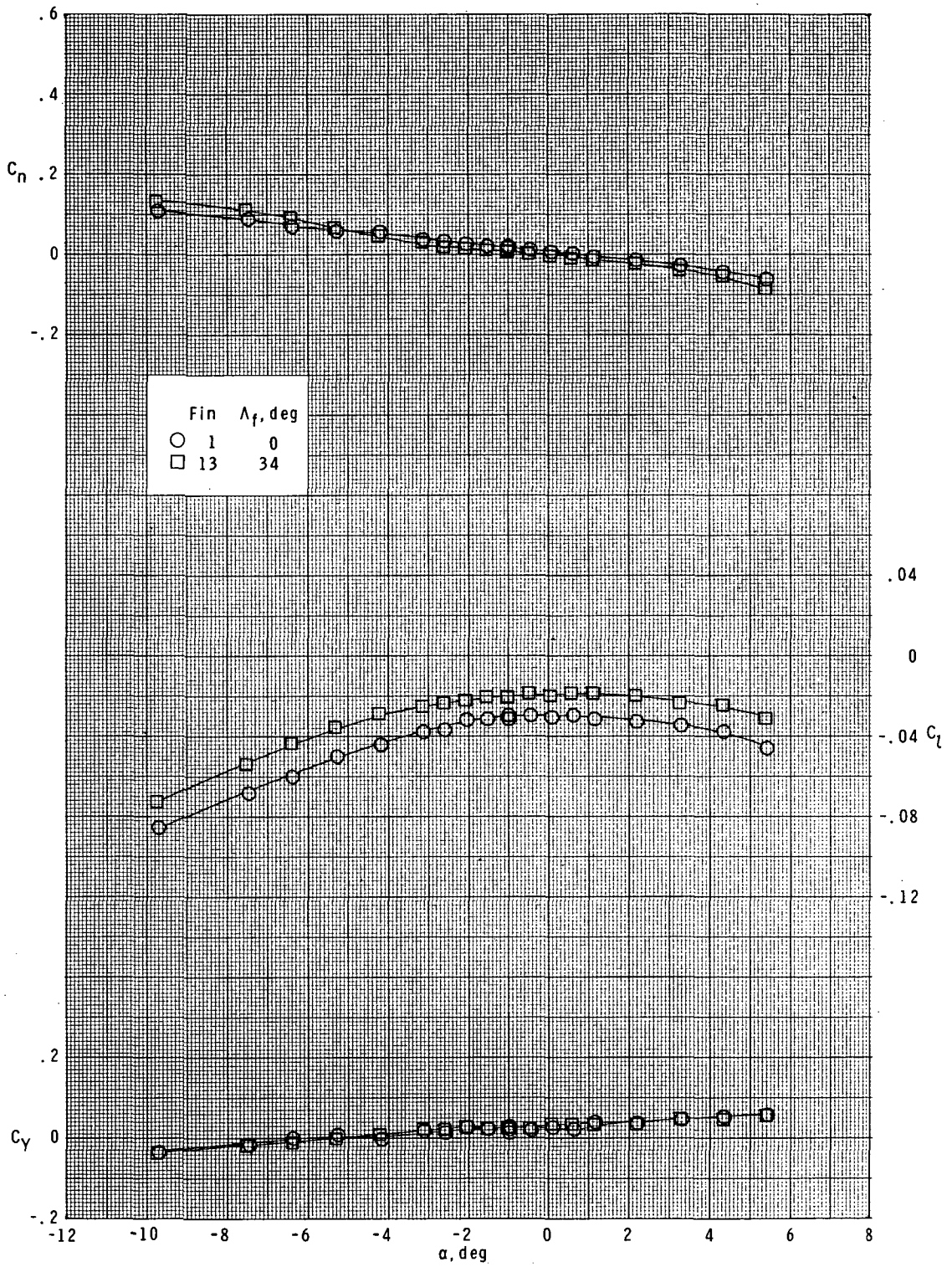

(d) M = 2.86.

Figure 29.- Concluded.

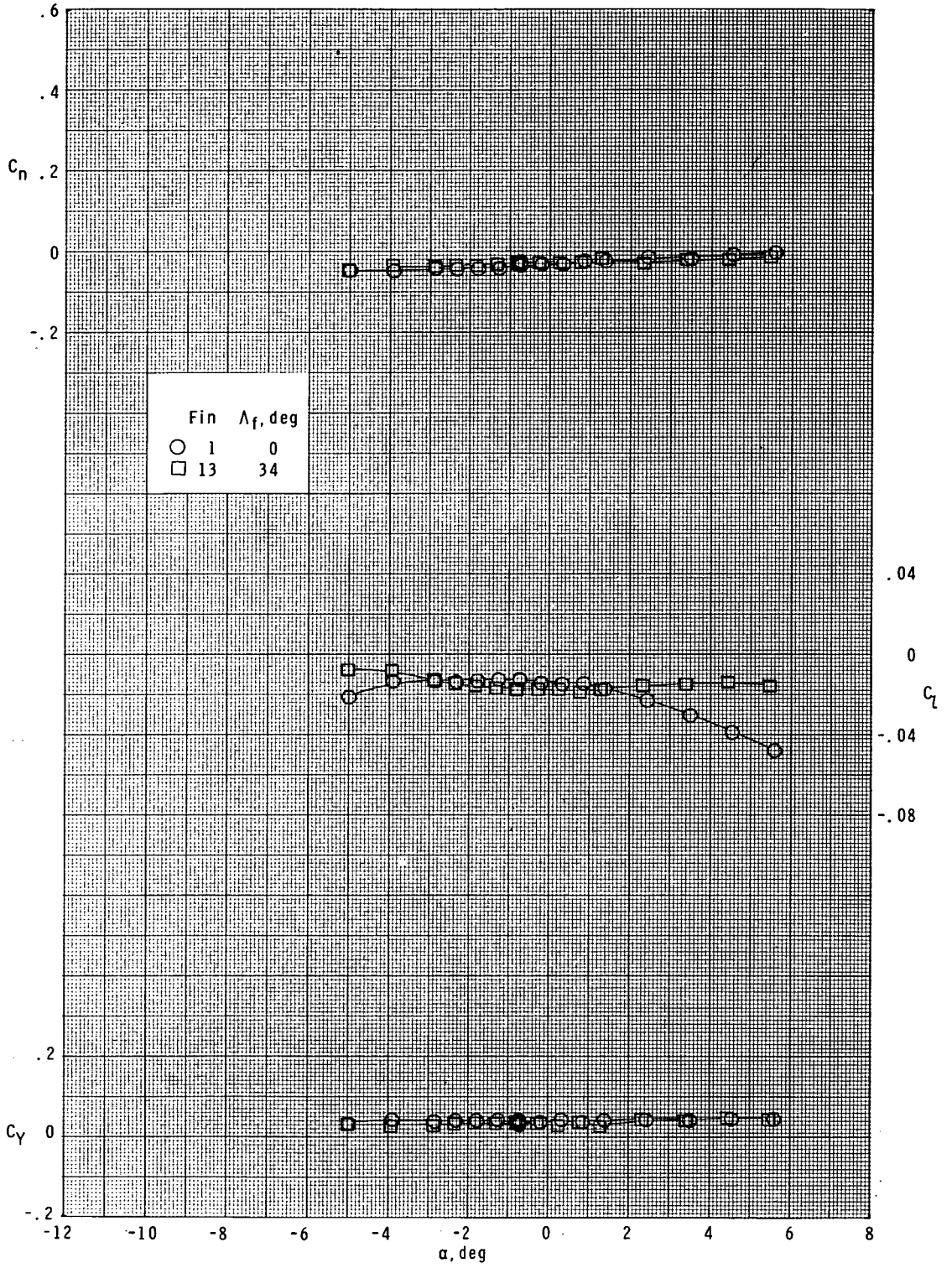

(a) M = 1.60.

Figure 30.- Effect of fin leading-edge sweep on lateral characteristics. Basic body (B_1); long-chord curved fins (F_1 and F_{13}); $\phi = 45^o$.

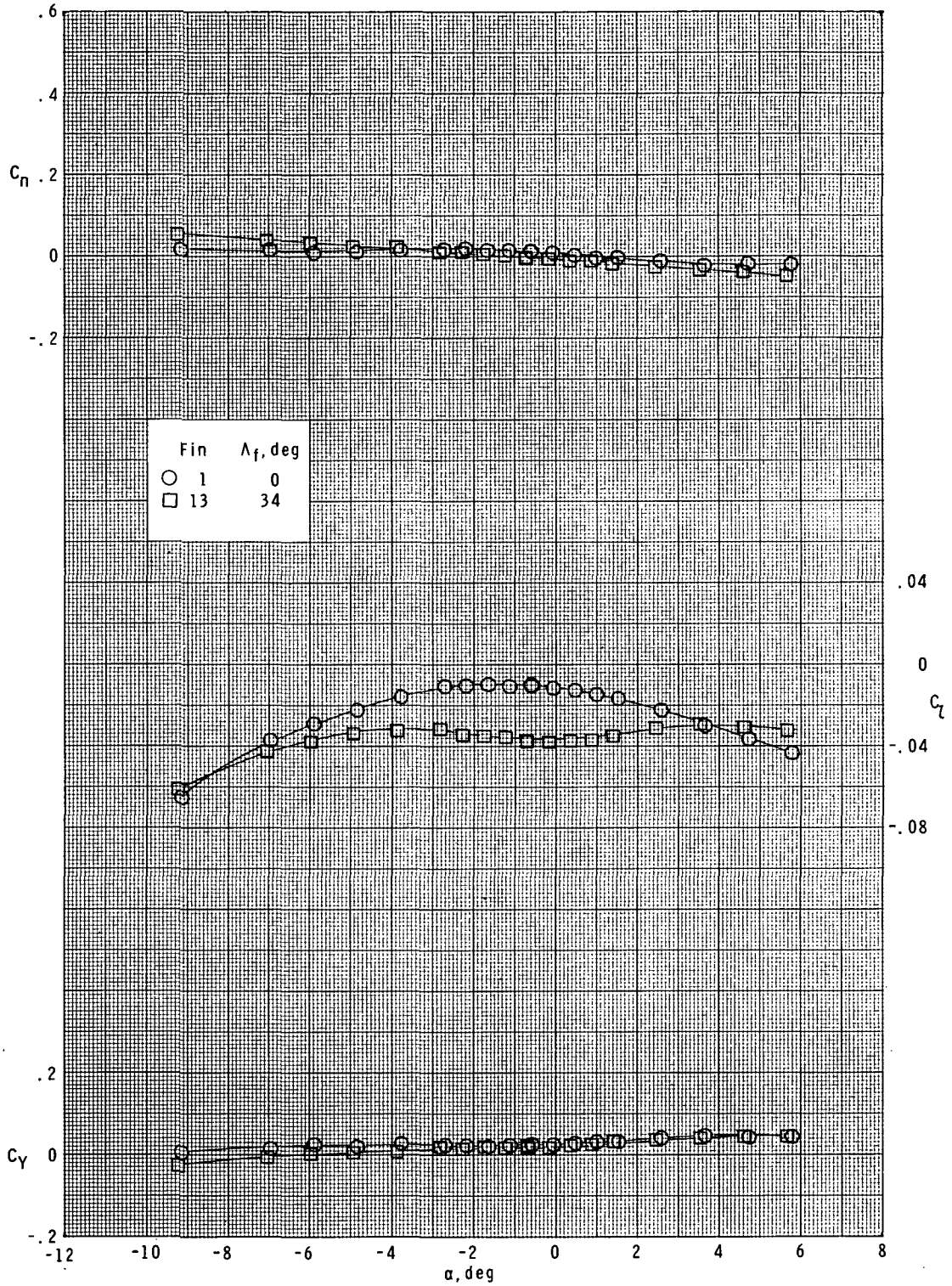

(b) M = 1.90.

Figure 30.- Continued.

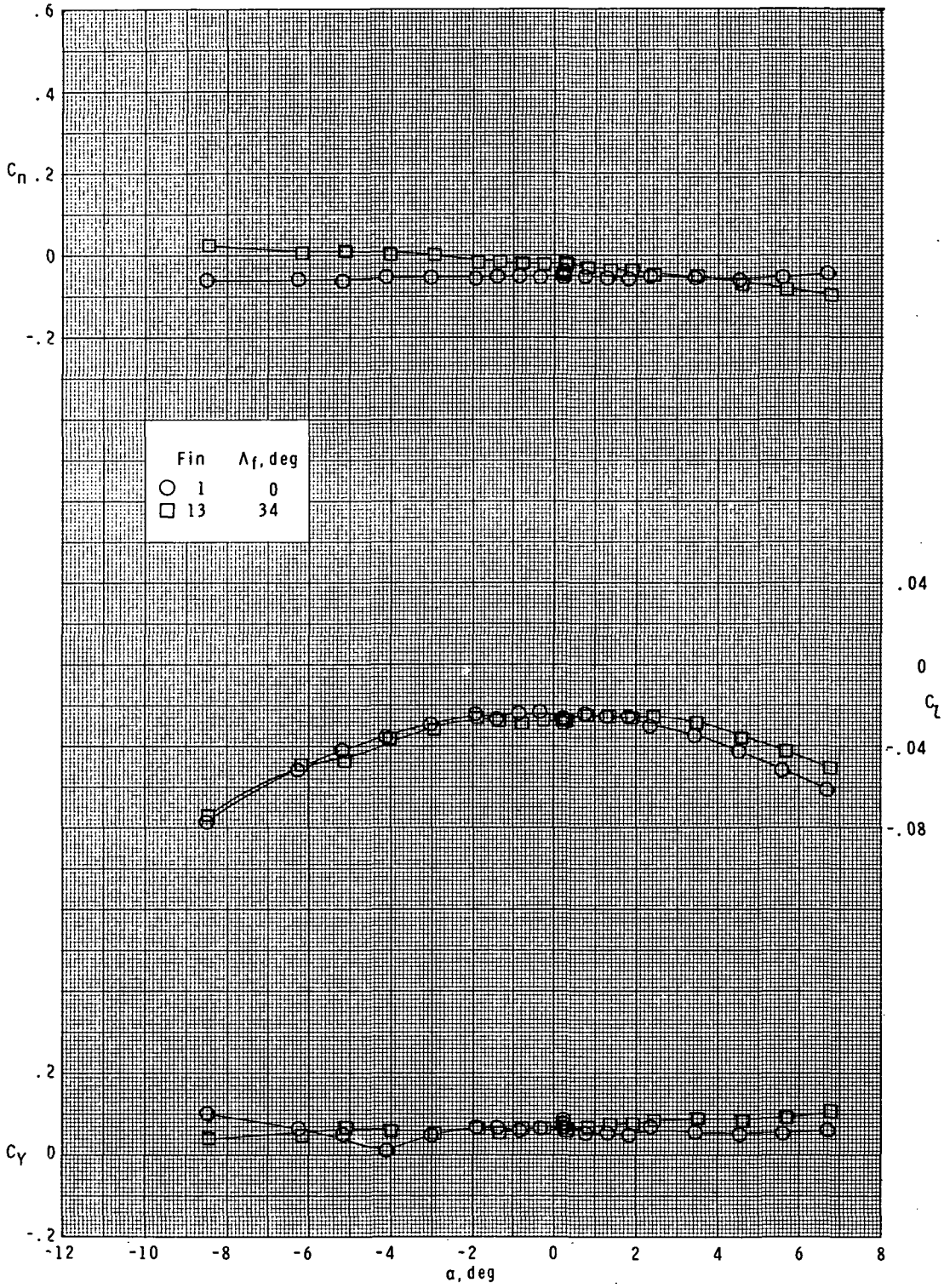

(c) M = 2.36.

Figure 30.- Continued.

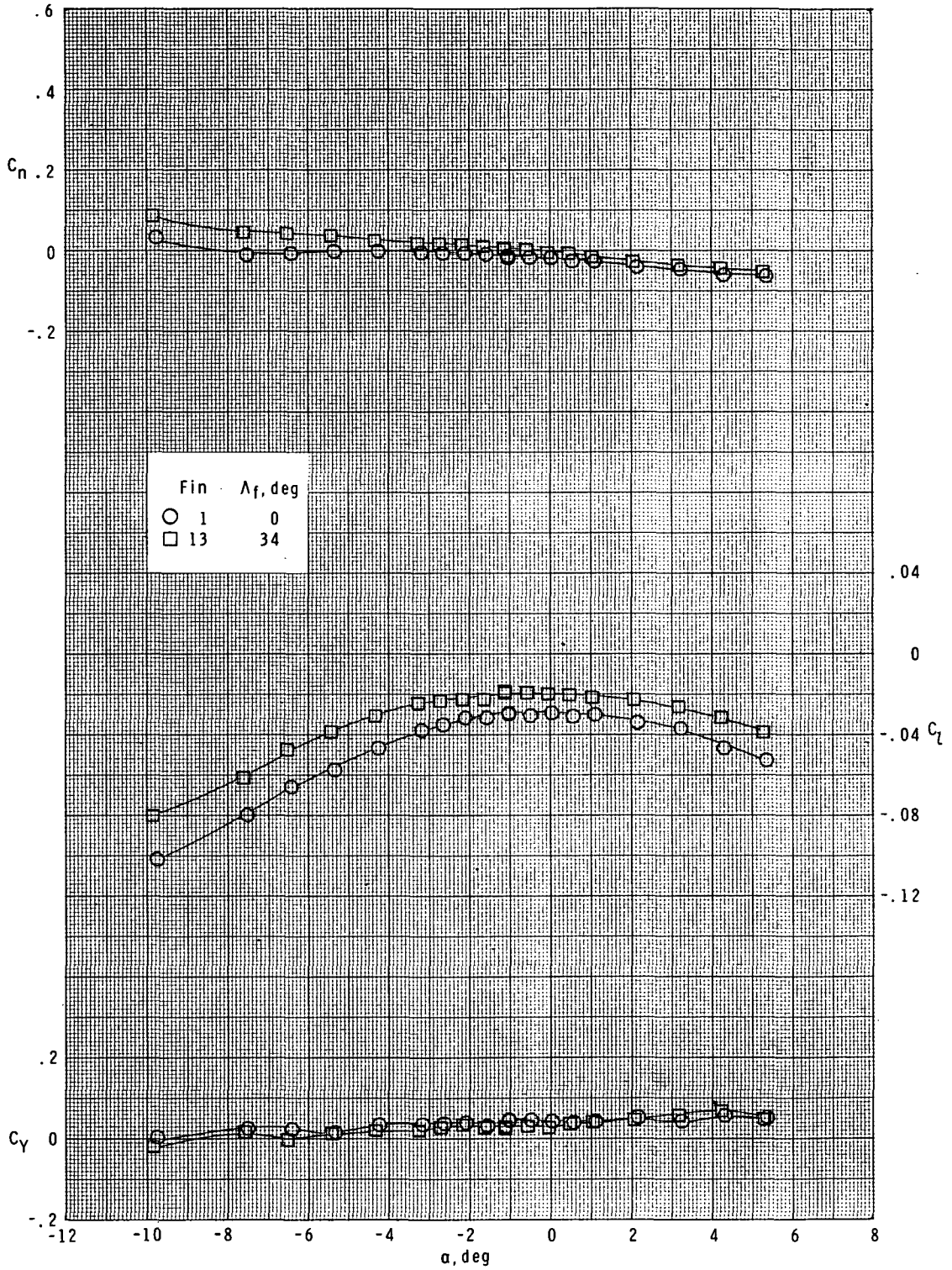

(d) M = 2.86.

Figure 30.- Concluded.

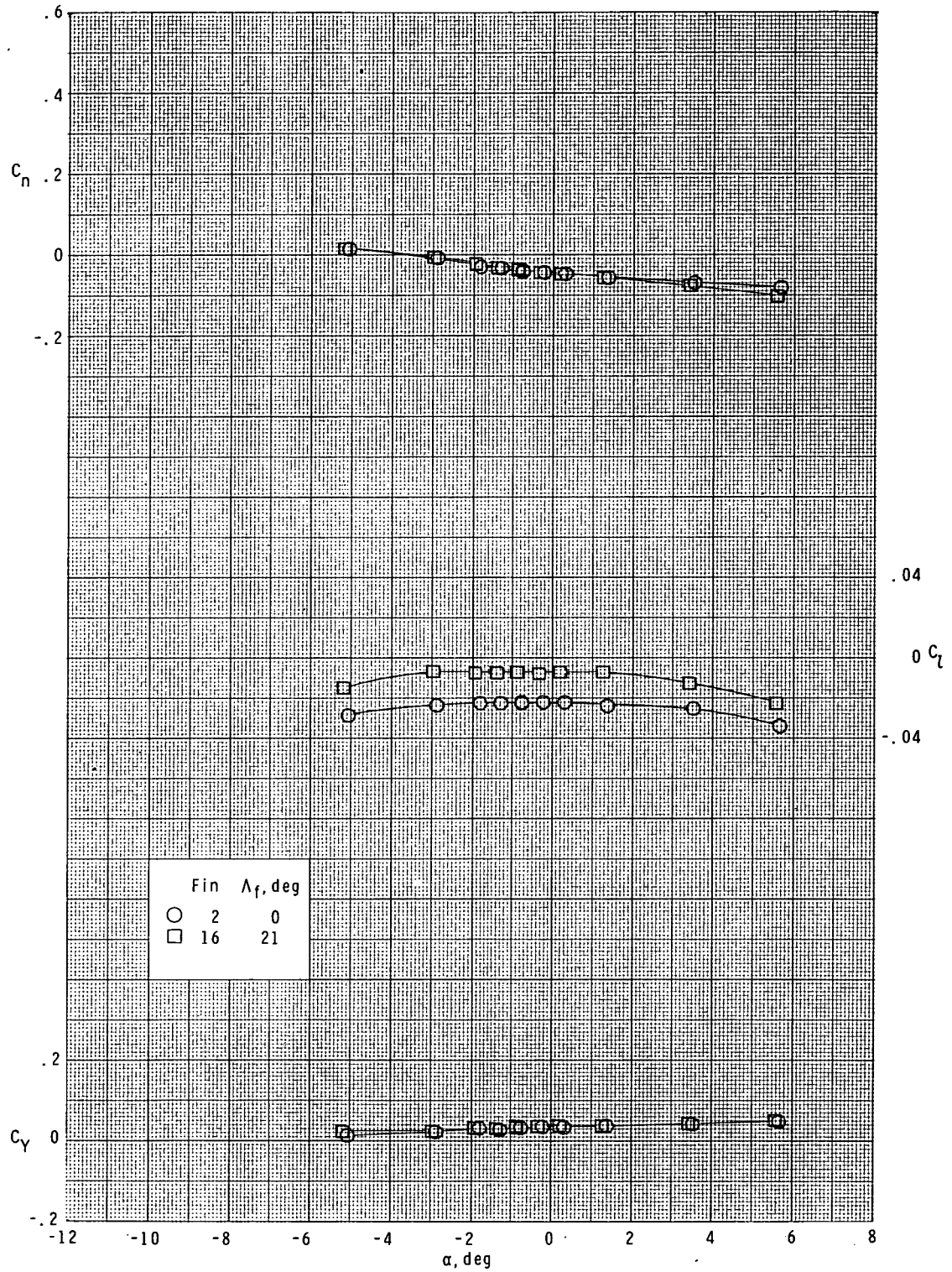

(a) M = 1.60.

Figure 31.- Effect of fin leading-edge sweep on lateral characteristics. Basic body (B_1); short-chord curved fins (F_2 and F_{16}); $\phi = 0^o$.

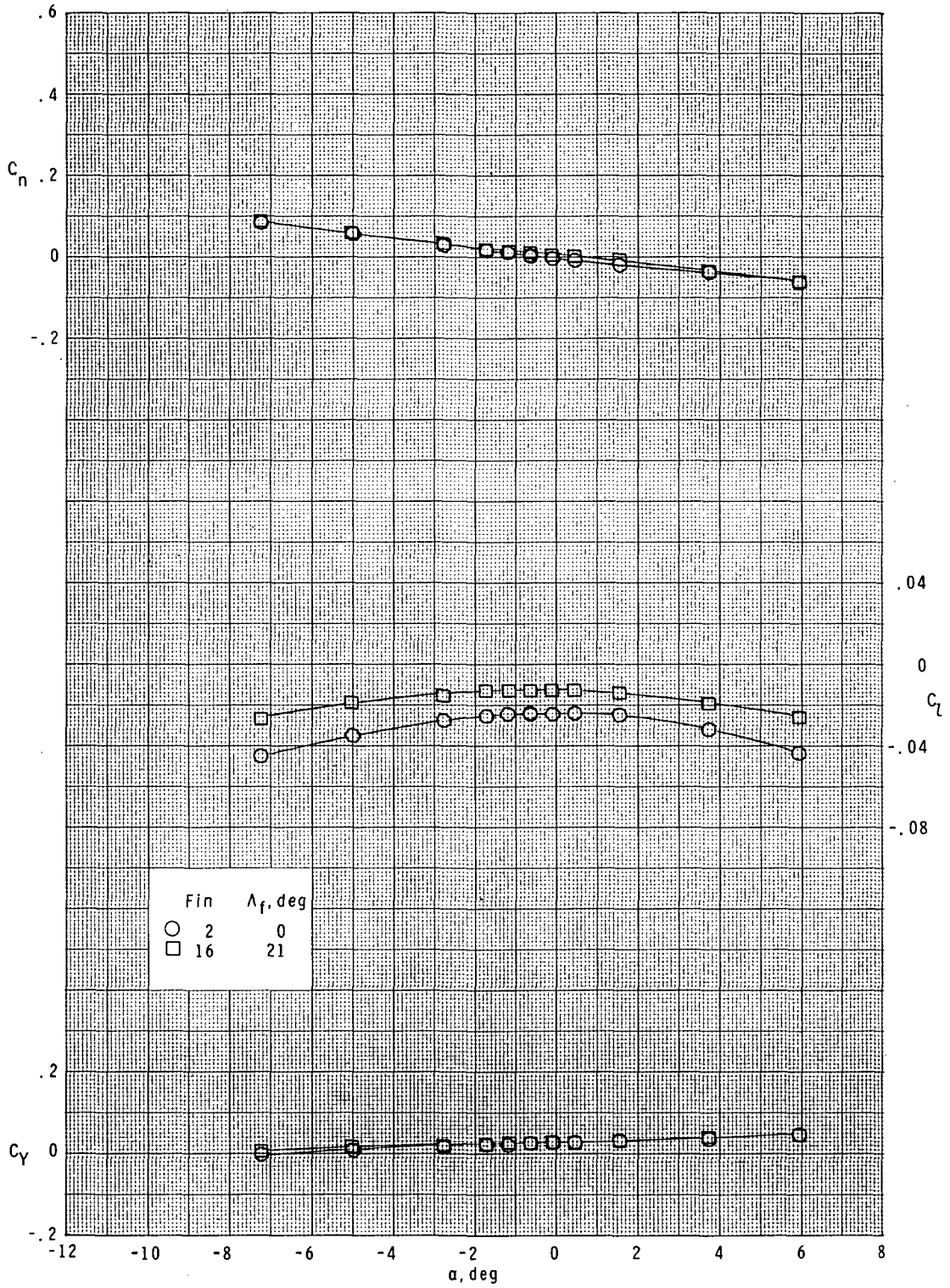

(b) M = 1.90.

Figure 31.- Continued.

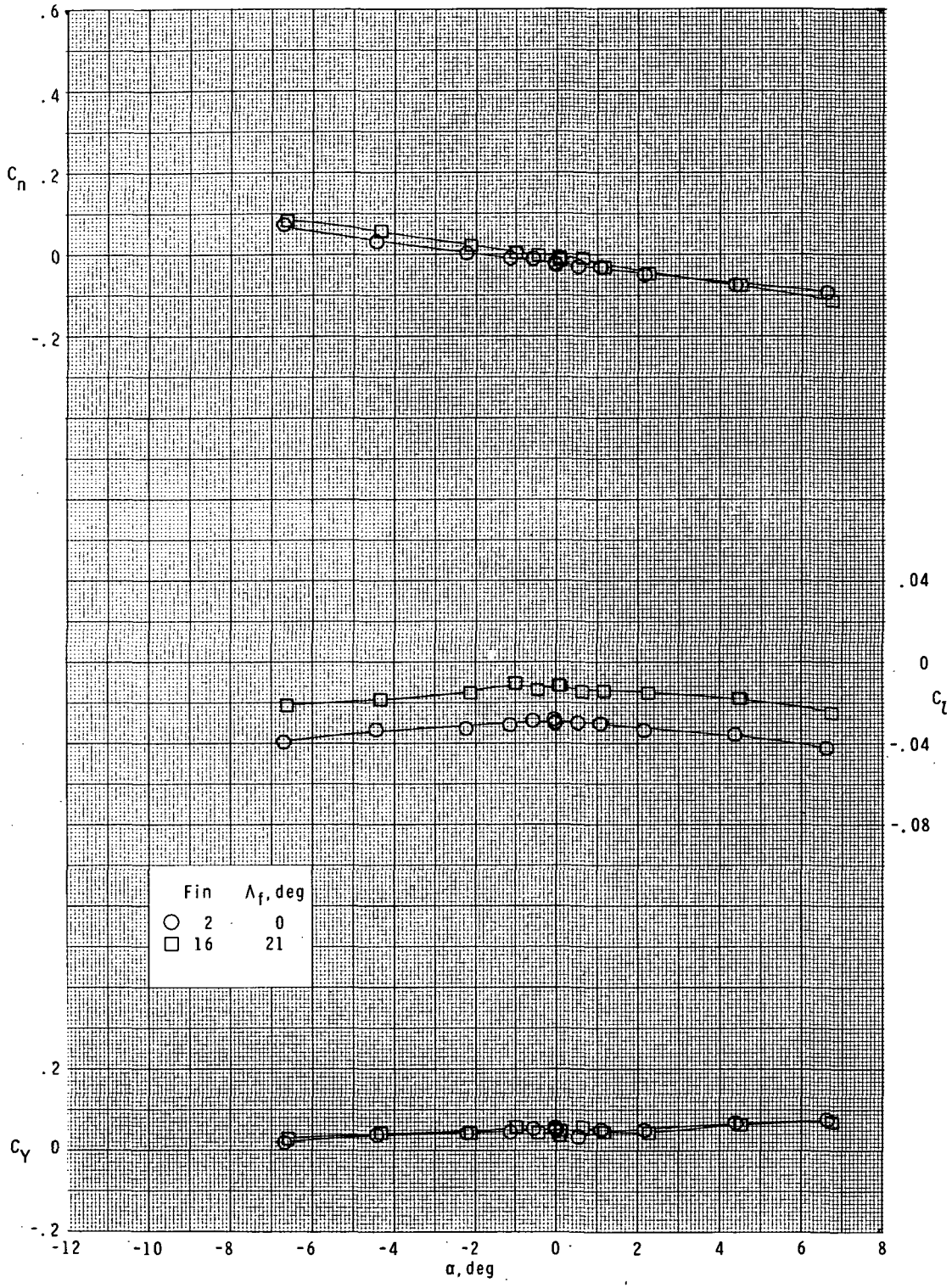

(c) M = 2.36.

Figure 31.- Continued.

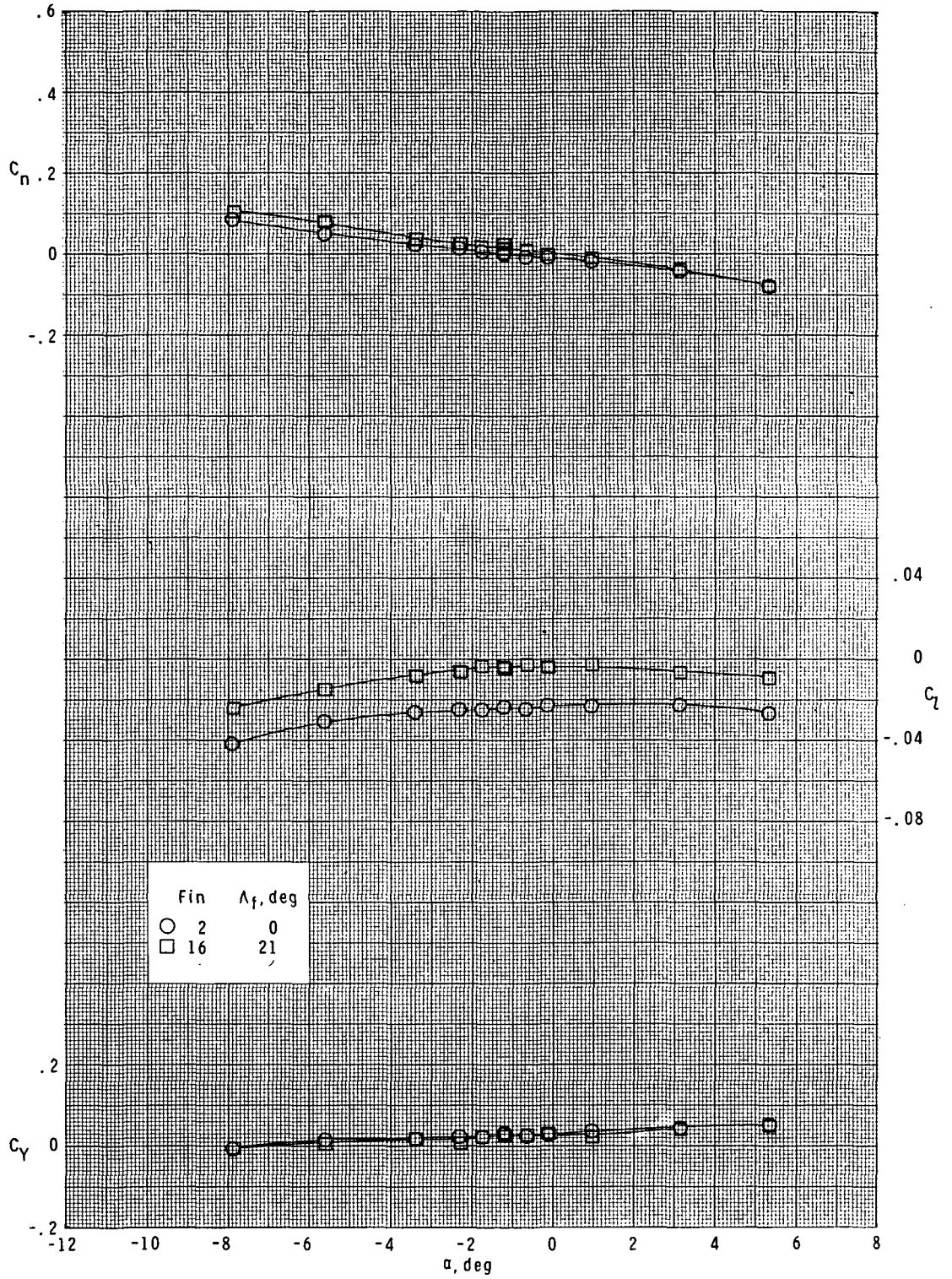

(d) M = 2.86.

Figure 31.- Concluded.

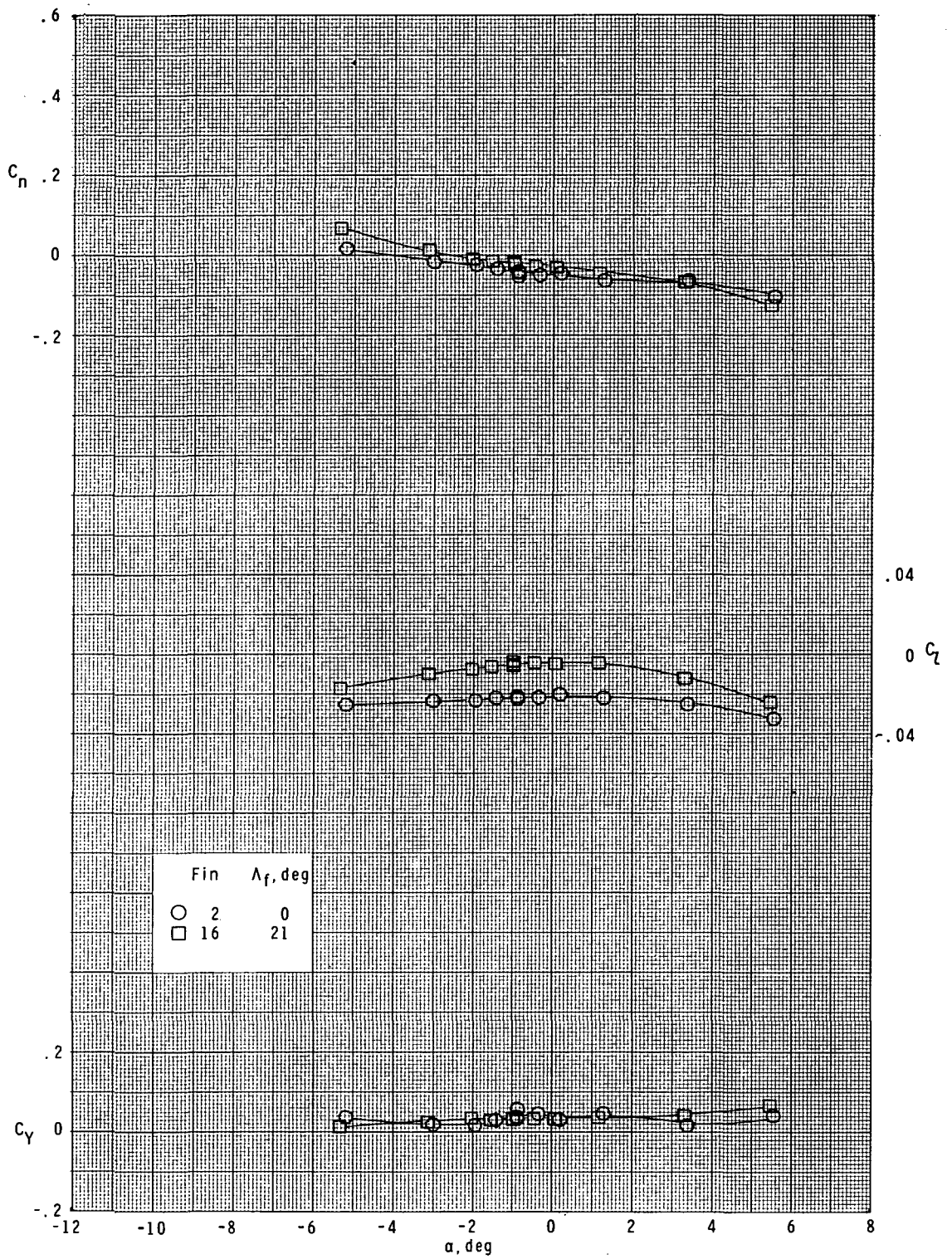

(a) M = 1.60.

Figure 32.- Effect of leading-edge sweep on lateral characteristics. Basic body (B_1); short-chord curved fins (F_2 and F_{16}); $\phi = 45^\circ$.

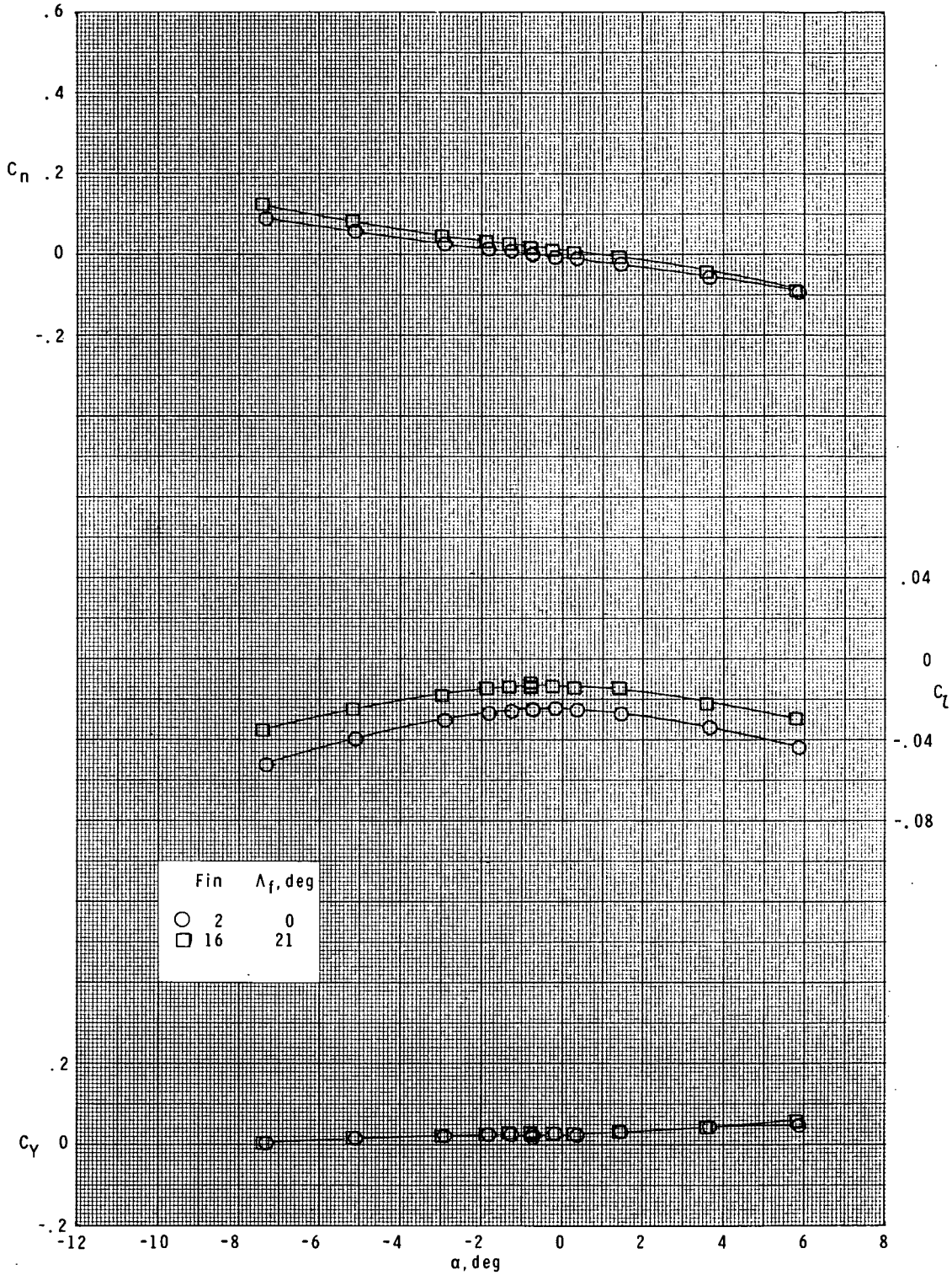

(b) M = 1.90.

Figure 32.- Continued.

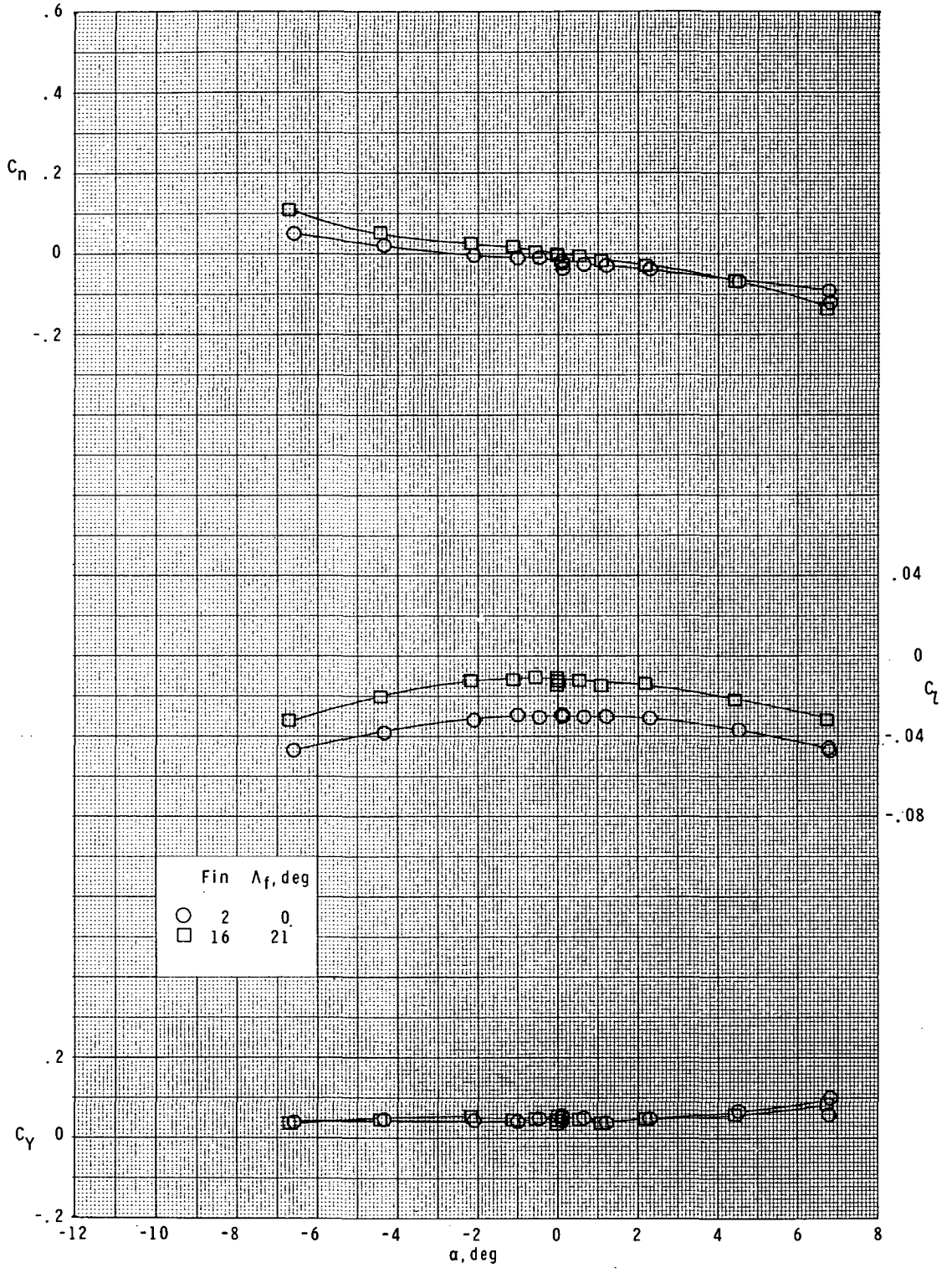

(c) M = 2.36.

Figure 32.- Continued.

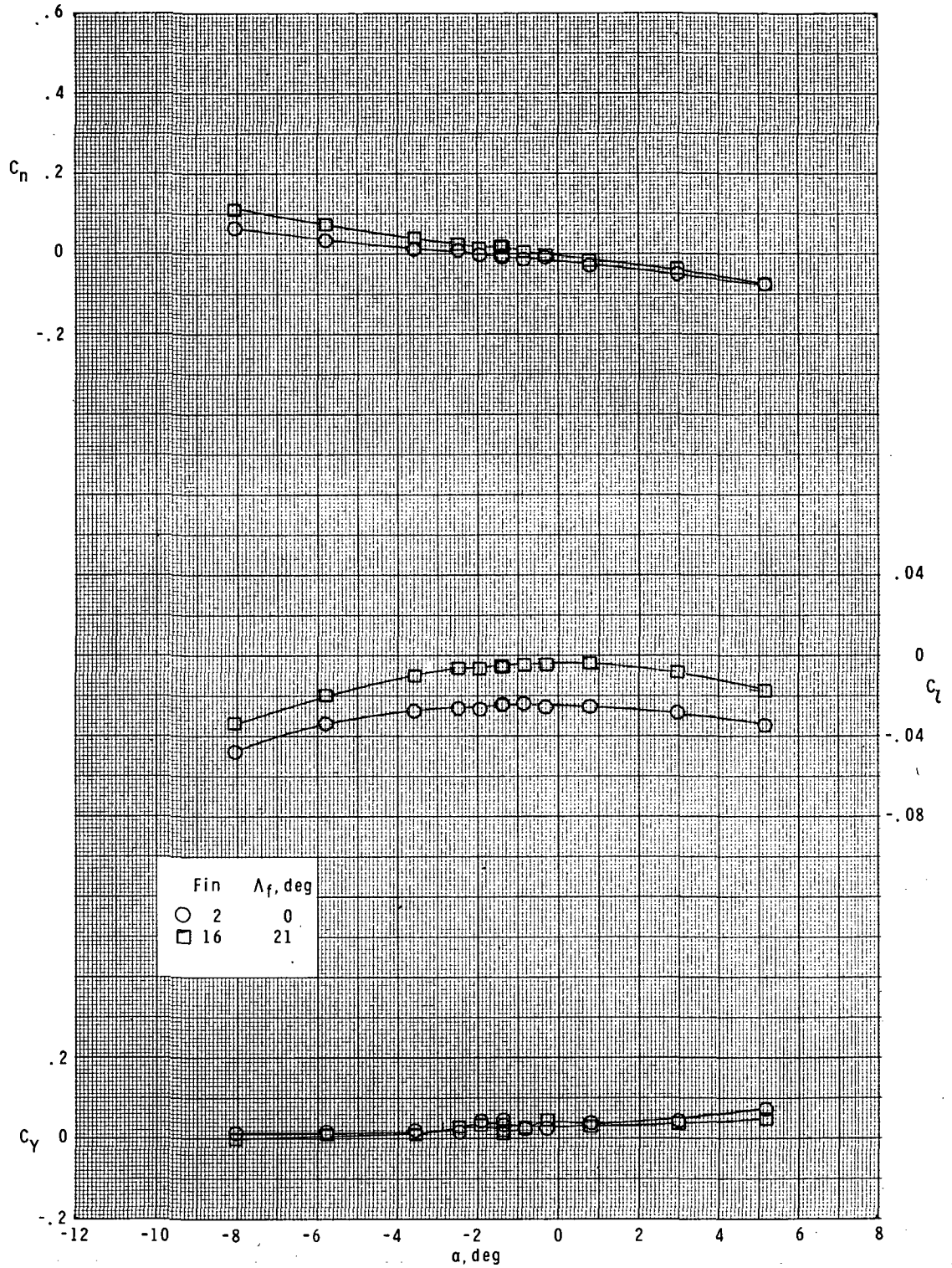

(d) M = 2.86.

Figure 32.- Concluded.

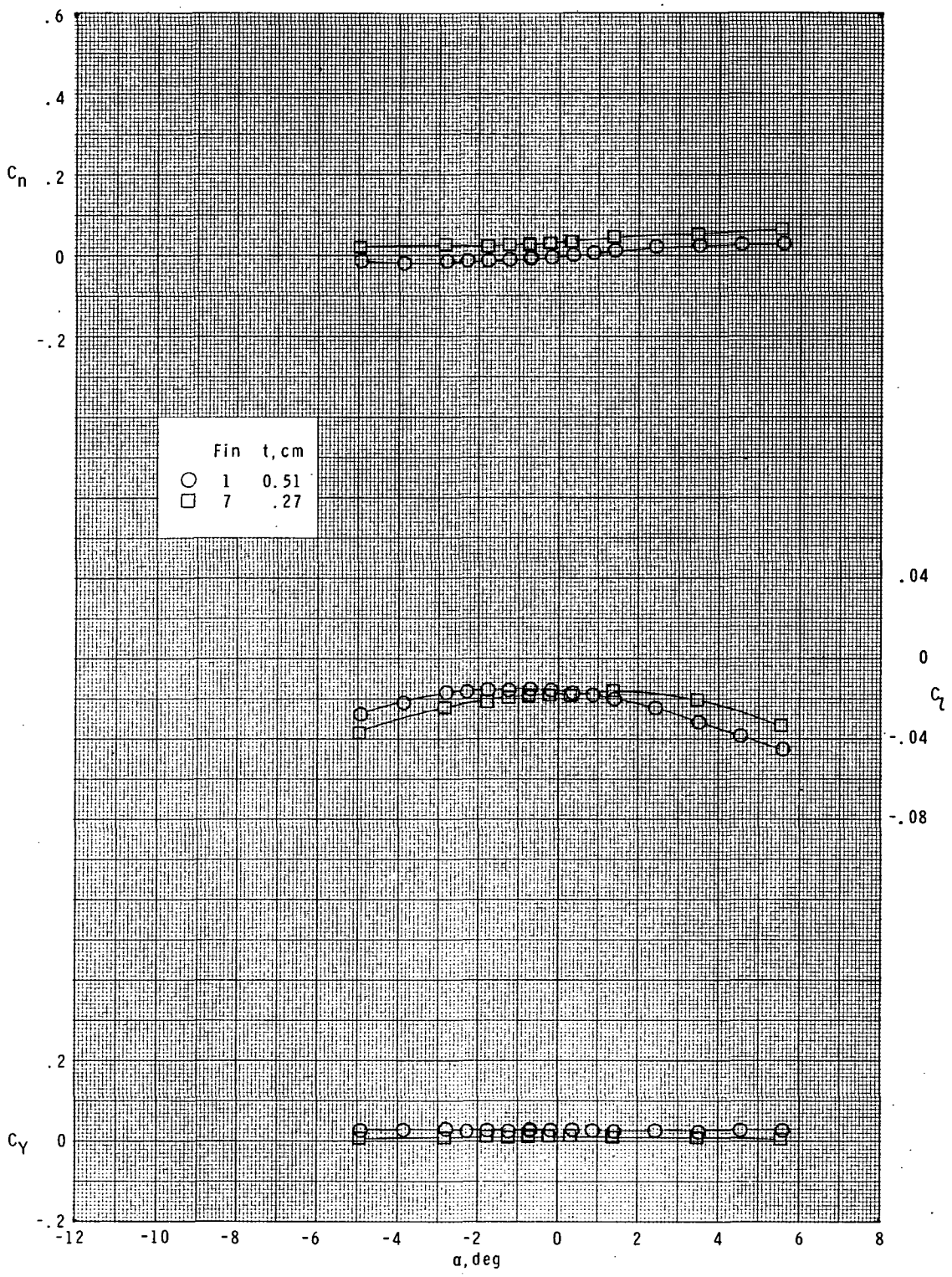

(a) M = 1.60.

Figure 33.- Effect of fin thickness on lateral characteristics. Basic body (B_1); long-chord curved fins (F_1 and F_7); $\phi = 0^o$.

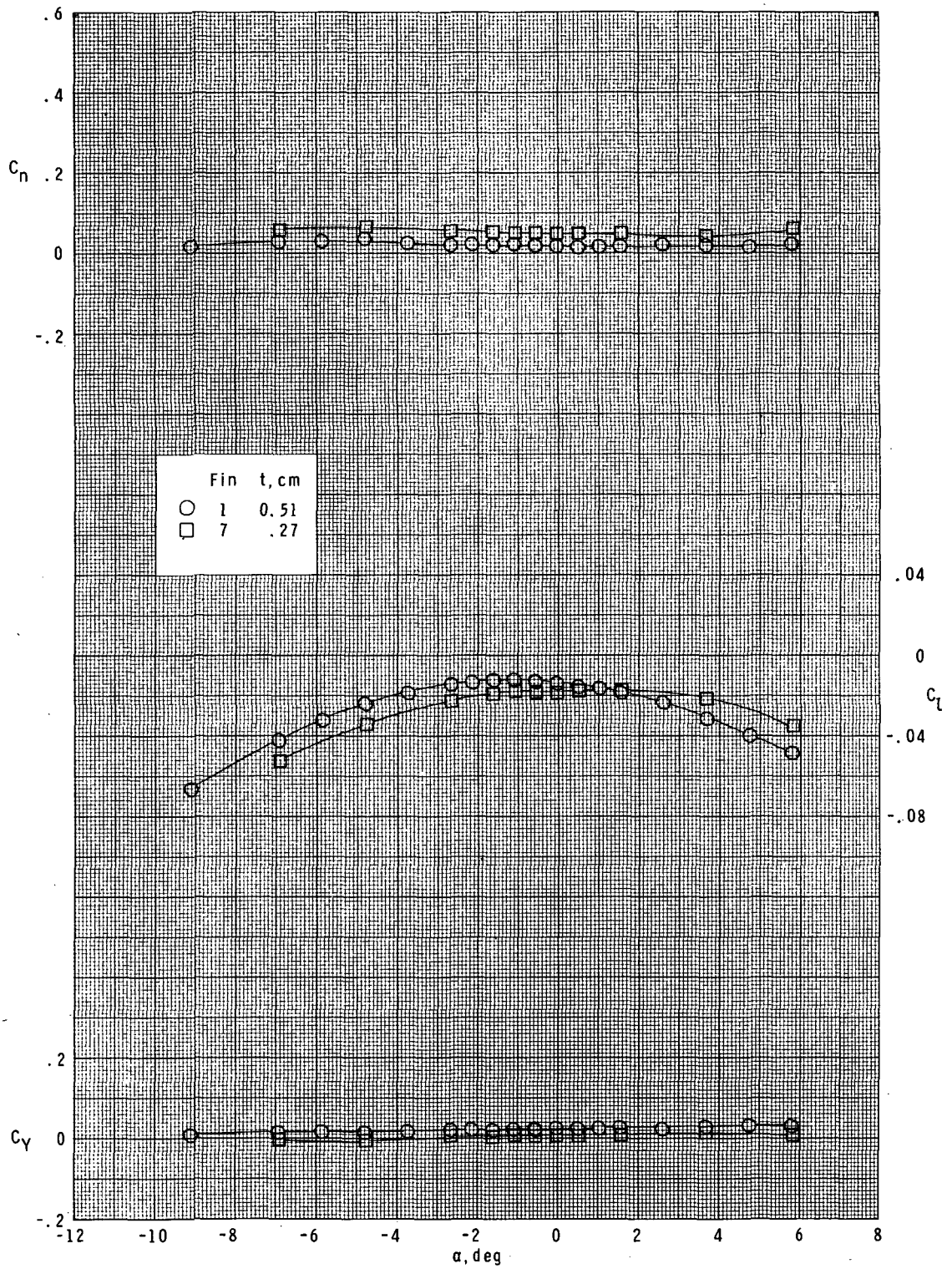

(b) M = 1.90.

Figure 33.- Continued.

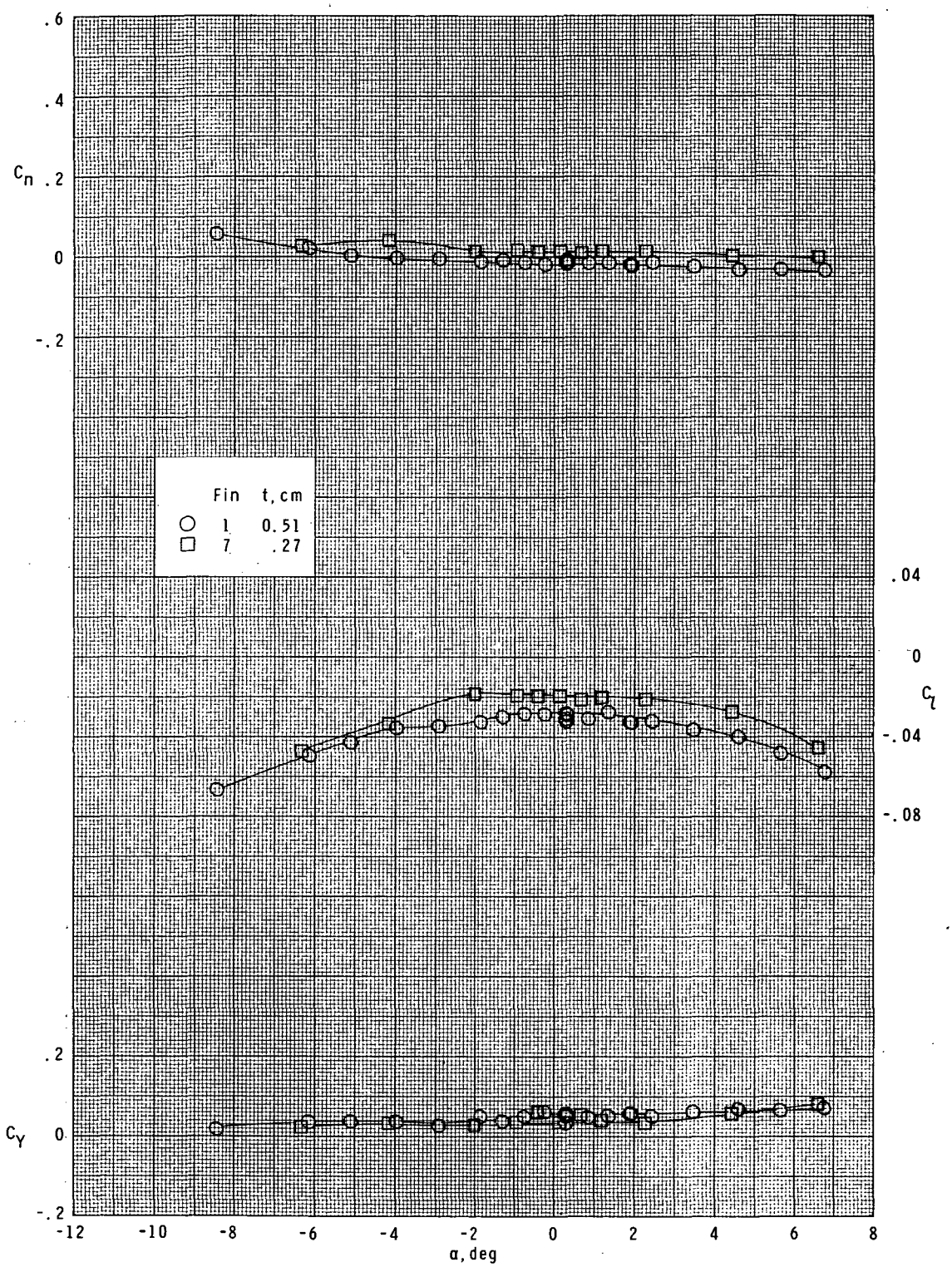

(c) M = 2.36.

Figure 33.- Continued.

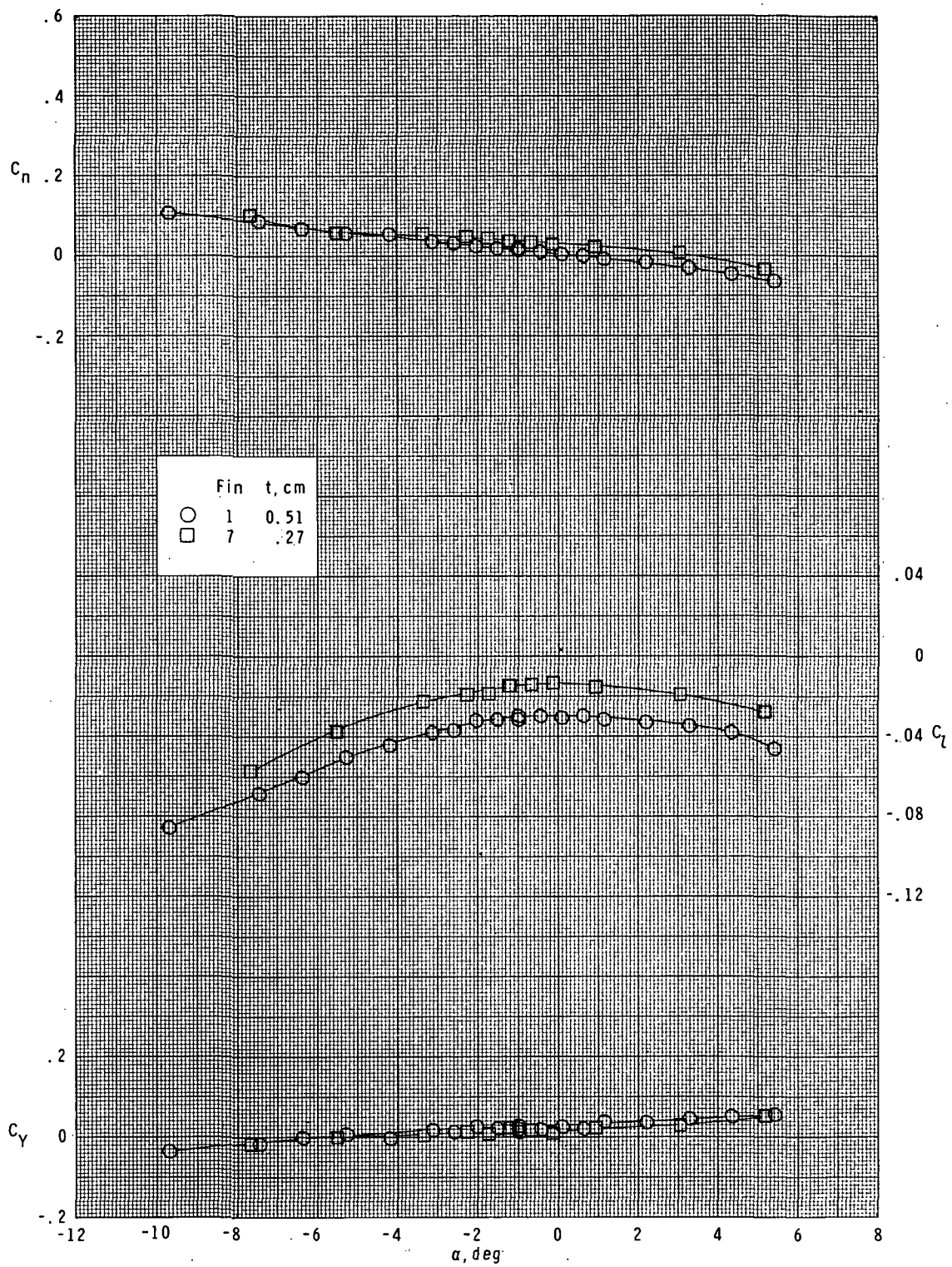

(d) M = 2.86.

Figure 33.- Concluded.

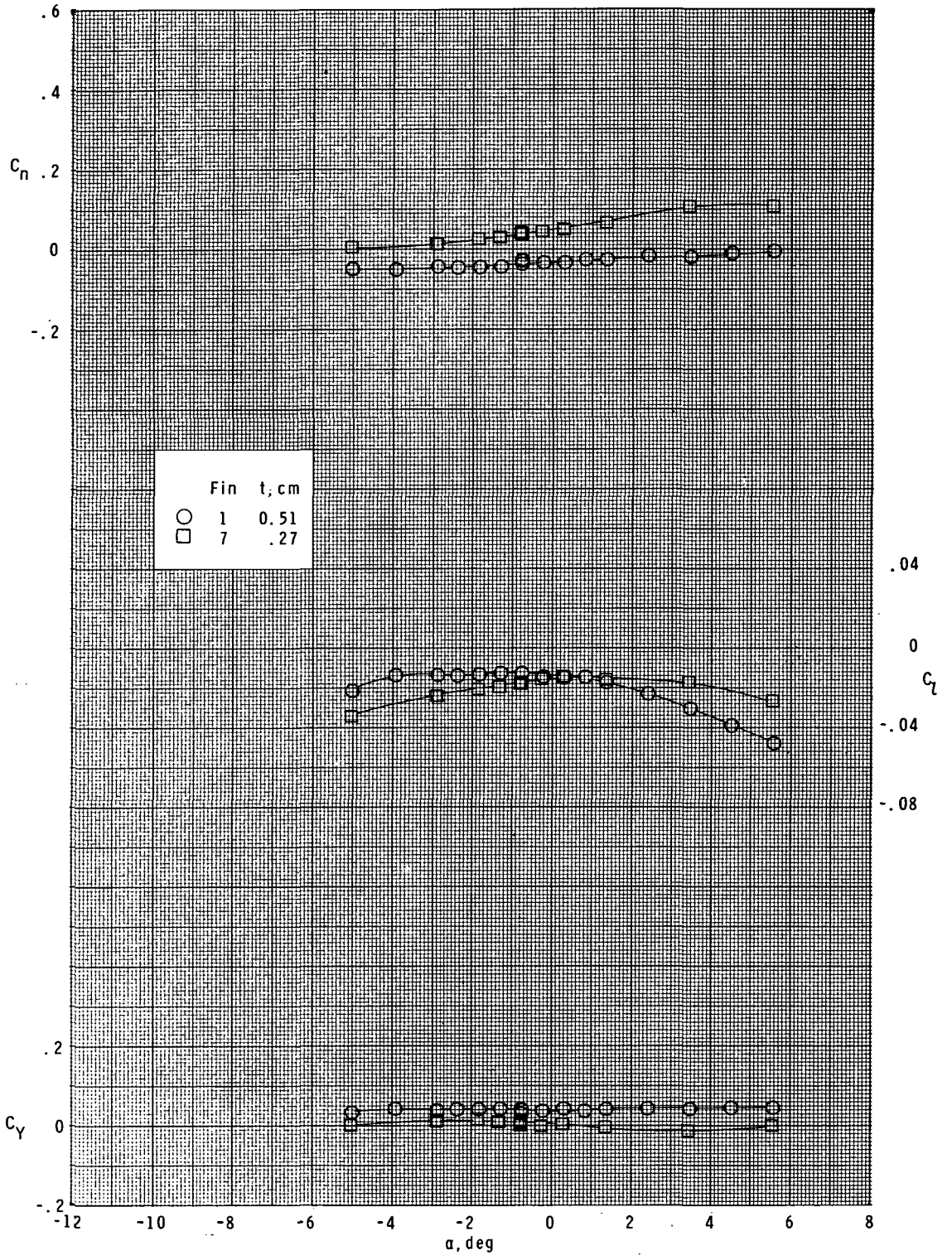

(a) M = 1.60.

Figure 34.- Effect of fin thickness on lateral characteristics. Basic body (B_1); long-chord curved fins (F_1 and F_7); $\phi = 45^\circ$.

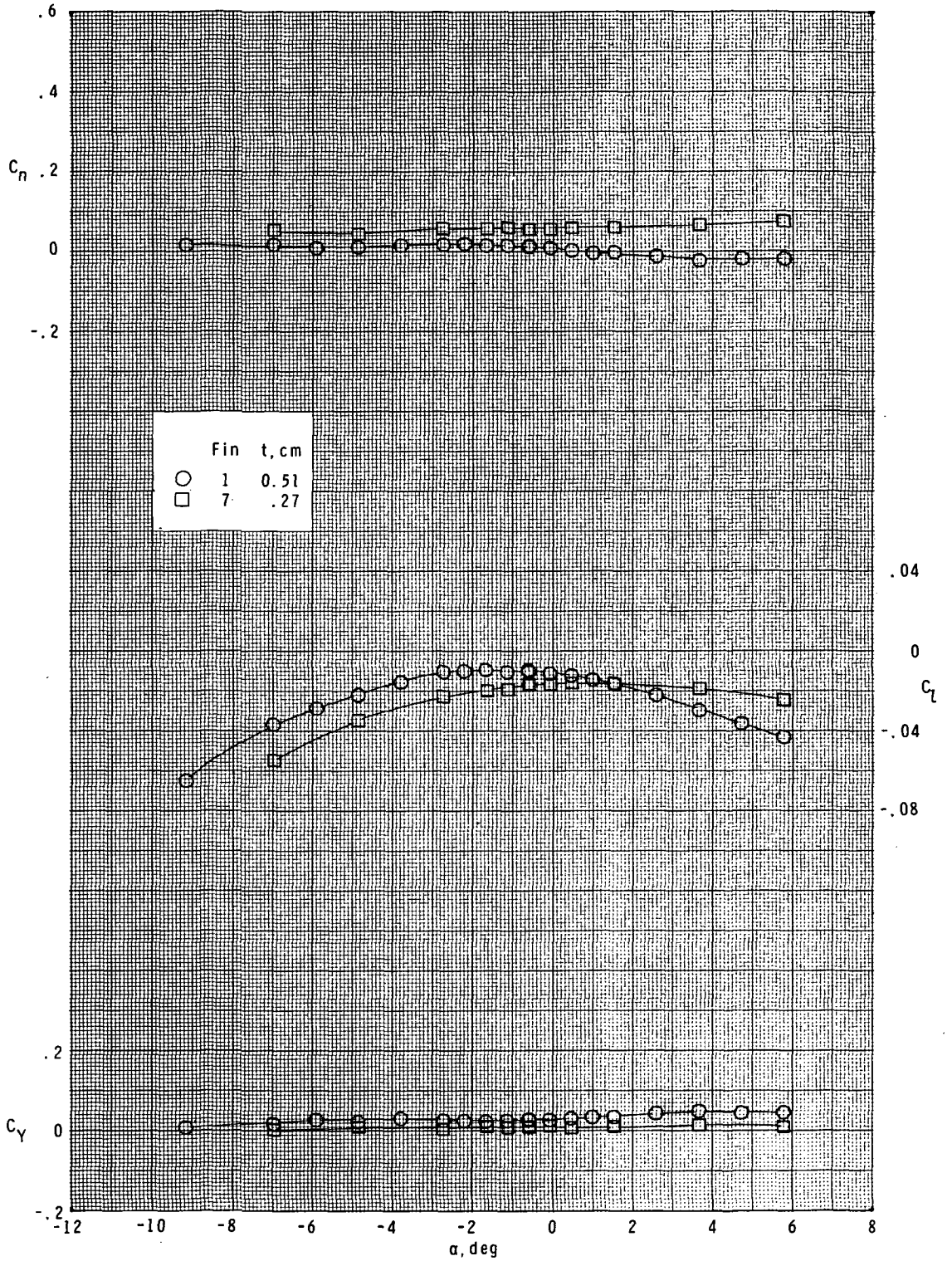

(b) M = 1.90.

Figure 34.- Continued.

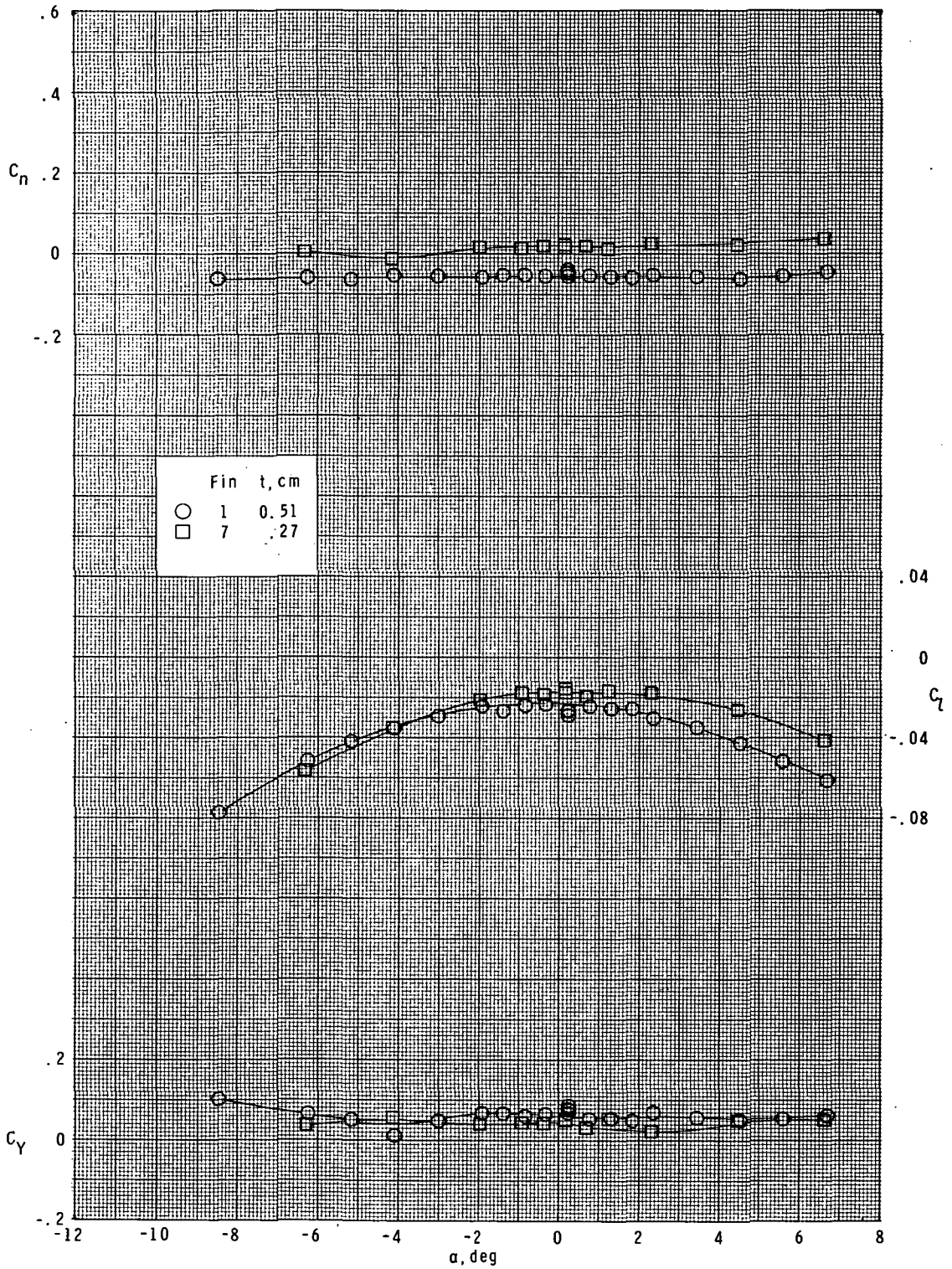

(c) M = 2.36.

Figure 34.- Continued.

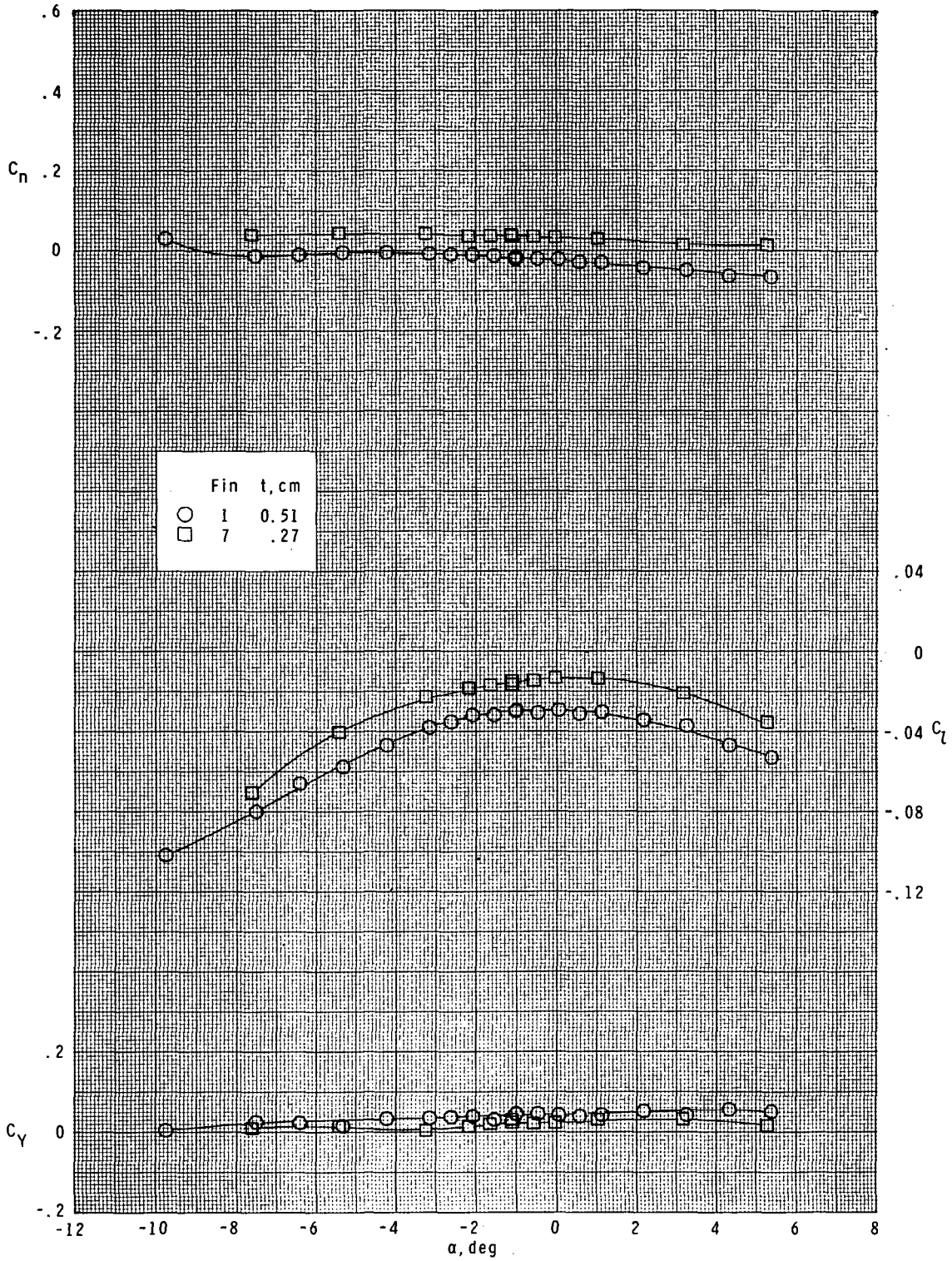

(d) M = 2.86.

Figure 34.- Concluded.

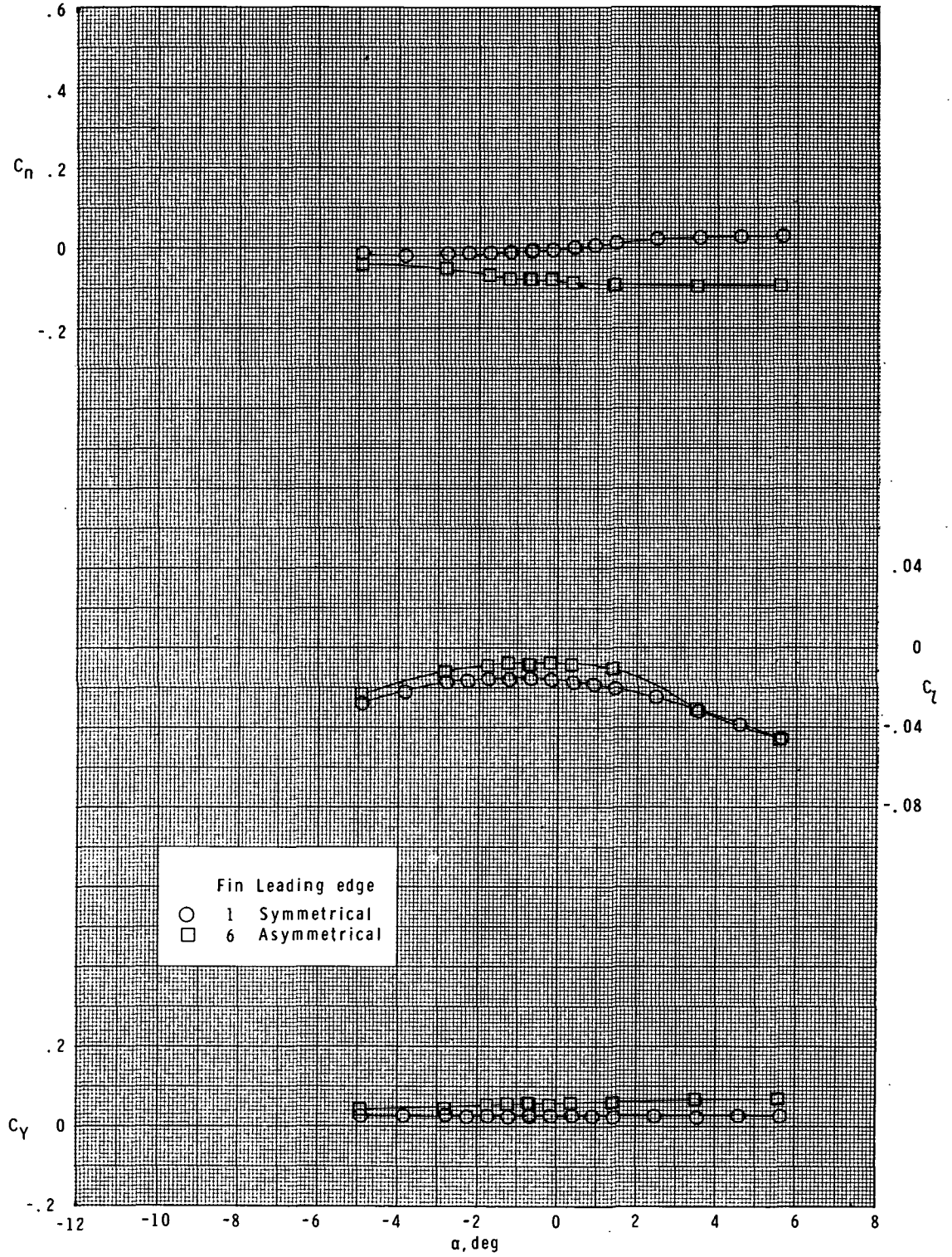

(a) M = 1.60.

Figure 35.- Effect of fin leading-edge shape on lateral characteristics. Basic body (B_1); long-chord curved fins (F_1 and F_6); $\phi = 0^o$.

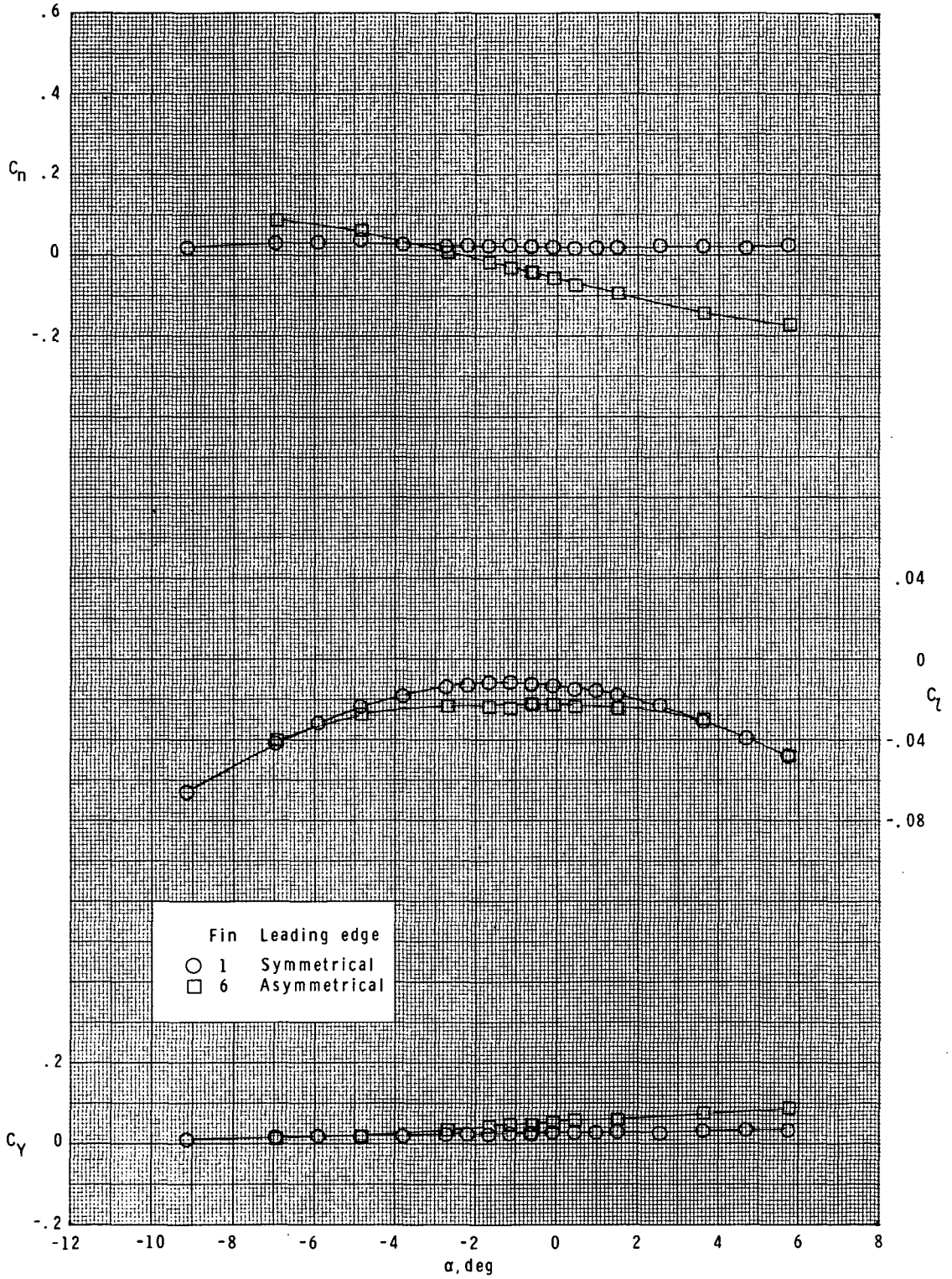

(b) M = 1.90.

Figure 35.- Continued.

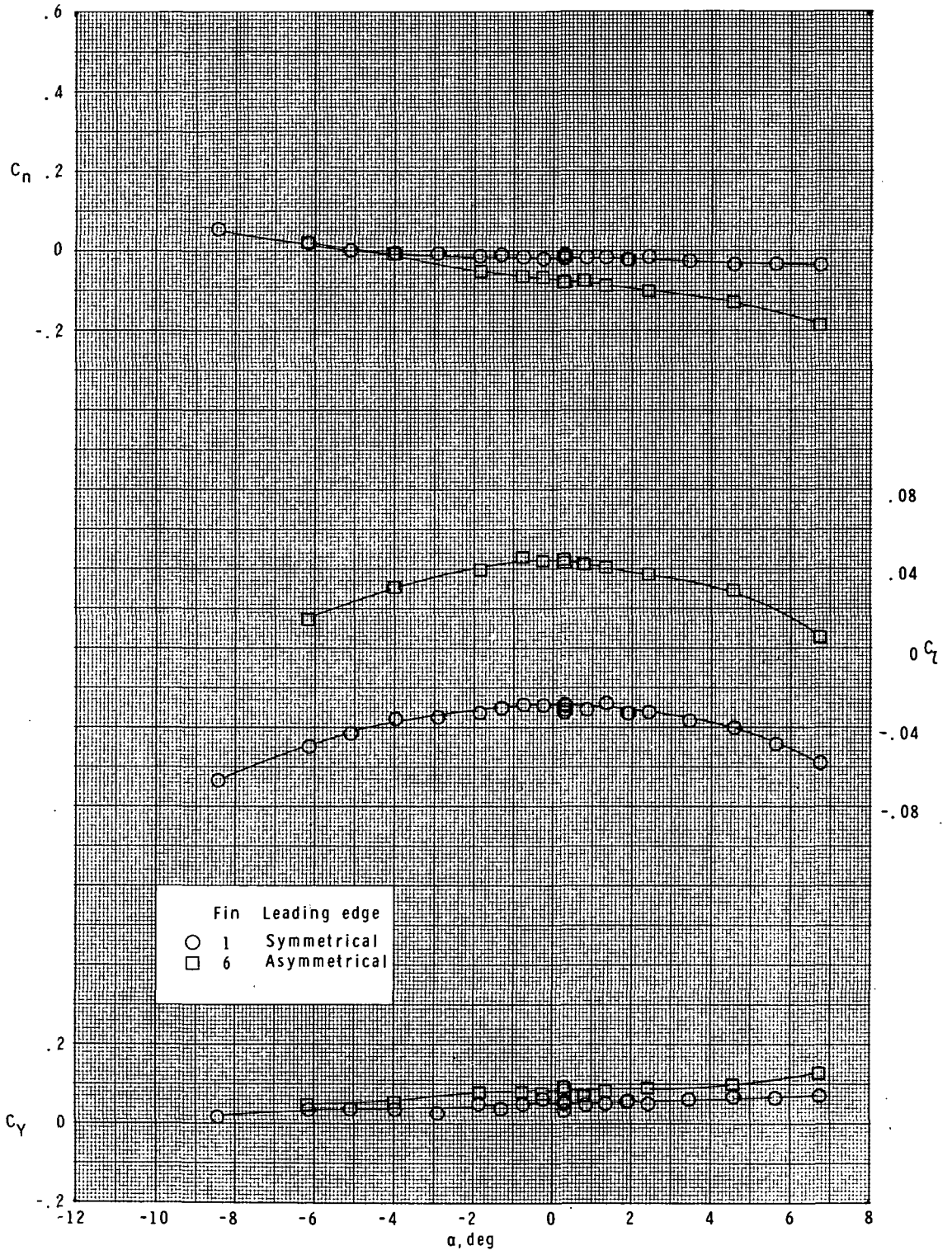

(c) M = 2.36.

Figure 35.- Continued.

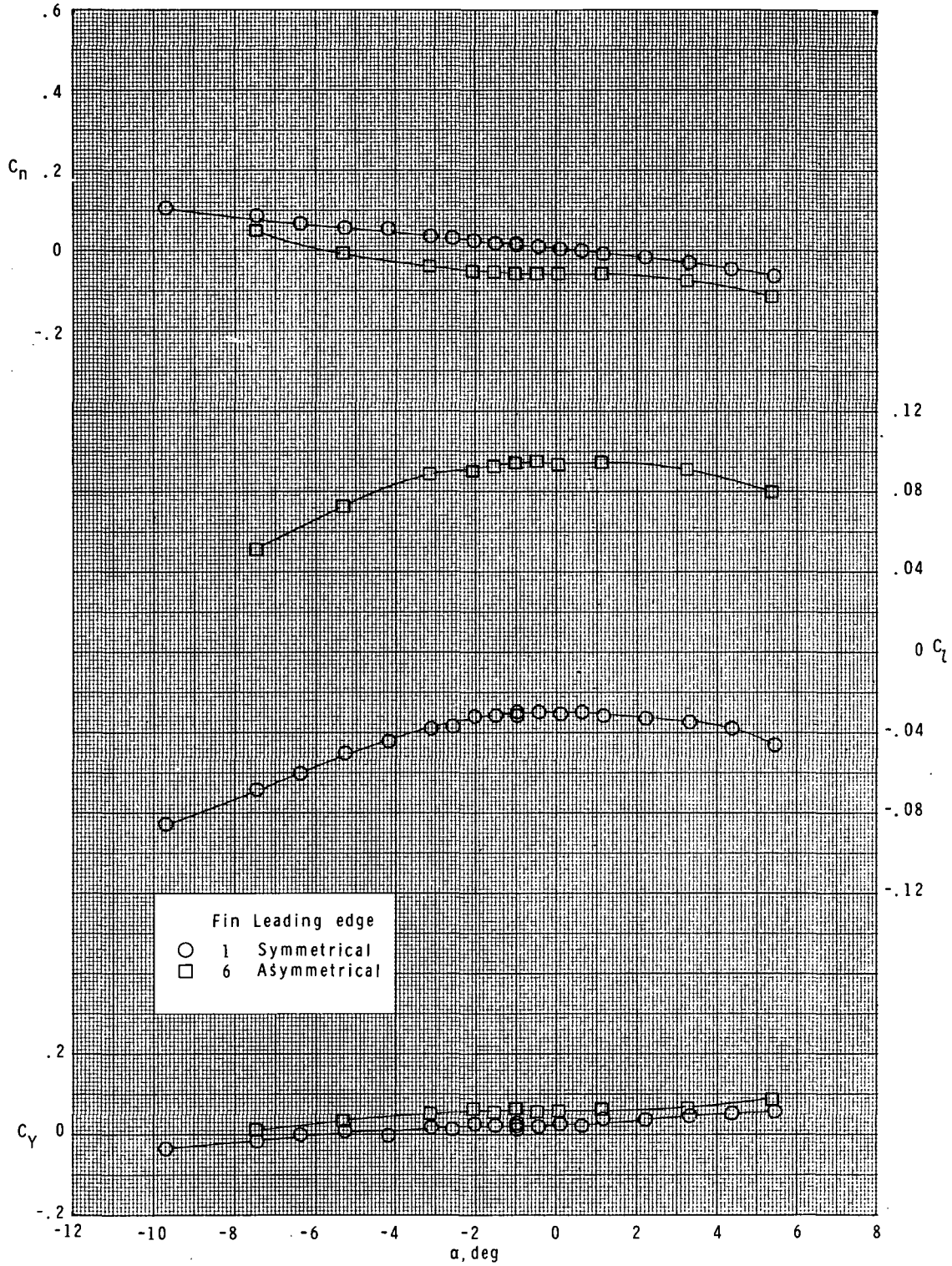

(d) M = 2.86.

Figure 35.- Concluded.

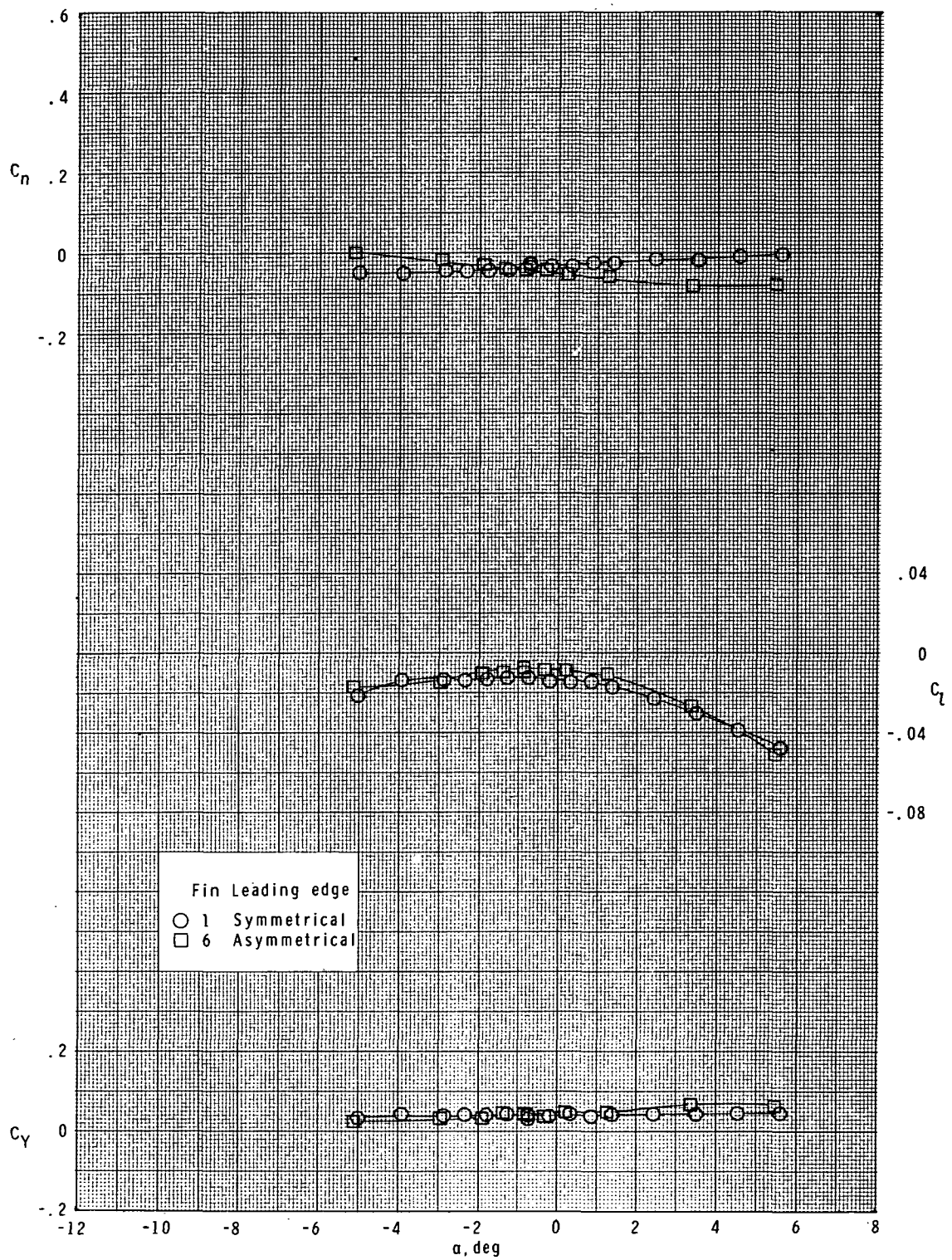

(a) M = 1.60.

Figure 36.- Effect of fin leading-edge shape on lateral characteristics. Basic body (B_1); long-chord curved fins (F_1 and F_6); $\phi = 45^o$.

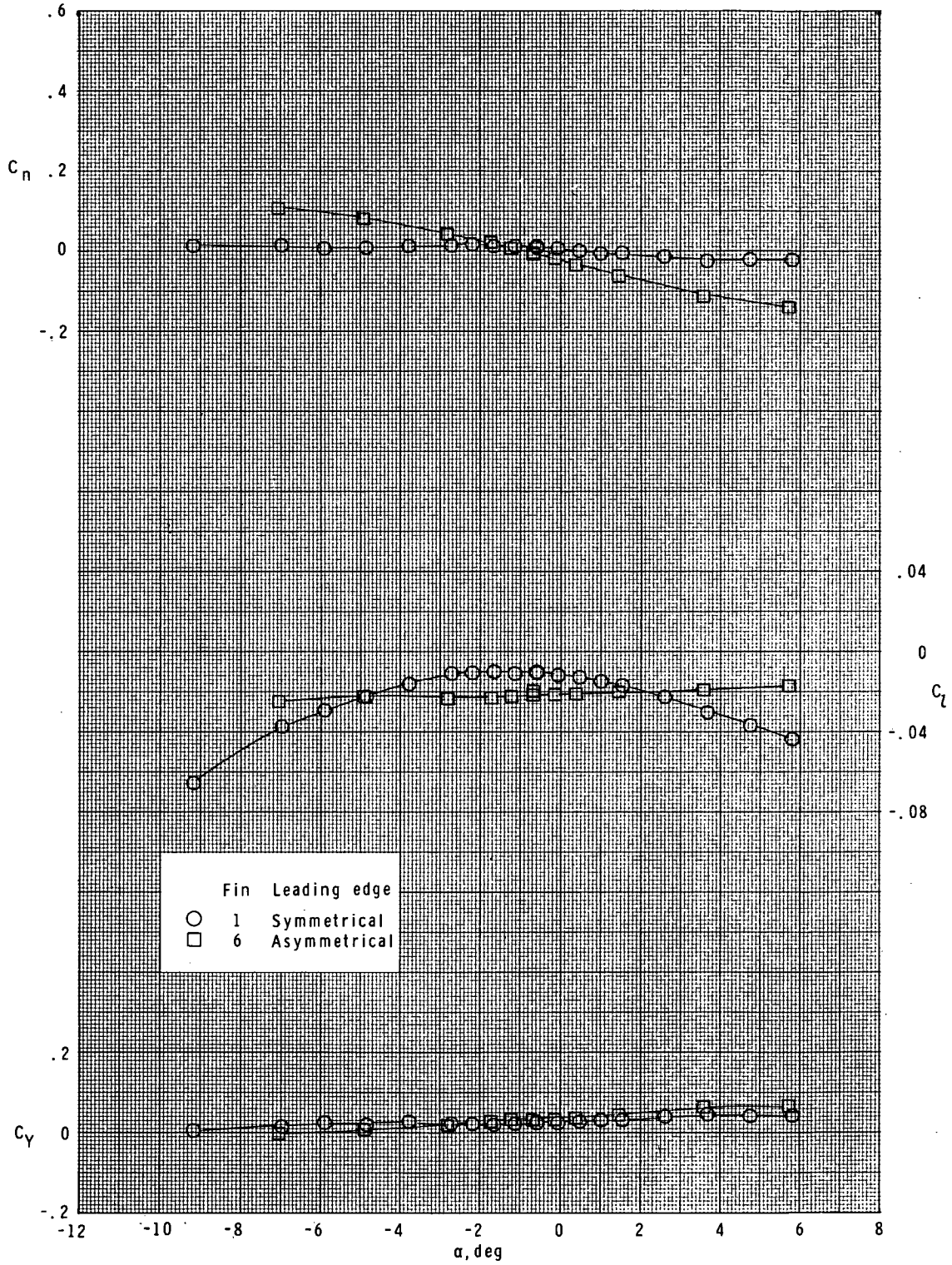

(b) M = 1.90.

Figure 36.- Continued.

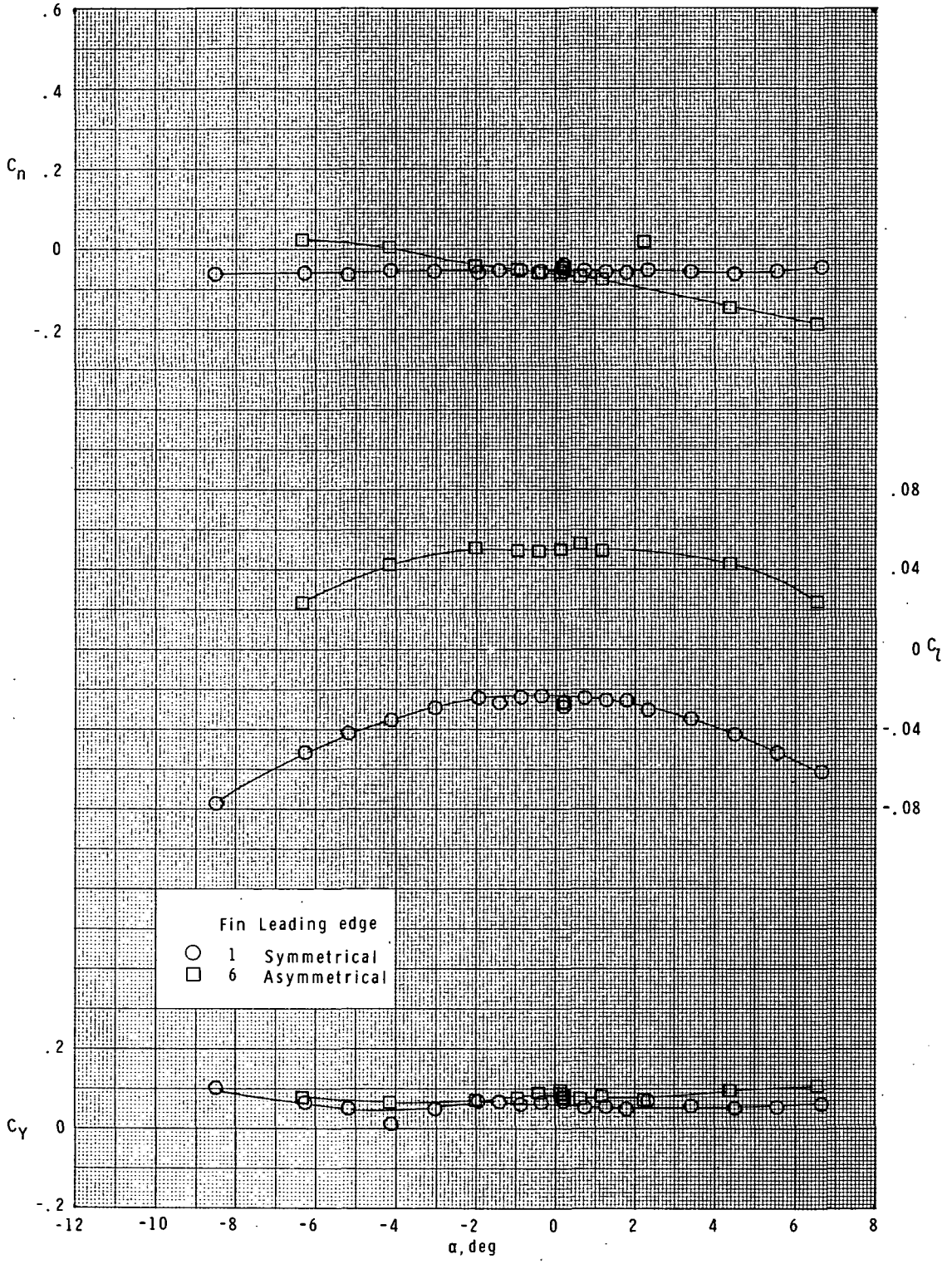

(c) M = 2.36.

Figure 36.- Continued.

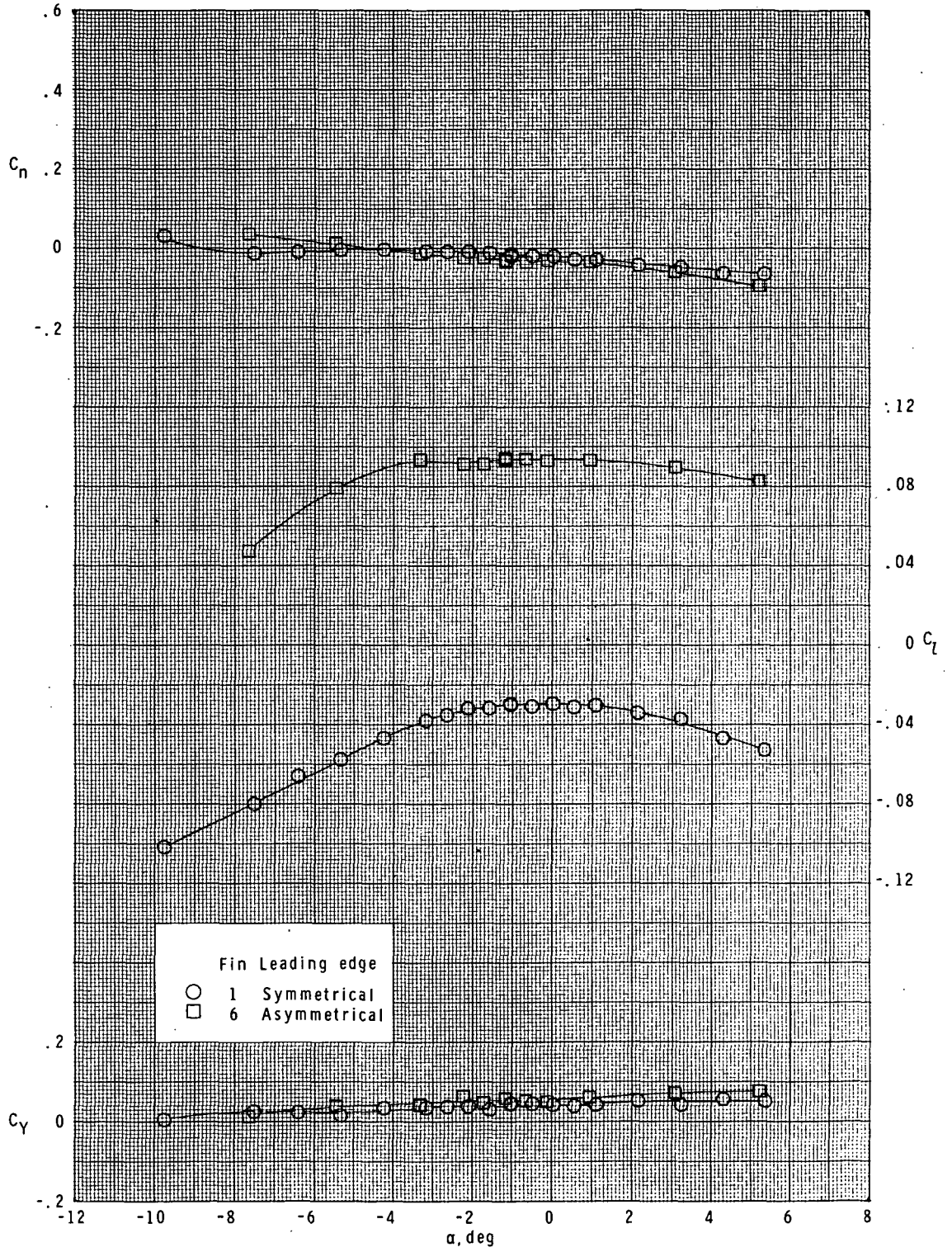

(d) M = 2.86.

Figure 36.- Concluded.

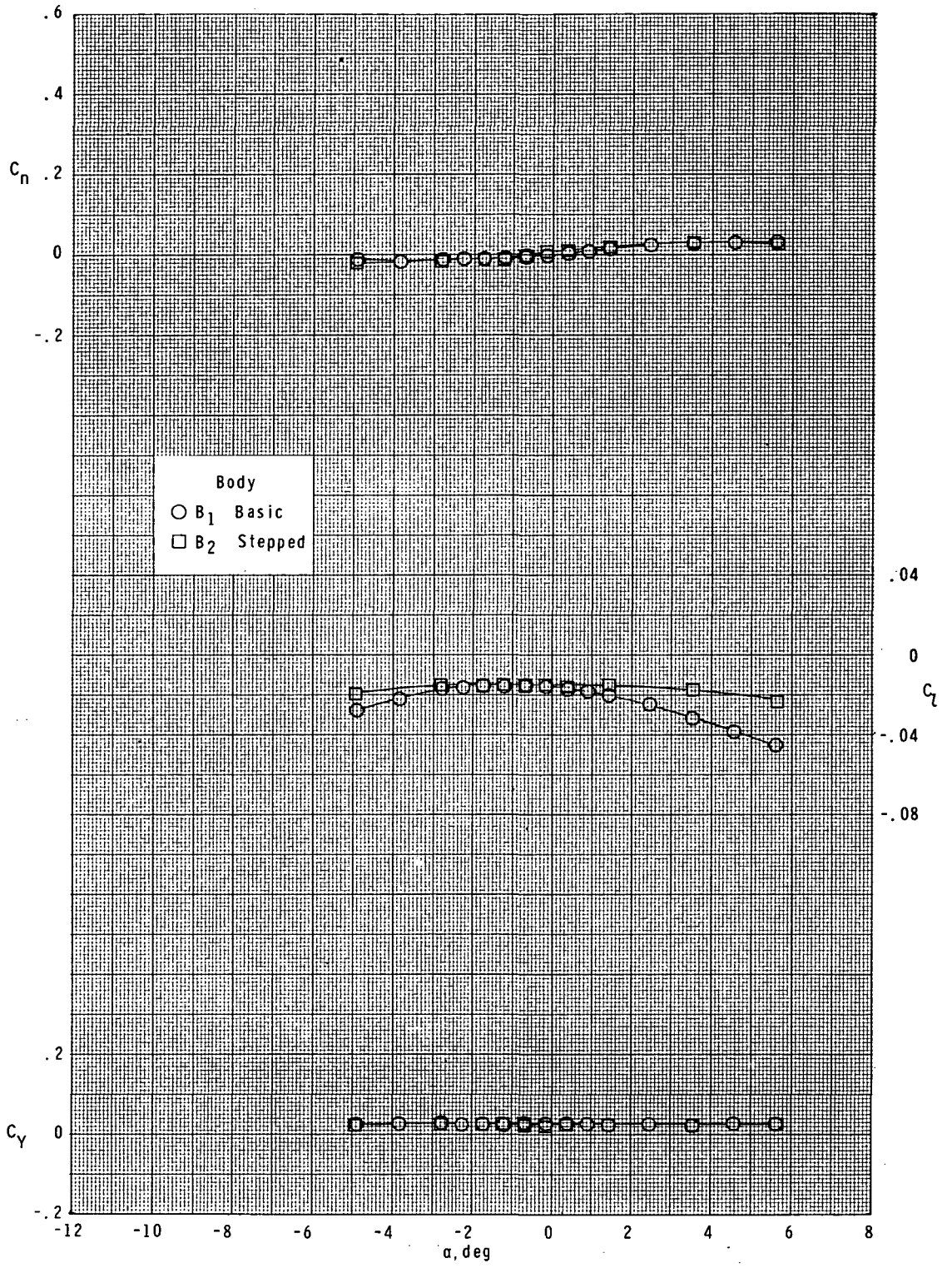

(a) M = 1.60.

Figure 37.- Effect of afterbody diameter on lateral characteristics. Long-chord unswept curved fin (F_1); bodies (B_1 and B_2); $\phi = 0^o$.

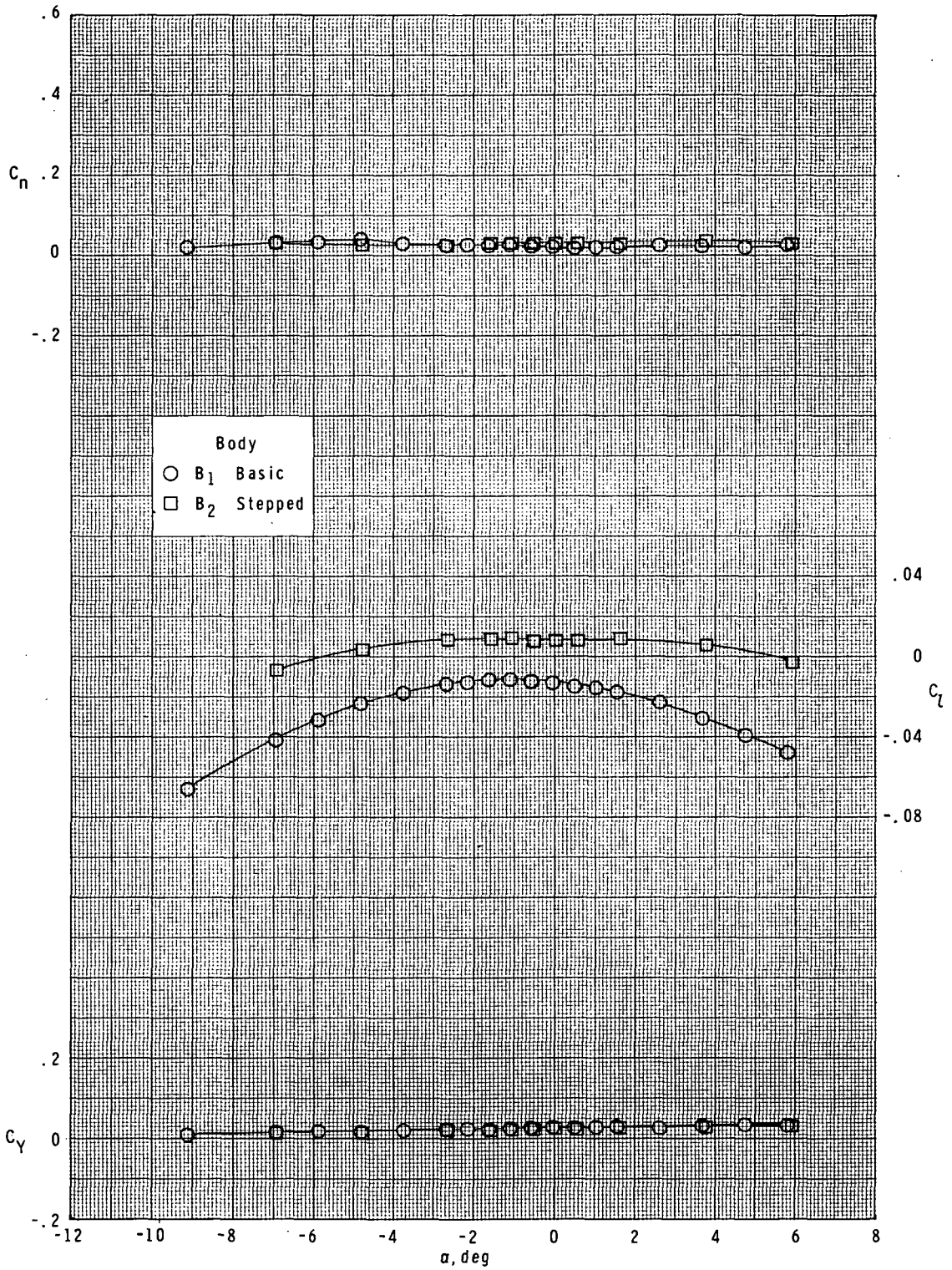

(b) M = 1.90.

Figure 37.- Continued.

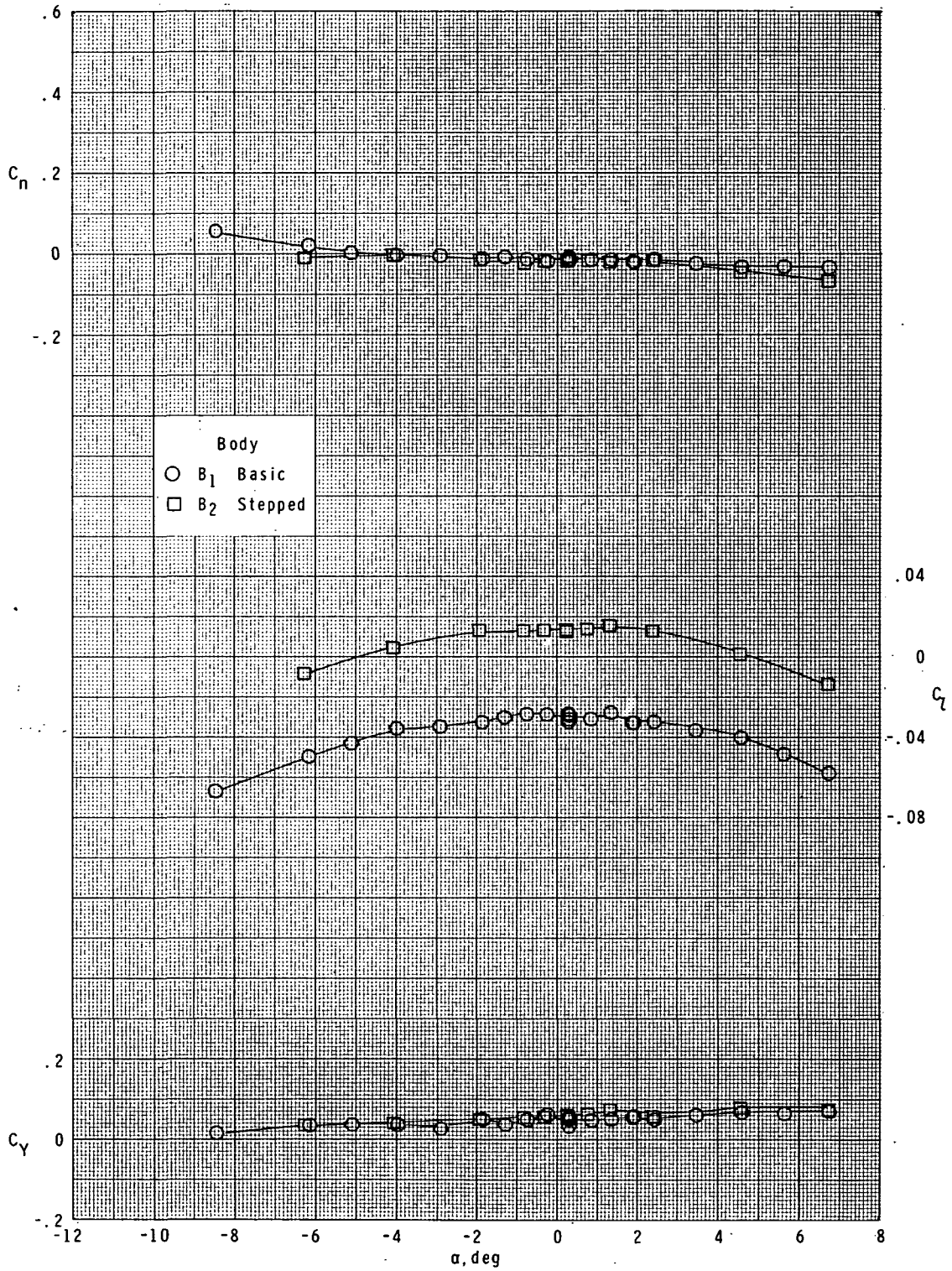

(c) M = 2.36.

Figure 37.- Continued.

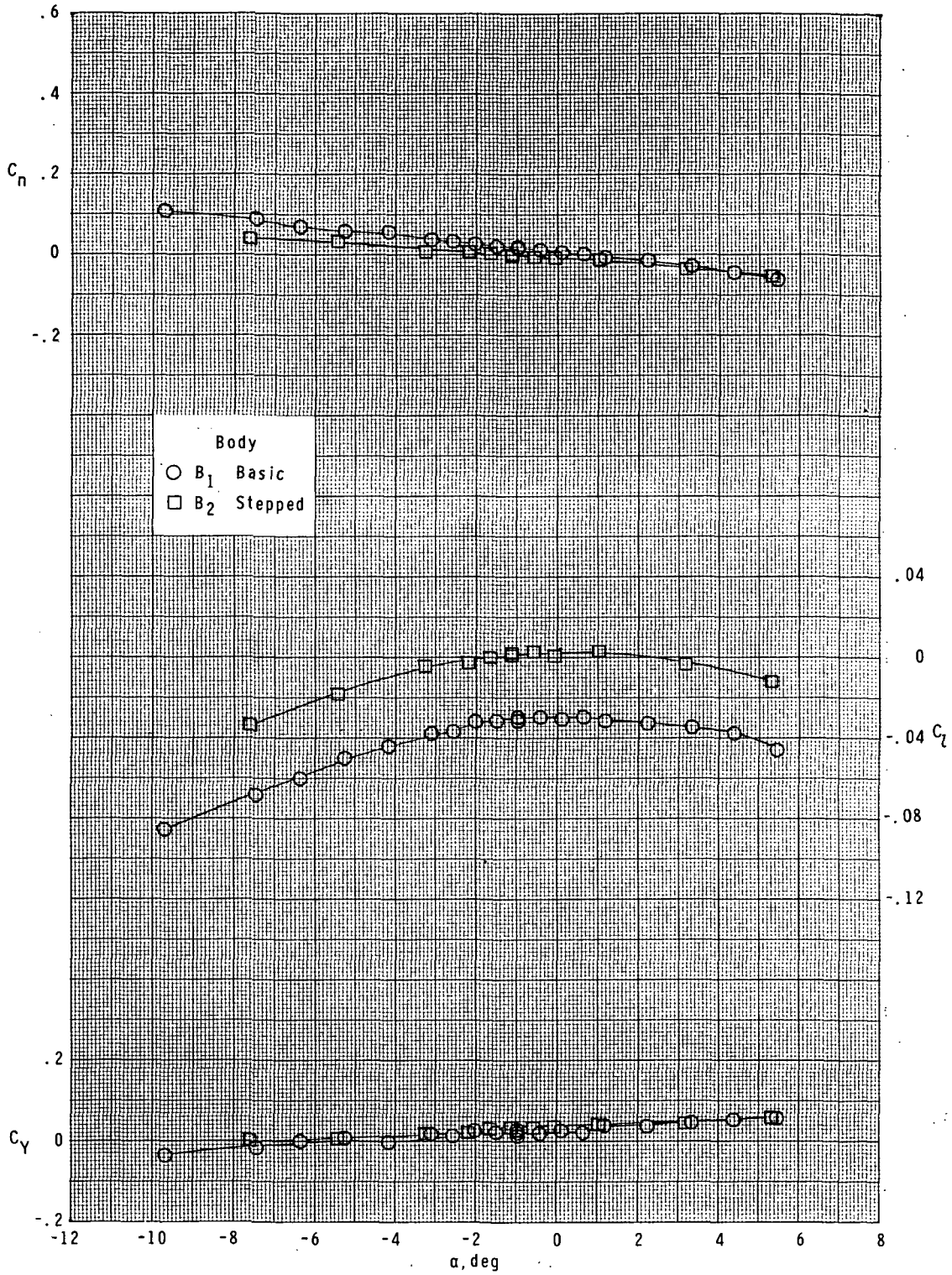

(d) M = 2.86.

Figure 37.- Concluded.

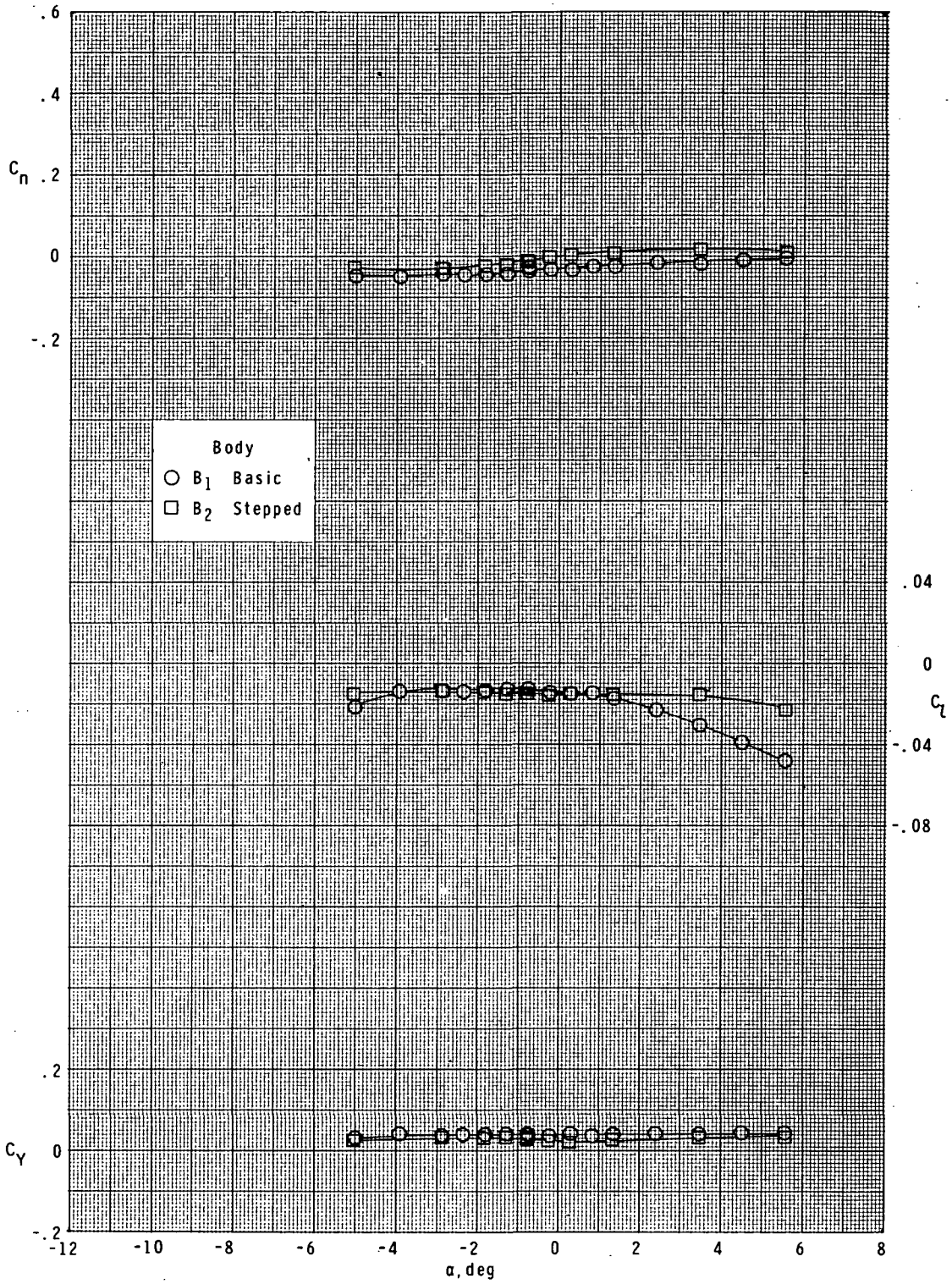

(a) M = 1.60.

Figure 38.- Effect of afterbody diameter on lateral characteristics. Long-chord unswept curved fin (F_1); bodies (B_1 and B_2); $\phi = 45^\circ$.

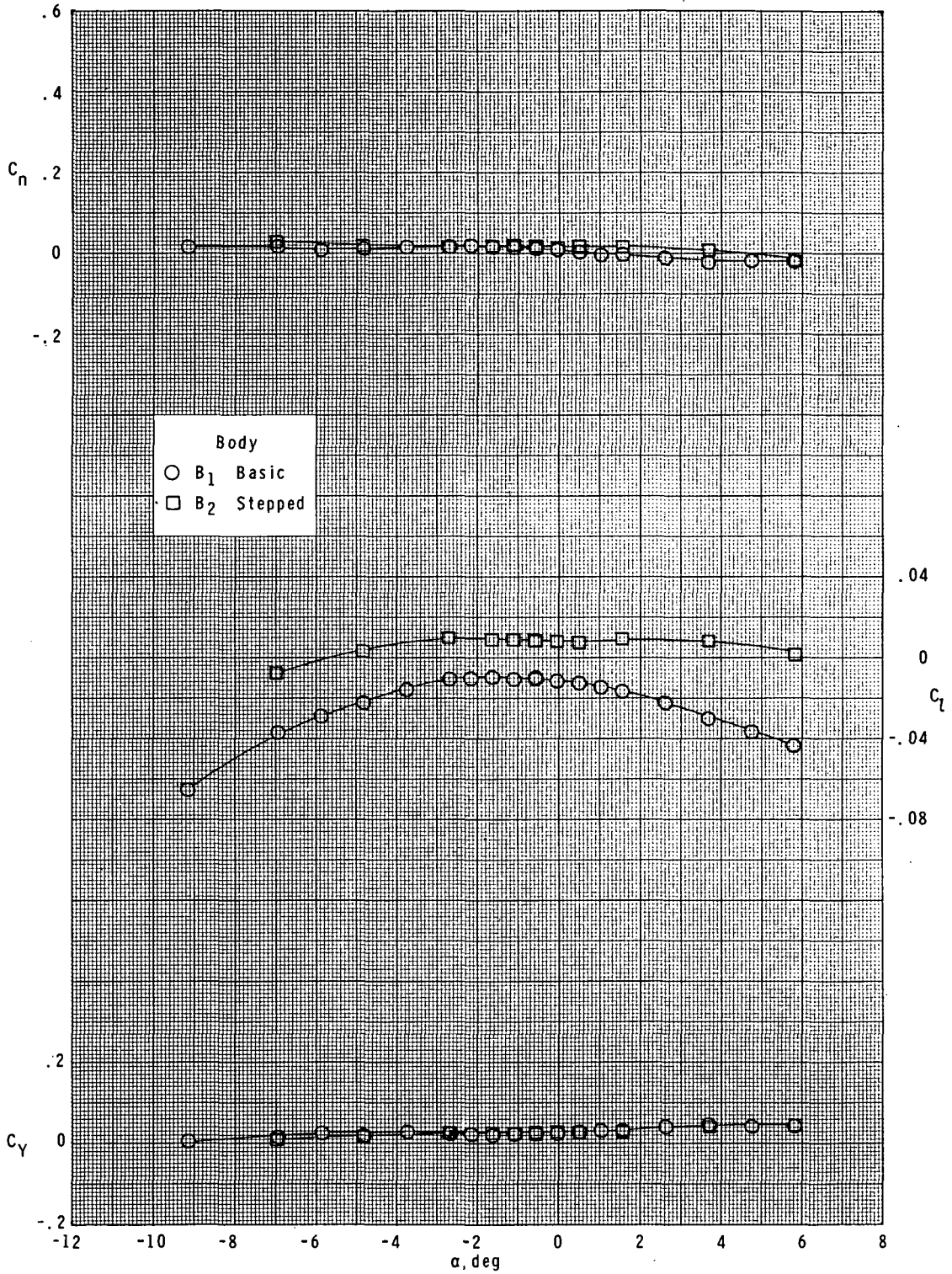

(b) M = 1.90.

Figure 38.- Continued.

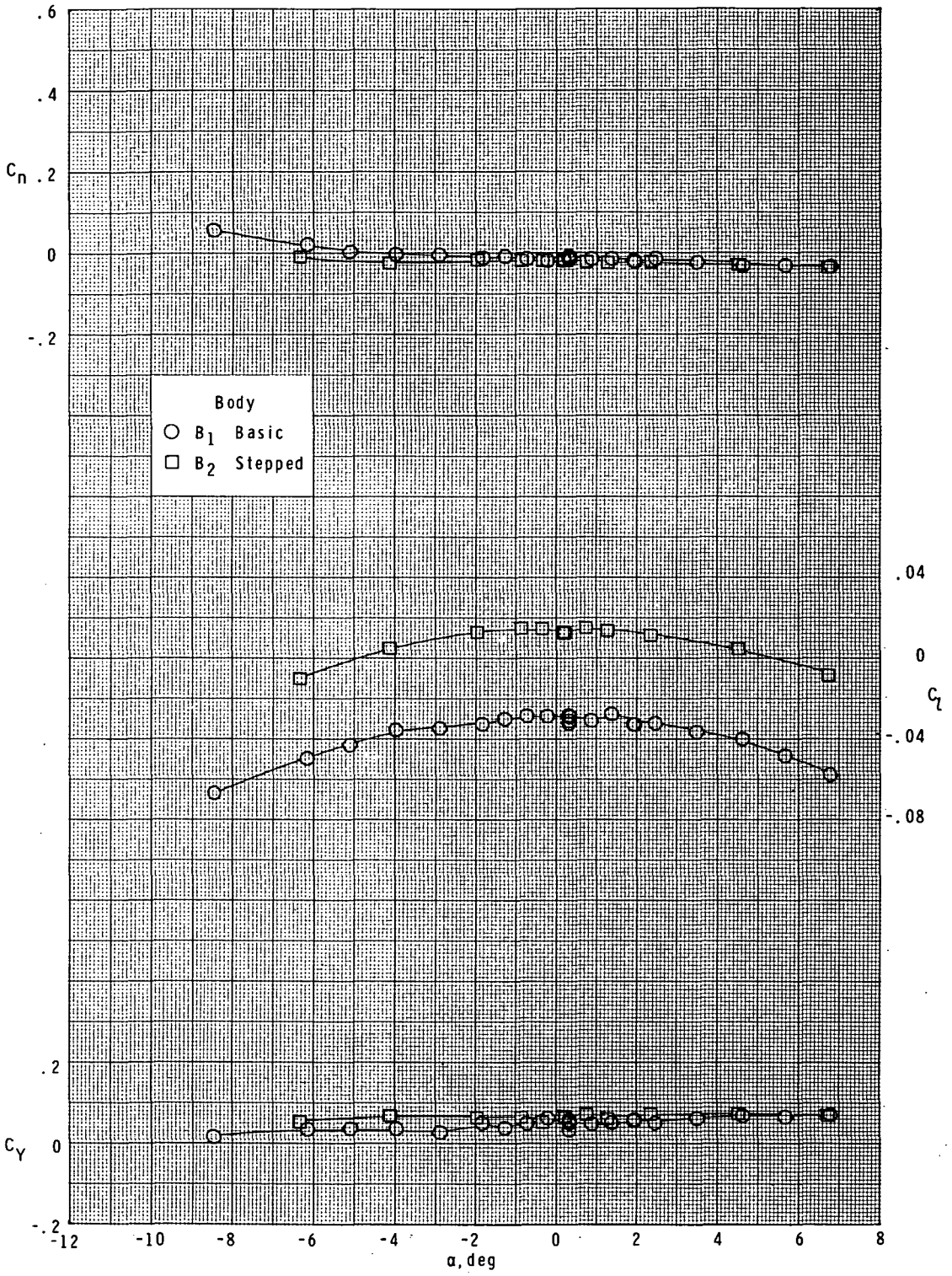

(c) M = 2.36.

Figure 38.- Continued.

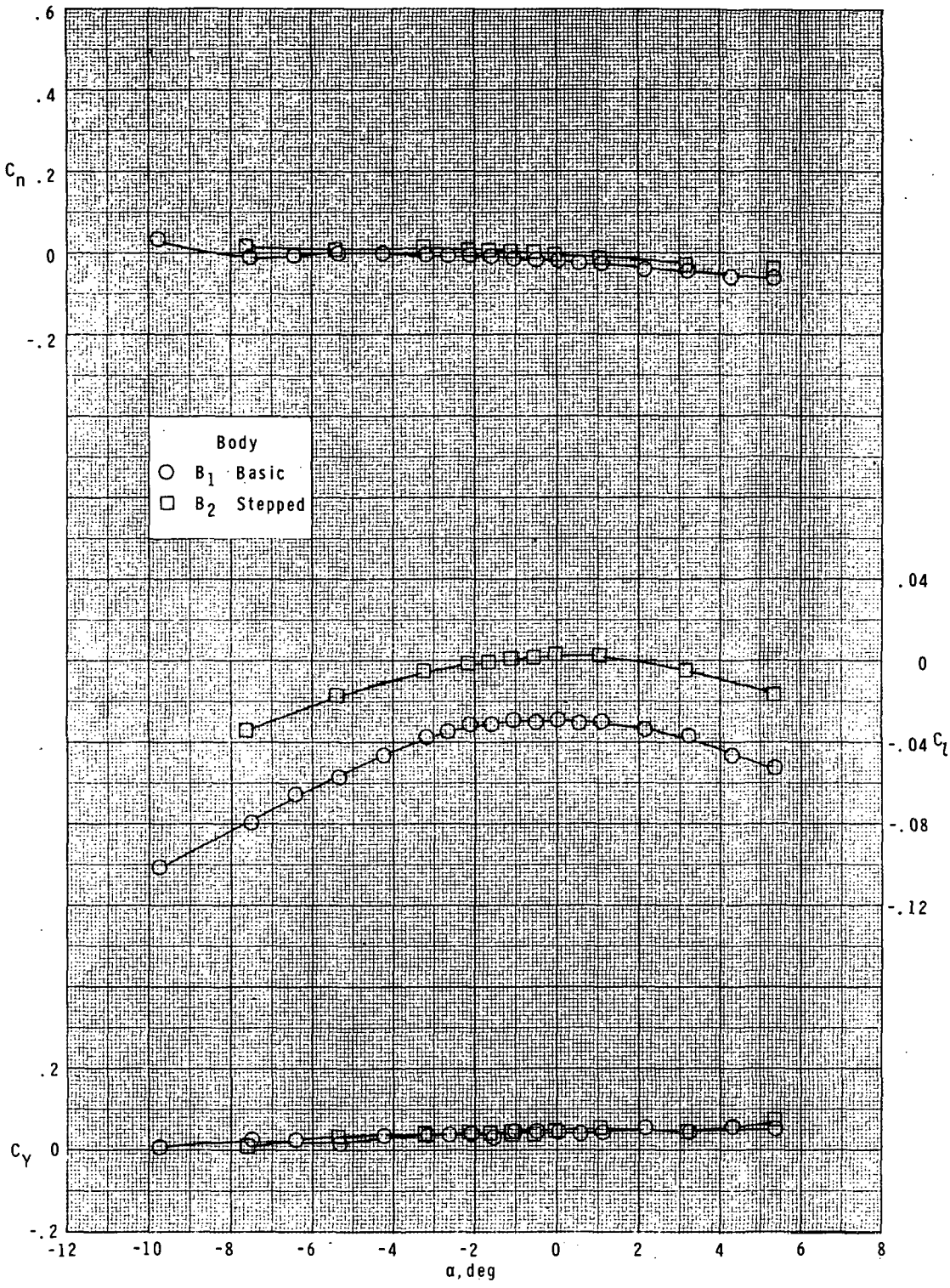

(d) M = 2.86.

Figure 38.- Concluded.

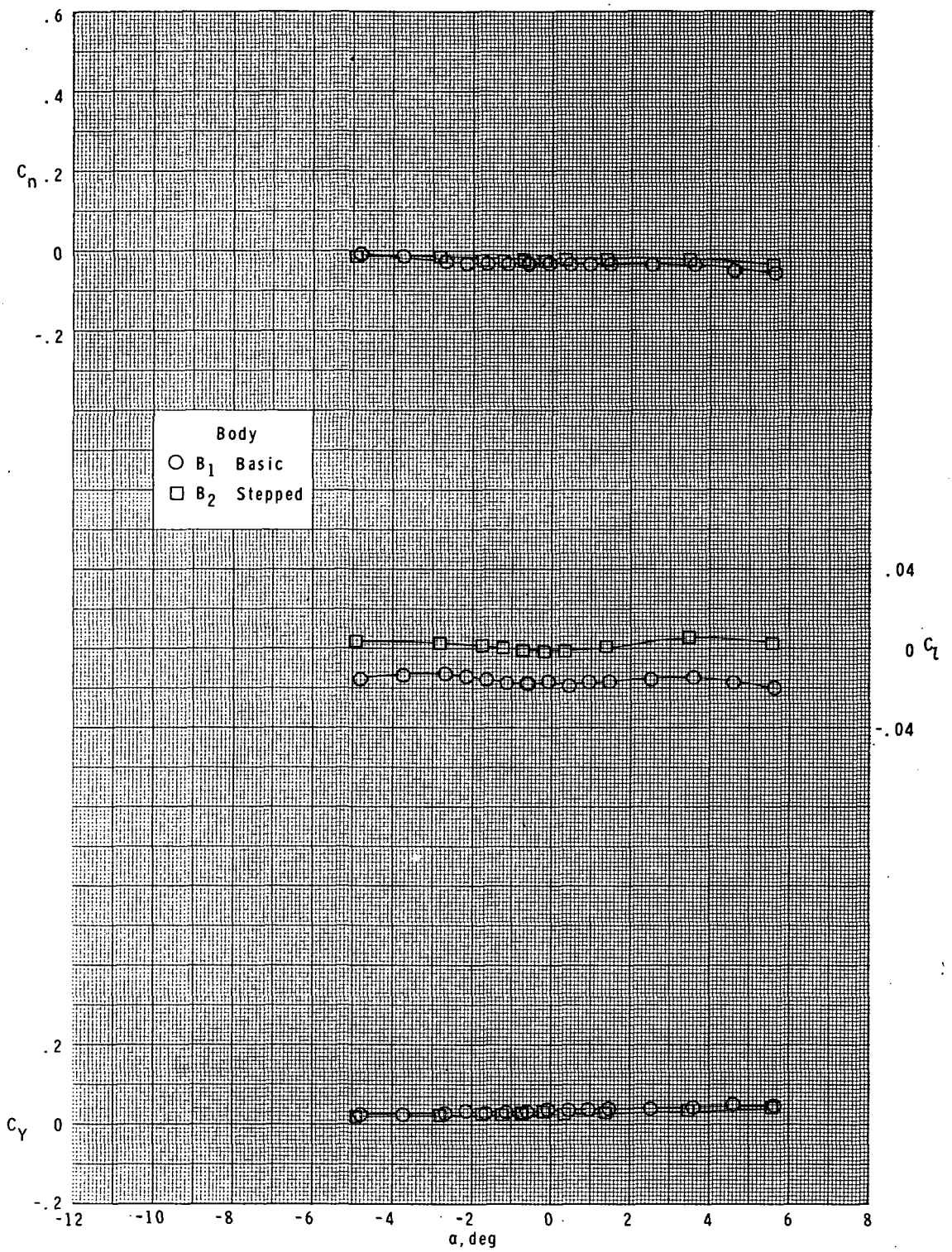

(a) M = 1.60.

Figure 39.- Effect of afterbody diameter on lateral characteristics. Long-chord swept curved fin (F_{13}); bodies (B_1 and B_2); $\phi = 0^o$.

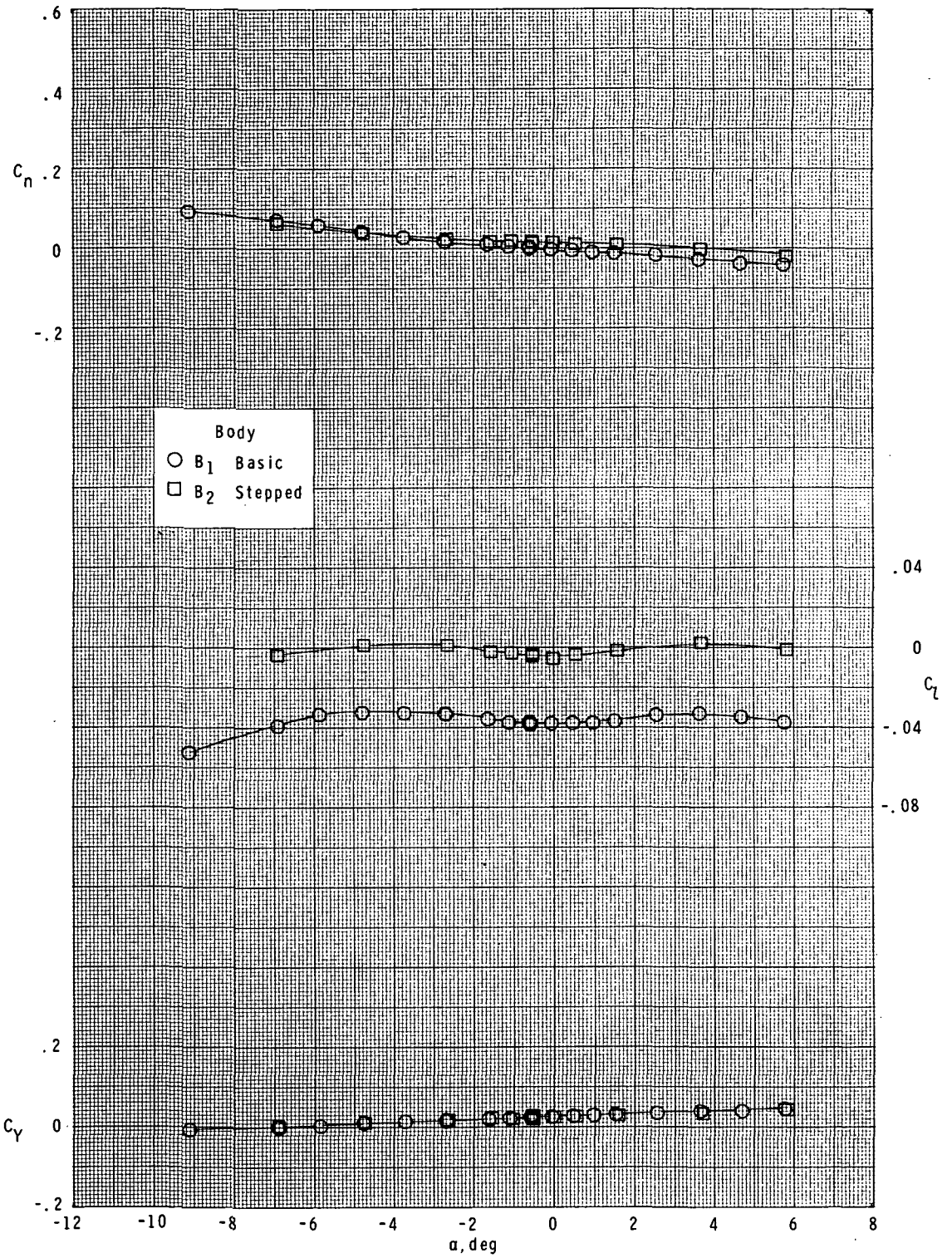

(b) M = 1.90.

Figure 39.- Continued.

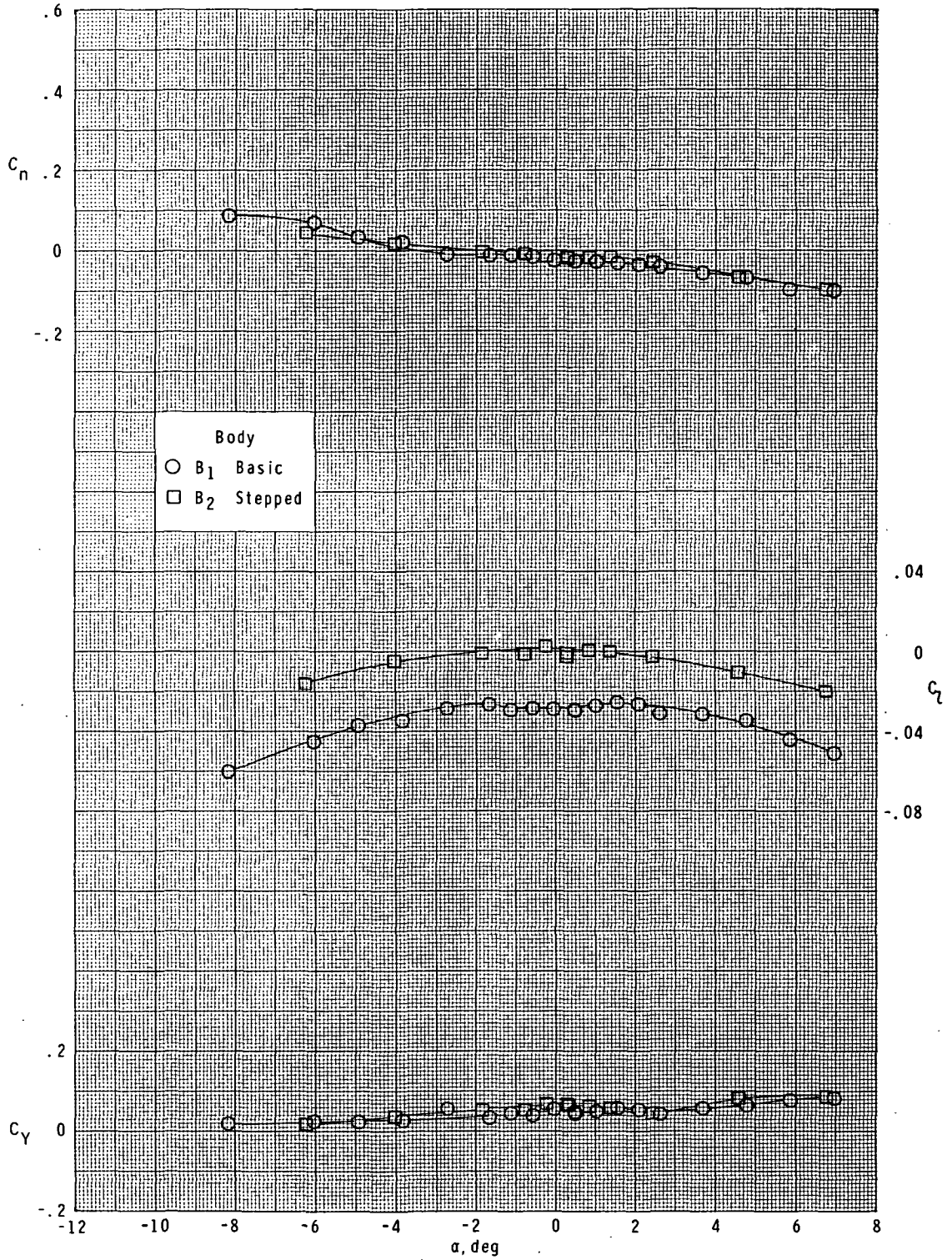

(c) M = 2.36.

Figure 39.- Continued.

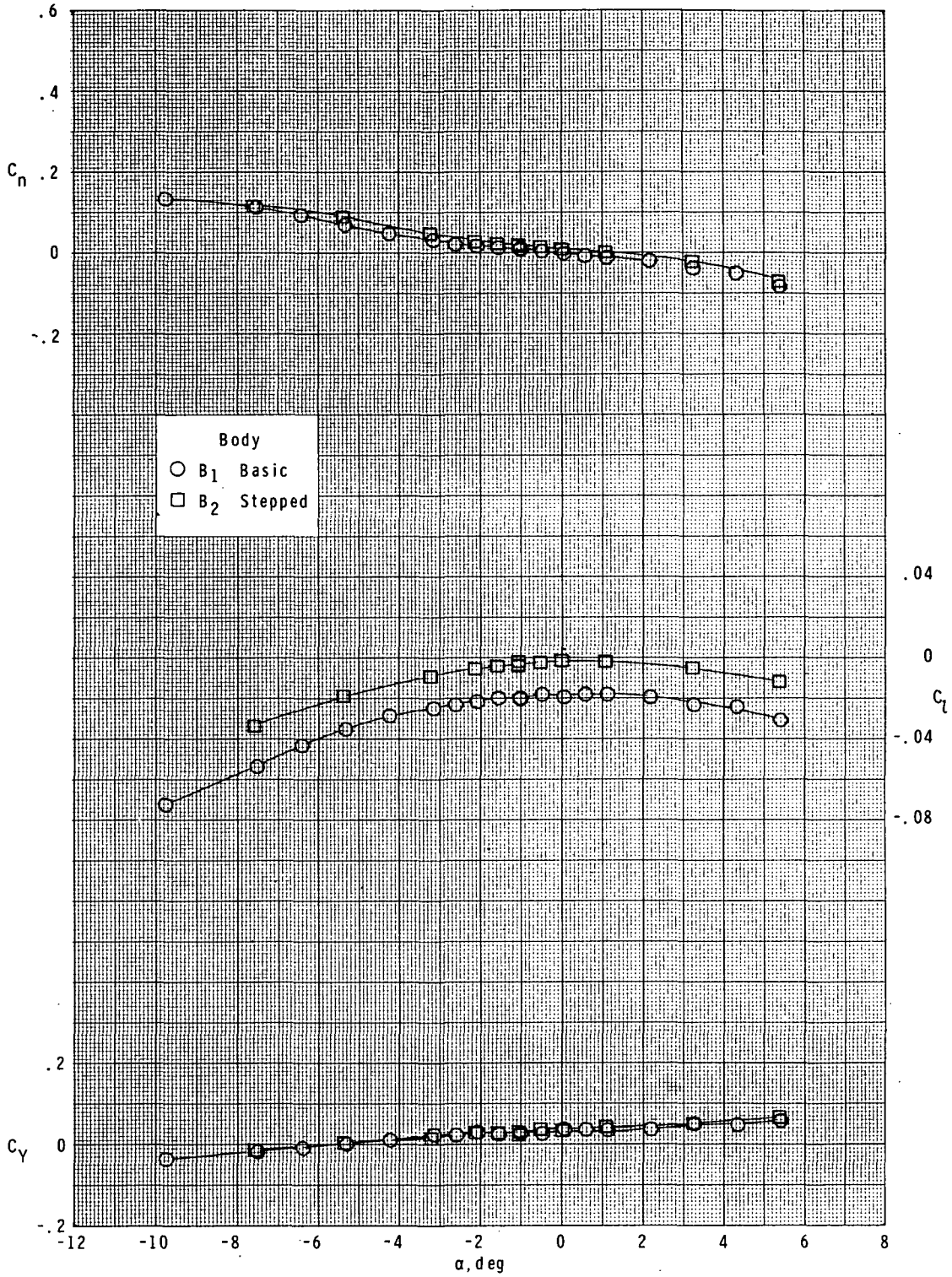

(d) M = 2.86.

Figure 39.- Concluded.

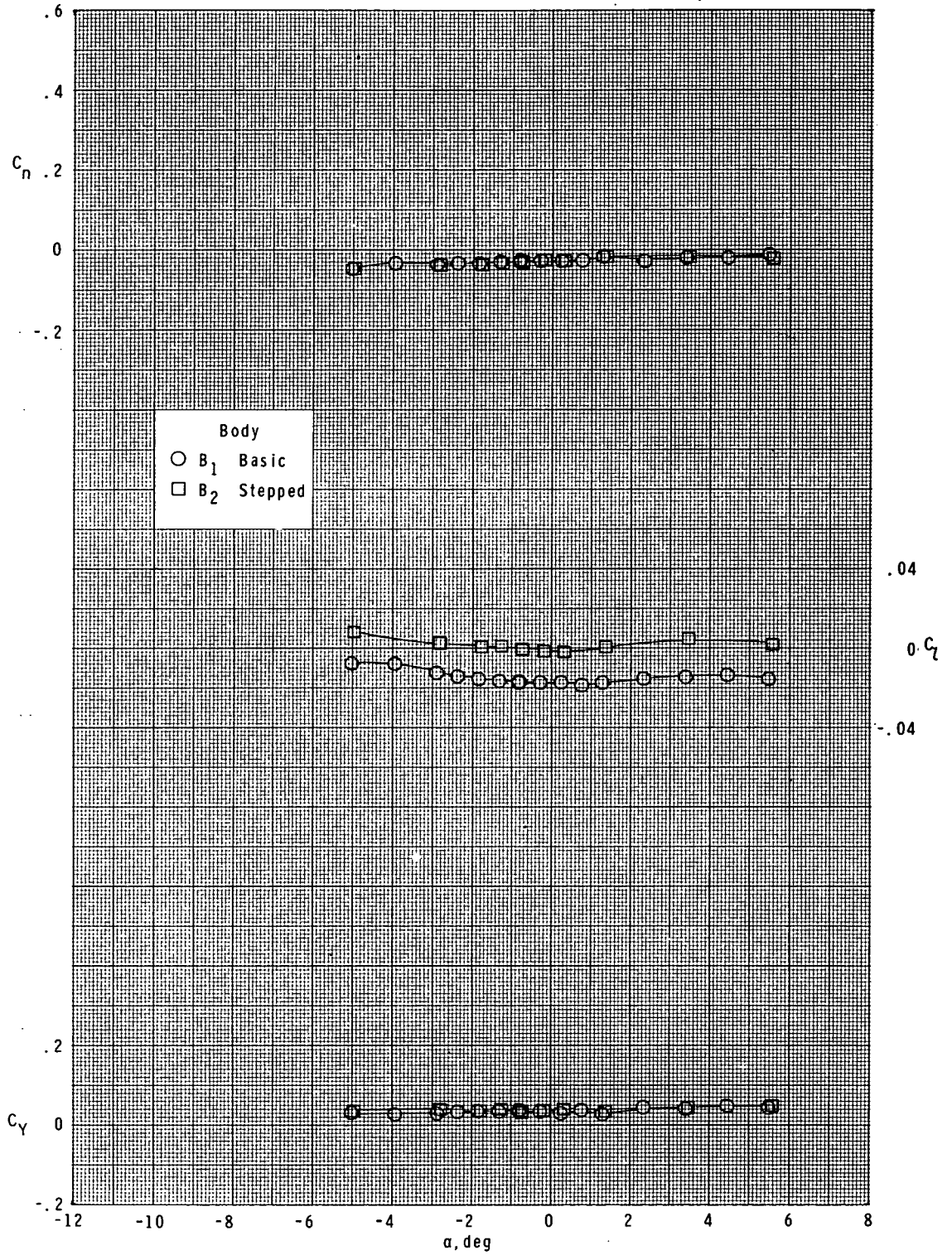

(a) M = 1.60.

Figure 40.- Effect of afterbody diameter on lateral characteristics. Long-chord swept curved fin (F_{13}); bodies (B_1 and B_2); $\phi = 45^{\circ}$.

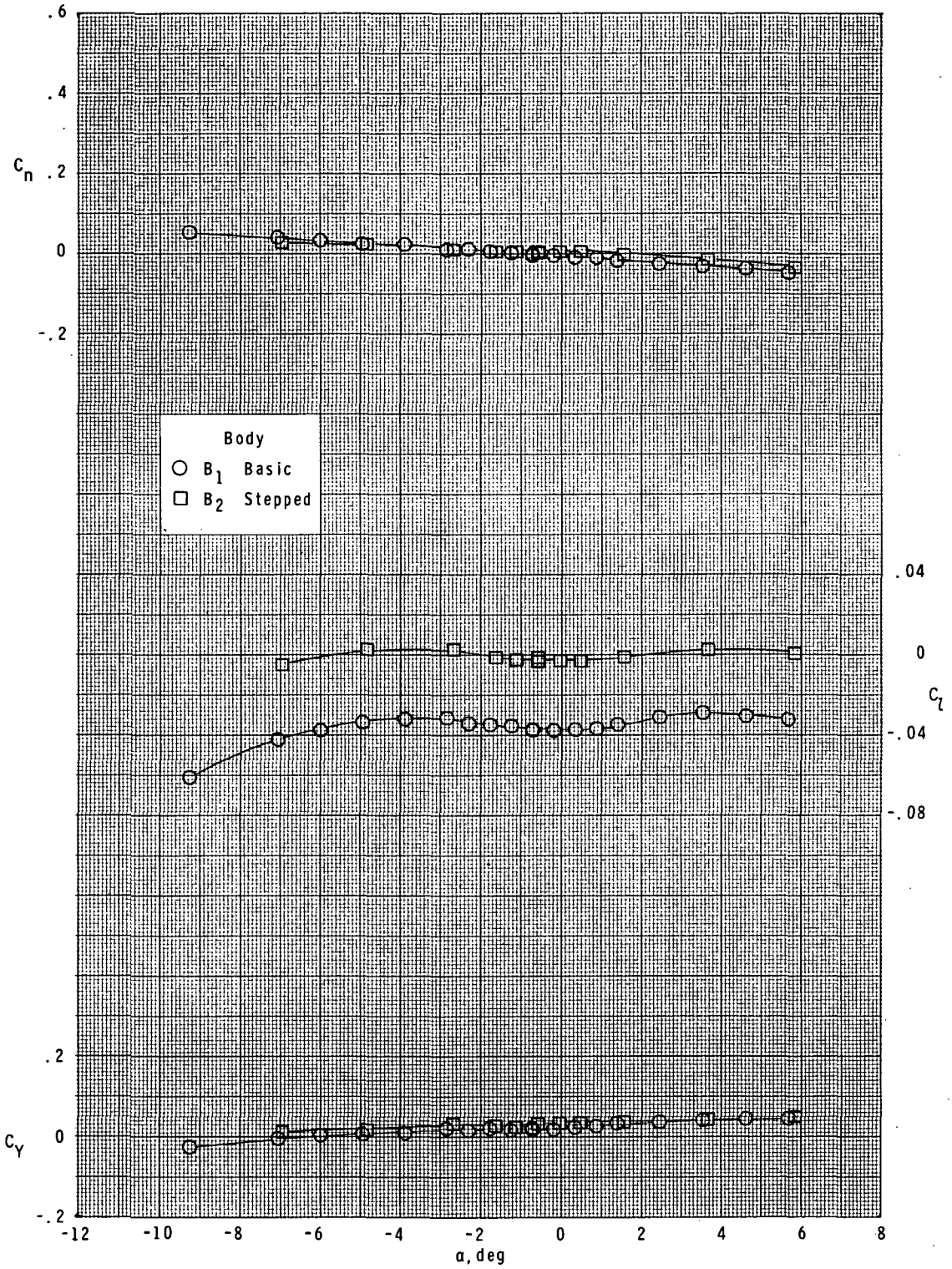

(b) M = 1.90.

Figure 40.- Continued.

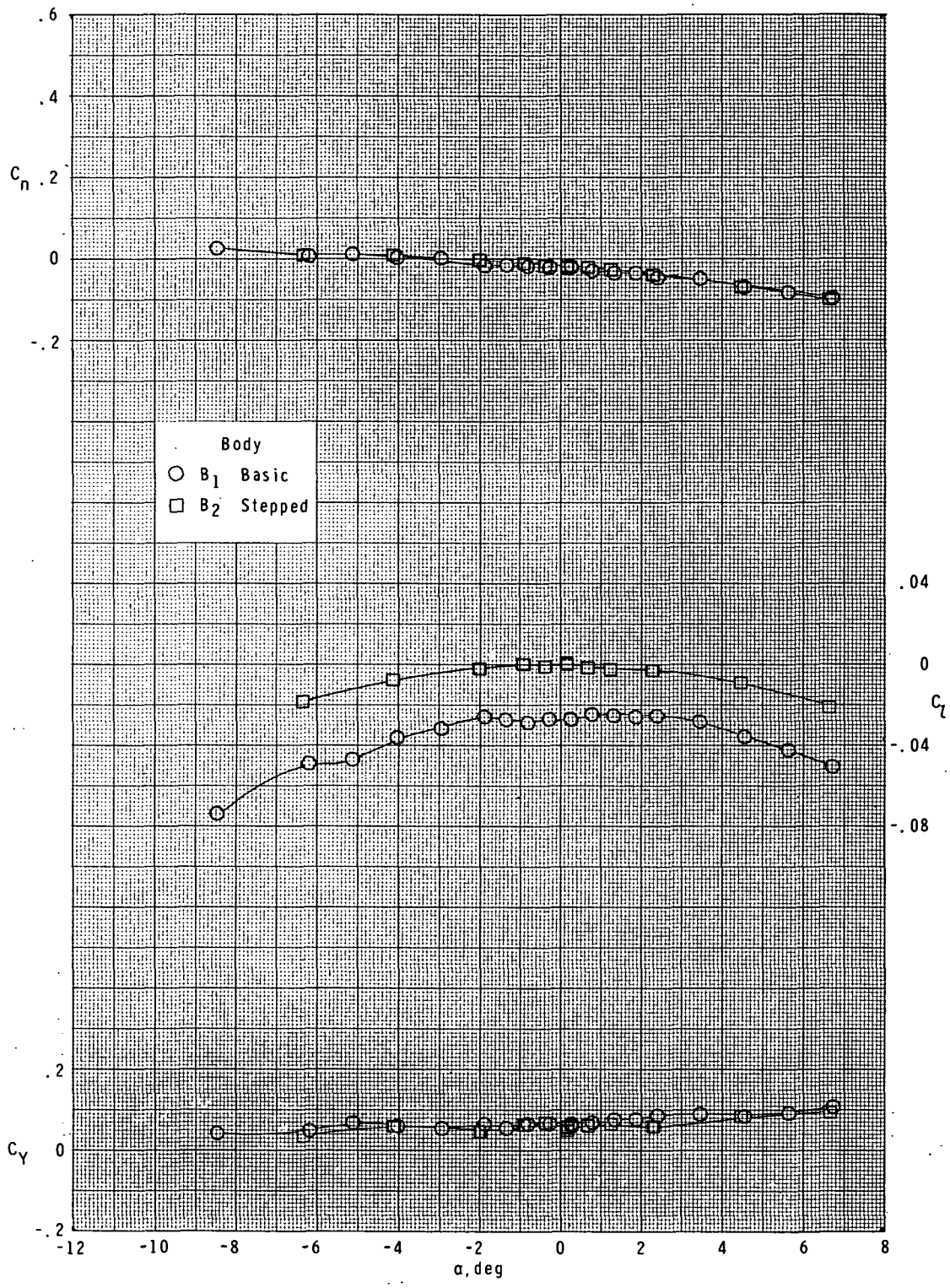

(c) M = 2.36.

Figure 40.- Continued.

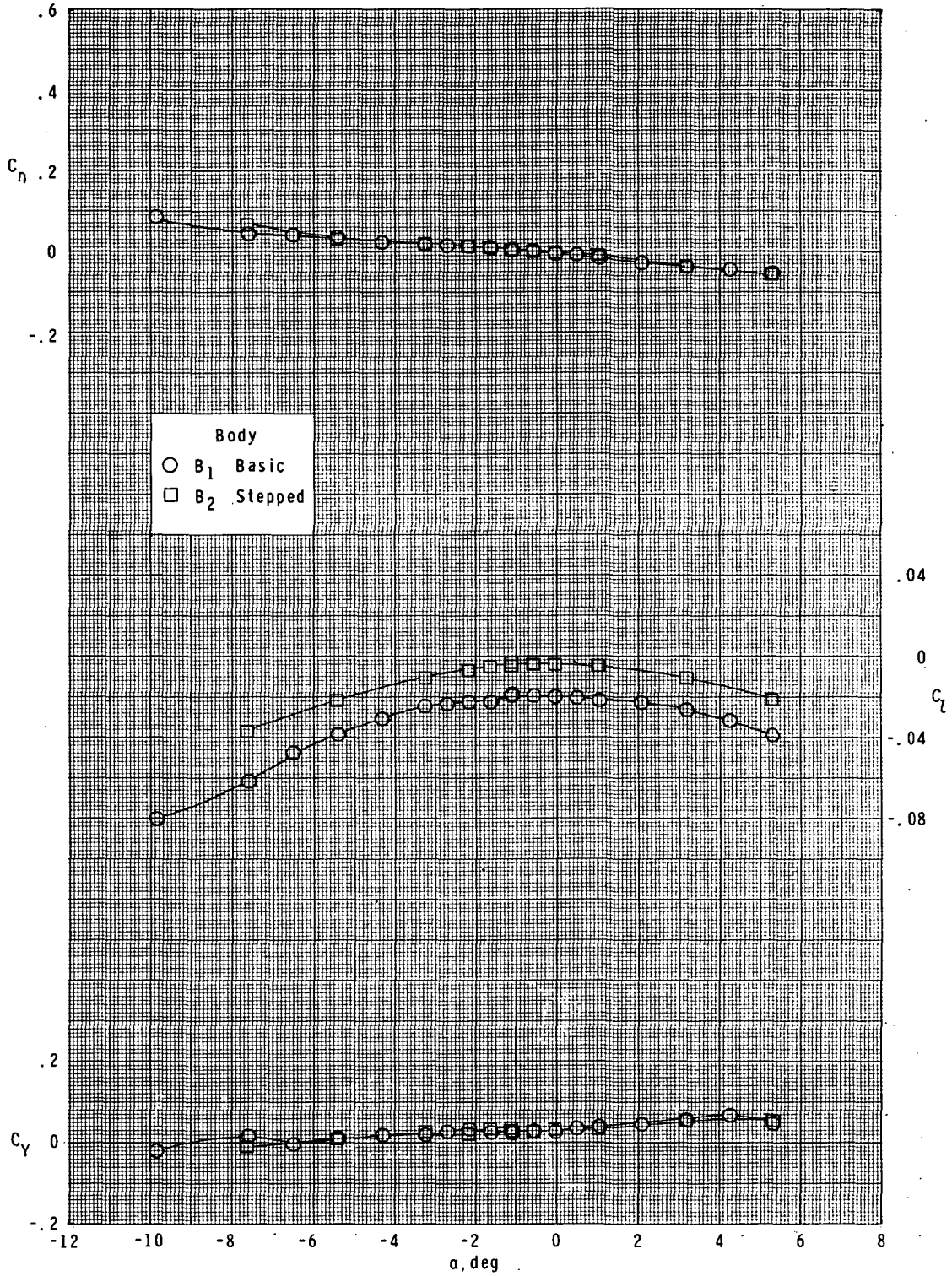

(d) M = 2.86.

Figure 40.- Concluded.

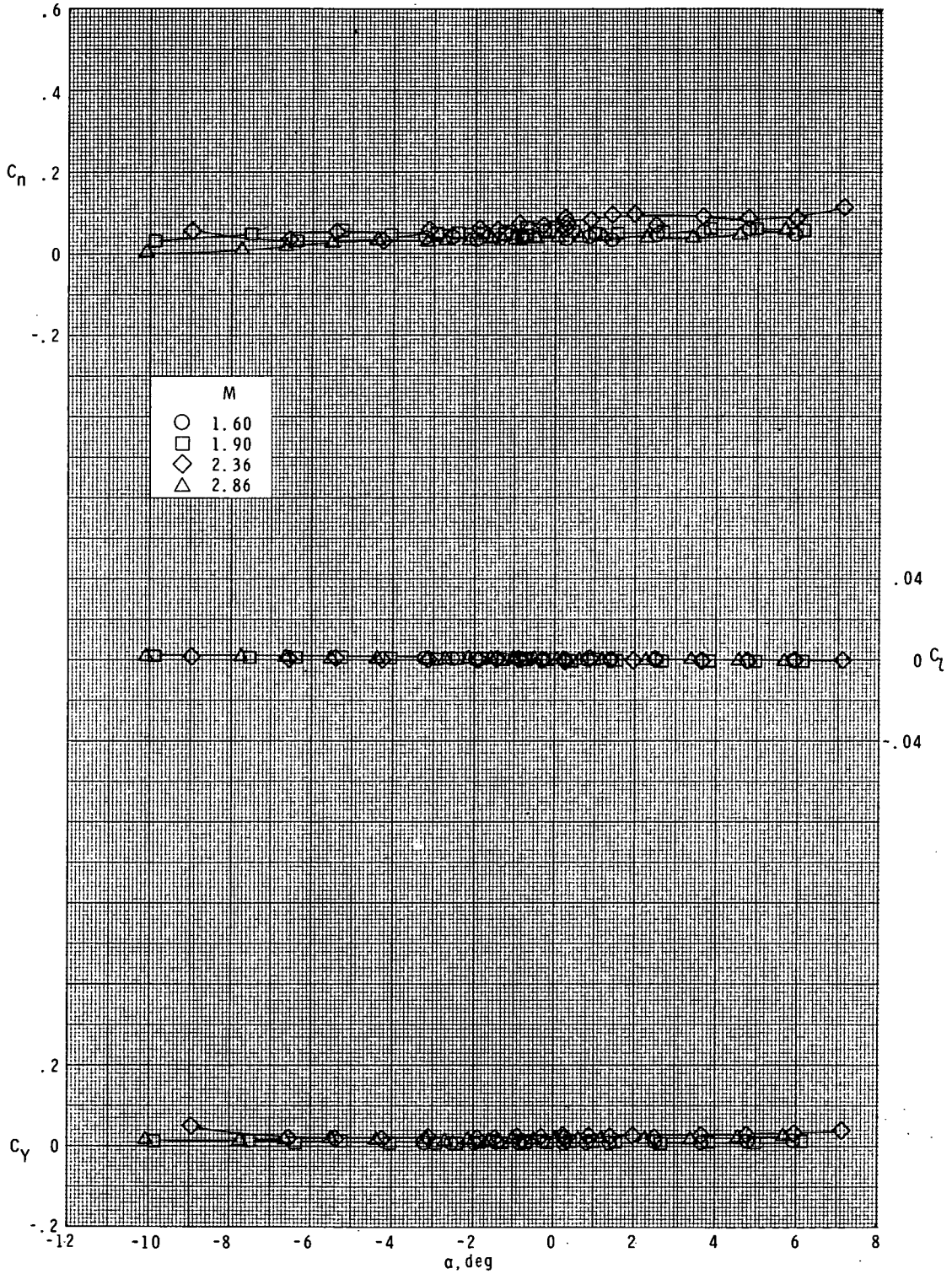

Figure 41.- Lateral characteristics of basic body (B_1).

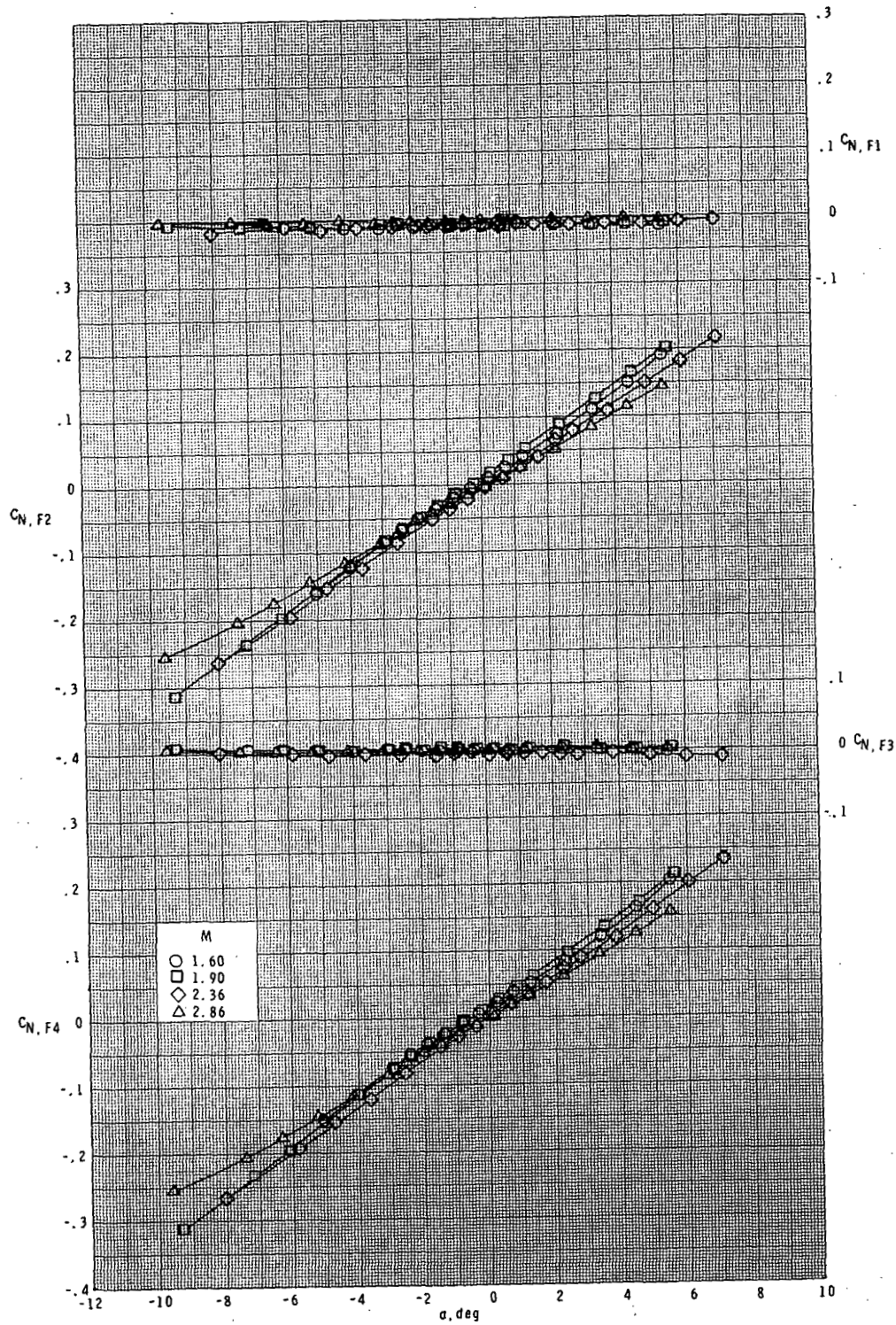

(a) $\phi = 0^{\circ}$.

Figure 42.- Variation of fin normal-force coefficient with angle of attack. Basic body (B_1); long-chord straight unswept fin (F_9).

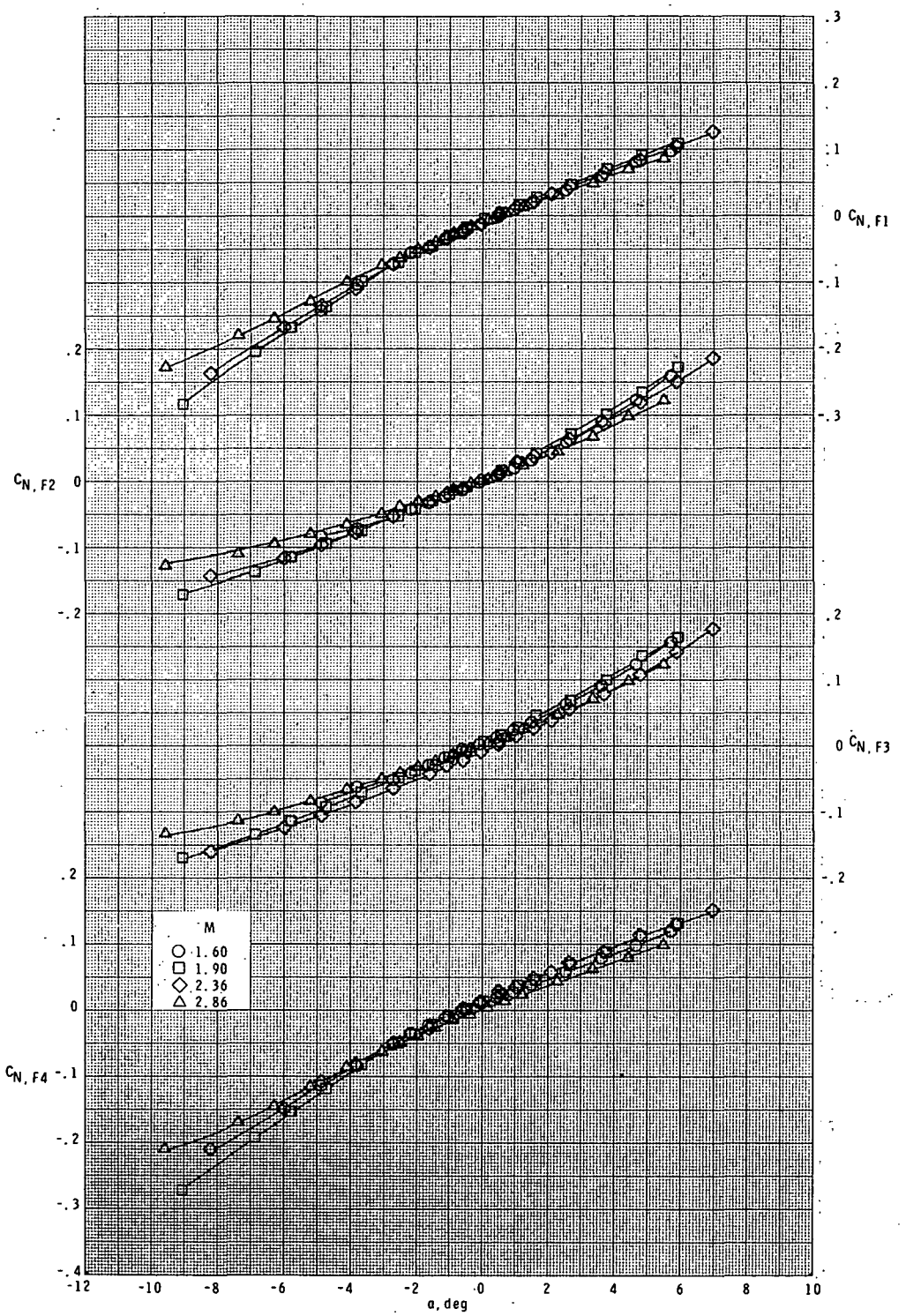

(b) $\phi = 45°$.

Figure 42.- Concluded.

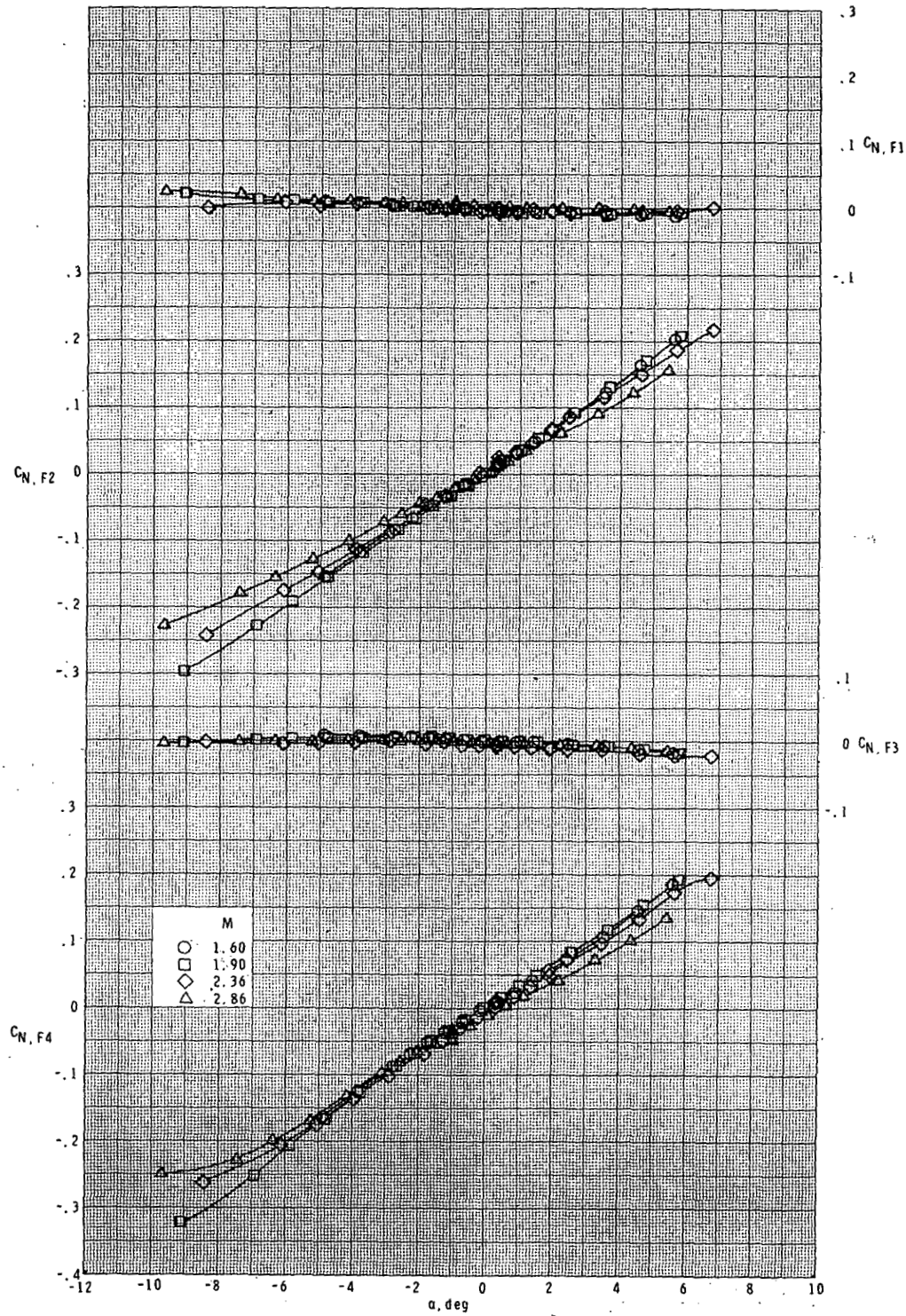

(a) $\phi = 0^{\circ}$.

Figure 43.- Variation of fin normal-force coefficient with angle of attack. Basic body (B_1); long-chord curved unswept fin (F_1).

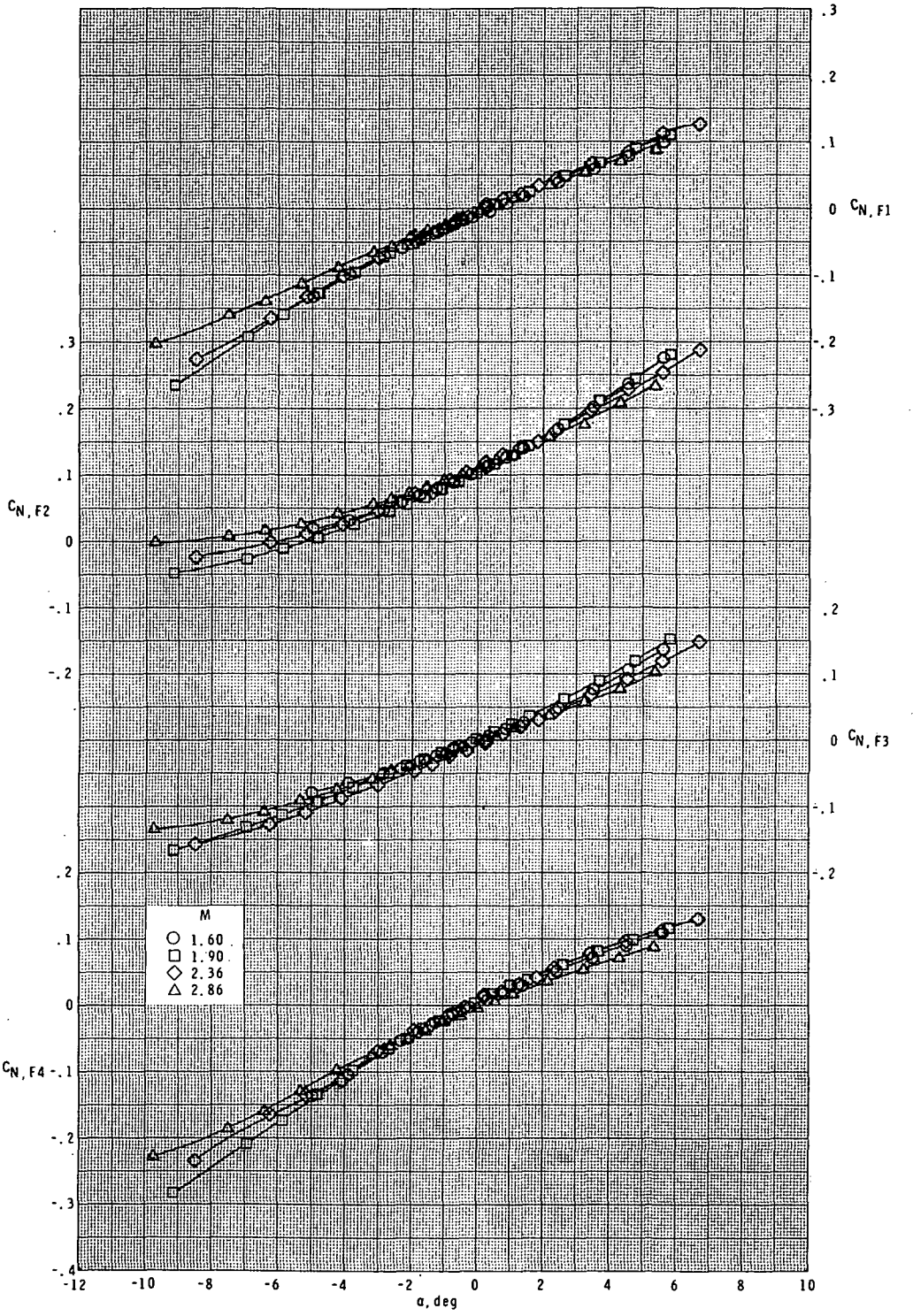

(b) $\phi = 45^{\circ}$.

Figure 43.- Concluded.

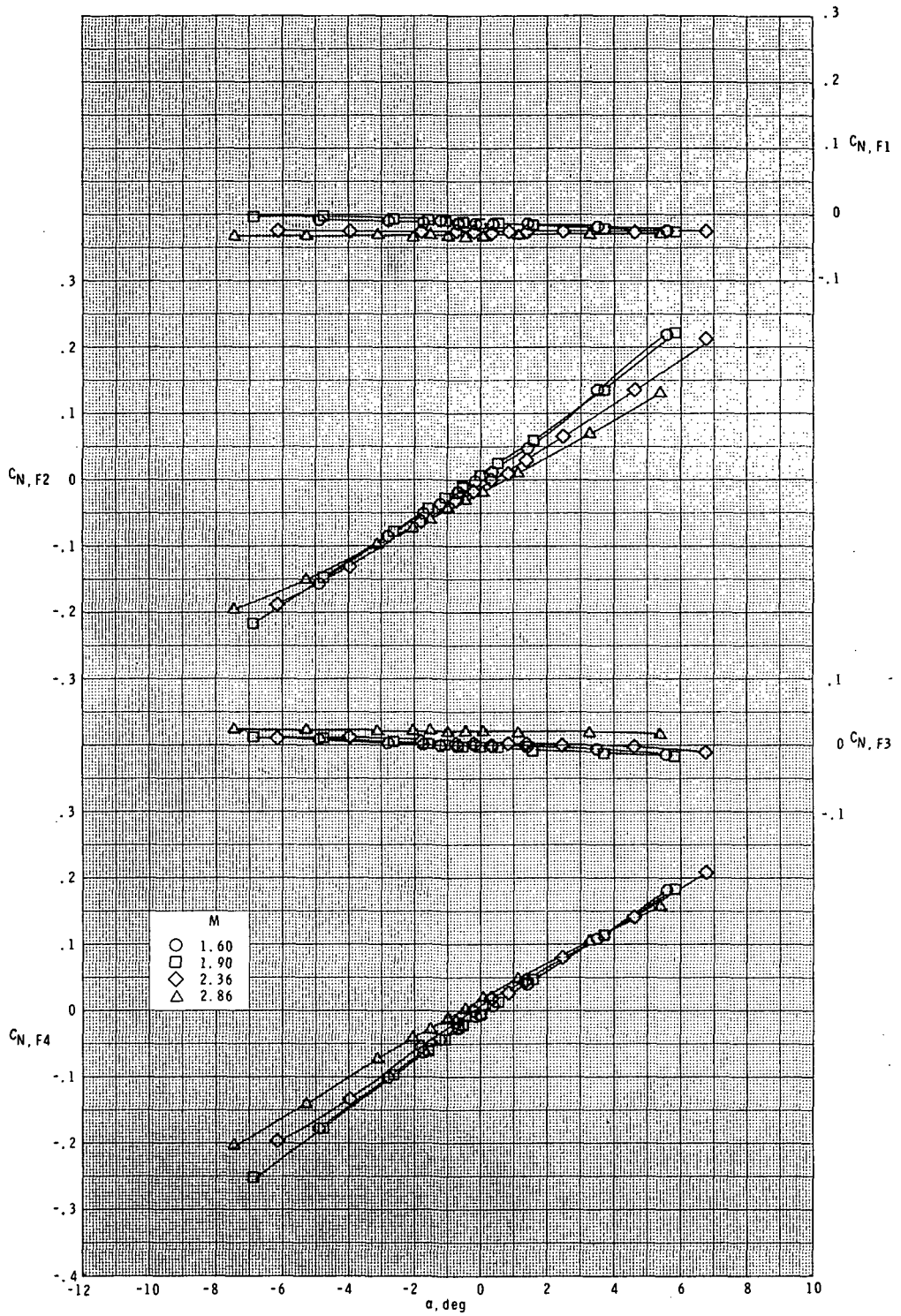

(a) $\phi = 0^{\circ}$.

Figure 44.- Variation of fin normal-force coefficient with angle of attack. Basic body (B_1); long-chord curved unswept fin (F_6) with asymmetrical leading edge.

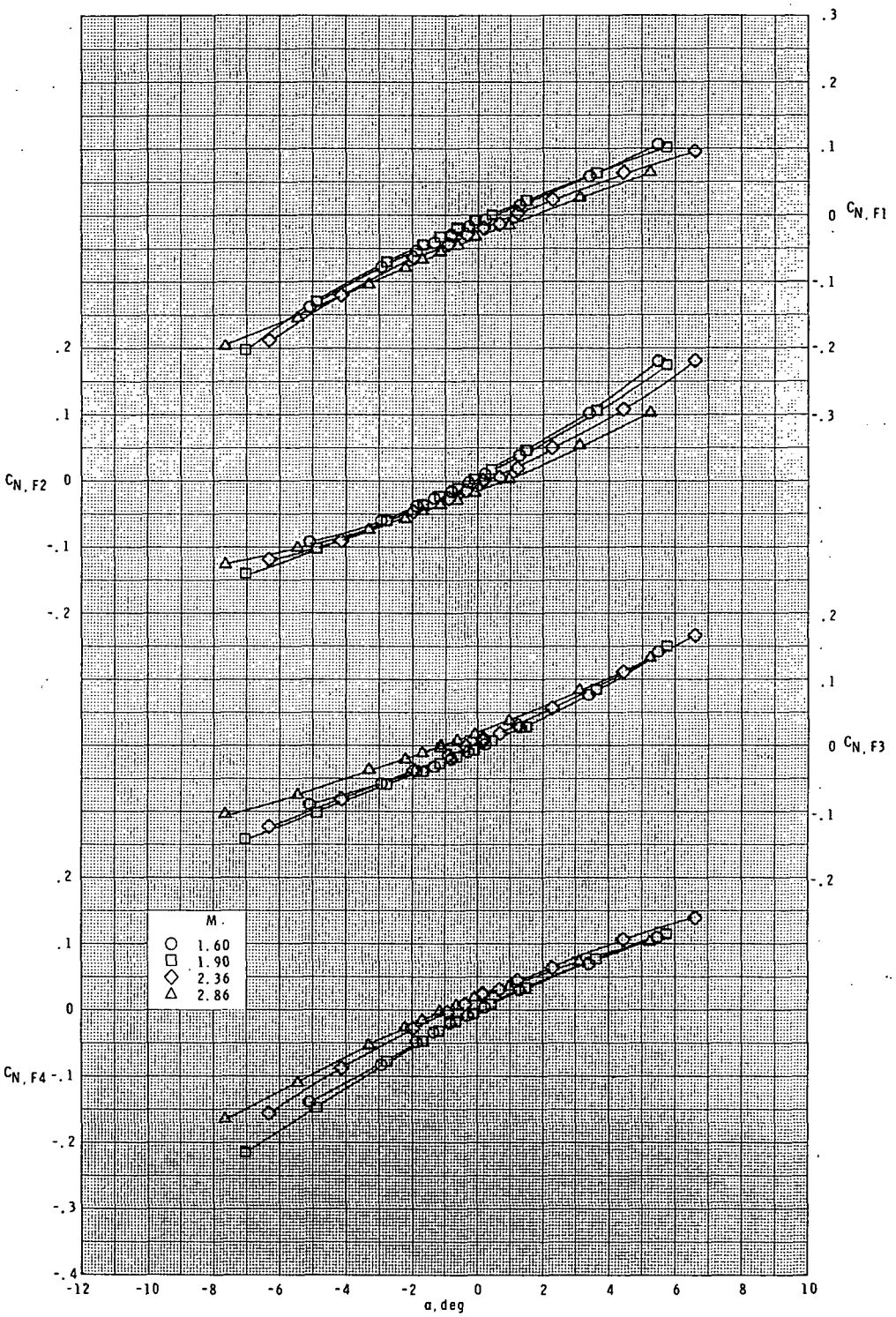

(b) $\phi = 45^{\circ}$.

Figure 44.- Concluded.

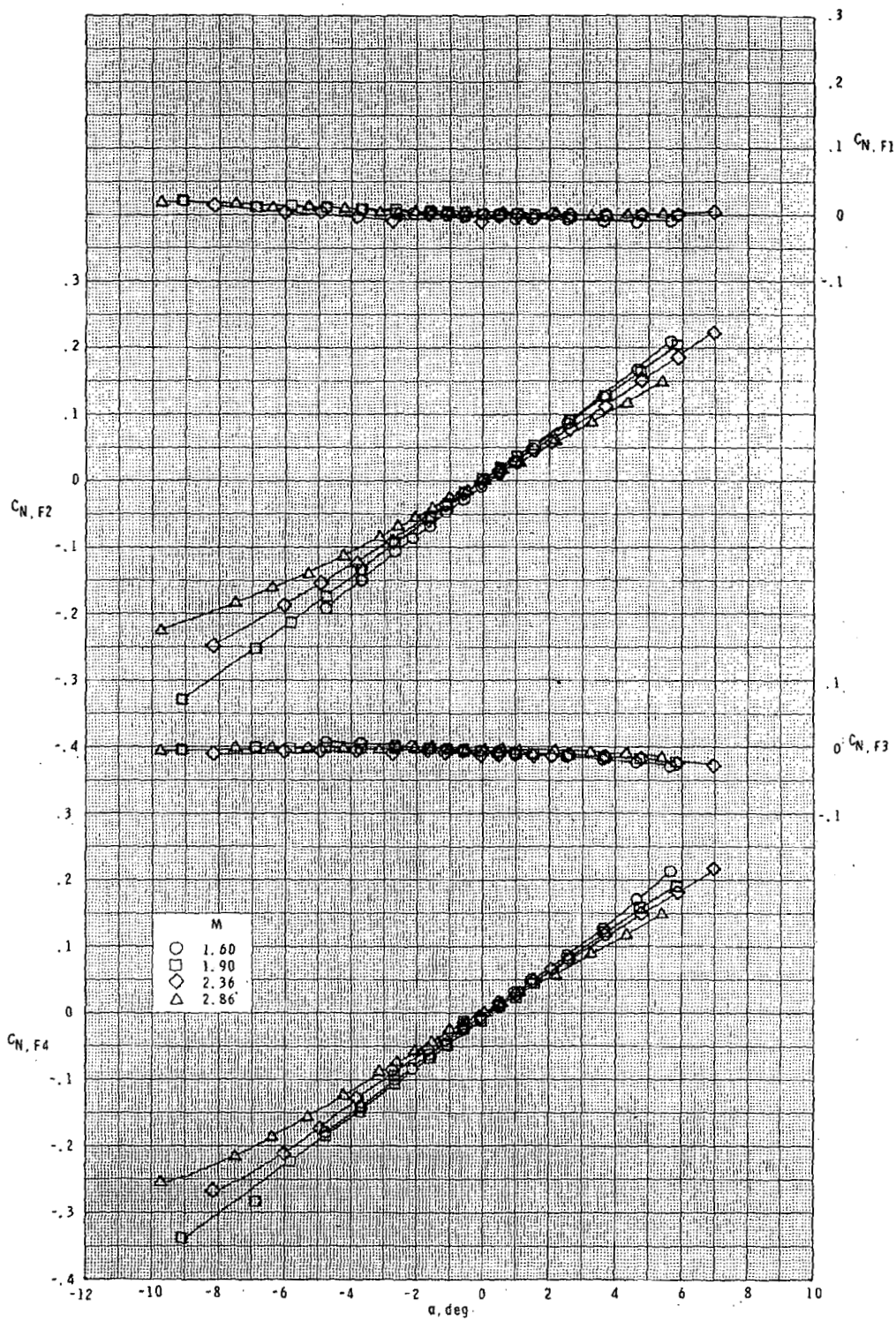

(a) $\phi = 0^{o}$.

Figure 45.- Variation of fin normal-force coefficient with angle of attack. Basic body (B_1); long-chord curved swept fin (F_{13}).

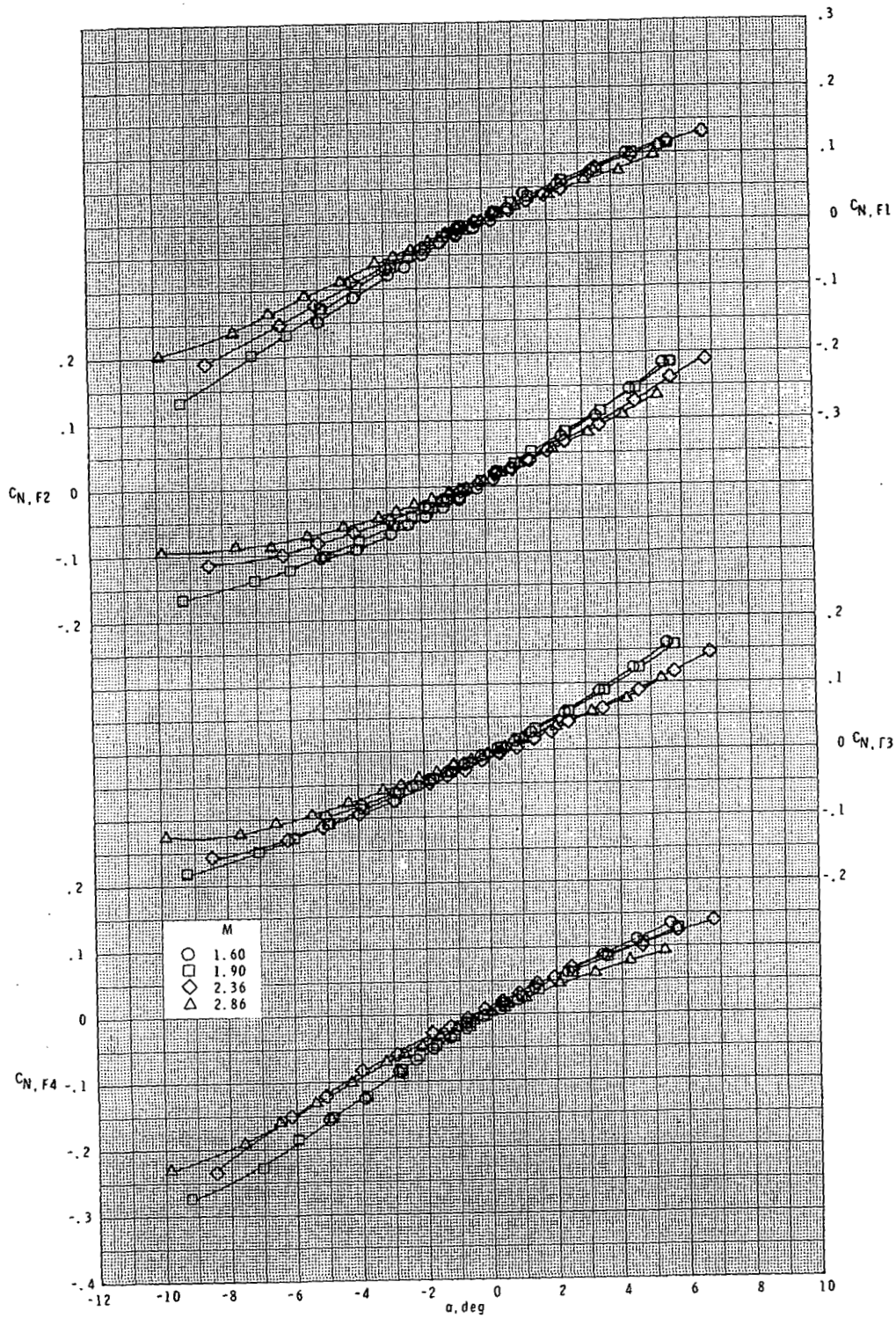

(b) $\phi = 45^{\circ}$.

Figure 45.- Concluded.

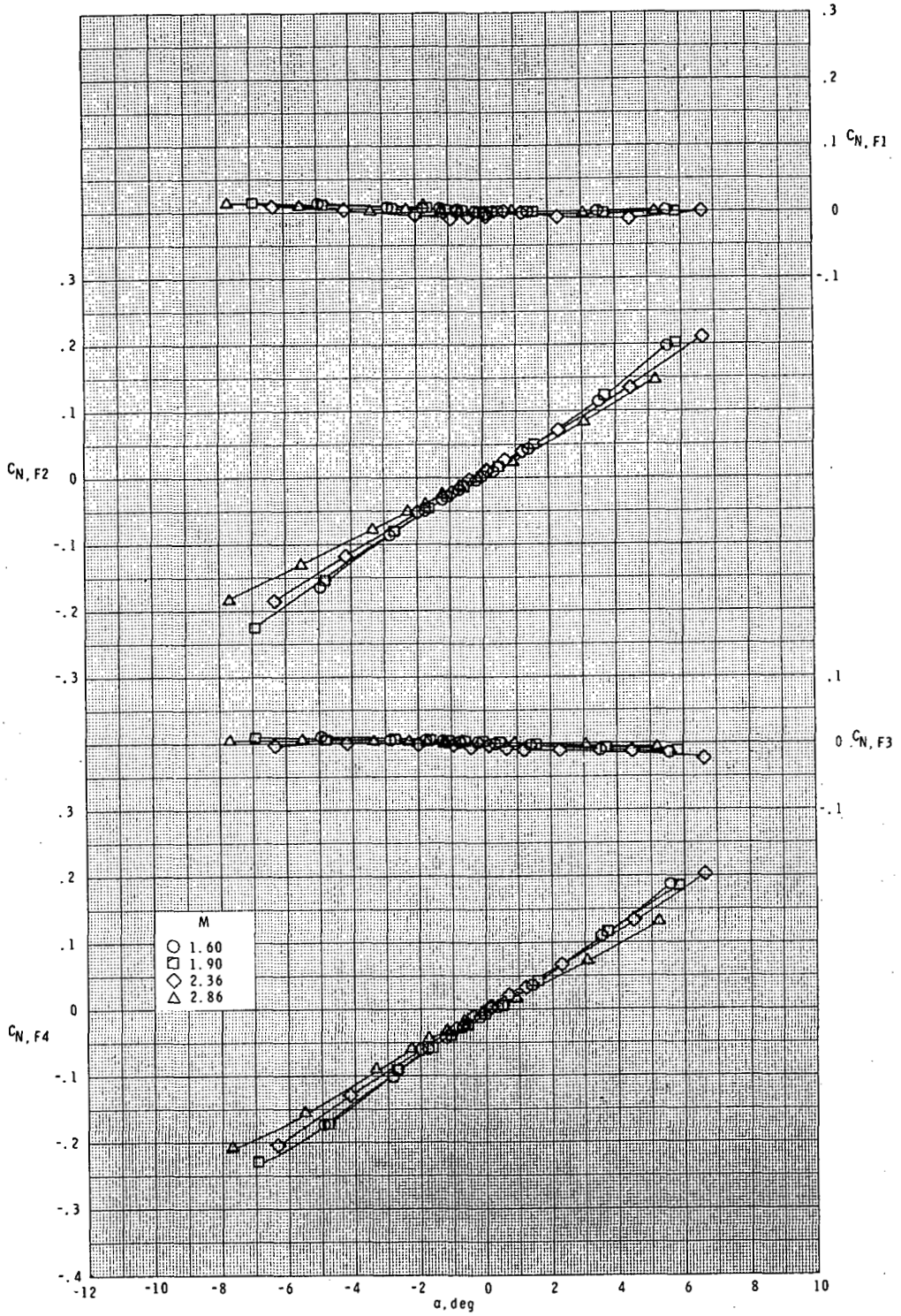

(a) $\phi = 0^{\circ}$.

Figure 46.- Variation of fin normal-force coefficient with angle of attack. Basic body (B_1); long-chord thin curved fin (F_7).

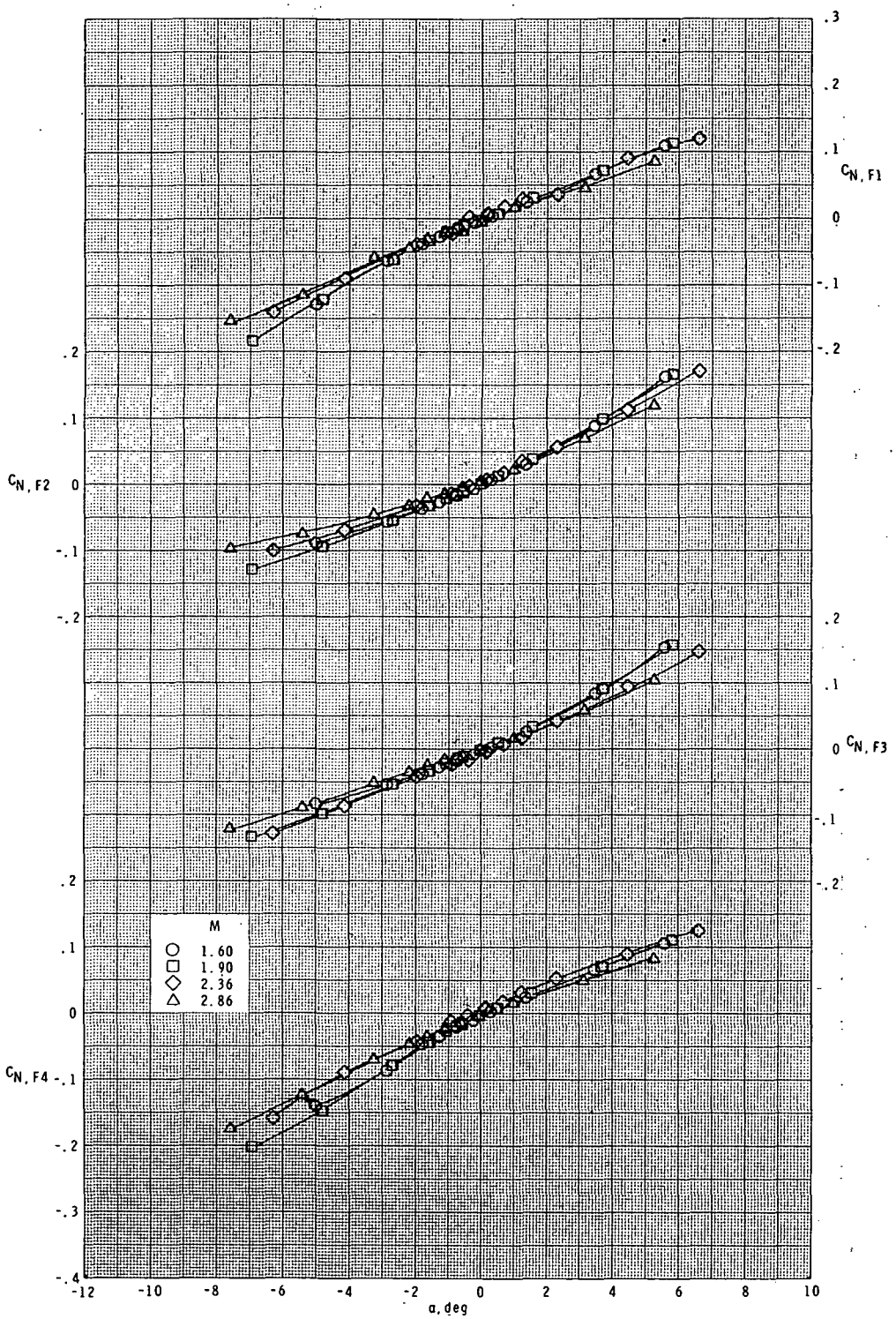

(b) $\phi = 45°$.

Figure 46.- Concluded.

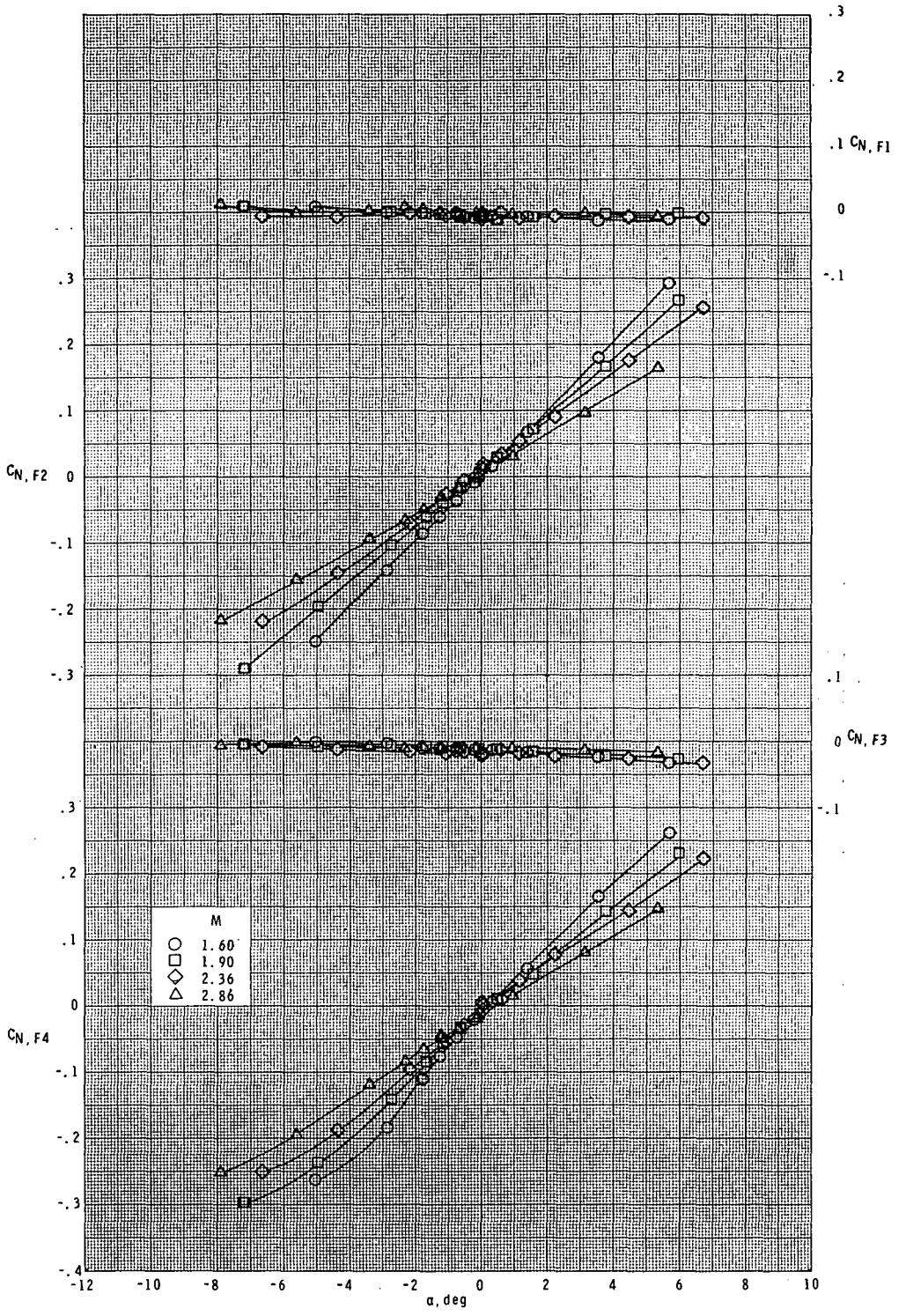

(a) $\phi = 0^{\circ}$.

Figure 47.- Variation of fin normal-force coefficient with angle of attack. Basic body (B_1); short-chord curved unswept fin (F_2).

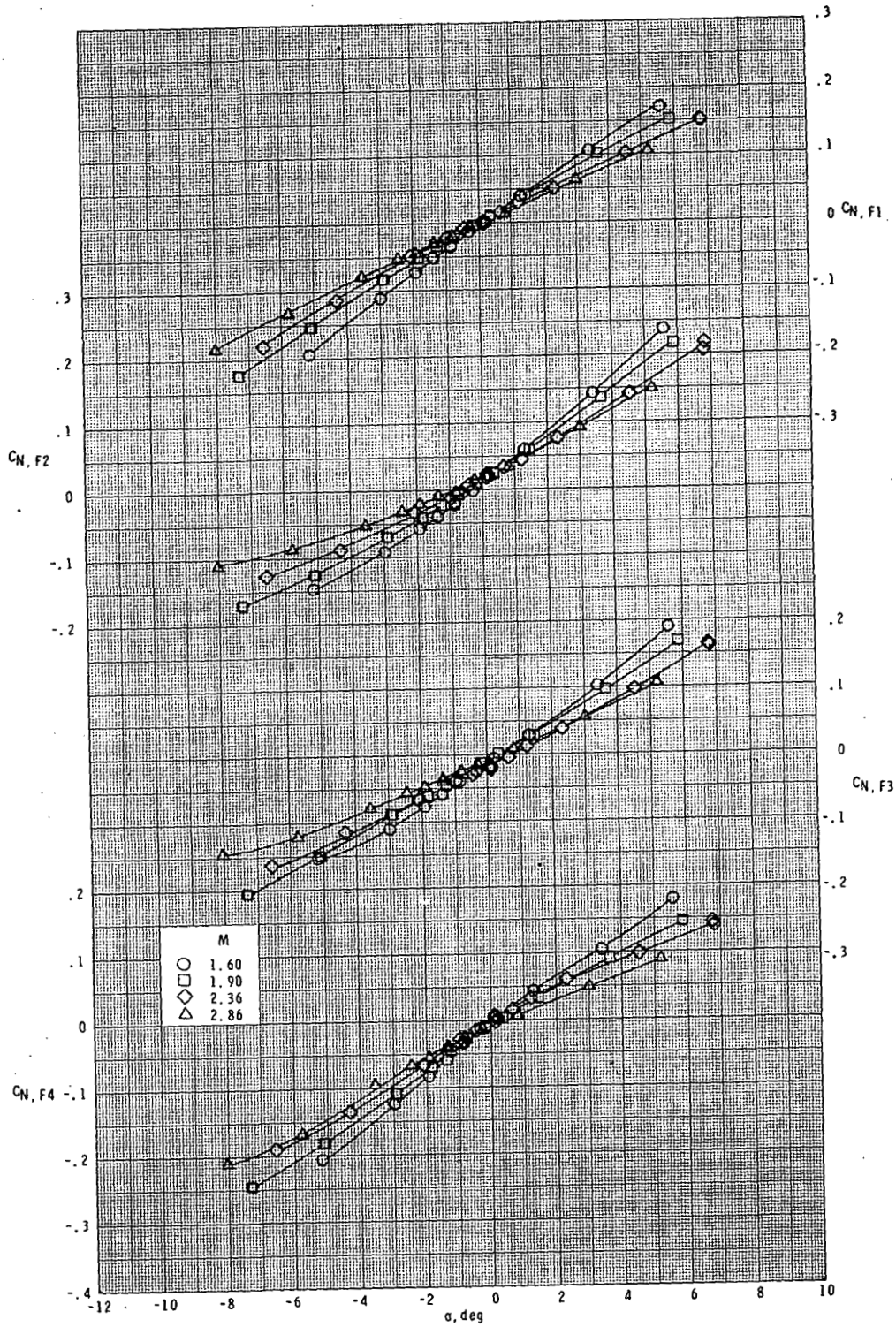

(b) $\phi = 45^{\circ}$.

Figure 47.- Concluded.

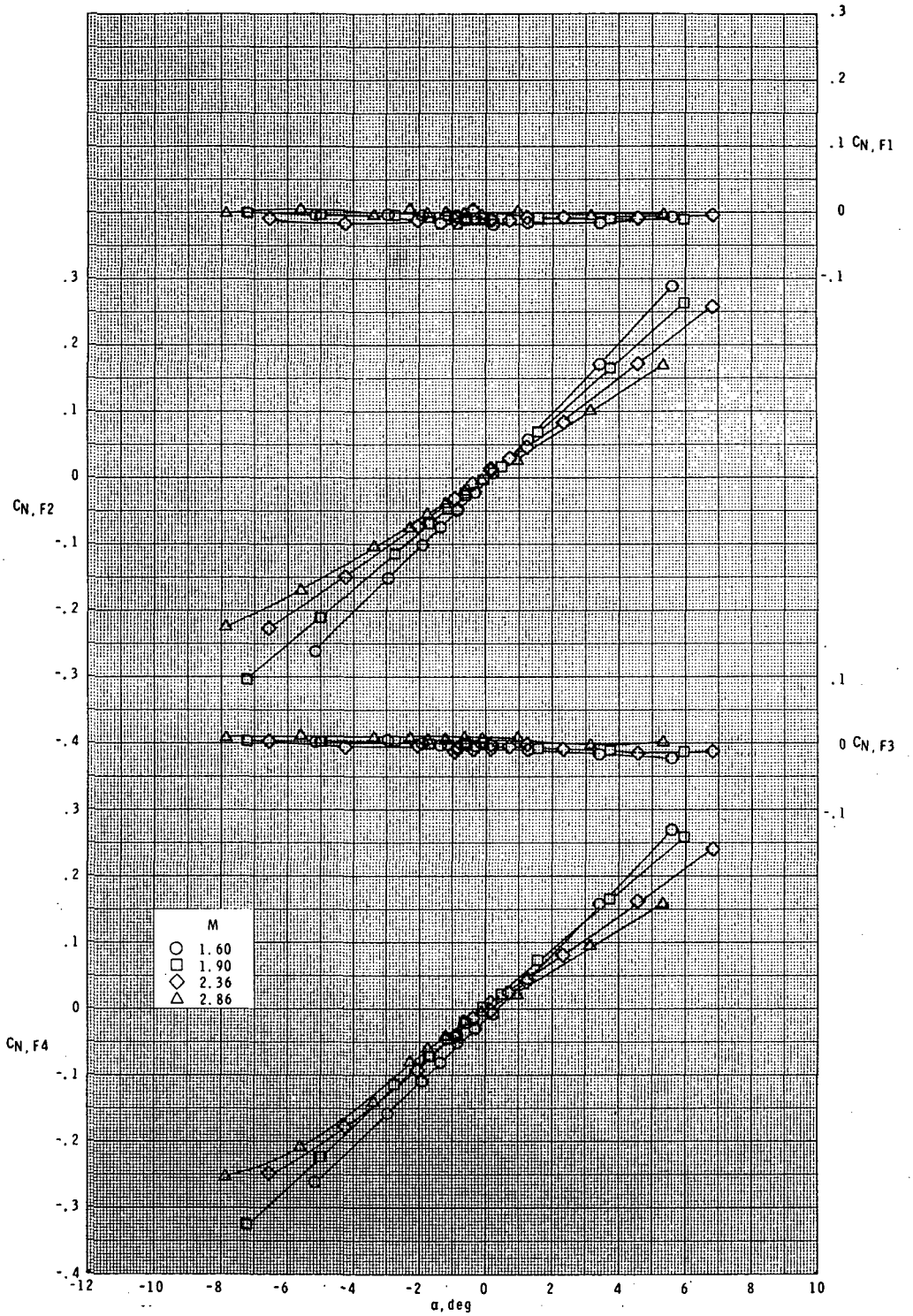

(a) $\phi = 0^{\circ}$.

Figure 48.- Variation of fin normal-force coefficient with angle of attack. Basic body (B_1); short-chord curved swept fin (F_{16}).

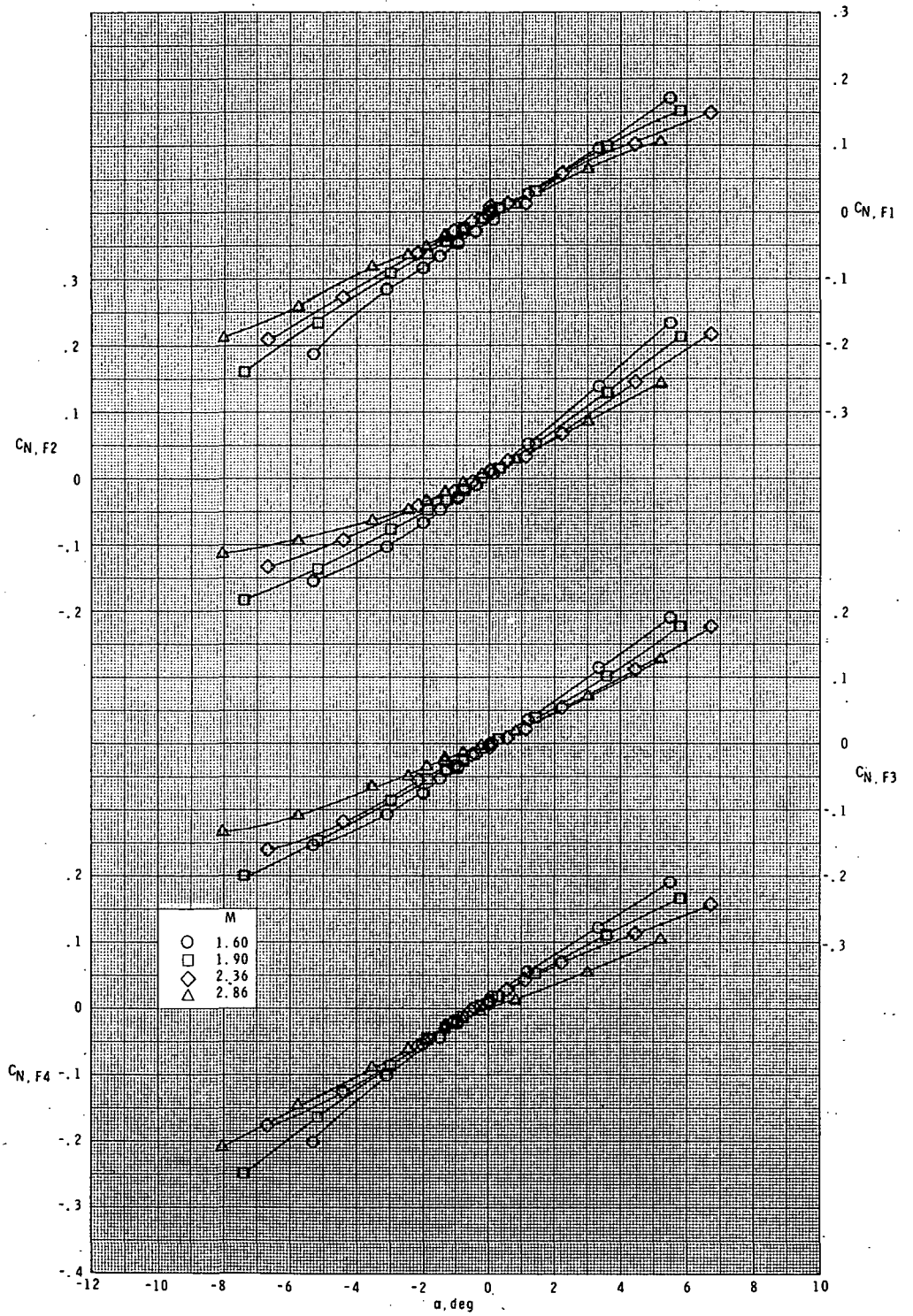

(b) $\phi = 45°$.

Figure 48.- Concluded.